Yizhak Marcus

Ions in Water and Biophysical Implications

From Chaos to Cosmos

Springer

Ions in Water and Biophysical Implications

Yizhak Marcus

Ions in Water and Biophysical Implications

From Chaos to Cosmos

Springer

Yizhak Marcus
Institute of Chemistry
The Hebrew University of Jerusalem
Jerusalem
Israel

ISBN 978-94-007-4646-6 ISBN 978-94-007-4647-3 (eBook)
DOI 10.1007/978-94-007-4647-3
Springer Dordrecht Heidelberg London New York

Library of Congress Control Number: 2012945903

Printed on acid-free paper

Springer is part of Springer Science+Business Media (www.springer.com)

Preface

It is so often stated that water is a ubiquitous liquid on earth and a general solvent for many kinds of solutes that such statements sound as clichés. Nevertheless, they are correct and merit discussion. Other common statements are that the properties of water are unique among liquids and are difficult to understand: "No one really understands water. It's embarrassing to admit it, but the stuff that covers two-thirds of our planet is still a mystery. Worse, the more we look, the more the problems accumulate: new techniques probing deeper into the molecular architecture of liquid water are throwing up more puzzles." (Ball 2008). Unfortunately, to date this situation keeps being rather true and should be accorded a more comprehensive treatment.

On the other hand, ions are found in a large variety of environments. These include a non-environment where the ions are isolated in vacuum, as generated for example in a mass spectrometer. Ions in a gaseous phase include clusters of ionized water vapour relating to cloud formation. Ions in condensed phases may occur in solids, whether crystalline or disordered (glasses) but also in liquids, including room temperature ionic liquids or molten salts at higher temperatures. In such condensed phases the ions are in close vicinity to one another with strong coulombic interactions between their charges that tend to order the ions (at least over short distances in liquids) with alternating positive and negative charges.

Ions also exist in liquid solutions in a variety of solvents, whether non-aqueous, aqueous, or mixed. When ions are placed in a solvent, by the dissolution of an electrolyte capable of extensive ionic dissociation, the properties of such solutions cannot be estimated simply as weighted sums of the properties of the individual components, solvent and ions. This results from the strong interactions between the ions and the solvent molecules, which merit intensive investigation in order to comprehend the properties of such solutions. The ions tend to be solvated in solution with a solvation shell around them, the solvent separating the ions from one another, their mutual distance apart depending on their concentration. For a binary electrolyte, consisting of one cation C and one anion A at a molar concentration c their average distance apart is inversely proportional to the cube root of the concentration: ${d^{\mathrm{av}}}_{\mathrm{C-A}} = (2cN_{\mathrm{A}})^{-1/3}$ (Marcus 2009). If each of the ions has one solvent molecule attached to it in the space between them, there is hardly space for a further solvent molecule between the solvated ions at a concentration of 1 mol per litre. Therefore, the

properties of dilute and mildly concentrated solutions differ considerably. Moreover, electrolyte solutions may be homogeneous but also colloidal dispersions and their properties vary from those in the bulk to those near surfaces. The interactions of ions at solution surfaces, whatever the phase at the other side of the surface—a gas, an immiscible liquid, a solid (e.g., an electrode), or dispersed colloidal particles (including biopolymers)—are also a subject that requires attention.

Both biological systems and their physiology are based on the water that is present in all living things, which is essential to life, as well as on solutions of ions in the water. Furthermore, these solutions exist in rather heterogeneous situations, in the vicinity of surfaces of organic substances that are partly hydrophilic and partly hydrophobic and which may carry charges on their ionisable groups. Therefore, the biophysical implications of such solutions are consequences of the above-mentioned interactions. There exists thus a wide spread of topics that should be dealt with in a book such as the present one.

The term "entropy", meaning "transformation" in Greek, was introduced by Clausius for this well known but perhaps less well understood thermodynamic quantity. This entity is often interpreted as "disorder" in a system, equivalent to "chaos", but also as "lack of knowledge" in terms of information theory (Ben-Naim 2008). It is the purpose of this book to fill the gap in ordered knowledge about the above mentioned topics of ions in water, and lead the reader from "chaos" to "cosmos", which means in Greek "order" and "harmony". Therefore, "from chaos to cosmos" is an apt subtitle for this book, in particular because ions in aqueous solutions relating to biophysical phenomena are classified as "chaotropic" or "kosmotropic". The justification of the use of these terms in the context of biological systems is critically assessed in this book. The author does not belong to the biophysics research establishment, hence his efforts to bring order to the use of such terms such as chaotropic and kosmotropic ions and the Hofmeister effect and series is like tilting at windmills. Still, he is confident that the suggestions made in this book may infiltrate into this establishment and might be accepted in the long run.

This book, being written by a single author, cannot be a comprehensive treatise on the subject of ions in water. It does present the author's physicochemical point of view, but is annotated with a large number of references to the original literature. In the present millennium already some 700 books have been published that have "water" in their title, but only very few have bearing on the present spread of problems. Some, indeed "ancient", books on aqueous electrolyte solutions, however, should be mentioned here, because they contain the physicochemical basis for the present discussions: the books by Harned and Owen (1958) and by Robinson and Stokes (1965). More recently the books by Conway (1981) and by Marcus (1985) and a special journal issue edited by Harding (2001) bear directly on the problems dealt with here. Other books are mentioned in the chapters dealing with the specific topics.

The author acknowledges gratefully very useful comments from Prof. Werner Kunz (Regensburg) and Prof. Bernd Rode (Innsbruck) on some parts of this book. However, the opinions presented are solely the author's.

References

Ball P (2008) Water: Water—an enduring mystery. Nature 452:291–292
Ben-Naim A (2008) Entropy Demystified. World Scientific, New Jersey
Conway BE (1981) Studies in physical and theoretical chemistry, Vol. 12. Ionic Hydration in chemistry and biophysics, Elsevier, Amsterdam
Harding SE (2001) The hydration problems in solution biophysics. Biophys Chem 93:87–246
Harned HS, Owen BB (1958) The Physical Chemistry of Electrolyte Solutions, 3rd edn. Reinhold, New York
Marcus Y (1985) Ion Solvation, Wiley, Chichester
Marcus Y (2009) On water structure in concentrated salt solutions. J Solution Chem 38:513–516
Robinson RA, Stokes RH (1965) Electrolyte Solutions, 2nd edn. Butterworths, London, (revised)

Yizhak Marcus

Contents

List of Symbols

Symbol Description (Units (SI))

Acronyms

cmc	Critical micelle concentration
EoS	Equation of state
ITIM	Identification of truly interfacial molecules
MC	Monte Carlo computer simulation
MD	Molecular dynamics computer simulation
PVT	Pressure-volume-temperature
SAFT	Statistical associated fluid theory
SHG	Second harmonic generation spectroscopy
SPT	Scaled particle theory
STI	Surface tension increment
VLE	Vapour/liquid equilibrium
VSFG	Visible sum frequency generation spectroscopy

Symbols for units (not in the general SI list) Roman font

m	Molality (mol kg solvent^{-1})
M	Molarity (mol dm^{-3})

Universal constants in *italics* font

e	Unit electrical charge: 1.602177×10^{-19} (C)
F	Faraday's constant: 9.64853×10^{4} (C mol^{-1})
k_B	Boltzmann's constant: 1.380658×10^{-23} (J K^{-1})
N_A	Avogadro's number: 6.022136×10^{23} (mol^{-1})
R	Gas constant: 8.31451 (J K^{-1} mol^{-1})
ε_0	Permittivity of vacuum: 8.854188×10^{-12} (C^2 J^{-1} m^{-1})

Symbols for physical quantities in Roman *italics* font

A	Helmholz energy, molar (kJ mol^{-1})
a	Attractive parameter in an EoS (J^2 Pa^{-1} mol^{-2})
B	Virial coefficient (m^3)
b	Scattering length (nm)
b	Co-volume parameter in an EoS (m^3)
C_P	Heat capacity at constant pressure, molar (J K^{-1} mol^{-1})
C_V	Heat capacity at constant volume, molar (J K^{-1} mol^{-1})
c	Concentration, molar scale (mol dm^{-3})
D	Diffusion coefficient (m^2 s^{-1})
d	Interatomic distance (nm)
E	Energy, molar (kJ mol^{-1})
e_{HB}	Energy of an H-bond per mole of bonds (kJ mol^{-1})
f	Fugacity (kPa)
f_i	Fraction of water molecules with i H-bonds
G	Gibbs energy, molar (kJ mol^{-1})
g	Kirkwood dipole orientation parameter
$g(r)$	Pair correlation function
H	Enthalpy, molar (kJ mol^{-1})
h_i	Hydration number, ionic
I	Ionic strength (mol dm^{-3})
I	Intensity of scattered or absorbed radiation
K	Equilibrium constant (dm^3 mol^{-1})
$K^O{}_W$	Octanol/water partition coefficient
K_W	Ion product of water (dm^6 mol^{-2})
k	Variable, function of diffraction angle (m^{-1})
k	Rate constant (s^{-1})
L_g	Ostwald coefficient of gas solubility
M	Mass, molar (kg mol^{-1})
m	Mass, molecular (kg)
m	Molality (mol kg^{-1})
N	number of components
N	Number of molecules or ions
N_{co}	Coordination number
n	Refractive index (at specified frequency)
$<n_{HB}>$	Average number of H-bonds per water molecule
P	Pressure (MPa)
P_i	Internal pressure (MPa)
p	Vapor pressure (kPa)
p(event)	Probability of an event
r	Radial distance from a particle (nm)
r_i	Radius, ionic (nm)
S	Entropy, molar (J K^{-1} mol^{-1})

$S(k)$	Structure factor
s	Solubility (mol dm^{-3})
T	Temperature (absolute) (K)
T_1	Spin-lattice nmr relaxation time (s)
t	Temperature (centigrade) (°C)
t_i	Transference number, ionic
U	Configurational energy of system, molar (kJ mol^{-1})
u	Sound velocity (m s^{-1})
u_i	Mobility, ionic (m s^{-1} V^{-1})
V	Volume, molar (m^3)
v	Specific volume (m^3 kg^{-1})
v	Velocity, molecular (m s^{-1})
x	Mole fraction of specified component or species
Y	Generalized thermodynamic function or solvatochromic parameter
y	Activity coefficient, molar scale
Z	Compressibility factor *PV/RT*
Z	Lattice parameter
z	Charge number, algebraic

Symbols for physical quantities in Greek *italics*

α	Kamlet-Taft H-bond donation ability index
α	Polarizability, molecular (m^{-3})
α_P	Expansibility, isobaric (K^{-1})
β	Kamlet-Taft H-bond acceptance ability index
γ	Activity coefficient, molal scale
δ	NMR chemical shift (ppm)
δ_H	Hildebrand solubility parameter ($MPa^{1/2}$)
ε_r	Relative permittivity
ζ	Reciprocal of the friction coefficient
η	Dynamic viscosity (mPa s^{-1})
θ	Angle between two dipoles or three atoms (°)
θ_{ca}	Contact angle between a solid and a sessile drop (°)
κ_S	Compressibility, adiabatic (GPa^{-1})
κ_T	Compressibility, isothermal (GPa^{-1})
Λ	Conductivity, molar (Ω^{-1} m^2 mol^{-1})
λ_i	Conductivity, ionic equivalent (Ω^{-1} m^2 mol^{-1})
μ	Dipole moment (C m)
μ	Chemical potential (kJ mol^{-1})
ν	Wave number (cm^{-1})
ξ	Correlation length (m)
π^*	Kamlet-Taft polarity/polarizability index
ρ	Density (kg m^{-3})
σ	Diameter, molecular (nm)

τ Relaxation or correlation time (ps)
φ Volume fraction
φ Osmotic coefficient
χ Number of H-bonds of any given water molecule
ω Frequency (s^{-1})
ω Pitzer's acentric factor

Sub- and superscripts

* Pure substance or scaling parameter
$^{\circ}$ Standard state
$^{\infty}$ Infinite dilution
$_{ass}$ Association
$_{c}$ Critical
$_{D}$ Dielectric or Debye, or self diffusion
$_{E}$ Excess thermodynamic quantity
$_{f}$ Of formation (thermodynamic quantity)
$_{g}$ Of a gas
$_{ig}$ Ideal gas
$_{i}$ Of an individual ion
$_{r}$ Reduced, divided by the critical quantity
$_{V}$ Of vaporization
$_{W}$ Of water
$_{\sigma}$ Saturation (VLE equilibrium)

Chapter 1
Water

Water is a ubiquitous liquid substance in our world, is essential for life as we know it, and has by all accounts striking properties that set it aside from other liquids. It has therefore been investigated from many points of view and the results have been published in innumerable papers in journals and in many books. Some 70 years ago Dorsey (1940) published a compendium of data on the water substance and Eisenberg and Kauzmann (1969) published a book on the structure and properties of water. A collective set of volumes, edited by Franks (1972) some 40 years ago, was devoted to water and solutions in it. Since then numerous more books and review articles have been devoted to the properties of water, both for itself and as a solvent for various substances, including electrolytes and their constituent ions. The recent review by Malenkov (2006) of the structure and dynamics of liquid water covers the developments in these subjects since the earlier books mentioned above. Recent works on the properties of water are the collection of review papers edited by Pratt (2002) and the book by Ben-Naim (2009) on understanding water.

1.1 Liquid Water

1.1.1 The Properties of Water in the Liquid State

The limits of existence of water in a thermodynamically stable liquid state extend from the triple point, at which it is in equilibrium with ice I, the solid state of water under ordinary pressures, to the critical point, at which the distinction between liquid and vapour phases vanishes. The former limit, the triple point, is at 0.01 °C (T_t = 273.16 K) and P_t = 0.61166 kPa. The latter limit, the critical point, is at 374.93 °C (T_c = 647.096 K) and P_c = 22.064 MPa. Liquid water also exists in a meta-stable sub-cooled state, theoretically down to the glass transition point, 139 K, but experimentally to 232 K (−41 °C) before spontaneous nucleation and freezing sets in. Liquid water is at equilibrium with water vapour along the so-called saturation curve, $p_\sigma(T)$, where p_σ is the vapour pressure, but it exists as a liquid also at higher external pressures. Wagner and Pruss (2002) reported the IAPWS 1995 formulation

Y. Marcus, *Ions in Water and Biophysical Implications,*
DOI 10.1007/978-94-007-4647-3_1, © Springer Science+Business Media Dordrecht 2012

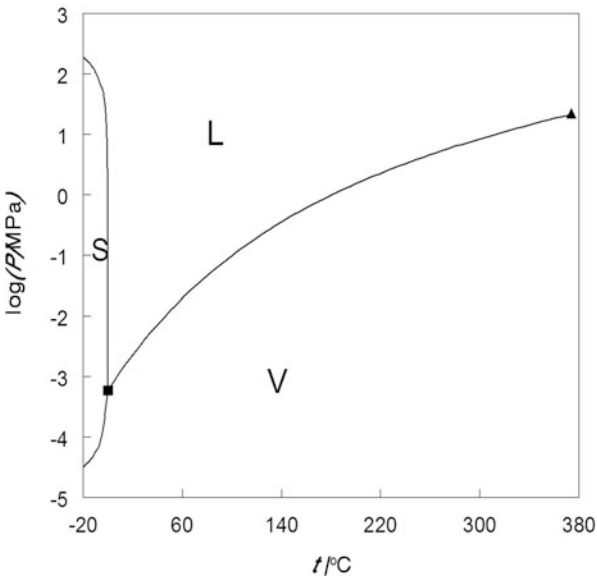

Fig. 1.1 A part of the phase diagram of water, showing the domains of the solid (iceI, *S*), the liquid (*L*), and the vapour (*V*). The square denoted the triple point and the triangle the critical point. (From data in (Dorsey 1940))

for the thermodynamic properties of water; it seems to be so far the last word on the subject. The expression for the saturation (equilibrium) vapour pressure of liquid water, $p_\sigma(T)$, takes the following form:

$$\ln\left(\frac{p_\sigma}{P_c}\right) = (1-\theta)^{-1}\left[a_1\theta + a_2\theta^{1.5} + a_3\theta^3 + a_4\theta^{3.5} + a_5\theta^4 + a_6\theta^{7.5}\right] \qquad (1.1)$$

where $\theta = 1 - T/T_c$ and with the following coefficients: $a_1 = -7.8595$, $a_2 = 1.84408$, $a_3 = -11.78665$, $a_4 = 22.68074$, $a_5 = -15.96187$, and $a_6 = 1.801225$. The relevant part of the phase diagram of water is shown in Fig. 1.1.

The properties of water are important for the understanding of the effects ions have on it. The molecular properties pertain to isolated water molecules in the ideal gas state. Some of these properties are shown in Table 1.1 for ordinary water, H_2O, and also for heavy water, D_2O, where known. The properties of these substances as liquids are, of course, also of large significance in the context of this book and are shown in Table 1.1 too.

The thermophysical and thermodynamic properties of liquid water as well as its chemical properties, all depend on the temperature and the pressure. The thermophysical and thermodynamic properties include the density ρ, the molar volume $V = M/\rho$, the isothermal compressibility $\kappa_T = \rho^{-1}(\partial\rho/\partial P)_T = -V^{-1}(\partial V/\partial P)_T$, the isobaric expansibility $\alpha_P = -\rho^{-1}(\partial\rho/\partial T)_P = V^{-1}(\partial V/\partial T)_P$, the saturation vapour pressure p_σ, the molar enthalpy of vapourization $\Delta_V H$, the isobaric molar heat capacity C_P, the Hildebrand solubility parameter $\delta_H = [(\Delta_V H - RT)/V]^{1/2}$, the surface tension γ, the dynamic viscosity η, the relative permittivity ε_r, the refractive index (at the sodium D-line) n_D, and the self-diffusion coefficient D. These are shown in Table 1.2, at the ambient pressure of 0.1 MPa (1 bar, 0.986923 atm) as a function

Table 1.1 Properties of light and heavy water. (Jasnsco and Van Hook 1974; Marcus 1985, 1998)

Molecular properties	H_2O	D_2O
O–H(D) bond length, (pm)	95.72	95.75
H–O–H angle, (°)	104.523	104.474
Moment of inertia, ($I_A/10^{-30}$ kg m^{-2})	0.10220	0.18384
Moment of inertia, ($I_B/10^{-30}$ kg m^{-2})	0.19187	0.38340
Moment of inertia, ($I_C/10^{-30}$ kg m^{-2})	0.29376	0.56698
Hydrogen bond length, (pm)	276.5	276.6
Dipole moment, (μ/D)	1.834	1.84
Electrical quadrupole moment, ($\theta/10^{-39}$ C m^2)	1.87	
Polarizability, ($\alpha/10^{-30}$ m^3)	1.456	1.536
Collision diameter, (σ/pm)	274	
Potential energy minimum, (u/k_B)/K	732	
O–H(D) bond energy at 0 K, (kJ mol^{-1})	44.77	
Proton (deuteron) affinity, (kJ mol^{-1})	762	772
Symmetrical stretching frequency, (cm^{-1})	3656.65	2671.46
Asymmetrical stretching frequency, (cm^{-1})	3755.79	2788.05
Bending frequency, (cm^{-1})	1594.59	1178.33
Zero point vibrational energy, (kJ mol^{-1})	55.31	40.44
Thermodynamic properties		
Triple point, K (°C)	273.15 (0.00)	276.97 (3.82)
Normal boiling point, K (°C)	373.15 (100.00)	374.57 (101.42)
Critical temperature, K (°C)	647.3 (374.1)	644.1 (370.9)
Critical pressure, (MPa)	22.12	21.86
Molar mass, (M/kg mol^{-1})	0.018015	0.020031
Van der Waals volume, (V_{vdW}/cm^3 mol^{-1})	12.4	12.4
Van der Waals surface area, ($A_{vdW}/10^4$ m^2 mol^{-1})	22.6	22.6
Ideal gas heat capacity, (C_P/J K^{-1} mol^1)	33.578	34.238
Ideal gas entropy, (S/J K^{-1} mol^1)	188.72	198.23
Enthalpy of vapourization, (kJ mol^{-1})	44.04	45.46
Properties of the liquid at 25 °C		
Isobaric heat capacity, (J K^{-1} mol^{-1})	75.27	84.52
Isochoric heat capacity, (J K^{-1} mol^{-1})	74.48	83.7
Isothermal compressibility, (GPa^{-1})	0.457	0.4678
Isobaric expansibility, (10^{-3} K^{-1})	0.2572	0.1911
Surface tension, (mN m^{-1})	71.97	71.85
Viscosity, (mPa.s)	0.890	1.103
Magnetic susceptibility, ($\chi/10^{-6}$ cm^3 mol^{-1})	−12.9	
Relative permittivity, (ε_r)	78.46	78.06
$(\partial\ \ln\varepsilon_r/\partial T)_P$ (10^3 K^{-1})	−4.59	−4.64
$(\partial\ \ln\varepsilon_r/\partial P)_T$ (GPa^{-1})	0.471	
Self-diffusion coefficient, ($D/10^{-9}$ m^2 s^{-1})	2.299	2.109
Cooperative relaxation time (at 20 °C), (τ/ps)	9.55	12.3
Refractive index at Na D line	1.33250	1.32841

of the temperature, in the range relevant for liquid water, i.e., at 0 °C $\leq t \leq$ 100°C, where the vapour pressure is $p_\sigma \leq$ 1atm = 0.101325 MPa.

Finally, some chemical properties of water, such as the polarity and solvatochromic indices, are listed in Table 1.3 for 25 °C. The self-ionic-dissociation, of water is the most important chemical property of water. Its equilibrium constant, K_W,

Table 1.2 Thermohysical and thermodynamic properties of water at ambient pressure (0.1 MPa) and varying temperatures (0°C $\leq t \leq$ 100°C)

t (°C)	ρ (g cm^{-3})	V (cm^3 mol^{-1})	α_P (mK^{-1})	κ_T (GPa^{-1})	p_σ (kPa)	$\Delta_v H$ (KJ mol^{-1})	C_p (J K^{-1} mol^{-1})	δ_H (MPa$^{1/2}$)	γ (mN m^{-1})	η (mPa s)	ε_r	n_D	D^a (10^{-9}m^2 s^{-1})
0	0.99984	18.019	−0.0681	0.5089	0.611	45.03	75.98	48.71	75.62	1.792	87.81	1.33395	1.099
10	0.99970	18.021	+0.0880	0.4781	1.228	44.67	75.52	48.46	74.20	1.307	83.99	1.33374	1.525
20	0.99820	18.048	0.2068	0.4585	2.338	44.24	75.34	48.13	72.75	1.002	8.027	1.33298	2.023
25	0.99705	18.069	0.2572	0.4525	3.169	44.04	45.29	47.96	71.96	0.890	78.46	1.33250	2.299
30	0.99565	18.095	0.3032	0.4477	4.245	43.84	75.27	47.79	71.15	0.798	76.67	1.33195	2.594
40	0.99222	18.157	0.6853	0.4424	7.381	43.46	75.28	47.44	69.55	0.653	73.22	1.33066	3.238
50	0.98804	18.234	0.4576	0.4417	12.35	43.09	75.31	47.07	67.90	0.547	69.90	1.32909	3.956
60	0.98320	18.324	0.5231	0.4450	19.92	42.74	75.38	46.71	66.17	0.467	66.73	1.32730	4.748
70	0.97777	18.425	0.5837	0.4516	31.18	42.40	75.47	46.33	64.41	0.4041	63.70	1.32526	5.615
80	0.97180	18.538	0.6411	0.4614	47.38	42.09	75.60	45.96	62.60	0.354	60.81	1.32302	6.557
90	0.96532	18.663	0.6962	0.4743	70.12	41.79	75.75	45.58	60.74	0.313	58.05	1.32061	7.574
100	0.95836	18.799	0.7501	0.4902	101.325	41.50	75.95	45.20	58.85	0.278	55.41	1.31805	8.667

[a]From (Easteal et al. 1989)

Table 1.3 Chemical properties of light and heavy water at 25 °C

Property	H_2O	D_2O
Dimrot-Reichard polarity index, ($E_T(30)$/kcal mol^{-1})	63.1	62.5
Normalized Dimrot-Reichard polarity index, ($E_T{}^N$)	1.000	0.991
Kamlet-Taft polarity/polarizibility, (π^*)	1.09	
Kamlet-Taft electrom pair donicity, (β)	0.47	
Kamlet-Taft hydrogen bond donicity, (α)	1.17	
Gutmann donor number	18.0	
Gutmann-Maier acceptor number	54.8	
Marcus softness parameter, (μ)	0.00	
Ion product, pK_W (Pentz and Thornton 1967)	13.996	14.860

Table 1.4 Some temperature dependent chemical properties of water

t(°C)	κ(μS m^{-1})[a]	p$K_{W(m)}$[b]	S_y
0	1.19	14.944	0.4883
10	2.33	14.535	0.4960
20	4.20	14.167	0.5046
25	5.48	13.996	0.5091
30	7.06	13.833	0.5139
40	11.1	13.535	0.5241
50	16.7	13.262	0.5351
60	24.0	13.016	0.5470
70	33.4	12.796	0.5599
80	45.5	12.598	0.5739
90	59.9	12.420	0.5891
100	76.4	12.260	0.6056

[a]From Light (1984)
[b]From Harned and Owen (1958)

for the ion product resulting from the autoprotolysis, has been studied extensively by many authors, and the book by Bates (1973) may be consulted for details. Table 1.4 shows pK_W, the negative of the logarithm of the ion product equilibrium constant, (on the molal scale, mol (kg water)$^{-1}$). Also relevant are the specific conductance κ, and the limiting slope of the Debye-Hückel expression for the activity coefficients of 1:1 electrolytes S_y (on the molar, M, scale). The values of these properties are shown for 0 °C $\leq t \leq$ 100 °C in Table 1.4.

Such data are available also in the compendium by Riddick et al. (1986) on the properties of solvents and in the book by Marcus "Ion Solvation" (1985) among other sources. The latter book also summarizes interpolation functions for some of these variables. Some of these data are also available there for heavy water, D_2O and for sub-cooled liquid water, down to −35 °C, and heated liquid water along the saturation line to the critical point and at elevated pressures.

1.1.2 Water as a Structured Liquid

There exists consensus among researchers that water is a highly structured liquid due to an extensive network of hydrogen bonds (HBs). However, no agreement exists

on how the structure is to be defined and on how the extent of hydrogen bonding is to be measured or computed. Only recently have the intermolecular distances $d(O_W–O_W)$, $d(O_W–H_W)$, and $d(H_W–H_W)$ (pertaining to the water oxygen and hydrogen atoms) and the orientations of the water molecules been determined satisfactorily in liquid water by diffraction measurements and computer simulations (Head-Gordon and Hura 2002).

The molecular structure of liquids, as measured by x-ray and neutron diffraction, is presented in the first place as the structure factors $S(k)$. The diffraction methods yield the intensities I of the diffracted beams at various angles θ at a fixed wavelength λ of the radiation for the defined variable k:

$$k = \lambda^{-1} 4\pi \sin\left(\frac{\theta}{2}\right) \tag{1.2}$$

The structure factors are then obtained as

$$S(k) \approx \frac{I(k) - I(0)}{I(\infty) - I(0)} \tag{1.3}$$

This expression uses the intensities measured at very small angles $I(0)$ and at very large angles $I(\infty)$ to normalize the intensities and eliminate the effect of the incoherent scattering on the relative intensities. Note that $\lim S(k \to 0) = \rho k_B T \kappa_T \sim 0.01$ (nominally $S(0) = 0$) where ρ is the number density of the diffracting atoms, and also that $S(\infty) = 1$.

The structure factor is related to the radial distribution function of the liquid $n(r)$ and, in turn, to the pair correlation function $g(r)$ of the diffracting atoms, see below. The former of these quantities is the probability of finding a particle in a spherical shell of thickness $\mathrm{d}r$ at a distance r from a given particle. At large distances there are no interactions between the particles so that $\mathrm{d}n(r \to \infty, \mathrm{d}r) = \rho 4\pi r^2 \mathrm{d}r$, is proportional to the number density of the particles. At short distances, where attraction and repulsion forces between the particles play a role, the presence of a given particles at the origin affects the probability for another one to be in a volume element at the distance r from it: they are correlated. Hence the pair correlation function is defined by the conditional probability of finding another particle at a distance r from a given one:

$$\mathrm{d}n(r, \mathrm{d}r) = g(r)\rho 4\pi r^2 \mathrm{d}r \tag{1.4}$$

Since there is no correlation between the particles at large distances from each other $g(r \to \infty) = 1$. On the other hand, at very small distances the large repulsion of the electronic shells of the atoms prevent their overlapping and $g(r < \sigma) = 0$, where σ is the diameter of the particles. Integration of Eq. (1.4) from σ to any distance r yields the number of neighbouring molecules around the particle at the origin, i.e., the coordination number up to that distance. Generally $g(r)$ peaks at $r = \sigma + \varepsilon$, i.e., at a distance slightly beyond σ, and "undulates" further out reaching unity asymptotically, but practically beyond 3σ and possibly up to 5σ. The coordination numbers reach plateaus (have small slopes) at $r \sim \sigma$, that is the first coordination shell, and possibly also for the second shell at $r \sim 2\sigma$.

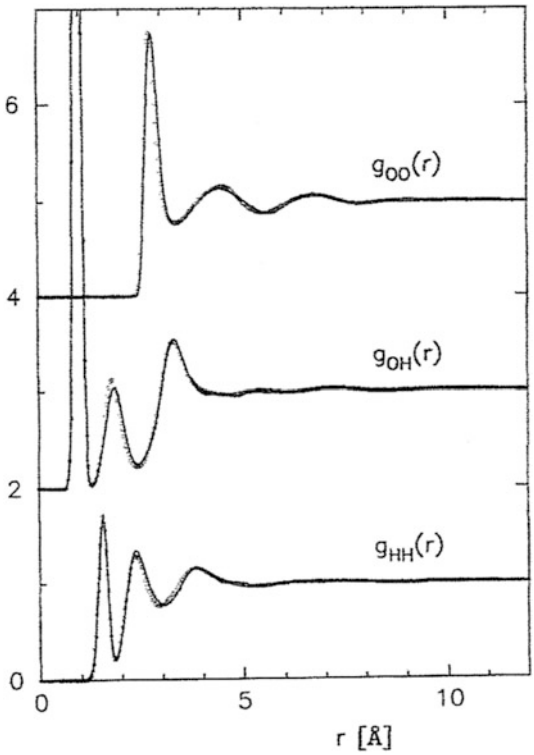

Fig. 1.2 The three partial pair correlation functions: $g(O_W–O_W, r)$, $g(O_W–H_W, r)$, and $g(H_W–H_W, r)$, for water at ambient conditions. (Reproduced from (Soper 2000) with kind permission of © The American Institute of Physics)

The structure factors yield after Fourier transformation the total pair correlation function $g(r)$:

$$g(r) = \left(2\pi^2 \rho r\right)^{-1} \int_0^\infty (S(k) - 1)k \sin(kr)\, \mathrm{d}k \tag{1.5}$$

Here "total" means that $g(r)$ pertains to all the diffracting atoms. Application of x-ray diffraction results in the structure of liquid water, in terms of $g(O_W–O_W, r)$, since only the oxygen atoms, but not the hydrogen atoms, diffract x-rays. This function resembles to some extent that of liquid argon, a non-structured liquid by all accounts (Fisenko et al. 2008), as demonstrated by Marcus (1996). There is, thus, more in the notion of the structure of water than what is measurable by $g(r)$, which is dominated by the strong repulsion of molecules that are too closely packed together.

Special techniques, isotope substitution in neutron diffraction with empirical potential structure refinement, permit partial pair correlation functions to be obtained. The three partial pair correlation functions: $g(O_W–O_W, r)$, $g(O_W–H_W, r)$, and $g(H_W–H_W, r)$, provide more information on the molecular structure of water as discussed below. Those for water at ambient conditions are shown in Fig. 1.2 (Soper 2000).

Table 1.5 The "structuredness" of some highly hydrogen-bonded solvents at 25 °C compared with other common electrolytic solvents

Solvent	*Stiffness* $(\delta_H^2 - P_i)$/ MPa	*Order* $(\Delta\Delta_{vap}S/R)$	$\Delta C_P/V$ (J K^{-1} cm^{-3})	KDOCP (*g*)	*Openness* $(1 - V_X/V)$
Water	2,129	7.82	2.31	2.90	0.076
1,2-Ethanediol	548	21.20	0.92	2.08	0.091
Glycerol	541	39.50	1.41	2.13	0.034
2-Ethanolamine	490	23.20	0.67	2.25	0.090
Formamide	1,014	7.58	1.56	1.67	0.091
Methanol	570	6.26	0.92	2.82	0.243
Acetonitrile	186	4.38	0.74	0.74	0.236
N, N-Dimethylformamide	101	4.00	0.74	1.03	0.249
Dimethyl sulphoxide	187	5.07	0.89	1.04	0.140

The first peak in the $g(O_W–O_W, r)$ function pertains to nearest water molecule neighbours, the second peak to next-nearest-neighbours, etc. The extent of the correlation (the height of the peak) is seen to diminish with increasing distances. The very large first peak in $g(O_W–H_W, r)$ pertains to the O−H covalent bond and is not relevant to the structure of water, but the second and further peaks yield information on the mutual orientation of the water molecules and on the hydrogen bonding. The latter item can also be retrieved from $g(H_W–H_W, r)$.

Before going into the details of the hydrogen bonding, there are other features of structured liquids in general and of water in particular that ought to be discussed. The notion of "structuredness" that was introduced by Marcus (1992) relates to more subtle interactions characterizing bulk properties of a liquid. Following Caldin and Bennetto (1971), Marcus described the structuredness of liquids in terms of the "stiffness", "order", and "openness" of a liquid in general.

The work that must be expended in order to create a cavity in a liquid measures its stiffness. Such a cavity is required in order to accommodate a molecule of the liquid itself, condensing into it from the vapour, or of a solute particle. This work per unit volume of the cavity can be obtained from the thermodynamic quantities characterizing the liquid: its molar enthalpy of vapourization $\Delta_v H$, its molar volume V, its isobaric expansibility α_P, its isothermal compressibility κ_T, and its vapour pressure p_σ, all at the temperature of interest T. These yield the difference between the cohesive energy density $ced = {\delta_H}^2 = [\Delta_v H - RT]/V$ and the internal pressure $P_i = T\alpha_P/\kappa_T - p_\sigma$. The *ced* is the square of the Hildebrand solubility parameter. According to Marcus (1999):

$$stiffness = {\delta_H}^2 - P_i = [(\Delta_v H - RT)/V] - T(\alpha_P/\kappa_T) - p_\sigma \qquad (1.6)$$

Water is a very stiff liquid, with ${\delta_H}^2 - P_i = 2,129$ MPa at 25 °C, much beyond other liquids, even those with a hydrogen bonded network, Table 1.5.

The deficit of the molar entropy of a liquid with respect to the same substance in the ideal gas phase is a measure of the "order" existing in the liquid. Trouton's constant, $\Delta_{vap}S(T_b) = \Delta_v H(T_b)/T_b$ is the negative of this deficit, where T_b is the

normal boiling point at atmospheric pressure (0.101325 MPa) and $\Delta_v S$ and $\Delta_v H$ are the molar entropy and enthalpy of vapourization. Trouton's constant of an ordered liquid is $\Delta_{vap} S(T_b)/R > 12$. The value for water is 13.15, but it shares this property with a great many other liquids that are ordered (Marcus 1992). However, water vapour at the boiling point is associated and thus has a lower entropy than it would have in the ideal gas state. For a more refined criterion for order possible association in the vapour phase is taken into account according to Marcus (1996) by equating order with $\Delta\Delta_v S/R$. This eliminates liquids, such as normal alkanes, that are deemed to be unordered and vapour phase association:

$$order = \Delta\Delta_v S/R = [\Delta_v S_{liquid}(T, P^\circ) - \Delta_v S_{alkane}(T, P^\circ)]/R + (P^\circ/R)\mathrm{d}(B_{liquid} - B_{alkane})/\mathrm{d}T \quad (1.7)$$

In this expression $\Delta_v S(T, P^\circ) = S(\text{vapour}, T, P^\circ) - S$ (liquid, T, P°) is the molar entropy difference between the vapour and the liquid at the standard pressure $P^\circ = 0.1$ MPa and the temperature of interest, T. The comparison of $\Delta_v S(T, P^\circ)$ of the test liquid is with this quantity of a saturated alkane having the same skeleton as the molecules of the liquid. For this purpose, non-carbon atoms are converted: halogen $-$X to $-CH_3$, ethereal oxygen $-O-$ to $-CH_2-$, carbonyl $>C=O$ to $-CH(CH_3)-$, etc. as appropriate. The temperature derivative of the difference between the second virial coefficients B of the vapours of the liquid of interest and of the alkane takes into account association of the vapour.

This criterion for the existence of "order" in a given liquid is $\Delta\Delta_v S/R > 2$, and at 25 °C water has $\Delta\Delta_v S/R = 7.94$, larger than many liquids deemed structured by any criterion (Marcus 1998). However, this quantity is by no means larger than for all structured liquids, see Table 1.5. When the "order density" in a structured liquid is expressed by division of $\Delta\Delta_v S$ by V, the molar volume of the liquid, water ($\Delta\Delta_v S/V = 3.23$ J K^{-1} cm^{-3}) becomes quite similar to 1,2-ethanediol (3.15) and 2-ethanolamine (3.21), having a somewhat lower value than glycerol (4.20), but a higher one than formamide (1.58) and methanol (1.28).

The molar heat capacity at constant pressure of a liquid, $C_P(l)$, is the amount of energy that must be invested in order to increase its temperature. This energy is consumed by re-ordering the liquid molecules in addition to that going into internal degrees of freedom. The latter amount of energy is taken into account by subtraction of the ideal gas quantity. Hence, a further measure of the order in liquids is the heat capacity density (Marcus 1996):

$$order = \frac{\Delta C_P}{V} = \frac{C_P(1) - C_P(\text{i.g.})}{V(1)} \quad (1.8)$$

Structured liquids have values of $(\Delta C_P/V)$/J K^{-1} cm$^{-3} > 0.6$, that for water being 2.32, larger than the values of some other structured liquids, see Table 1.5. This is due to the small molar volume of water and mainly to the extensive hydrogen bonded network that absorbs the energy.

Another measure for order in a liquid is the Kirkwood dipole orientation correlation parameter (KDOCP) g, but this pertains only to dipolar liquids:

$$g = \frac{(9k_B\varepsilon_o/N_A)\,VT\mu^{-2}\left(\varepsilon_r - 1.1{n_D}^2\right)\left(2\varepsilon_r + 1.1{n_D}^2\right)}{\varepsilon_r\left(2 + 1.1{n_D}^2\right)^2} \tag{1.9}$$

Here μ is the dipole moment of the molecules of the liquid, ε_r is the relative permittivity of the liquid, and ${n_D}^2$ is the square of its refractive index at the frequency of the sodium D-line. The theoretical expression requires ${n_\infty}^2$, the square of the infinite frequency refractive index to represent the polarizability of the molecules of the liquid, but $1.1{n_D}^2$ is a good empirical approximation of it. The KDOCP of a non-structured liquids is ideally $g = 1$, but in practice $g = 1.0 \pm 0.3$ holds for such liquids, whereas for ordered liquids $g > 1.7$ (Marcus 1992). Water has the value $g = 2.90$ at 25 °C, comparable with other hydrogen-bonded liquids, see Table 1.5, but by no means outstandingly large (compare, e.g., N-methylformamide with $g = 3.97$) (Marcus 1992).

The "openness" of a liquid measures its free volume, which is the difference between its bulk molar volume and its intrinsic molar volume. The latter can be expressed as the van der Waals volume of its molecules per mole. A liquid cannot be compressed by an external pressure to have a lower molar volume. The van der Waals molar volume of water is $V_{vdW} = 12.4\ \text{cm}^3\ \text{mol}^{-1}$ at 25 °C. Another measure of the intrinsic volume of a liquid takes into account the exclusion volume adjacent to a given molecule, where another particle cannot penetrate because the crevices between the peripheral atoms are smaller than any atomic size. This is the McGowan intrinsic volume, which for water is $V_X = 16.7\ \text{cm}^3\ \text{mol}^{-1}$ (Abraham and McGowan 1987). Both of these measures of the intrinsic molar volume of water are considerably smaller than its molar volume at 25 °C, $V = 18.07\ \text{cm}^3\ \text{mol}^{-1}$, (Marcus 1998) leaving some free volume. The fractions of free volume according to these two measures are $(1 - V_{vdW}/V) = 0.314$ and $(1 - V_X/V) = 0.076$. The former is less relevant for the discussion of solutions, because it does not allow for the exclusion volume.

Contrary to expectations from the open tetrahedral hydrogen-bonded structure of ice, liquid water is a close-packed rather than an open liquid. It shares this property with 1,2-ethanediol, glycerol, and formamide, among common solvents, see Table 1.5. These four liquids have $(1 - V_X/V) < 0.1$, whereas most other common solvents for ions have larger values of this quantity. Liquids that have large fractions of free volume, i.e., are "open", are quite compressible, and there exists a moderate positive correlation of $(1 - V_X/V)$ with the isothermal compressibility. Water shares a low isothermal compressibility, $\kappa_T = 0.457\ \text{GPa}^{-1}$ at 25 °C, with the above named "low-openness" solvents for which $\kappa_T < 0.5\ \text{GPa}^{-1}$, whereas for other common solvents the values range from 0.524 (dimethylsulfoxide) to 1.706 (*n*-hexane) (Marcus 1998).

Over the temperature range of the existence of water as a liquid at the standard pressure $P^\circ = 0.1$ MPa, i.e., at $0\ ^\circ\text{C} \le t \le 100^\circ\text{C}$, the structuredness of water diminishes with rising temperatures, as is shown in Table 1.6 (Marcus 2009). This feature, common to other solvents as well, is due to the increased order-destroying

Table 1.6 The temperature dependence of the "structuredness" of water

t(°C)	*Stiffness* $(\delta_H{}^2 - P_i)$/MPa	*Order* $\Delta\Delta_{vap}S/R$	$\Delta C_P/V$ (J K^{-1} cm^{-3})	KDOCP (g)	*Openness* $(1 - V_X/V)$
0		8.35	2.37	2.96	0.0731
10	2,284	8.17	2.34	2.94	0.0733
20	2,179	8.01	2.32	2.91	0.0747
25	2,129	7.94	2.32	2.90	0.0757
30	2,078	7.87	2.31	2.89	0.0770
40	1,975	7.74	2.29	2.86	0.0802
50	1,877	7.63	2.28	2.83	0.0841
60	1,782	7.52	2.27	2.81	0.0886
70	1,686	7.43	2.26	2.78	0.0936
80	1,599	7.35	2.25	2.76	0.0991
90	1,508	7.28	2.24	2.73	0.1051
100	1,416	7.22	2.23	2.71	0.1116

thermal motion of the molecules and the general thermal expansion (above 4 °C). Whereas the *stiffness* decreases by 47 % between 25 and 100 °C and the *openness* increases by 50 % over this temperature range, the other measures of the 'structuredness" change (diminish) only much more moderately: the *order* by 10 %, the heat capacity density by 4 %, and the KDOCP g by 7 %. The *stiffness* and *openness* are governed mainly by the thermal expansion, whereas the other measures depend more on the strength and extent of the hydrogen bonding, which change only moderately with the thermal motion of the water molecules, see below.

With rising pressures at a given temperature water compresses and its density increases, so that its openness diminishes. At 25 °C but under 100 bar (10 MPa) pressure $(1 - V_X/V) = 0.0743$ compared with 0.0757 at ambient pressure. It decreases to 0.0578 at 500 bar and to 0.0402 at 1000 bar (0.1 GPa). The "free volume" practically vanishes at very high pressures ($\geq$2.4 GPa at 25 °C), water being then "completely" compressed. As will be discussed in Chap. 2, such pressures are prevailing in the vicinity of ions, due to their extremely large electric fields.

1.1.3 The Hydrogen Bonded Structure of Water

The "structuredness" of liquid water described in Sect. 1.1.2. is qualitatively ascribed there to its extensive hydrogen bonded network. This network of liquid water resembles the low-density tetrahedral arrangement in ice, but with a certain fraction of the number of water molecules being in interstitial positions. Mixture models for water have been suggested over the years, which refer either to at least two distinct species or domains, or to a continuum of species with different hydrogen bonding characteristics. Röntgen (1892) was possibly the first to propose a two-state model for liquid water: a low-density ice-like one and a high density domain of interstitial water

molecules. The former has nearly fully hydrogen bonded water molecules, each donating two HBs to and accepting two HBs from their neighbours. The latter domains consist either of individual molecules with few HBs each or of oligomeric clusters. Such a model was given a detailed statistical thermodynamic basis by Ben-Naim (1972).

Robinson and coworkers (Vedamuthu et al. 1994, Cho et al. 2002) have subsequently developed this two-state model of water (bulky and dense) with respect to its volumetric properties at temperatures that vary from −30 to +100 °C and at pressures in the range of 0.1 MPa to 0.77 GPa. Such models depend on the consideration of the hydrogen bonding in liquid water in comparison with the various polymorphs of solid water, i.e., of ice. Each of the two states is represented by several hydrogen bonding schemes. Thus, the bulky one is not confined to ice Ih that has exactly tetrahedral O···O···O angles of 109.5 ° and next-nearest oxygen atom distances of 0.45 nm, but allows for some bending of this angle and shortening of the distance. The dense state does not consist of interstitial molecules only but involves domains where the O···O···O angles are severely bent, down to even 80 °, leading to next-nearest oxygen atom distances of 0.32 nm.

According to this two-state model, at the ambient pressure of 1.01325 bar (≈0.1 MPa) the fraction of the bulky state decreases from 0.4746 at 0 °C via 0.3855 at 25 °C to 0.2705 at 70 °C, its corresponding molar volumes being 20.017, 20.242, and 20.645 $cm^3\ mol^{-1}$. The fraction of the dense state makes up the rest to unity and the molar volumes of the dense state are 16.112, 16.705, and 17.594 $cm^3\ mol^{-1}$ at the respective temperatures (Cho et al. 2002). It was expected that other forms of broken down hydrogen bonded structures are present above 70 °C. At higher pressures the fraction of the bulky state is reduced, of course, the more the lower the temperature. The molar volumes of the two states also diminish with higher pressures, the more so for the bulky state than for the dense state, as expected, and for the latter being more sensitive to the temperature. The temperature and pressure variation of other bulk properties of water, such as the viscosity and the refractive index, could also be interpreted in terms of the two-state model and the respective fractions of these two states.

According to this model a major portion of liquid water, nearly 40 % at ambient conditions, is made up of the bulky domains, and this is in accord with the fact that the coordination number of a water molecule is somewhat larger than four. Tanaka (2000) argued that the major portion should be the dense domains, called 'background water', disordered and with few HBs, and only a minor portion is what he called 'locally favoured structures' of high symmetry and possibly an 'octameric unit' of hexagonal ice (ice Ih) with a void core. Such a 'locally favoured structure' has a volume larger than 'background water' by $\Delta V \sim 10\ cm^3\ mol^{-1}$ and an energy larger by $\Delta E = 15\ kJ\ mol^{-1}$. The average fraction of the locally favoured structures is $8 \times 10^{-5} \exp[(\Delta E - P\Delta V)/RT]$, i.e., quite small, about 4 % at ambient conditions. Its temperature dependence is able, however, to explain quantitatively the anomalous density maximum of water, the minima in the isothermal compressibility and heat capacity, and the anomalous pressure dependence of the viscosity, with the use of only a few fitting parameters (Tanaka 2000).

Rull (2002) recently provided Raman spectroscopic evidence supporting the mixture model, a major fraction consisting of domains with linear HBs in a tetrahedral like configuration, the other of interstitial molecules, with either bifurcated or else weak or no HBs. Soper (2010) commented on the two-state model that the different domains must be very short lived, in view of the rapid diffusion of the water molecules, one of them moving over 150 molecular diameters away in 1 ms.

Ordinary structural investigations of water using neutron or x-ray scattering provide the pair correlation functions of pairs of atoms (see above). The hydrogen bonding that takes place is inferred from the atom pair distances and the angles of the O–H···O configurations. Specific experiments aimed at the investigation of the HB network itself have recently been reported by two research groups who applied to liquid water x-ray absorption and x-ray Raman scattering at the oxygen K edge. The absorption spectrum is characterized by a small pre-edge at 535 eV, a main peak around 538 eV and a post-peak shoulder near 541 eV. The interpretation of these features and the temperature dependence of the corresponding intensities in terms of the hydrogen bonding has been controversial, however.

The group around Nilsson contented that the data point to the presence of one strong HB donated by each water molecule that accepts a strong HB from a neighbouring water molecule, the network being maintained by further weak HBs with bent O–H···O configurations (a 'chain and rings' model) (Näslund et al. 2005). The group around Saykally (Smith et al. 2004, 2006) preferred the interpretation in terms of fully coordinated ("ice-like" model, with two donor and two acceptor HBs) and distorted (broken-donor) configurations, responsible for the post-edge and pre-edge absorptions, respectively. The latter view is compatible with the two-state notion of Cho et al. (2002) in that a 20–25 % reduction in the bulky domain occurs over a 37 K temperature increase around 0 °C, and with results of molecular dynamics (MD) simulations. A more recent paper from the Nilsson group (Tokushima et al. 2008) using x-ray emission rather than absorption reverted to a two-state (tetrahedral and strongly distorted) description of liquid water near room temperature, at a ratio near 1:2, not too different from the value given above from the density data: 1:1.59 at 25 °C (and it is 1:2.04 at 45 °C) (Cho et al. 2002).

The x-ray absorption data were in all cases supported by computer simulations. The results of Prendergast et al. (2005, Prendergast and Galli 2006) on the electronic structure showed reasonable results when a classical potential was applied to the so-called the "standard" model, i.e., the tetrahedral "ice-like" model for liquid water at ambient conditions (Soper 2000). This has $\chi = 3.6$ HBs per each molecule, or, since two molecules are involved in each HB, there are on the average $\langle n_{\mathrm{HB}} \rangle = 1.8$ HBs donated per water molecule in liquid water at ambient conditions. Further calculations by Wang et al. (2006) confirm this view of the water hydrogen-bonded network, with $\chi = 3.2 \pm 0.1$ HBs per water molecule, about two thirds of them belonging to the double-donor category.

It is instructive to consider the relative number of HBs in which the water molecules are donors (d_n) and those in which they are acceptors (a_n). A tetrahedrally fully hydrogen bonded molecule (as in ice) would be $\mathrm{a}_2\mathrm{d}_2$ and in the case of bifurcated HBs n may be as large as 3. Simulation of 3,456 water molecules at 24 °C

and a density of 997 kg m^{-3} (Malenkov 2006) yielded 50.7 % a_2d_2, 13.6 % a_3d_2, 12.9 % a_1d_2, 7.1 % a_2d_3, and 6.6 % a_2d_1, with smaller fractions ($\leq$ 2.4 %) of other HB configurations, but none of water molecules with no HBs at all. These results depend, of course, on the criteria used to define the hydrogen bonding: $d_{O-O}/nm \leq 0.33$ and $d_{O-H}/nm \leq 0.26$. On the other hand, rather than having $>$ 77 % of the molecules as double donors (d_2), an interpretation of recent x-ray absorption and x-ray Raman spectroscopic results shows that a typical water molecule is a single donor (d_1) one (Näslund et al. 2005).

Since the average number of HBs per water molecule present in the liquid is a very useful measure for the structuredness of water, an important issue in this respect is the definition of an "intact" HB as distinct from a "broken", "bent", or non-existent one. This issue is crucial for the interpretation of computer simulation results for whatever potential function of water is being employed.

Xenides et al. (2006) applied recently an ab initio Hartly-Fock level quantum mechanical/molecular mechanical (QM/MM) MD simulation of liquid water at 298 K and ambient pressure, involving 500 water molecules. The resulting radial distribution functions agreed well with experimental neutron diffraction and x-ray absorption and Raman diffraction data. In this manner they could describe the first and second solvation shells of any central water molecule, having coordination numbers ranging from 3 to 6 and centering around 4 (53 % occupancy,) and ranging from 16 to 24 and centering around 20 (21 % occupancy), respectively. The geometric criteria for the existence of a HB between adjacent water molecules that emerged from this simulation are:

1. the angle of the O–H$\cdots$O configuration has to be $\theta \geq 100°$,
2. the distance between two oxygen atoms of neighbouring water molecules has to be $0.25 \leq d_{O-O}/nm \leq 0.35$, and
3. the HB distance has to be $0.15 \leq d_{O-H}/nm \leq 0.25$.

Thus, the HBs can be bent to a considerable degree but still be reckoned as being intact, provided the other criteria are adhered to. According to these criteria each oxygen atom of a water molecule accepts on the average 1.96 HBs from its neighbours, but also donates via its covalently bound hydrogen atoms further HBs. The peak of the O–O–O angle distribution is at 101°, smaller than the regular tetrahedral angle of 109.5°, so that the average tetrahedral structure is distorted. Subsequent considerations from the same group by Rode (2007, personal communication) distinguished between "strong" HBs, characterized by $d_{O-H}/nm \leq 0.21$, of which there are 1.81 per water molecule, and "weak" HBs up to $d_{O-H}/nm \approx 0.23$, of which there are 1.29, to produce altogether $\chi = 3.1$ bonds on the average per water molecule, a number not very sensitive to θ, the O–H$\cdots$O angle.

The Raman intensities of the O–D stretching vibration in dilute HOD in H_2O was employed to provide information on the energy difference between "strong" and "weak" HBs in liquid water (Walrafen 2004). The derivative at a given wavenumber ν_j of the Raman scattering intensity I_j with respect to the reciprocal of the temperature yields the energy $E_j = -R[\partial \ln I_j/\partial(1/T)]_P$. Short, "strong", and linear HBs are characteristic of Ida ice at 4 K, measured at $\nu_j = 2{,}440\ cm^{-1}$. Long, "weak",

and bent HBs are characteristic of supercritical HDO in H_2O at 0.9 g cm^{-3} density and 673 K, and are measured at ν_j 2,650–2,675 cm^{-1}. The difference in energy is 21.3 ± 2.1 kJ (mol HBs)$^{-1}$ (Walrafen 2004), but this appears to be excessive in view of the total energy of hydrogen bonding in water inferred from the sublimation energy of ice. In fact, a much smaller value was obtained by other spectroscopic results and their temperature dependence. These were interpreted in terms of structures with mainly tetrahedral hydrogen bonding though with long and bent HBs included ("ice-like" model). The energy difference between the "strong" and "weak" HBs, obtained from data in supercooled water at − 22 °C up to water at 15 °C, is 6.3 ± 2.1 kJ (mol HBs)$^{-1}$ (Smith et al. 2004), a more plausible value.

Kumar et al. (2007) discussed in detail the criteria for HBs in water, considering both geometrical and energetic ones. They suggested somewhat more restrictive geometrical criteria than those described above:

1. the angle of the O–H· · ·O configuration has to be $\theta \geq 130$ °, and
2. the distance between two neighbouring oxygen atoms has to be $d_{O-O}/\text{nm} \leq 0.330$, and
3. the HB distance has to be $d_{O\cdots H}/\text{nm} \leq 0.241$,
   but also specified the energetic criterion:
4. the interaction energy between the hydrogen bonded water molecules should be more negative than − 12.9 kJ mol^{-1}.

Application of the criteria (1)–(4) in molecular dynamic calculations employing the SPC/E water model for obtaining the numbers of HBs per water molecule χ at 300 K yielded between 3.2 and 3.4 such bonds. Double-donor water molecules provided according to criterion (3) 1.66 HBs, the rest coming from acceptor molecules (Kumar et al. 2007). These authors also considered electronic structure definitions for the occurrence of HBs between water molecules. Considering the electron donor-acceptor nature of the HB (rather than the hydrogen atom donor-acceptor mode discussed above), the relevant molecular orbital is the $\sigma_{OH}{}^*$ antibonding one of the acceptor that is empty in monomeric water. The occupancy of this orbital, once HBs are formed in liquid water, is the criterion to be used:

5. the occupancy of the σ^* orbitals has to be ≥ 0.0085.

This criterion is reasonably compatible with the former ones, leading to $\chi = 3.4$ HBs per water molecule. The dynamics of the hydrogen bonding also plays an important role, as discussed in Sect. 1.1.4.

To these criteria may be added a dynamic hydrogen bonding one, considering for how long before a given moment and after it two water molecules fulfilled the geometric and energetic criteria. If the criteria are met only very transiently, a HB is not considered to exist (Malenkov et al. 1999). This criterion may be formulated as:

6. The geometric and energetic criteria are met together for the duration of at least 0.2 ps.

On the whole, the formation and breaking of HBs in liquid water is a cooperative phenomenon as discussed by Luck (1998). If a HB is being formed between two

water molecules not so bonded previously, other HBs are preferably formed in their vicinity. On the other hand, if a HB is broken by the thermal movement of the water molecules that are partners to this bond, other HBs in the vicinity are also disrupted. This is because a HB induces enhanced partial positive charges on the hydrogen atoms bonded covalently to the oxygen atom to which the HB is donated and reduces the partial negative charge of the oxygen atom that donates this HB.

Long ago Bernal and Fowler (1933) introduced the concept of the 'structural temperature' of aqueous solutions. This is that temperature, T_{str}, at which pure water would have effectively the same inner structure as the water in a solution at the temperature T. They suggested that T_{str} could be estimated from viscosity, x-ray diffraction, Raman spectroscopy, etc., but did not provide explicit methods and values. The D_2O vs. H_2O isotope effects on x-ray Raman spectra indicate (Bergmann et al. 2007) that D_2O has a structural temperature lower by 20 K than H_2O at ambient conditions. This is ascribed to the inherently stronger hydrogen bonding in the heavy water. The concept of structural temperature has by now been practically abandoned, however.

The number of HBs present per water molecule in liquid water was obtained from both x-ray absorption and Raman scattering experiments and computer simulations for room temperature, although the experimental studies included sub-cooled water and water heated to 90 °C. Different approaches to ascertain the mean number of HBs in which a water molecule in liquid water is engaged are based on thermodynamic data and statistical thermodynamics. Recently, Fisenko et al. (2008) compared the reduced molar volumes of water and argon and argued that the difference, due to the hydrogen bonding, is related to the number of the HBs per water molecule. The reduced values of the volumes, v_r, were not with respect to the critical volumes but normalized to the reciprocal of the number densities 0.052613 nm^{-3} for water and 0.079033 nm^{-3} for argon. The comparison then yielded the linear dependence $v_{r(W)}(T_r) = 0.84 v_{r(A)}(T_r) + 0.028(1 - 0.83T_r)$, where T_r is the reduced temperature with respect to the critical one of water. This then led to:

$$\chi = 4(1 - 0.83T_r) \tag{1.10}$$

The resulting values are considerably smaller than obtained by the scattering, spectroscopic, and computer simulation methods described above: the value resulting from Eq. (1.10) of $\chi = 2.47$ at 25 °C is to be compared with 3.1–3.6 from these methods. The values of χ according to Fisenko et al. (2008) dropped to 2.09 and 1.88 at 100 and 140 °C, respectively. Lagodzinskaya et al. (2002) used the temperature dependent ^1H NMR chemical shifts of liquid water compared with monomeric water (dilute water vapour), $\Delta\delta_{HB}$ (ppm), and the HB energy, ΔE_{HB} to calculate the mean number of HBs in water. The resulting values, read from a figure, decrease from 3.96 at 0 °C through 3.75 at 25 °C to 3.12 at 100 °C.

Another approach was provided by Marcus and Ben-Naim (1985) 24 years ago, based on an earlier work of Ben-Naim (1975) and the following ideas. The molecular parameters of light and heavy water are very similar (Table 1.1), except those that depend on the mass (moments of inertia) (Marcus 1998). For H_2O and D_2O molecules the bond lengths O–H and O–D are 0.09572 and 0.09575 nm, the bond angles H–O–H

and D–O–D are 104.523 and 104.474 degrees, for a pair of gaseous molecules the lengths of the HBs O–H···O and O–D···O are 0.2765 and 0.2766 nm, the dipole moments are 1.834 and 1.84 D (1 D = 3.33564 × 10^{-30} C m), and the polarizabilities are 1.456 × 10^{-3} and 1.536 × 10^{-3} nm^3 respectively. However, the strengths of the O–H···O and O–D···O HBs in these two kinds of water differ. A comparison of the properties of H_2O and D_2O as isolated molecules (vapours), liquids, and crystalline solids (ices) is thus the basis for obtaining the extent of hydrogen bonding in liquid water.

When ice is sublimed, all the HBs between the water molecules are broken. Each water molecule in ice is hydrogen bonded to four neighbouring molecules, and two molecules are involved in each HB. When a mole of ice sublimes to form a dilute water vapour, which is assumed to be an ideal gas, $2N_A$ HBs are therefore completely broken. On comparison of the sublimation energies of the ices, the energy contributions of the multipole interactions and internal bond vibrations of the H_2O and D_2O ices are assumed to cancel out, in view of the similarities of the properties of the individual water molecules noted above. Therefore, the difference between the molar sublimation enthalpies of the D_2O and H_2O ices measures the difference $\Delta^{HD}e_{HB}$ in the strength (energy) e_{HB} of the HBs per mole of HBs.

$$\begin{aligned}\Delta^{HD}e_{HB} &= e_{HB}(D_2O) - e_{HB}(H_2O)\\ &= -[\Delta_{subl}H(D_2O, cr) - \Delta_{subl}H(H_2O, cr)]/2\\ &= [(859 \pm 314) - (4.721 \pm 0.828) \times 10^5/(T/K)]\ J\ mol^{-1}\end{aligned} \tag{1.11}$$

The numerical expression results from the temperature dependence of the vapour pressures of the ices over the range $-40°C \le t \le 0\ °C$, reported by Pupezin et al. (1972). It is then assumed that Eq. (1.11) can be extrapolated to higher temperatures in the range of existence of liquid water. An estimate, $\Delta^{HD}e_{HB} \approx -929\ J\ mol^{-1}$ at $T = 298.15$ K that has been employed (Marcus 1986, 1994, 2008) is within the range of values provided by Eq. (1.11).

The next step considers the difference in the molar Gibbs energy of condensation of a water molecule of each isotopic kind from the vapour into its corresponding liquid. This process involves the addition of one water molecule from a fixed position in the vapour to a fixed position in the liquid containing already N water molecules. This difference is proportional to the average number of prevailing HBs, $\langle n_{HB}{}^{HD}\rangle$, the proportionality factor being the difference in the hydrogen bonding energy:

$$\Delta^{HD}\Delta_{cond}G = \Delta^{HD}e_{HB}\langle n_{HB}{}^{HD}\rangle \tag{1.12}$$

Note that $\langle n_{HB}{}^{HD}\rangle$ pertains to the average over all the water molecules, each HB involving two water molecules. However, the mean number of HBs per individual water molecule is $\chi = 2\langle n_{HB}{}^{HD}\rangle$. The superscript^{HD} refers to 'mean water', assuming $\langle n_{HB}{}^{HD}\rangle = 0.5[\langle n_{HB}(H_2O)\rangle + \langle n_{HB}(D_2O)\rangle]$. The molar condensation Gibbs energy of each of the two kinds of water is obtained experimentally from the molar masses M, the saturated vapour pressures p_σ, and the densities ρ:

$$\Delta_{cond}G = RT\ln(p_\sigma M/RT\rho)_{D_2O} - RT\ln(p_\sigma M/RT\rho)_{H_2O} \tag{1.13}$$

Table 1.7 The average number of hydrogen bonds per water molecule at ambient pressures according to various approaches

Approach	Temperature (°C)	$\chi = 2\langle n_{HB}\rangle$	Reference
X-ray absorption	Ambient	3.6	Prendergast et al. 2005; Prendergast and Gali 2006
X-ray absorption	Ambient	3.2 ± 0.1	Wang et al. 2006
MM/MD simulation	Ambient	3.1 (1.81 + 1.29)[a]	Rode 2007
SPC/E simulation	Ambient	3.4 (1.66 + 1.74)[b]	Kumar et al. 2007
Simulation	24	4.25	Malenkov 2006
Reduced volumes	25, 100	2.47, 2.09	Fisenko et al. 2008
NMR chemical shifts	25, 100	3.75, 3.12	Lagodzinskaya et al. 2002
D_2O/H_2O comparison	25, 100	3.50[c], 2.45[c]	Marcus 1985

[a] Strong and weak hydrogen bonds
[b] Double-donor and other hydrogen bonds
[c] Prorated from $\langle n_{HB}{}^{HD}\rangle$ according to the difference between D_2O and H_2O

The average number of HBs per water molecule for liquid 'mean water', $\langle n_{HB}{}^{HD}\rangle$, as a function of the temperature is then obtained from a combination of Eqs. (1.11)–(1.13) and the respective data.

A refinement, depending on the addition of data for tritiated water, T_2O, enabled the evaluation of the individual $\langle n_{HB}(H_2O)\rangle$ and $\langle n_{HB}(D_2O)\rangle$ values (Marcus 1985). The latter is larger than the former, by 8 % at 5 °C and up to by 17 % at 100 °C. This is in conformity of the structural temperature of D_2O being lower than that of H_2O (Bergmann et al. 2007) (see above). It is indeed generally agreed that heavy water, D_2O, is more strongly hydrogen bonded (structured) than light water, H_2O.

Table 1.7. summarizes the values of n_{HB} for water under ambient conditions resulting from the various approaches presented above.

1.1.4 The Dynamics of Water Molecules

The dynamics of the molecules in liquid water involve their translation, measured by the self-diffusion coefficient (see Table 1.2), their rotational re-orientation, involving the breaking and re-making of HBs, and the exchange of protons between the molecules. From the self-diffusion coefficient D_W is follows that at ambient conditions a water molecule moves the distance of some 150 molecular diameters, d_W, away from its original position in 1 ms (Soper 2010). The average residence time of a water molecule in the immediate vicinity of another one is obtained from the Einstein–Smulochovski relationship, $\tau_W = d_W{}^2/2D_W = 17$ ps at 25 °C. This value is 100 times smaller than the value reported by Samoilov (1957), apparently from similar data.

The intra-molecular vibrations, including librations, of the O–H (respectively, O–D) bonds present information on the motions of the water molecules. The HB

dynamics in liquid water can be traced back to the flickering cluster model of Frank and Wen (1957). It involves short lived hydrogen bonded clusters with several intermolecular HBs for each water molecule surrounded by non- or single-hydrogen-bonded water molecules, but see the comments of Soper (2010) on this. It has been studied by means of several experimental techniques as well as computer simulations. The former include dielectric spectroscopy, NMR signal relaxation, and vibrational spectroscopy. The latter are based on MD simulations enhanced by ab-initio quantum mechanical calculations. What is actually measured and simulated are the re-orientation (molecular rotation) relaxation times. The re-orientation of a water molecule involves the breaking and re-formation of HBs, so that in fact the dynamics of the hydrogen bonding is reported.

For the dielectric re-orientational times of the water molecules, the Debye relaxation expression holds:

$$\begin{aligned}\varepsilon(\omega) = \varepsilon(\infty) + \sum\nolimits_{\mathrm{j}} (\varepsilon_{\mathrm{j}} - \varepsilon(\infty))/[1 + (\mathrm{i}\omega\tau_{\mathrm{j}})^{1-\alpha \mathrm{j}}]^{\beta_{\mathrm{j}}} \approx \varepsilon(\infty) \\ + \sum\nolimits_{\mathrm{j}} (\varepsilon_{\mathrm{j}} - \varepsilon(\infty))/[1 + (\mathrm{i}\omega\tau_{\mathrm{j}})]\end{aligned} \tag{1.14}$$

Here the complex permittivity ε, related to the ability of the dipoles of water to re-orient in the direction of the electric field, is expressed as a function of the frequency ω of the field. At infinite frequency the dipoles cannot any more follow the alternation in the field direction and only the atomic and electron polarizations are relevant, given by the square of the refractive index at infinite frequency, $\varepsilon(\infty)$. The relaxation times τ_{j} express the average time the dipole re-orientation requires. The sum extends over as many independent relaxation steps j as are required and the second expression on the right hand side, assuming that all $\alpha_{\mathrm{j}} = 0$ and all $\beta_{\mathrm{j}} = 1$, was found to be a good approximation. Furthermore, a relationship between the re-orientation relaxation time, τ_θ, if only one relaxation time is required, and the temperature dependent viscosity of the fluid was shown to hold according to the Stokes–Einstein–Debye equation. In the case of dipolar aprotic solvents, i.e., those devoid of hydrogen bonding, the relaxation time pertains to individual molecules and is

$$\tau_\theta = \frac{4\pi r^3 \eta}{k_{\mathrm{B}} T} \tag{1.15}$$

where r is the molecular radius. However, the dynamics of hydrogen bonded solvents, such as water, is governed by the cooperative relaxation of their hydrogen bonded networks (Buchner and Hefter 2009).

Values of the dielectric relaxation times of water were determined already long ago. According to Collie et al. (1948) the values of τ_θ decrease from 17.7 ps at 0 °C to 3.23 ps at 75 °C, and $\tau_\theta = 8.28$ ps at 25 °C was reported by Haggis et al. (1952). Barthel et al. (1990) increased the available frequency to 89 GHz and found two distinct dielectric relaxation times: $\tau_{\theta 1} = 8.32$ ps and $\tau_{\theta 2} = 1.02$ ps at 25 °C. A further increase in the available frequency to 410 GHz led to more accurate values: $\tau_{\theta 1} = 8.38$ ps and $\tau_{\theta 2} = 1.1$ ps at 25 °C, with data also reported for 0.2 °C $\leq t \leq$ 35 °C

(Buchner and Hefter 2009). The former relaxation time can be attributed to a concerted reorientation of several dipoles in a water cluster, due to the co-operative nature of the hydrogen bonding, and the latter, shorter, re-orientation time to the movement of a single water molecule, but its relaxation time was later revised on measurements from 410 GHz to 18 THz frequencies to $\tau_{\theta 2} = 0.42$ ps (Fukasawa et al. 2005). Malenkov (2006) reviewed the temperature dependence of y, representing the longer $\tau_{\theta 1}$ values, between − 23 and 97 °C, and described it by:

$$y = y_0 \left[\frac{(T - T_s)}{T_s} \right]^{\gamma} \tag{1.16}$$

with $y_0 = 1.45$ ps, $T_s = 228$ K, and $\gamma = 1.55$. The values of $\tau_{\theta 1}$ diminish with increasing pressures. It should be stressed that the re-orientation relaxation times measured by dielectric relaxation pertain to the rotation of the *dipoles* of the water molecules.

NMR longitudinal relaxation times T_1 are related to the rotational dynamics (Ropp et al. 2001):

$$1/T_1 = \left[3\pi^2 (2I + 3)/10I^2(2I - 1) \right] {\chi_q}^2 \left(1 + \eta^2/3 \right) \tau_r \tag{1.17}$$

Here I is the spin number of the relaxing nucleus ($I = 1$ for ^{2}H and $I = 5/2$ for ^{17}O), χ_q is the quadrupole coupling constant, η is the asymmetry parameter, and τ_r is the rotational correlation time. For deuterium ${\chi_q}^2(1 + \eta^2/3) = 68.86(T/\mathrm{K}) + 42.64$ and for ^{17}O it is $0.0788(T/\mathrm{K}) + 76.04$ (Ropp 2001), so that τ_r can be directly derived from T_1 by means of Eq. (1.17).

Jonas et al. (1976) measured the spin-lattice relaxation times T_1 for both H_2O and D_2O at three temperatures (10, 30, 90 °C) over a large pressure range, up to 900 MPa by means of pulsed NMR. The resulting re-orientational relaxation times τ_r at ambient pressure, 0.1 MPa, were 3.63, 2.07, and 0.85 ps for H_2O at the three temperatures and 4.76, 2.51, 0.86 ps for D_2O. The isotope effect thus diminishes with increasing temperatures. Hardy et al. (2001) have more recently re-measured the isotope effect from NMR relaxation times. The values were only reported in a plot of the logarithm of the rotational diffusion coefficients D_{rot} vs. the reciprocal temperatures between 10 and 80 °C. The correlation times, τ_c in ps, are related to the D_{rot} in rad^2 ps^{-1} as $\tau_r = 1/6D_{rot}$, and the values are for H_2O 2.22, 1.39, 1.00, and 0.51 ps at 10, 25, 40 and 80 °C, compared with 2.87, 1.85, 1.41, and 0.62 ps at these temperatures for D_2O. Ropp et al. (2001) used 99 % deuterium-enriched water at 2–77 °C to obtain the rotational correlation time for the O–D bond vector, ranging from 5.8 ps through 1.94 ps (at 27 °C) to 0.86 ps over this temperature range, whereas the out-of-plane vector correlation time is from 4.4 ps through 1.24 ps (at 27 °C) to 0.64 ps over this range, i.e., only some 70 % of the former times. This was interpreted as an indication of the anisotropic rotation of the water molecules. It should be noted that the rotational relaxation times measured by NMR pertain to the rotation of the *mass vector* of the water molecules, not directly their dipole vectors.

Krynicki (1966) related the longitudinal relaxation times T_1 of ^{1}H NMR measurements at 28 MHz in air-free water over the temperature range $0\ ^\circ\mathrm{C} \le t \le 75\ ^\circ\mathrm{C}$ to the dielectric relaxation times, the product it is independent of the temperature:

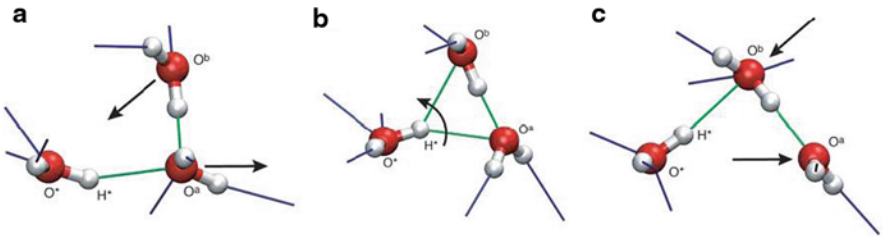

Fig. 1.3 Schematics of the rotation of hydrogen bonded water molecules. (Reproduced from Laage and Hynes (2006a) with kind permission of © Elsevier)

$(T_1\ \tau_\theta)^{-1} = 3.37 \times 10^{10}\ s^{-2}$ to within ± 3 %. The product $(T_1\ \tau_\theta)^{-1}$ for D_2O was obtained from quadrupole relaxation ^2H NMR by Woessner (1964); it is $4.79 \times 10^{10}\ s^{-2}$.

The use of vibrational spectroscopy as a probe for the dynamics of liquid water was recently reviewed by Bakker and Skinner (2010). For both infrared and Raman spectroscopic studies, the use of dilute HOD in either H_2O or D_2O is not only useful but practically mandatory, so that the stretching frequencies of O–D bonds in H_2O and of O–H bonds in D_2O are not coupled to other vibrations and are independently measurable. The Raman line shapes indicate that 10–15 % of the time a given hydrogen atom is *not* hydrogen bonded. The spectral diffusion is the fluctuation in time of the stretching frequency. Ultra-fast three-pulse infrared vibrational spectroscopy showed for the stretching frequency an initial inertial time decay within 50 fs (or 70–80 fs (Elsaesser 2009)), then an under-damped oscillation at about 180 fs, and a long time decay constant of $\sim$1.4 ps (Bakker and Skinner 2010). The latter is related to the structural relaxation, either of the HB making and breaking of an individual HOD molecule or also of a more long-range slightly slower collective effect. The rotational time correlation function has a relaxation time of 2.5–3.0 ps, longer than that of the spectral diffusion, so that only a fraction of the HB breakings leads to actual rotation of the water molecule. A schematic picture of the re-orientation of water molecules, due to Laage and Hynes (2006a, 2006b) is reproduced in Fig. 1.3.

In summary, the ultrafast vibrational spectroscopy indicates that a molecule may within 50 fs make short angular and translational excursions which lead to rapid but only partial loss of frequency and angular correlation. On a slightly longer time scale undamped oscillations—librations and HB stretches—take place, and at still longer times the molecule rotates and breaks old and forms new HBs. The water molecule rotates in a concerted HB switching mode through a transition state with weak bifurcated HBs (Fig. 1.3).

Computer simulations provided yet additional information on the dynamics of the hydrogen bonding. Voloshin and Naberukhin (2009) pointed out that it is necessary to distinguish between instantaneous, very short time (10–20 fs) excursions of the HB length beyond its d_{O-H} cut-off criterion, called spurious breaking, instantaneous close approaches of water molecules to the $< d_{O-O}$ cut-off criterion, called spurious making of HBs, and genuine breaking of such bonds, lasting for a time considerably longer than a single oscillation. They also considered the time interval between

successive formations of HBs between two neighbouring water molecules, called "non-lifetime". They applied the Poltev–Malenkov (Poltev et al. 1984) potential model to 3,456 water molecules at 37 °C and found an average lifetime of a HB to be $< \tau_{HB} > = 0.45$ ps, and an exponential decay time of 1.48 ps, as well as an average "non-lifetime" of 160 fs. Eaves et al. (2005) also found a very short relaxation time of non-hydrogen-bonded configurations between adjacent water molecules, when they can revert to hydrogen-bonded ones, of less than 200 fs. Xenides et al. (2006) in their quantum mechanical/molecular dynamics simulations predicted a mean residence time of the HB of 0.33 ps, adding that every 1.51 ps on the average a molecule leaves the first coordination shell of a given water molecule or enters it and remains ≥ 0.5 ps in the new position, but only for one in 4.6 "attempts" the exchange is successful. The rearrangement of the hydrogen bonding, as a function of the libration and other kinds of relative movement of water molecules is on a ps time scale, and the local HB relaxation time is around 1.5 ps (Kumar et al. 2007). The self-diffusion of water indicates that water molecules tend to reside for an average of 3.1 ps near their oscillating equilibrium positions before they move to a neigbouring position (Novikov et al. 1994). Molecular dynamic computer simulations at 24 °C of several water trajectories (Voloshin et al. 2007) showed that concerted movements of two or more water molecules take place. They may reside at a distance apart of 0.28 nm, at which a HB between them is formed, for ~7 ps, and then move together, so that the HB persists for at least 12.6 ps. The average lifetime of a correlated pair of molecules is 6.8 ps, commensurate with the cooperative Debye relaxation time of the permittivity $\tau_\theta = 8.3$ ps at 25 °C (see above).

The rotational dynamics have been simulated by Svishchev and Kusalik (1994) at 25 °C by the SPC/E model with 256 water (H_2O, D_2O, and T_2O) molecules. They found different orientation self times of individual molecules rotating around the three principal axes for each kind of isotopic water, i.e., the rotation is anisotropic. The resulting Debye relaxation time $\tau_\theta = 9.7$ ps was somewhat larger than the experimental value, 8.3 ps. Van der Spoel et al. (1998) compared several water potential models at 28 °C, including the SPC/E one, with 216 and 820 H_2O molecules. The resulting τ_θ values, 6.9 or 9.7 ps for SPC/E water, depended on the cut-off distance r_{co}, but are larger than those obtained with other models (≤ 5.5 ps). For the rotational correlation times of the O–H and out-of-plane vectors of H_2O they found $\tau_{OH} = 1.6$ and 1.1 ps at 28 °C, compared with $\tau_{OD} = 1.94$ and 1.24 ps with this model at 27 °C for $D_2{}^{16}O$ and $D_2{}^{17}O$ obtained in simulations by Ropp et al. (2001). The former isotope effect (1.21) is larger than that reported by Svishchev and Kusalik (1994) but the latter (1.13) is in agreement with it. A new model, involving three molecule interaction, proposed by Kumar and Skinner (2008) improves over the SPC/E model, bringing the calculated values of $\tau_{OD} = 2.1$ ps nearer to the experimental (NMR) ones of Ropp et al. (2001) 2.4 ps. Chang and Dang (2008) presented their computation results for the out of plane vector rotational times, τ_{OD}, at five temperatures between −23 and 77 °C, albeit only in a figure, claiming agreement with experimental values at ≥ 27 °C. Schmidt et al. (2007) again compared various models for water, and found that the SPC/E model provides the overall best agreement with experiment, considering the Debye relaxation time τ_θ and the τ_{HH} reorientation time. Paesani et al. (2006) showed

Table 1.8 Re-orientation times of water molecules for various processes involving the dynamics of the hydrogen bonding: collective Debye relaxation time $\tau_{\theta 1}$, individual Debye relaxation time $\tau_{\theta 2}$, OH vector rotational re-orientation time (in parenthesis for D_2O) ${\tau_r}^{OH}$, and mean hydrogen bond life time τ_{HB}

Method	t (°C)	$\tau_{\theta 1}$ (ps)	$\tau_{\theta 2}$ (ps)	${\tau_r}^{OH}$ (ps)	τ_{HB} (ps)	Reference
Dielectric	0	17.3				Collie et al. 1948
spectroscopy	75	3.2				
	25	8.3				Haggis et al. 1952
	25	8.32	1.02			Barthel et al. 1990
	25	8.38	1.1			Buchner et al.1999
	25		0.42			Fukasawa et al. 2005
	−15	34				Malenkov 2006
	25	9.0				
	85	3.5				
NMR T_1	0			3.63 (4.76)		Jonas et al.1976
	30			2.07 (2.51)		
	90			0.85 (0.86)		
	10			2.29 (2.87)		Hardy et al. 2001
	25			1.39 (1.85)		
	40			1.00 (1.41)		
	80			0.51 (0.62)		
	2			(5.8)		Ropp et al. 2001
	27			(1.94)		
	77			(0.86)		
Infrared/	r.t.		1.4	2.5 (3.0)		Bakker and Skinner 2010
Raman	31				0.2	Elsaesser 2009
Computer	25	9.7				Svishchev and Kusalik 1994
simulation	28	6.9–9.7				Van der Spoel et al. 1998
	27			1.60 (1.94)		Ropp et al. 2001
	27			1.5		Lawrence and Skinner 2003
	27			2.5		Laage and Hynes 2006a
	27		1.5		0.33	Xenides et al. 2006
	25			2.1		Kumar and Skinner 2008
	25	8.3		1.95		Paesani et al. 2006
	37		1.48		0.45	Voloshin and Naberukhin 2009

that a force-matched centroid MD calculation provided the best agreement with the experimental values (at 25 °C) of $\tau_\theta = 8.3$ ps, and the second rank vector rotational correlation times ${\tau_2}^{HH} = 2.0$ ps, ${\tau_2}^{OH} = 1.95$ ps, and ${\tau_2}^{\mu} = 1.9$ ps, the latter for the dipole vector. Malenkov (2006) showed that on following the MD trajectories long enough then once in ca. 10 ps a water molecule would flip over by 180°, keeping its new orientation for 8 ps. The fully hydrogen bonded (and most probable) configuration d_2a_2 (see above) has an average lifetime of 0.7 ps and a maximal one of 7.4 ps (Malenkov et al. 2003), those of less probable configurations are shorter.

Table 1.8 summarizes the re-orientation times of water molecules for various process involving the HB dynamics.

Another kind of information concerning the dynamics in liquid water is the rate of exchange of protons between water molecules, or in other words the mean "life time"

or "residence time" of a proton on a given oxygen atom of a water molecule in bulk neutral water. Lamb et al. (1981) used pulsed ^{1}H-NMR in samples containing 3 % $H_2{}^{17}O$ to obtain these life times that range from 0.53 ms at 0 °C through 0.37 ms at 25 °C down to 0.10 ms at 100 °C. In this time interval, at ambient conditions, diffusion of the water molecule takes it away some 60 molecular diameters from its original position (Soper 2010). Lagodzinskaya et al. (2002) reported the proton exchange rate in neutral water ($c(H^+) = c(OH^-) = 10^{-7}$ M) as 1100 s^{-1}, i.e., a residence time of 0.91 ms at 25 °C, but did not explain the discrepancy with the Lamb et al. data shown above. The mean life time between two hops in the process of structural diffusion was reported as 1.7 ps, commensurate with the rotational correlation time, 2.7 ps (Lagodzinskaya et al. 2002).

1.2 Water as a Solvent

The dissolution of a solute (subscript$_S$) in a solvent, in the present case water (subscript$_W$), can be thought of as proceeding by means of the following steps. (1) the solute molecule is freed from its neighbours (if in a condensed phase) and transferred to a fixed position in the ideal gas state; (2) a cavity for the accommodation of the solute of proper size is created in the solvent at a fixed position; (3) the solute is transferred from the ideal gas state into the cavity; (4) the solute interacts with the solvent in its immediate surroundings by means of van der Waals forces, ion-dipole, dipole-dipole or dipole-induced dipole and similar interactions, as well as HBs and hydrophobic interactions; (5) the solvent molecules disturbed from their normal dispositions in the bulk solvent are re-arranged to their new equilibrium state; (6) the constraint to fixed positions in the ideal gas and solution phases is relaxed.

The solute is solvated by the solvent; the solvation process proper pertains to the imagined steps (2)–(5) (Ben-Naim and Marcus 1984) and constitutes the so-called 'unitary' part of the solvation. Step (6) is the so-called 'cratic' part of the process, which depends solely on the standard states in the gas and solution phases employed. (The terms 'unitary' and 'cratic' are no longer commonly used).

The standard molar Gibbs energy of dissolution, $\Delta_{dis}G^\circ$, for a given solute in a series of solvents depends mainly on the properties of the solvents for steps (2) and (5). For a given solvent (here water) and a series of solutes it depends solely on the properties of the solutes for step (1), whereas for steps (4) and (5) it depend on the properties of both the solvent and the solutes. Since the dissolution step (3) takes place from a fixed position of the solute (assumed an electrically neutral species) in the ideal gas phase to a fixed position in the solution (Ben-Naim and Marcus 1984) there is no contribution from this step to $\Delta_{dis}G^\circ$. This quantity, $\Delta_{dis}G^\circ$, then describes the difference in the molar Gibbs energy between the neat solute and solvent on the one hand and the solution on the other, that is the net solvation of the solute transferring from and to its standard states.

The standard molar Gibbs energy of dissolution is related directly to the activity of the dissolved solute in the saturated solution of a crystalline or liquid solute, a_{Ssat},

provided that the solvent does not alter the neat solute (solvate the crystalline solute or mix with the liquid solute). Then the activity of the pure solute is unity, and:

$$\Delta_{\text{dis}}G^{\circ}(\text{S in W}) = -RT\ln a_{\text{S sat}} = -RT\ln(x_{\text{S sat}}f_{\text{S}}) \tag{1.18}$$

The last quantity on the rhs contains the product of the mole fraction of the solute in the saturated solution, x_{Ssat}, and its activity coefficient that describes the solute-solute interactions. In the case of poorly soluble solutes the saturated solution is very dilute so that the solute-solute interactions can be ignored and $f_{\text{S}} \approx 1$. Solubilities are commonly presented as s_{S} on the molar scale (M), so that $\Delta_{\text{dis}}G^{\circ}{}_{\text{c}}(\text{S in W}) = -RT\ln(s_{\text{S}}y_{\text{S}})$, subscript$_{\text{c}}$ on the standard molar Gibbs energy of dissolution denoting the molar scale. The solubility is $s_{\text{S}} = c_{\text{Ssat}}$ and y_{S} is the activity coefficient on the molar scale. For poorly soluble solutes $y_{\text{S}} \approx 1$, hence $\Delta_{\text{dis}}G^{\circ}{}_{\text{c}}(\text{S in W}) = -RT\ln(10)\log s_{\text{S}}$. Conversion from the mole fraction to the molar scales involves the number of moles of the solvent, water, per 1 dm^3, and for poorly soluble solutes in water at 25 °C this is $1{,}000\rho_{\text{W}}/M_{\text{W}} = 55.35$ M. Thus

$$\log s_{\text{S}} = \log x_{\text{S sat}} + \log(55.34) = \log x_{\text{S sat}} + 1.74. \tag{1.19}$$

1.2.1 The Aqueous Solubility of Gases

The solubility of gases in water is of importance especially for the atmospheric gases, oxygen, nitrogen and carbon dioxide, and to a lesser extent also for argon and other gases. Naturally, the solubility of oxygen in water, fresh as well as oceanic, is important for aquatic life and the solubility of nitrogen in water (and blood) strongly affects divers. Carbon dioxide reacts with water to form carbonic acid and eventually carbonate salts, and the dissolution and possible equilibrium of CO_2 with the oceans will eventually determine the global warming, because CO_2 is an important hothouse constituent of the atmosphere. In the case of gases dissolving in water the virtual step (1) in the thought process described above will be absent at low pressures (typically ≤ 0.1 MPa $\sim$ 1 atm).

Data bases of aqueous gas solubilities have been published, among others, by Wilhelm et al. (1977), Cosgrove and Walkely (1981), and Crovetto et al. (1982), the latter over a very wide temperature range, $298 \leq T/\text{K} \leq 548$, and most recently by Battino and Clever (2007).

The solubility of gases is generally described by the Ostwald coefficient $L = V_{\text{S}}/V_{\text{W}}$, where subscripts $_{\text{S}}$ and $_{\text{W}}$ denote the solute and the solvent (water), and V_{S} denotes the volume of pure gas at a given temperature and pressure sorbed by (dissolved in) a volume V_{W} of pure water. For the standard pressure of $P^{\circ} = 0.1$ MPa ≈ 1 atm (the Ostwald coefficient is not appreciably dependent on the pressure at moderate pressures) the standard state molar volume of the gas is $V_{\text{S}}{}^{\circ} = RT/P^{\circ} + B_{\text{SS}}$, the second term is the second virial coefficient of the gas (describing interactions of the gas molecules with each other) and generally $B_{\text{SS}} << RT/P^{\circ}$ and can be ignored. The molar concentration (in $V_{\text{W}} = 1$ dm^3 of water) of the gas is then LP°/RT (with

$R = 0.08206$ dm^3 atm K^{-1} mol^{-1}), and its mole fraction (unless reacting with the water so that its concentration is high) is:

$$x_S = \frac{1{,}000 L M_W P^\circ}{\rho_W R T} \tag{1.20}$$

where $M_W/\rho_W = V_W{}^*$ is the molar volume of water (0.01807 dm^3 mol^{-1} at 25 °C).

Cabani et al. (1981) were among those who related the solubility of gases in water to their properties, namely in terms of group contributions of the solute molecules. They reproduced the solubilities at 25 °C of 209 hydrocarbons and mono-functional molecules in the gaseous state in terms of log$L$(S(g) in W) with a standard deviation of 0.09. (Actually, they dealt with $\Delta_{hyd}G^\circ = -RT\ln(10)\ \log L$, as well as with derived enthalpies, entropies, heat capacities and volume changes.) The group contribution approach, however, does not provide much insight into the factors that affect the solubility of gases in water. Still, the authors recognized the importance of hydrophobic interactions, because hydrophobic groups are contributing much more than hydrophilic ones to increasing $\Delta_{hyd}G^\circ$ (hence, reducing the solubility). Among hydrophilic groups, those capable of HB formation decrease $\Delta_{hyd}G^\circ$ (hence, lead to increased solubilities) as could be expected. The entropy change on hydration (dissolution) does not play an important role and its contribution is negative for all the groups considered.

Abraham et al. (1994) have more recently applied the linear solvation energy relationships (LSER) approach to the aqueous solubility of a large number of organic compounds in the gaseous state:

$$\log L = -1.00 + 0.58 R_S + 2.55\pi^* + 3.81\alpha + 4.84\beta - 0.0087 V_X \tag{1.21}$$

Here R_S is the "excess molar refraction of the solute over that of an alkane with the same characteristic volume" (Abraham et al. 1990) (not further specified). The Kamlet-Taft solvatochromic parameters of the solute (Kamlet et al. 1983) are: π^*, the polarity/polarizibility, α the HB donation (electron pair acceptance) ability, and β the HB acceptance (electron pair donation) ability. The volume of the solute is represented by the Abraham-McGowan volumes V_X (Abraham and McGowan 1987), based on invariant atom and bond contributions. The parameters α and β pertain to the monomeric solutes (measured in dilute solutions thereof). The correlation coefficient for Eq. (1.21) for 408 solutes is 0.998 and the standard deviation is 0.15.

This correlation does not apply to the noble gases and permanent gases, such as oxygen and nitrogen. Their solubilities in water at 25 °C are shown in Table 1.9.

A quite different approach to gas solubilities in water was taken by Scharlin et al. (1998). They considered the surface of the gaseous molecule accessible to the solvent, A_{SAS}, as the surface generated by the centre of a solvent molecule, considered as a rigid sphere, as it rolls around the van der Waals surface of the molecule. The number of water molecules adjacent to the solute molecule is then $N_W = A_{SAS}/(2r_W)^2$, where $(2r_W)^2$ is the effective area occupied by a water molecule. It was found that linear correlations of the standard molar Gibbs energy of dissolution, $\Delta_{dis}G^\circ$/kJ mol^{-1} $= -RT\ln x_{Ssat}$ with N_W could be obtained according to the classes of gaseous

Table 1.9 The solubilities of noble gases and some other gaseous small molecules in water at 25 °C (partial pressure of the gas is 1 atm). (From Wilhelm et al. 1977)

	log$L$	$10^4 x_S$	$10^4 c_S$[b]
Helium	−2.024	0.0698	3.86
Neon	−1.958	0.0813	4.50
Argon	−1.468	0.252	13.95
Krypton	−1.216	0.449	24.85
Xenon	−0.978	0.776	42.95
Radon	−0.644	1.675	92.71
Hydrogen	−1.718	0.1413	7.82
Deuterium	−1.73[a]	0.1461[c]	8.09[c]
Oxygen	−1.507	0.2298	12.72
Nitrogen	−1.799	0.1173	6.49
Nitrous oxide	−0.23[a]	4.349	240.7[a]
Carbon monoxide	−1.632	0.1724	9.54
Carbon dioxide	−0.082	6.111	338.2
Methane	−1.469	0.2507	14.13
Ethane	−1.344	0.3345	18.84
Tetrafluoromethane	−2.286	0.0382	1.705

[a]From (Abraham et al. 1994)
[b]$c_S = 55.35 x_S$ at 25 °C
[c]From (Scharlin et al. 1998)

compounds: $39 - 0.76N_W$ for the noble gases, $24 + 0.09N_W$ for alkanes up to *n*-pentane, $32 - 0.74N_W$ for halomethanes, $71 - 1.68N_W$ for freons (fluorocarbons) that have no hydrogen atoms, and $46 - 1.12N_W$ for freons that have them. The negative coefficients of N_W (except for the alkanes) signify that the more water molecules are involved with van der Waals interactions with the solute, the higher is the solubility, but no reason for the opposite (though weak) trend of the alkanes is apparent.

1.2.2 Water as Solvent for Non-Electrolytes

The solubility of non-electrolytes has been treated in several books, including those of Hildebrand and Scott (1950), Gerrard (1976), Shinoda (1978), and especially for water as a solvent by Yalkowsky and Banerjee (1992). Several approaches have been employed for relating the solubility to properties of the solutes and solvents.

If the interactions are confined to van der Waals ones and the solution conforms to the restrictions of regular solution theory (Hildebrand and Scott (1950)) then the well known Scatchard–Hildebrand solubility parameter expression can be applied:

$$\ln x_{S\ sat} = \frac{-V_S \varphi_W{}^2 (\delta_{HW} - \delta_{HS})^2}{RT} \tag{1.22}$$

This has been done for the solubilities of many kinds of solutes in many kinds of solvents, provided these are not highly polar. Here V_S is the molar volume of the solute, φ_W is the volume fraction of the solvent (≈ 1 for poorly soluble solutes) and

the δ_H's are the Hildebrand solubility parameters. The solubility, thus, diminishes on increasing the molar volumes of the solutes, when direct solute-solvent interactions are disregarded. Highly soluble solutes (in the case of liquid solutes, even those miscible in all proportions) have in general solubility parameters near those of the solvent.

In principle, the regular solution theory and Eq. (1.22) should not be applicable to the polar and hydrogen bonded water as the solvent. Empirically, the solubility parameter of water is 48 $MPa^{1/2}$, whereas those of non-polar non-electrolytes are ≤ 20 $MPa^{1/2}$, hence they are expected to be poorly soluble in water. All that can be learned from Eq. (1.22) on solubilities of non-electrolytes in water is its counteractive dependence on the molar volume of the solute. The latter is directly related to the size of the cavity required for its accommodation, thought process step 2) mentioned above.

For macroscopic bodies dispersed in water the cavity creation may be the most important contribution. This could be related to the surface tension of water, γ_W, which at room temperature is 72 mN m^{-1} (Table 1.2), much larger than those of non-polar liquid solutes, $\gamma_S \leq 30$ mN m^{-1}, and to the surface area of the cavity accommodating the solute, A_S. The relevant expression for the mole fraction solubility for solutes that are liquid in their standard state is then, in analogy to Eq. (1.22):

$$\ln x_{S\ sat} = -\frac{A_S\left(\gamma_W{}^{1/2} - \gamma_S{}^{1/2}\right)^2}{RT} \tag{1.23}$$

This approach was taken by Yalkowsaki and co-workers (Amidon et al. 1974, 1975; Valvani et al. 1976) also for molecular-sized solutes. The surface area of the cavity was calculated in their earlier papers on addition of an annular layer of thickness 0.15 nm (about the radius of a water molecule) to the actual van der Waals surface of the solute molecule, in order to represent the exclusion region of the solvent around the solute and obtain A_{SAS}. Corrections have to be applied for the mutual surface tension of the solute and water, γ_{WS}, using this quantity rather than $(\gamma_W{}^{1/2} - \gamma_S{}^{1/2})^2$, and for the curvature of the cavity (since the surface tension is measured for flat surfaces of infinite radius of curvature). This approach was applied successfully to various kinds of mono-functional aliphatic solutes.

In both the solute volume and surface area approaches the solute is considered to be a liquid in its standard state, hence for crystalline solutes an important part of the virtual step (step 1) in the thought process of dissolution dealt with above is thereby disregarded. (Note that the solubility parameter in Eq. (1.22) takes care of the vaporization of the *liquid* to the ideal gas state.) For solid solutes the term

$$\ln x_{cryst} = -\Delta_F H(T_F - T)/RT_F T + \Delta C_p[(T_F - T)/T - \ln(T_F T)]/R \tag{1.24}$$

should be added on the right hand side of Eqs. (1.22) and (1.23), where $\Delta_F H$ is the molar enthalpy of fusion of the solute at its fusion temperature T_F and ΔC_p is the heat capacity change on fusion. The second term on the rhs of Eq. (1.24) is generally much smaller than the first and can usually be ignored.

According to the above two approaches, the outstanding property of water that counter-acts the solubility of non-polar solutes is the large value of the relevant property of water relative to those of the solutes: the solubility parameter δ_W and the surface tension γ_W. These are consequences of the hydrogen bonded network of the water, discussed above (Sects 1.1.2. and 1.1.3.).

In a subsequent paper Yalkowsky and Valvani (1980) related the solubility of non-electrolytes in water, polar as well as non-polar, to their distribution quotients between 1-octanol and water and, in the case of crystalline solutes, to their fusion temperatures, T_F, and entropies of fusion, $\Delta_F S$. This approach was taken for the aqueous solubilities of drug molecules and places the burden of explaining the interactions on the octanol/water distribution quotients, $D^O{}_W$, or on $P^O{}_W = \log D^O{}_W$, that have been dealt with extensively by Hansch and Leo (1979) among others. The empirical expression used for solubility at 25 °C was:

$$\log s_S = -1.00 P^O{}_W - 1.11 \Delta_F S(T_F/\mathrm{K} - 298.15)/298.15 \ln(10) R + 0.54 \quad (1.25)$$

Here s_S is the solubility of a drug in water on the molar scale (M; at 25 °C $\log s_S = 1.74 + \log x_{Ssat}$ for poorly soluble solutes, see above). The first term in Eq. (1.25) assumes that the drug molecule has a molar cohesive energy similar to that of 1-octanol, so that the logarithm of the activity coefficient of the drug in water should be equal to $P^O{}_W$, the logarithm of the distribution ratio between 1-octanol and water. This, in turn, can be related to the constitution and structure of the drug (Hansch and Leo 1979). The second term, involving the molar entropy of fusion of the drug molecule, is taken as zero for liquid solutes (at 25 °C) but non-zero for crystalline drugs. In summary, Eq. (1.25) predicted the aqueous solubility of 167 drug and related organic solutes with a correlation coefficient of 0.994 and a standard deviation of 0.24 in $\log s_S$.

A crucial component of this treatment is the value of $P^O{}_W$ for the distribution of the solute molecules between 1-octanol and water. This could be estimated from group contributions (Hansch and Leo 1979) but could also be related to other properties of the solutes, namely, their solvatochromic parameters according to Kamlet et al. (1984, 1988). Their equation was tested for 245 solutes of all kinds with a correlation coefficient of 0.996 and a standard deviation of 0.13. Earlier, Kamlet, Taft and coworkers (Taft et al. 1985, Kamlet et al. 1986) applied the LSER concept directly to the solubility of non-electrolytes in water, independently of the octanol/water distribution. Subsequently, important differences between aliphatic and aromatic solutes were stressed (Kamlet et al. 1987). For liquid aliphatic solutes the expression:

$$\log s_S(\text{aliphatic}) = 0.05 - 0.0585 V_I + 1.09 \pi^* + 5.23 \beta \quad (1.26)$$

holds for 115 solutes with a correlation coefficient of 0.994 and a standard deviation of 0.15. Eq. (1.26) was subsequently (Kamlet et al. 1988) modified for aromatic solutes to

$$\log s_S(\text{aromatic}) = 0.27 - 0.0529 V_I + 3.93 \beta - 0.0096(T_F/\mathrm{K} - 298.15\mathrm{K}) \quad (1.27)$$

as applied to 139 solutes (including polychlorinated biphenyls and solutes with up to six fused rings) with a correlation coefficient of 0.993 and a standard deviation of 0.29. In these equations V_I is the computer-generated (Leahy 1986) intrinsic (van der Waals) volume of the solute and the last term in (1.27) pertains only to solutes that are solid at 25 °C. The solvatochromic parameters of the solute are as before: π^* its polarity/polarizibility and β its HB acceptance (electron pair donation) ability. The solute molar volume, related to the cavity formation process in water, is the endoergic contribution (for non-crystalline solutes) to the solubility. The parameters π^* and β are scaled to the same range (roughly between 0 and 1), so that the coefficients of these variables in Eq. (1.26) mean that the HB acceptance ability dominates over the polarity/polarizibility of the solute in determining its exoergic term (and the π^* term is insignificant for aromatic solutes). Thus, the main properties of water as the solvent are its stiffness, Eq. (1.5), resisting the creation of the cavity, and its ability to donate HB to the solute.

In a critique of the LSER approach based on the solvatochromic parameters Yalkowsky et al. (1988) produced a simplified form of Eq. (1.24), namely:

$$\log s_S = -1.00 P^O{}_W - 0.01(T_F/K - 298.15) + 0.8 \tag{1.28}$$

again based on the 1-octanol/water distribution constants that they claimed are much more widely available (Dunn et al. 1986) and applicable than the solvatochromic parameters.

Abraham and Le (1999) compared many methods for the description, estimation, and prediction of the aqueous solubility of diverse compounds, some methods involving a training set and a subsequent test set of solutes. Standard deviations of the multi-parameter correlations of $\log s_S$ were generally not smaller than 0.5 (a factor of 3 in the solubility!). They then reverted to an LSER-type expression:

$$\begin{aligned}\log s_S = {} & 0.57 - 0.0408 V_X + 3.39\beta + 1.23\alpha + 0.98\pi^* \\ & - 0.576 R_S - 0.010(T_F/K - 298.15)\end{aligned} \tag{1.29}$$

The use of the computer-generated solute volumes, V_I, rather than the molar volumes V_S, in the later formulations of Kamlet et al. (1988), Eqs. (1.26) and (1.27), is inconvenient. Here the Abraham-McGowan molar volumes V_X (Abraham and McGowan 1987) are employed, based additively on invariant atom and bond contributions. The β and α are the summation solvatochromic parameters (for poly-functional solutes) and the new solute parameter R_S is an excess molar refraction (measuring solute polarizibility). Eqation (1.29) was applied to 411 solutes, liquids and solids, aliphatic and aromatic, including drugs and environmentally important substances, with a correlation coefficient of 0.957 and a standard deviation of 0.56. Abraham and Le (1999) suggested that a cross term in $\alpha \times \beta$ could be used for the self interactions in both liquid and solid solutes, rather than incorporating the fusion temperature term.

Although the thought process for the dissolution of a solute in a solvent delineated at the beginning of Sect. 1.2 is generally adhered to by investigators of solubilities, this is not universally accepted. The mobile order theory of Huyskens and Siegel

(1988) assumes a non-ergodic behaviour of the systems, i.e., that the time averages are not the same as the ensemble averages of the molecules. The consequence of this treatment is that the dissolution is at least as much entropy driven as enthalpy driven. According to Ruelle and Kesselring (1998) the overall solubility expression for the volume fraction of the solute in the saturated solution is:

$$\ln\varphi_{S\ sat} = -A + B - F - D + (O - OH) \tag{1.30}$$

The following contributions have to be considered additively, the letters in parenthesis designate the terms in Eq. (1.30): the solute must be fluidized (A), there is a combinatorial entropy term (B), there is a solvophobic effect on a self-associated solvent such as water (F), a change in non-specific forces (D) occurs, and hydrogen bonding or donor–acceptor interactions take place (O and OH).

The aqueous solubility of hydrophobic compounds (aliphatic hydrocarbons and polychlorinated diphenyl ethers) at 25 °C is then simply given by:

$$\ln\varphi_{S\ sat} = -0.02278(T_F/\mathrm{K} - 298.15) - 1.948 - 0.083V_S + 0.5\ln V_S \tag{1.31}$$

Here the first term corresponds to A (the coefficient is ln(10) times that in Eqs. (1.27)–(1.29) and is zero for liquid solutes) and the other three terms correspond to $B+F$, whereas $-D+(O-OH)=0$ for such solutes that are devoid of specific interactions. The molar volumes for solid solutes were estimated from group contributions rather than from the densities of the solids. The full solubility expression was applied to 150 solutes, including in addition to those above also polycyclic aromatic hydrocarbons, halogenated hydrocarbons and various pollutants, drugs, and related compounds, with an overall standard deviation in $\ln\varphi_{Ssat}$ of 0.45 (Ruelle and Kesselring 1998). The hydrophobic contribution remains dominant even when hydrophilic groups are present in the solute molecule, which reduce somewhat the counter-active hydrophobic effect on the solubility.

More recently Yalkowsky and coworkers (Jain and Yalkowsky 2001, Yang et al. 2002) revived and revised their general solubility equation (GSE) (Yalkowsky and Valvani 1980) to read:

$$\log s_S = -1.031P^{O}{}_W - 0.0102(T_F/\mathrm{K} - 298.15) + 0.424 \tag{1.32}$$

instead of Eq. (1.28). This accounts for the aqueous solubility of a large number of non-electrolytes, including drugs and pollutants. This two (or three) parameter approach was compared with that of Abraham and Le (1999), Eq. (1.30), requiring six descriptors of the solutes, for 664 compounds, and very similar predictive powers for the two treatments were found (Yang et al. 2002).

Still further expressions have been suggested for the description and prediction of the solubility of non-electrolytes in water with emphasis on drugs and environmental pollutants, e.g. very recently (Sprunger et al. 2007, 2009; Jain and Yalkowsky 2010). It is not the purpose of this section to present the best available solubility expressions, but to show the properties of water as a solvent for such solutes. The emerging picture, well known for many years, is that the solubility is governed by the hydrophobic-hydrophilic balance of the solute. This is dominated by the former, except for small

aliphatic solutes, and is the same whether called 'cavity formation' and dominated by the endoergic V_X term in Eq. (1.29) or described by the entropic term of the 'mobile order theory' in Eq. (1.31). The self-interaction of the solute, also endoergic, is given by the $(T_F/K - 298.15)$ term, but does not relate to the solvent properties of water. The exoergic hydrophilic effects are due to the ability of water to donate and accept HBs, expressed in the LSER approach, Eq. (1.28), by the terms in *solute* β and α, with a minor contribution of the polarity and polarizibility of water, expressed by the *solute* R_S and π^*, respectively. Similarly, the $D + (O - OH)$ terms of the 'mobile order theory', Eq. (1.30) involve modified solubility parameters (cf. Eq. (1.22)) for non specific interactions, the number of protogenic and proton accepting groups of the solute, and stability constants of their interactions with water.

1.2.3 Water as Solvent for Electrolytes

For the purpose of this section electrolytes (subscript$_E$) are considered as neutral combinations of ions (Chap. 2) that are capable of ionic dissociation in water. It is recognized that some electrolytes are gaseous (e.g. HCl) or liquid (H_2SO_4) at the temperature range considered here (0–100 °C), also that they may be only partly dissociated ($NH_4^+OH^-$) in dilute solutions or associate to ion pairs in more concentrated ones ($Mg^{2+}SO_4^{2-}$), or that they are surface active ($C_{12}H_{25}SO_3^-Na^+$) or are polymeric ($-[CH(CH_3)CO_2^-Na^+]_n-$). However, typical electrolytes dealt with in this section are salts, such as Na^+Cl^-, which are practically completely dissociated in dilute solutions and consist of small ions.

Such salts are crystalline in the pure state and have very large lattice energies, cohesive energies or solubility parameters. The values of $\delta_{HE}/MPa^{1/2}$ for salts having melting temperatures $T_F > 470$ K, are appreciably larger than that of water: $\delta_{HW}/MPa^{1/2} = 48$; they range between 79 (CsI) and 254 (LiF) (Marcus 2010), so that according to Eq. (1.22) these salts should be completely insoluble on water. Since this is not the case, this self-interaction must be counter-balanced for the salt to dissolve in water by the strong hydration of the ions.

The molar lattice energy of a salt, U_{latE}, is the energy that has to be invested in the crystalline salt at zero K in order to separate a mole of its ions from their near proximity and mutual interactions in the crystalline phase to form individual ions at infinite distance apart in the ideal gas state. The values of $U_{lat\,E}$ of many salts are available from the compilation of Jenkins and Roobottom (2002), the estimated error in them being about ± 10 kJ mol^{-1}, due to the various modes of obtaining $U_{lat\,E}$. In order to obtain the cohesive enthalpy of a salt at 298.15 K it is necessary to subtract $[H_{298} - H_0]_E$ from $U_{lat\,E}$ and add $298.15\nu_E R$ to it. Here $[H_{298} - H_0]_E$ is the tabulated molar enthalpy value (Wagman et al. 1982) for the crystalline salt at 298.15 K relative to its value at 0 K and ν_E is the total number of ions a formula unit of the salt dissociates into.

The enthalpies of hydration of the ions transferring from the ideal gas state into their standard state in the aqueous solution, $\Delta_{hyd}H^\circ_I$, have been tabulated for

Table 1.10 The lattice energies U_{lat} (at 0 K), cohesive energies, $V_S\delta_S{}^2$ (at $T = 1.1T_F$) and the sums of the standard molar enthalpies of hydration of the constituent ions $-\sum\Delta_{hyd}H^\circ$ (at 298.15 K), all in kJ mol^{-1}, of some uni-univalent salts

Salt	U_{lat}	$V_S\delta_S^2$	$-\sum\Delta_{hyd}H^\circ$
LiF	1,030	956	1041
LiCl	834	825	898
LiBr	788	735	867
LiI	730	681	822
NaF	910	891	926
NaCl	769	694	783
NaBr	732	665	752
NaI	682	613	707
KF	808	725	844
KCl	701	622	701
KBr	671	594	670
KI	632	558	625
RbF	774	695	818
RbCl	680	614	675
RbBr	651	589	644
RbI	617	560	599
CsF	744	674	793
CsCl	657	590	650
CsBr	632	563	619
CsI	600	531	575
AgF	953	934	993
AgCl	810	880	850
AgBr	897	867	819
AgI	881	849	774
LiOH	1021	954	1051
$LiNO_3$	848	790	843
$LiBF_4$	699	629	758
$LiCH_3CO_2$	911	851	956
NaOH	887	826	736
NaSCN	682	672	727
$NaNO_3$	755	693	728
$NaBF_4$	657	563	643
$NaCH_3CO_2$	828	766	841
KOH	789	735	854
KSCN	623	583	645
KNO_3	685	617	646
KBF_4	611	490	561
KCH_3CO_2	749	684	759
RbOH	766	715	828
$RbNO_3$	662	613	620
CsOH	721	678	803
$CsNO_3$	648	574	595
$AgNO_3$	820	772	795

298.15 K (Marcus 1997), derived for individual ions by using an extra-thermodynamic assumption, see Sect. 2.3. However, the sums of such values for complete salts, $\Delta_{hyd}H^\circ{}_E = \sum\Delta_{hyd}H^\circ{}_I$ are independent from such an assumption, since they are based on measurable values, and have estimated errors of about $\pm$ 6 kJ mol^{-1}.

Table 1.10 shows the lattice energies, $U_{lat\,E}$, applicable at zero K, the molar cohesive energies of the molten salts, i.e., the products of the molar volumes V_E

and $\delta_{HE}{}^2$, recorded at $T = 1.1T_F$, and the negatives of the sums of the standard molar hydration enthalpies of the ions, $\sum \Delta_{hyd}H^\circ{}_I$, measured at 298.15 K, for typical uni-univalent salts. All these values are commensurate with each other for a given salt, but should not be compared directly, because they pertain to different temperatures. The lattice and cohesive energies and hydration enthalpies of salts involving multivalent ions are typically $0.5\sum \nu_I z_I{}^2$ those of uni-univalent ones, where ν_I is the number of z_I-valent ions in a formula unit of the salt.

The solubilities of salts in water are, of course, related to the Gibbs energy changes rather than to the enthalpies. The solubility product of a sparingly soluble salt, K_{SP}, the product of the ion concentrations in the saturated solution, is related to the Gibbs energy changes by

$$\log K_{SP} = -RT\Delta_{diss}G^\circ/\ln(10) = -RT(G^\circ{}_{lat} + \Delta_{hyd}G^\circ)/\ln(10) \qquad (1.33)$$

where $\Delta_{diss}G^\circ$ ranges at ambient conditions from -80 to $+80$ kJ mol^{-1}. This expression is valid as long as the activity coefficients of the ions are well approximated by unity, i.e., the saturated solution is very dilute. Thus, since the lattice and hydration enthalpies are commensurate, the entropies of solution also play a role in the determination of the solubility, in addition to the enthalpies exhibited above. Since $G^\circ{}_{lat} = H^\circ{}_{lat} - TS^\circ{}_{lat}$, conversion of the lattice enthalpy, $H^\circ{}_{lat} = U_{lat} - [H_{298} - H_0]_E + \nu_E RT$ to the lattice Gibbs energy involves subtraction of $TS_{lat} \approx T\,\Sigma_I(1.5R\ln M_I - 3.9\,\text{J K}^{-1}\,\text{mol}^{-1})$, where M_I is the dimensionless relative ionic (atomic) mass of the ions. The approximation is according to Latimer's rule and the logarithmic dependence on M_I means that the variation of the lattice entropies among various salts is minor. Consequently, also $\Delta_{hyd}G^\circ = \Delta_{hyd}H^\circ - T\Delta_{hyd}S^\circ$ is required for the estimation of the salt solubility. Therefore, the hydration enthalpies and hydration entropies are to be considered for assessing the role of water as a solvent for typical salts. The details of the thermodynamics of hydration of ions are discussed in Sect. 2.3.

In summary, the role of the water as the solvent for salts is to provide a medium of high relative permittivity, $\varepsilon_r = 78.46$ at 25 °C, so the salt can dissociate into its constituent ions. Cavities must then be created to accommodate the ions, with work being done against the stiffness of the water (its large cohesive energy) and a concomitant lowering of the entropy. The water molecules provide electron pairs to hydrate cations and HBs to hydrate anions in a first hydration shell. Water has a moderate propensity to donate electron pairs: its Kamlet-Taft β solvatochromic parameter in bulk water is 0.47 and its Gutmann donor number is $DN = 18.0$, compared with a solvent such as dimethylsulfoxide ($\beta = 0.76$, $DN = 29.8$) (Marcus 1998). However, the small size of a water molecule, permitting several of them to hydrate the cations, compensates for this. Water does have a pronounced ability to donate HBs to anions: its Kamlet-Taft α solvatochromic parameter is 1.17 and its Gutmann-Maier acceptor number is $AN = 54.8$, compared with a solvent such as N-methylformamide ($\alpha = 0.62$, $AN = 32.1$) that has an even larger relative permittivity, $\varepsilon_r = 182.40$ at 25 °C (Marcus 1998). It turns out that the enthalpies of hydration of cations and anions of the same sizes are similar, and as mentioned above, the sum of these values for

complete salts are commensurate with the lattice energies. The hydrogen bonding of water molecules beyond the hydration shell with those inside it, as well as the disturbance of the water structure by the hydrated ion is a further aspect that water as a solvent exhibits much beyond other structured solvents and must be reckoned with. Further consideration of the quantities pertaining to ions and relevant to salt solubilities are presented in Sect. 2.3, p. 64 ff.

1.2.4 Mixed Aqueous-Organic Solvents

For many purposes it is advantageous to add an organic solvent to water in order to enhance or modify its solvent powers. For instance, formulations for drugs that are poorly soluble in water may be optimized by the addition of a suitable organic solvent. For other purposes the properties of water may be tuned as needed by such an addition. There are many solvents that are miscible with water in all proportions, such as the lower alcohols (up to C_3, as well as tert-butanol), alkane-diols, glycerol, certain ethers (tetrahydrofuran, dioxane), acetone, certain esters (ethylene carbonate, γ-butyrolactone), lower and cyclic amines and pyridine, acetonitrile, various amides, and certain sulphur compounds (sulfolane and dimethylsulfoxide), among others (Marcus 1998). Although the properties of such mixed aqueous solvents are generally in between those of the components, the possibility of preferential solvation of solutes must be taken into account. This aspect complicates the situation considerably, so that specification of the bulk properties of the mixtures (Marcus 2002a, b) requires further information in order to be of use in assessing the solvent powers of such a mixture.

The bulk properties are conveniently described by Redlich-Kister-type expressions for binary mixtures of water (W) and a co-solvent (S):

$$\begin{aligned} Y = {} & x_W Y_W + x_S Y_S + x_W x_S [y_0 + y_1(1 - 2x_S) \\ & + y_2(1 - 2x_S)^2 + y_3(1 - 2x_S)^3 + \cdots] \end{aligned} \tag{1.34}$$

Here Y denotes a general bulk property, Y_W that of pure water and Y_S that of the pure co-solvent, and the y_i are listed coefficients, generally up to $i = 3$ being required. Annotated data are provided in (Marcus 2002) for the viscosity η, relative permittivity ε_r, refractive index (at the sodium D-line) n_D, excess molar Gibbs energy G^E, excess molar enthalpy H^E, excess molar isobaric heat capacity ${C_P}^E$, excess molar volume V^E, isobaric expansibility α_P, adiabatic compressibility κ_S, and surface tension γ of aqueous mixtures with many co-solvents. These include methanol, ethanol, 1-propanol, 2-propanol, 2-methyl-2-propanol (tert-butanol), 1,2-ethanediol, tetrahydrofuran, 1,4-dioxane, pyridine, acetone, acetonitrile, N, N-dimethylformamide, and dimethylsulfoxide and a few others.

The solvent powers of solvents and solvent mixtures are described by the solvatochromic parameters, see Sect. 1.2.2. The solvatochromic parameters of aqueous mixtures with co-solvents, symbolized by Y, are generally in between those of the

pure components, but usually in a manner non-linear with the mole-fraction composition. The parameters Y considered are the Dimroth-Reichard general polarity $E_T(30)$ ($Y_W = 63.3$) and the Kamlet-Taft polarity/polarizibility π^* ($Y_W = 1.09$), electron pair donicity/HB acceptance β ($Y_W = 0.47$), and electron pair acceptance/HB donicity α, ($Y_W = 1.17$). The deviations ΔY from linearity may be positive or negative and are listed (Marcus 2002) for $x_S = 0.15, 0.35, 0.50, 0.65, 0.85$ as well as are the Y_S of pure S for the above-mentioned co-solvents.

Binary mixtures of water with water-miscible solvents show a balance between the self-association and the mutual association of the components. This aspect has been studied by the use of many methods, but the most definite information is given by the preferential solvation parameter $\delta_{W(S)} = x_{W(S)}{}^{L} - x_W$, where $x_{W(S)}{}^{L}$ is the *local* mole fraction of W around S. Obviously, what is excess in one component must be deficiency in the other, so that $\delta_{W(S)} = -\delta_{S(S)}$ and $\delta_{W(W)} = -\delta_{S(W)}$. Also, $\delta_{W(S)}(x_W = 0) = 0 = \delta_{W(S)}(x_W = 1)$ and necessarily also $\delta_{W(S)} \leq x_W$. The experimental errors in the data required for the calculation of the preferential solvation parameters lead to values $|\delta_{W(S)}| \leq 0.010$ to be insignificant, but larger values mean that water is preferred around S rather than S molecules, i. e., self-associated S. Similarly, $\delta_{W(W)} \geq 0.010$ means that self-association of water is preferred over mutual association with the co-solvent S. Another manner of presenting this information is in terms of the solvent sorting parameter P_{ss}:

$$P_{ss} = (x_{W(S)}{}^{L}/x_{W(W)}{}^{L})/(x_S/x_W) = (x_{W(S)}{}^{L}/x_S)/(x_{W(W)}{}^{L}/x_W) \tag{1.35}$$

When $P_{ss} > 1$ mutual association of water with the co-solvent is preferred over their self-association and vice versa when $P_{ss} < 1$, and $P_{ss} = 1.00 \pm 0.02$ means absence of preferential solvation.

The preferential solvation in binary aqueous–co-solvent mixtures leading to values of the local mole fractions and the preferential solvation parameters has been studied extensively by two methods. One is the quasi-lattice quasi-chemical (QLQC) treatment of Marcus (1983) and the other is the inverse Kirkwood-Buff integral (IKBI) treatment of Ben-Naim (1977). The former, QLQC, is approximate, in that it involves several simplifying assumptions, and is confined to the first solvation shell of a given molecule, but is less demanding on the accuracy of the input data. On the contrary, the latter, IKBI, is rigorous and presents information also on more than one solvation shell, but is highly demanding regarding the accuracy of the input data that cannot in many cases be adequately met. For the present purposes only the working expressions for these two treatments are shown here; further details can be obtained from the original publications cited above and from (Marcus 2002).

In the QLQC treatment a lattice parameter is assigned for each component: Z_W and Z_S, and for the mixtures the mean lattice parameter is:

$$Z(x) = wZ_W + (1 - w)Z_S \tag{1.36}$$

where the weighting factor w is given by:

$$w = x_S{}^{r}\exp(\Delta)\left[x_W{}^{r} + x_S{}^{1/r}\exp(\Delta)\right] \tag{1.37}$$

with $r = Z_S/Z_W$ and:

$$\Delta = \left(2/RT\,{Z_W}^2\right)\left[\Delta_V H_W + r^{-2}\Delta_V H_S + \left(r^{-2} - 1\right)RT\right] \tag{1.38}$$

where $\Delta_V H$ is the molar enthalpy of vapourization. The interaction energy of a water molecule with a neighbouring water molecule (assumed independent of the nature of its other neighbours) is given by:

$$e_{WW} = \frac{\Delta_V H_W - RT}{Z_W N_A} \tag{1.39}$$

Similarly, e_{SS} and e_{WS} are the corresponding interaction energies of two nearest neighbour solvent molecules and nearest neighbour water-solvent molecules. The neighbour exchange energy is:

$$\Delta e_{WS} = e_{WW} + e_{SS} - 2e_{WS} = 2k_B T \ln\left\{2\exp\left[-2{G^E}_{(x=0.5)}/Z(x)RT\right] - 1\right\} \tag{1.40}$$

and is obtained from the excess Gibbs energy of mixing at the equimolar composition. The entire $G^E(x)$ curve can then be fitted by:

$$\begin{aligned} G^E(x) = (Z(x)RT/2)\left[x_W \ln\left\{(x_W - (1-Q)/2P)/{x_W}^2\right\}\right. \\ \left. + x_S \ln\left\{(x_S - (1-Q)/2P)/{x_S}^2\right\}\right] \end{aligned} \tag{1.41}$$

where $Q = (1 - 4x_W x_S P)^{1/2}$ and $P = 1 - \exp(-\Delta e_{WS}/k_B T)$. This is a check on the correct assignment of the Z_S and Z_W values.

Finally, the local mole fraction of, say, water around S, is given by:

$${x_{W(S)}}^L = \left[1 - \{1 - 4x_W x_S(1-P)\}^{1/2}\right]/2Px_S \tag{1.42}$$

The required input values are thus the vapourization enthalpies of the components, $\Delta_V H_W$ and $\Delta_V H_S$ and their lattice parameters, Z_W and Z_S, and the excess molar Gibbs energy at the equimolar composition, ${G^E}_{(x\,=\,0.5)}$. The lattice parameter for the binary mixtures, $Z(x)$, is then given by Eqs. (1.36) to (1.38), the molar excess Gibbs energy of the binary mixtures $G^E(x)$ is given by Eq. (1.41), and the local mole fraction of W around S is given by Eq. (1.42) (Marcus 1983, 1989, 2002). A simplification can be achieved provided the $G^E(x)$ curve is nearly symmetrical by setting $Z_S = Z_W = Z(x)$ (hence, $r = 1$). For water $Z_W = 4$ was arbitrarily fixed, and Z_S was obtained (in the range 2.8–6.8) by fitting the experimental ${G^E}_{(x\,=\,0.5)}$ with Eq. (1.41). The treatment was applied to mixtures of water with the above mentioned co-solvents and a few others, noting preferential mutual solvation in some cases, preferential self-association in some others (Marcus 1989); representative curves are shown in Fig. 1.4. Mutual interactions of water with deimethylsulfoxide and with methanol are seen to prevail over the entire composition range, whereas in water-rich mixtures self-association of water dominates over mutual association in aqueous 2-propanol, acetone, and acetonitrile.

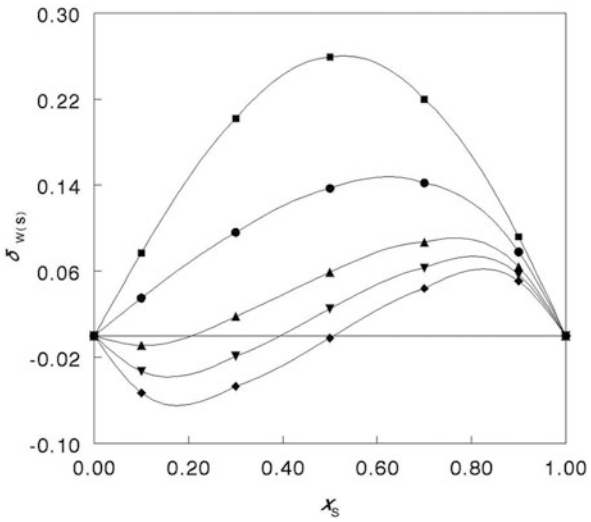

Fig. 1.4 The preferential mutual solvation parameters according to the QLQC treatment in binary mixtures of water with the co-solvents: ■ dimethylsulfoxide, • methanol, ▲ 2-propanol, ▼ acetone, and ♦ acetonitrile

The IKBI method requires, as said, highly accurate data, because it employs derivative thermodynamic functions of the composition, see below. Following are the working expressions for the Kirkwood-Buff integrals:

$$G_{WS} = RT\,[k_T - V_W V_S / VD] \tag{1.43}$$

$$G_{WW} = RT\left[k_T + (x_S/(1-x_S))\left({V_S}^2/VD\right)\right] - V/(1-x_S) \tag{1.44}$$

$$G_{ss} = RT\left[k_T + ((1-x_S)/x_S)\left({V_W}^2/VD\right)\right] - V/x_S \tag{1.45}$$

where κ_T is the isothermal compressibility of the mixture, V_W and V_S are the partial molar volumes of the components in the mixture, and V is the molar volume of the mixture. The partial molar volumes can be readily calculated from those of the pure components, the excess molar volume of the mixtures, $V^E(x_S)$, and its first derivative with respect to the composition. The function D is calculated from the second derivative of the excess Gibbs energy of the mixture, $G^E(x_S)$:

$$D = RT + x_S(1-x_S)\left(\partial^2 G^E/\partial {x_S}^2\right)_{T,P} \tag{1.46}$$

For both the partial molar volumes and the function D the derivatives of the general expression (1.34) and the coefficients listed in (Marcus 2002) can be used, but only for the volumes with sufficient accuracy. An alternative expression for the function D, assuming water to be the much more volatile component, requires only the first derivative and should be preferred when the data are available:

$$D = RT\left[1 + (1-x_S)(\partial \ln f_W/\partial(1-x_S))_{T,P}\right] \tag{1.47}$$

Here $f_W = p_W/(1-x_S)p_W{}^\circ$ is the activity coefficient of water, and p_W and $p_W{}^\circ$ are its fugacities above the mixture and pure water, respectively. Partial pressures can

be used instead of fugacities, if they are sufficient low, otherwise they must be corrected for the vapour virial coefficients. If the required isothermal compressibilities of the mixtures, $\kappa_T(x_S)$, are not known, they can be estimated with sufficient accuracy from adiabatic compressibilities as 1.1–1.4 times $\kappa_S(x_S)$ or interpolated linearly between $\kappa_{T(S)}$ and $\kappa_{T(W)}$ of the neat solvents. The Kirkwood-Buff integrals of many binary aqueous solvent systems were reported by Matteoli and Lepori (1984) and subsequently for many more by Marcus (1990, 1995, 2001, 2002a, 2003) among others.

Preferential solvation occurs, if at all, in the correlation volume, where a central molecule affects its environment. The correlation volume, $V_{cor}/cm^3\ mol\text{-}^1$, can be calculated for m consecutive spherical solvation shells, taking into account partial penetration of molecules from farther shells into nearer ones as well as the preferential solvation in these shells (Marcus 1990). The correlation volumes around W and S molecules are:

$$V_{cor\,W} = 2522.7\left\{(-0.085m) + (0.1363/2)V_W{}^{1/3} + 0.1363(m-0.5)\left[x_{WW}{}^{L}V_W + \left(1 - x_{WW}{}^{L}\right)V_S\right]^{1/3}\right\}^3 \tag{1.48}$$

$$V_{cor\,S} = 2522.7\left\{(-0.085m) + (0.1363/2)V_S{}^{1/3} + 0.1363(m-0.5)\left[x_{WS}{}^{L}V_W + \left(1 - x_{WS}{}^{L}\right)V_S\right]^{1/3}\right\}^3 \tag{1.49}$$

The numerical coefficients arise from the relationship between the molar volume and the mean molecular diameter, d, of the solvent, W or S. The calculation must be carried out iteratively, because it uses the local mole fractions implicit in the expressions (1.48) and (1.49) for $x_{WW}{}^{L}$ and $x_{WS}{}^{L}$. The latter, in turn, depend on the preferential solvation parameters presented in Eqs. (1.50) and (1.51) further below.

"Ideal" Kirkwood-Buff integrals, $G_{ij}{}^{id}$, are based solely on the relative molar volumes of the components and do not provide information on the molecular interactions leading to preferential solvation. The $G_{ij}{}^{id}$ are obtained on setting $G^E(x_S) = V^E(x_S) = 0$ in Eqs. (1.43) to (1.45) and conform to $G_{WW}{}^{id} + G_{SS}{}^{id} - 2G_{WS}{}^{id} = 0$. The "volume corrected" (Matteoli 1997) preferential solvation parameters are calculated using residual "volume-corrected" values of the Kirkwood-Buff integrals, $\Delta G_{ij} = G_{ij} - G_{ij}{}^{id}$, which then describe the preferential solvation due to the molecular interactions. The volume-corrected preferential solvation parameters are given by:

$$\delta x_{WW}{}' = x_W x_S \frac{(\Delta G_{WW} - \Delta G_{SW})}{[x_W \Delta G_{WW} + x_S \Delta G_{WS} + V_{corW}]} \tag{1.50}$$

$$\delta x_{WS}{}' = x_W x_S \frac{(\Delta G_{WS} - \Delta G_{SS})}{[x_W \Delta G_{WS} + x_S \Delta G_{SS} + V_{corS}]} \tag{1.51}$$

The local mole fractions are then given by $x_{WW}{}^{L} = x_W + \delta x_{WW}{}'$ and $x_{WS}{}^{L} = x_S + \delta x_{WS}{}'$. Representative curves of the water self-interaction volume-corrected

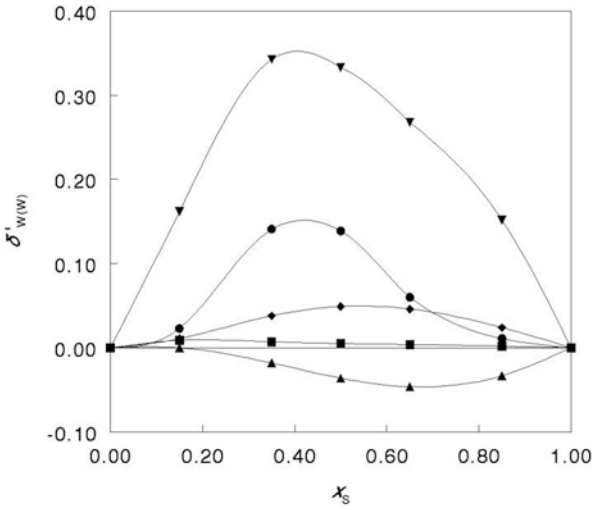

Fig. 1.5 The water self-preferential solvation parameters according to the IKBI treatment in binary mixtures of water with the co-solvents: ▼ tetrahydrofuran, ● ethanol, ♦ hexamethyl phosphoric triamide, ■ formamide, and ▲ 2-aminoethanol

preferential solvation parameters $\delta x_{WW}'(x_S)$ are shown in Fig. 1.5. Formamide is seen not to lead to appreciable self interaction of the water, contrary to tetrahydrofuran that does so, while the mutual interactions with 2-aminoethanol prevent any strong self association of the water.

Most of the solvents that are miscible with water eventually destroy its three-dimensional hydrogen bonded network. In organic-solvent-rich mixtures water tends to act as individual molecules or small clusters of them. However, in water-rich mixtures the cooperative hydrogen bonding may be enhanced, and such mixtures may have a greater extent of hydrogen bonding than pure water. One way to see this is to note that the partial molar volume of water in water-rich mixtures with some organic solvents is *larger* than the molar volume of pure water, or $V_W{}^E = V_W - V_W{}^* > 0$ (Marcus 2011). Figure 1.6. shows this for aqueous dimethyl-sulfoxide, N, N-dimethylformamide, and N, N-dimethylacetamide with data taken from Torres et al. (2006). $V_W{}^E > 0$ up to $x_S = 0.154$, 0.138, and 0.124, respectively. For the lower alcohols the data of Benson and Kiyohara (1980) lead to $V_W{}^E > 0$ up to $x_S = 0.154$ for methanol and $x_S = 0.014$ for ethanol at 25 °C (but at 10 °C $V_W{}^E > 0$ for ethanol beyond $x_S = 0.09$ according to Franks and Johnson (1962)), and $x_S \sim$ 0.11 (read from a plot) for 1,2-ethanediol (George and Sastry 2004) at 25 °C. This phenomenon means that some water is transferred from compact domains to bulky domains (having more hydrogen bonding and being more self-associating) according to the two-domain concept of water of Robinson et al. (Sect. 1.1.3). This can also be described in terms of the formation of the bulky and highly hydrogen bonded form of water in cages around the molecules of the co-solvent (Onori and Santucci 1996). However, $V_W{}^E > 0$, does not occur with some other co-solvents such as acetonitrile, dioxane, etc. Marcus 2011).

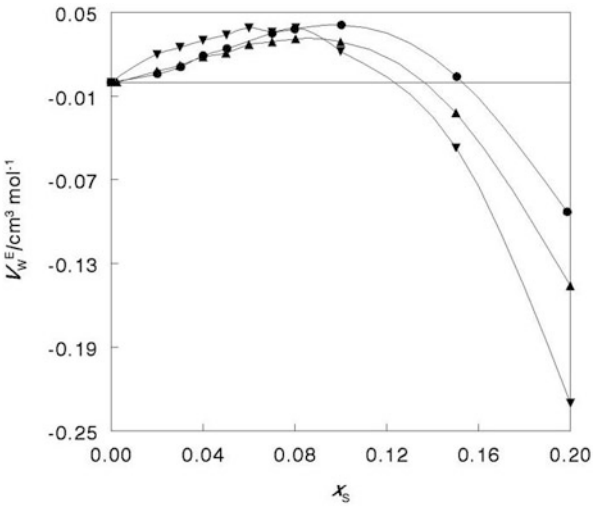

Fig. 1.6 Excess partial molar volumes of water in water-rich mixtures at 25 °C with: • dimethylsulfoxide, ▲ N, N-dimethylformamide, and ▲ N, N-dimethylacetamide. (From data of (Torres et al. 2006))

Another way to look at this enhanced hydrogen bonding in water-rich mixtures with co-solvents is in terms of the adiabatic compressibilities. These show composition dependencies that differ in form up to and beyond "signpost" values, $x_{S\,sp}$, of the co-solvent (D'Angelo et al. 1994). The $x_{S\,sp}$ are 0.11 for methanol, 0.060 for ethanol, 0.035 for 2-propanol, 0.030 for 1-propanol, and 0.025 for 2-methyl-2-propanol. A still further indication of the enhanced hydrogen bonding in water-rich aqueous alkanol mixtures is obtained from ^{17}O NMR relaxation times (Yoshida et al. 2006). The limits up to which such enhancement takes place are however larger: $x_S \sim 0.3$ for methanol, ~0.2 for ethanol, and ~0.1 for 1-propanol co-solvents. The activation energy for rotational correlation of the water molecules increases up to these limits, then diminishes. Similar observations of enhanced hydrogen bonding in water-rich mixtures of co-solvents were obtained also by other techniques mentioned in the references provided in these papers.

It is appropriate here to deal briefly with the effect of urea, $O=C(NH_2)_2$, on the structure and solvent properties of water. Although urea is not a solvent, since it is solid at ambient conditions, its aqueous solutions have been widely discussed in relation to the denaturation of proteins, possibly caused by its effects on the hydrogen bonding structure of water. A recent MD simulation study (Idrissi et al. 2010) summarizes the current state by noting that over the years controversial views were reported, based on the interpretation of experimental data and computer simulation studies, concerning the effect of urea on the structure of water. Some authors concluded that urea breaks the structure (it is chaotropic in analogy with certain salts, Chap. 3), others that it is indifferent in this respect, being well incorporated in the existing hydrogen bonded structure, and still others concluded that it enhances the structure of the water.

Concerning computer simulations, it is important to note that the structure of urea itself in aqueous solutions is rather indefinite—it reverts readily from planar

to non-planar configurations (Hermida-Ramon et al. 2007). Some simulation results (Stumpe and Grubmüller 2007) claim that urea strengthens the water structure in terms of HB energies and population. However, it is difficult to see how such claims are supported by the data, the number of HBs to water at 300 K (Fig. 7b in the paper) diminish linearly from ∼3.5 in pure water to ∼2.5 as the urea mole fraction increases to 0.29 while the total enthalpy due to hydrogen bonding per unit volume of the solution decreases (Fig. 8 in the paper) from 1.60 to 1.11 kJ mol^{-1} nm^{-3}. A more recent MD simulation study reports, on the contrary, that the structured tetrahedral arrangement of water molecules is reduced on increasing the urea mole fraction in favour of an unstructured one (Idrissi et al. 2010). This means that urea is a water structure breaker.

References

Abraham MH, McGowan JC (1987) The use of characteristic volumes to measure cavity terms in reversed phase liquid chromatography. Chromatographia 23:243–246

Abraham MH, Whiting GS, Doherty RM, Shuely WJ (1990) Hydrogen bonding. Part 14. The characterization of some *N*-substituted amides as solvents: comparison with gas-liquid chromatography stationary phases. J Chem Soc, Perkin Trans 2:1851–1857

Abraham MH, Andonian-Haftvan J, Whiting GS, Leo A, Taft RW (1994) Hydrogen bonding. Part 34. The factors that influence the solubility og gases and vapours in water at 298 K, and a new method for its determination. J Chem Soc, Perkin Trans 2:1777–1791

Abraham MH, Le J (1999) The correlation and prediction of the solubility of compounds in water using an amended solvation energy relationship. J Pharm Sci 88:858–880

Amidon GL, Yalkowsky SH, Leung S (1974). Solubility of nonelectrolytes in polar solvents II: solubility of aliphatic alcohols in water. J Pharm Sci 63:1858–1866

Amidon GL, Yalkowsky SH, Anik ST, Valvani SC (1975) Solubility of nonelectrolytes in polar solvents. V. Estimation of the solubility of monofunctional compounds in water using a molecular surface area approach. J Phys Chem 79:2239–2245

Bakker HJ, Skinner JL (2010) Vibrational spectroscopy as a probe of structure and dynamics in liquid water. Chem Rev 110:1498–1517

Barthel J, Bachhuber K, Buchner R, Hetzenbauer H (1990) Dielectric spectra of some common solvents in the microwave region. Water and lower alcohols. Chem Phys Lett 165:369–373

Bates RG (1973) Determination of pH: theory and practice. Wiley, New York

Battino R, Clever HL (2007) The solubility of gases in water and seawater. In: Letcher TM (ed) Developments and applications of solubility, RSC Publishing, Cambridge, pp. 66–77

Ben-Naim A (1972) Mixture-model approach to the theory of classical fluids. II. Application to liquid water. J Chem Phys 57:3605–3612

Ben-Naim A (1975) Structure-breaking and structure-promoting processes in aqueous solutions. J Phys Chem 79:1268–1274

Ben-Naim A (1977) Inversion of the Kirkwood-Buff theory of solutions: application to the water-ethanol system. J Chem Phys 67:4884–4890

Ben-Naim A (2009) Molecular theory of water and aqueous solutions. Part 1. Understanding water. World Scientific, New Jersey

Ben-Naim A, Marcus Y (1984) Solvation thermodynamics od non-ionic solutes. J Chem Phys 81:2016–2027

Benson GC, Kiyohara, O (1980) Thermodynamics of aqueous mixtures of nonelectrolytes. I. Excess volumes of water – n-alcohol mixtures at several temperatures. J Solution Chem 9:791–805

Bergmann U, Nordlund D, Wernet Ph, Odelius M, Petersson L, Nilsson A (2007) Isotope effects in liquid water probed by x-ray Raman spectroscopy. Phys Rev B 76:024202-01–024202-6

Bernal JD, Fowler RH (1933) A theory of water and ionic solution, with particular reference to hydrogen and hydroxyl ions. J Chem Phys 1:515–548
Buchner R, Barthel J, Stauber J (1999) The dielectric relaxation of water between 0 °C and 35 °C. J Chem Phys Lett 306:57–63
Buchner R, Hefter G (2009) Interactions and dynamics in electrolyte solutions by dielectric spectroscopy. Phys Chem Chem Phys 11:8984–8999
Cabani S, Gianni P, Mollica V, Lepori L (1981) Group contributions to the thermodynamic properties of non-ionic organic solutes in dilute aqueous solutions. J Solut Chem 10:563–595
Caldin EF, Bennetto HP (1971) Solvent effects on the kinetics of the nickel(II) and cobalt(II) ions with 2,2′-bipyridyl and 2,2′,2″-terpyridyl. J Chem Soc A 1971:2191–2198
Chang T-M, Dang LX (2008) Computational studies of liquid water and diluted water in carbon tetrachloride. J Phys Chem A 112:1694–1700
Cho CH, Urquidi J, Singh S, Park SC, Robinson GW (2002) Pressure effect on the density of water. J Phys Chem A 106:7557–7561 (and references therein)
Collie CH, Hasted JB, Ritson DM (1948) Dielectric properties of water and heavy water. Proc Roy Soc (London) B60:145–160
Cosgrove BA, Walkley J (1981) Solubilities of gases in water and deuterium oxide. J Chromatogr 216:161–167
Crovetto R, Fernandez-Prini R, Japas ML (1982) Solubilities of inert gases and methane in water and in heavy water in the temperature range of 300–600 K. J Chem Phys 76:1077–1086
D'Angelo M, Onori G, Santucci A (1994) Self-association of monohydric alcohols in water: compressibility and infrared absorption measurements. J Chem Phys 100:3107–3113
Dorsey NE (1940) Properties of ordinary water substance. Reinhold, New York (Facsimile ed., Hafner, New York, 1968)
Dunn WJ, Block JH, Pearlman RS (1986) Partition coefficient determination and estimation. Pergamon, New York
Easteal AJ, Price WE, Woolf LA (1989) Diaphragm cell for high-temperature diffusion measurements: tracer diffusion coefficients for water to 363 K. J Chem Soc, Faraday Trans 1(85):1091–1097
Eaves JD, Loparo JJ, Fecko CJ, Roberts ST, Tokmakoff A, Geissler PL (2005) Hydrogen bonds in liquid water are broken only fleetingly. Proc Natl Acad Sci (USA) 102:13019–13022
Eisenberg D, Kauzmann W (1969) The structure and properties of water. Clarendon Press, Oxford
Elsaesser T (2009) Two-dimensional infrared spectroscopy of intermolecular hydrogen bonds in the condensed phase. Acc Chem Res 42:1220–1228
Fisenko AI, Malomuzh NP, Oleynik AV (2008) To what extent are thermodynamic properties of water argon-like? Chem Phys Lett 450:297–301
Frank HS, Wen WY (1957) Structural aspects of ion-solvent interaction in aqueous solutions: a suggested picture of water structure. Disc Faraday Soc 24:133–140
Franks F (ed) (1972–1982) Water: a comprehensive treatise, vol I–VII. Plenum, New York
Franks F, Johnson HH (1962) Accurate evaluation of partial molar properties. Trans Faraday Soc 58:656–661
Fukasawa T, Sato T, Watanabe J, Hama Y, Kunz W, Buchner R (2005) Relation between dielectric and low-frequency Raman spectra of hydrogen-bond liquids. Phys Rev Lett 95:197802-1–197802-4
George J, Sastry NV (2004) Partial excess molar volumes, partial excess isentropic compressibilities and relative permittivities of water + ethane-1,2-diol derivative and water + 1,2-dimethoxyethane at different temperatures. Fluid Phase Equil 216:307–332
Gerrard W (1976) Solubility of gases and liquids. Plenum, New York
Haggis GH, Hasted JB, Buchanan TJ (1952) The dielectric properties of water in solutions. J Chem Phys 20:1452–1465
Hansch C, Leo A (1979) Substituent constants for correlation analysis in chemistry and biology. Wiley, New York
Hardy EH, Zygar A, Zeidler MD, Holz M, Sacher FD (2001) Isotope effect on the translational and rotational motion in liquid water and ammonia. J Chem Phys 114:3174–3181

Harned HS, Owen BB (1958) The physical chemistry of electrolyte solutions, 3rd ed. Reinhold, New York
Head-Gordon T, Hura G (2002) Water structure from scattering experiments and simulations. Chem Rev 102:2651–2670
Hermida-Ramon JM, Öhrn A, Karlström G (2007) Planar or nonplanar: what is the structure of urea in aqueous solutions? J Phys Chem B 111:11511–11515
Hildebrand JH, Scott RL (1950) The solubility of nonelectrolytes, 3rd ed. Dover, New York
Huyskens PL, Siegel GG (1988) Fundamental questions about entropy. I. Definitions: Clausius or Boltzmann? Bull Soc Chim Belg 97:809–814
Idrissi A, Gerrard M, Damay P, Kiselev M, Puhovsky Y, Cinar E, Lagant P, Vergoten G (2010) The effect of urea on the structure of water: a olacular dynamics simulation. J Phys Chem B 114:4731–4738
Jain N, Yalkowsky SH (2001) Estimation of the aqueous solubility I. Application to organic nonelectrolytes. J Pharm Sci 90:234–252
Jain N, Yalkowsky SH (2010) Prediction of aqueous solubility from SCRATCH. Int J Pharm 385:1–5
Jansco G, Van Hook WA (1974) Condensed phase isotope effects (especially vapour pressure isotope effects). Chem Rev 74:689–760
Jenkins HBD, Roobottom HK (2002) Lattice energies. In: Lide D (ed) CRC handbook of chemistry and physics, 2001–2002, 82nd ed. CRC Press, Baton Rouge, pp. 12-22–12-36
Jonas J, DeFries T, Wilbur DJ (1976) Molecular motions in compressed liquid water. J Chem Phys 65:582–588
Kamlet MJ, Abboud J-LM, Abraham MH, Taft RW (1983) Linear solvation energy relationships. 23. A comprehensive collection of the solvatochromic parameters π^*, α, and β, and some methods for simplifying the generalized solvatochomic equation. J Org Chem 48:2877–2887
Kamlet MJ, Abraham MH, Doherty RM, Taft RW (1984) Solubility properties in polymers and biological media. 4. Correlation of octanol/water partition coefficients with solvatochromic parameters. J Am Chem Soc 106:464–466.
Kamlet MJ, Doherty RM, Abboud J-LM, Abraham MH, Taft RW (1986) Linear solvation energy relationships: 36. Molecular properties governing solubilities of organic nonelectrolytes in water. J Pharm Sci 75:338–349
Kamlet MJ, Doherty RM, Abraham MH, Carr PW, Doherty F, Taft RW (1987) Linear solvation energy relationships. 41. Important differences between aqueous solubility relationships for aliphatic and aromatic solutes. J Phys Chem 91:1996–2004
Kamlet MJ, Doherty RM, Abraham MH, Marcus Y, Taft RW (1988) Linear solvation energy relationships. 46. An improved equation for correlation and prediction of octanol/water partition coefficients of organic nonelectrolyes (including strong hydroge bond donor solutes). J Phys Chem 92:5244–5255
Krynicky K (1966) Proton spin-lattice relaxation in pure water between 0 °CD and 100 °C. Phisica 32:167–178
Kumar R, Schmidt JR, Skinner JL (2007) hydrogen bond definitions and dynamics in liquid water. J Chem Phys 126:204107-1–204107-12
Kumar R, Skinner JL (2008) Water simulation model with explicit three-molecule interactions. J Phys Chem B 112:8311–8318
Laage D, Hynes JT (2006a) Do more strongly hydrogen-bonded water molecules reorient more slowly? Chem Phys Lett 433:80–85
Laage D, Hynes JT (2006b) A Molecular Jump Mechanism of Water Reorientation. Science 311:832–835
Lagodzinskaya GV, Yunda NG, Manelis GB (2002) H^+-catalyzed symmetric proton exchange in neat liquids with a network of N–H–N and O–H–O hydrogen bonds and molecular mechanism of Grotthus proton migration. Chem Phys 282:51–61
Lamb WJ, Brown DR, Jonas JJ (1981) Temperature and density dependence of the proton lifetime min liquid water. Phys Chem 85:2883–1887
Lawrence CP, Skinner JL (2003) Vibrational spectroscopy of HOD in liquid D_2O. III. Spectral diffusion, and hydrogen-bonding and rotational dynamics. J Chem Phys 118:264–272

Leahy DJ (1986) Intrinsic molecular volume as a measure of the cavity term in linear solvation energy relationships: octanol-water partition coefficients and aqueous solubilities. Pharm Sci 75:629–636
Light TS (1984) Temperature dependence and measurement of resistivity of pure water. Anal Chem 56:1138–1142
Luck WAF (1998) The importance of cooperativity for the properties of liquid water. J Mol Struct 448:132–142
Malenkov GG (2006) Structure and dynamics of liquid water. J Struct Chem 47:S1–S31
Malenkov GG, Tytik DL, Zheligovskaya EA (2003) Structural and dynamic heterogeneity of computer simulated water: ordinary, supercooled, stretched and compressed. J Mol Liq 106:179–198
Marcus Y(1983) A quasi-lattice quasi-chemical theory of preferential solvation of ions. Austr J Chem 36:1719–1738
Marcus Y (1985) Ion solvation. Wiley, Chichester
Marcus Y (1986) The hydration entropies of ions and their effects on the structure of water. J Chem Soc, Faraday Trans 1(82):233–240
Marcus Y (1989) Preferential solvation. Part 3. Binary solvent mixtures. J Chem Soc, Faraday Trans 1(85):381–388
Marcus Y (1990) Preferential solvation in mixed solvents. Part 5. Binary mixtures of water and organic solvents. J Chem Soc, Faraday Trans 1(86):2215–2224
Marcus Y (1992) The structuredness of solvents. J Solution Chem 21:1217–1230
Marcus Y (1994) Viscosity B-coefficients, structural entropies and heat capacities, and the effects of ions on the structure of water. J Solution Chem 23:831–847
Marcus Y (1995) Preferential solvation in mixed solvents. Part 7. Binary mixtures of water and alkanolamines. J Chem Soc, Faraday Trans 91:427–430
Marcus Y (1996) The structuredness of solvents. 2. Data for ambient conditions. J Solution Chem 25:455–469
Marcus Y (1997) Ion properties. Dekker, New York
Marcus Y (1998) The properties of solvents. Wiley, Chichester
Marcus Y (1999) The structuredness of water at elevated temperatures along the saturation line. J Mol Liq 79:151–165
Marcus Y (2001) Preferential solvation in mixed solvents. 10. Completely miscible aqueous co-solvent binary mixtures at 298.15 K. Monatsh Chem 132:1387–1411
Marcus Y (2002a) Solvent mixtures. Dekker, New York
Marcus Y (2002b) Preferential solvation in mixed solvents. 11. Eight additional completely miscible aqueous co-solvent binary mixtures and the relationship between the volume-corrected preferential solvation parameters and the structures of the co-solvents. Phys Chem Chem Phys 4:4462–4471
Marcus Y (2003) Preferential Solvation in Mixed Solvents. 12. Aqueous glycols. J Mol Liquids 107:109–126
Marcus Y (2008) On the relation between thermodynamic, transport and structural properties of electrolyte solutions. Elektrokhimiya 44:18–31; Russ J Electrochem 44:16–27
Marcus Y (2009) The effects of ions on the structure of water: structure breaking and making. Chem Rev 109:1346–1370
Marcus Y (2010) Cohesive energy of molten salts and its density. J Chem Thermodyn 42:60–64
Marcus Y (2011) Water structure enhancement in water-rich binary solvent mixtures. J Mol Liq 158:23–26
Marcus Y, Ben-Naim A (1985) A study of the structure of water and its dependence on solutes, based on the isotope effects on solvation thermodynamics. J Chem Phys 83:4744–4475
Matteoli E (1997) a study on Kirkwood-Buff integrals and preferential solvation in mixtures with small deviations from ideality and/or with size mismatch of components. Importance of a proper reference system. J Phys Chem B 101:9800–9810.
Matteoli E, Lepori L (1984) Solute-solute interactions in water. II. An analysis through the Kirkwood-Buff integrals for 14 organic solutes. J Chem Phys 80:2856–2863

Näslund L-Å, Lüning J, Ufuktepe Y, Ogasawara H, Wernet P, Bergmann U, Pettersson LGM, Nilsson A (2005) X-ray absorption spectroscopy measurements of liquid water. J Phys Chem B 109:13835–13839

Novikov AG, Rodnikova MN, Savostin VV, Sobolev OV (1994) Study of the diffusion of cesium ions in an aqueous solution of CsCl by a method of quasielastic scattering of slow neutrons. Zh Fiz Khim 68:1982–1986

Onori G, Santucci A (1996) Dynamical and structural properties of water/alcohol mixtures. J Mol Liq 69:161–181

Paesani F, Zhang W, Case DA, Cheatham TE III, Voth GA (2006) An accurate and simple quantum model for liquid water. J Chem Phys 125:184507-1–184507-11

Pentz L, Thornton ER (1967) Isotope effects on the basicity of 2-nitrophenoxide, 2,4-dinitrophenoxide, hydroxide, and imidazole in protium oxide-deuterium oxide mixtures. J Am Chem Soc 89:6931–6938

Poltev VI, Grokhlina TA, Malenkov GG (1984) Hydration of nucleic acid bases studied using novel atom-atom potential functions. J Biomol Struct Dyn 2:413–429

Pratt LR (2002) Introduction. Water Chem Rev 102:2625–2526 (and the other papers in this issue)

Prendergast D, Galli G (2006) X-ray absorption spectra of water from first principles calculations. Phys Rev Lett 96:215502-1–215502-4

Prendergast D, Grossman JC, Galli G (2005) The electronic structure of liquid water within density-functional theory. J Chem Phys 127:014501-1–014501-10

Pupezin J, Jakli G, Jansco G, Van Hook WA (1972) The vapour pressure isotope effect in aqueous systems. I. H_2O-D_2O ($-64\,^\circ$ to $100\,^\circ$) and $H_2^{16}O$-$H_2^{18}O$ ($-17\,^\circ$ to $16\,^\circ$). J Phys Chem 76:743–756

Riddick JA, Bunger WB, Sakano TK (1986) Organic solvents, 4th ed. Wiley-Interscience, New York

Rode BM (2007) personal communication

Röntgen WC (1892) Ann Phys Chim (Wied.) 45:91 (quoted by Vedamuthu et al. (1994))

Ropp J, Lawrence C, Farrar TC, Skinner JL (2001) Rotational motion in liquid water is anistropic: a nuclear magnetic resonance and molecular dynamics simulation study. J Am Chem Soc 123:8047–8052

Ruelle P, Kesselring UW (1998) The hydrophobic effect. 2. Relative importance of the hydrophobic effect on the solubility of hydrophobes and pharmaceuticals in H-bonded solvents. J Pharm Sci 87:998–1014

Rull F (2002) Structural investigation of water and aqueous solutions by Raman spectroscopy. Pure Appl Chem 74:1859–1870

Samoilov OYa (1957) A new approach to the study of hydration of ions in aqueous solutions. Disc Faraday Soc 24:141–146

Scharlin P, Battino R, Silla E, Tunon I, Pascual-Ahuir JL (1998) Solubility of gases in water: correlation between solubility and the number of water molecules in the first solvation shell. Pure Appl Chem 70:1895–1904

Schmidt JR, Roberts ST, Loparo JJ, Tokmakoff A, Fayer MD, Skinner JL (2007) Are water simulation models consistent with steady-state and ultrafast vibrational spectroscopy experiments? Chem Phys 341:143–157

Shinoda K (1978) Principles of solution and solubility. Dekker, New York

Smith JD, Cappa CD, Wilson KR, Messer BM, Cohen RC, Saykally RJ (2004) Energetics of hydrogen bond network rearrangements in liquid water. Science 306:851–853

Smith JD, Cappa CD, Wilson KR, Messer BM, Drisdell WS, Cohen RC, Saykally RJ (2006) Probing the local structure of liquid water by x-ray absorption spectroscopy. J Phys Chem B 110:20038–200345

Soper AK (2000) The radial distribution functions of water and ice from 220–673 K at pressures up to 400 MPa. Chem Phys 258:121–137

Soper AK (2010) Recent water myths. Pure Appl Chem 82:1855–1867

Sprunger L, Acree WE, Abraham MH (2007) Linear free energy relationship correlation of the distribution of solutes between water and sodium dodecyl sulfate (SDS) micelles and between gas and sds micelles. J Chem Inf Model 1808–1817

Sprunger LM, Gibbs J, Acree WE, Abraham MH (2009) Linear free energy relationship correlation of the distribution of solutes between water and cetytrimethylammonium bromide (CTAB) micelles. QSAR Combin Sci 28:72–88

Stumpe MC, Grubmüller H (2007) Aqueous urea solutions: structure, energetics, and urea aggregation. J Phys Chem B 111:6220–6228

Svishchev IM, Kusalik PG (1994) Dynamics in liquid H_2O, D_2O, and T_2O: a comparative simulation study. J Phys Chem 98:728–733

Taft RW, Abraham MH, Doherty RM, Kamlet MJ (1985) The molecular properties governing solubilities of organic nonelectrolytes in water. Nature 313:384–386

Tanaka H (2000) Simple physical model of liquid water. J Chem Phys 112:799–809

Tokushima T, Harada Y, Takahashi O, Senba Y, Ohashi H, Pettersson LGM, Nilsson A, Shin A (2008) High resolution X-ray emission spectroscopy of liquid water: the observation of two structural motifs. Chem Phys Lett 460:387–400

Torres RB, Marchiore ACM, Volpe PLO (2006) Volumetric properties of binary mixtures of (water + organic solvents) at temperatures between T = 288.15 K and T = 303.15 K at p = 0.1 MPa. J Chem Thermodyn 38:526–541

Valvani SC, Yalkowsky SH, Amidon GL (1976) Solubility of nonelectrolytes in polar solvents. VI. Refinements in molecular surface e area computations. J Phys Chem 80:829–835

Van der Spoel D, Van Maaren PJ, Berendsen JC (1998) A systematic study of water models for molecular simulation: derivation of water models optimized for use with a reaction field. J Chem Phys 108:10220–10230

Vedamuthu M, Singh S, Robinson GW (1994) properties of liquid water: origin of the density anomalies. J Phys Chem 98:2222–2230

Voloshin VP, Naberukhin YuI (2009) Hydrogen bond lifetime distributions in computer-simulated water. J Struct Chem 50:78–89

Voloshin VP, Malenkov GG, Naberukhin YuI (2007) Description of collective effects in computer models of water. J Struct Chem 48:1066–1072

Wagman DD, Evans WH, Parker VB, Schumm RH, Harlow I, Bailey SM, Churney KL, Nuttall RL (1982) The NBS tables of chemical thermodynamic properties. J Phys Chem Ref Data 11(Suppl. 2):2-1–2-390

Wagner W, Pruss A (2002) The IAPWS formulation 1995 for the thermodynamic properties of ordinary water substance for general and scientific use. J Phys Chem Ref Data 31:387–535

Walrafen GE (2004) Effects of equilibrium H-bond distance and angle changes on Raman intensities from water. J Chem Phys 120:4868–4876

Wang RLC, Kreuzer HJ, Grunze M (2006) Theoretical modelling and interpretation of x-ray absorption spectra of liquid water. Phys Chem Chem Phys 8:4744–4751

Wilhelm E, Battino R, Wilcock RJ (1977) Low-pressure solubility of gases in liquid water. Chem Rev 77:219–262

Woessner DE (1964) Molecular reorientation in liquids. Deuteron quadrupole relaxation in liquid deuterium oxide and perdeuterobenzene. J Chem Phys 40:2341–2348

Xenides D, Randolf BR, Rode BM (2006) Hydrogen bonding in liquid water: an ab initio QM/MM MD simulation study. J Mol Liquids 123:61–67

Yalkowsky SH, Banerjee S (1992) Aqueous solubility. Dekker, New York

Yalkowsky SH, Valvani SC (1980) Solubility and partitioning I: solubility of nonelectrolytes in water. J Pharm Sci 69:912–922

Yalkowsky SH, Pinal R, Banerjee SJ (1988) Water solubility: a critique of the solvatochromic approach. Pharm Sci 77:74–77

Yang G, Ran Y, Yalkowsky SH (2002) Prediction of the aqueous solubility: comparison of the general solubility equation and the method using an amended solvation energy relationship. J Pharm Sci 91:517–533

Yoshida K, Kitajo A, Yamaguchi T (2006) ^{17}O NMR relaxation study of dynamics of water molecules in aqueous mixtures of methanol, ethanol, and 1-propanol over a temperature range of 283–403 K. J Mol Liq 126:158–163

Chapter 2
Ions

Ions, defined as particles that carry electrical charges, exist in condensed phases (solids and liquids) as electrically neutral combinations of cations and anions: electrolytes. The ions may be bound or relatively free to migrate. Ions may be monatomic, such as K^+or Cl^-, they may consist of a few atoms, such as ammonium, $NH_4{}^+$, or sulfate, $SO_4{}^{2-}$, or even considerably more than a few, such as nitrobenzoate, $O_2NC_6H_4CO_2{}^-$, or tetrapropylammonium, $(C_3H_7)_4N^+$. They may even consist of very many atoms and may carry many dispersed charges and are then referred to as poly-ions, constituting the dissociated part of polyelectrolytes. Some biological moieties, such as polypeptides, proteins, and nucleic acids, as well as suitable synthetic molecules are examples of polyelectrolytes.

The treatment in the following deals mostly with ions in solution, though some discussion of isolated ions is also required. In dilute solutions strong electrolytes, such as NaCl, are those that are fully dissociated into their constituent ions, though they may associate to ion pairs in more concentrated ones, e.g., Na_2SO_4, forming $Na^+ + NaSO_4{}^-$. Weak electrolytes are hardly at all dissociated into ions in solution, but have the capability of doing so under special circumstances. They are ionogenic, that is, capable of ionizing by reaction with some component of the solution, including the solvent itself. A weak acid, such as benzoic acid, C_6H_5COOH, may donate a hydrogen ion to a basic environment and turn into an anion, $C_6H_5CO_2{}^-$. A weak base, such as aniline, $C_6H_5NH_2$, may add-on a hydrogen ion in an acidic medium and turn into a cation, anilinium, $C_6H_5NH_3{}^+$. Zwitterions may turn into anions or cations, depending on the pH of the medium, an example being alanine:$^+H_3NCH(CH_3)COO^-$, turning into$^+H_3NCH(CH_3)COOH$ in acidic media and into $H_2NCH(CH_3)COO^-$ in basic ones. The properties discussed in this chapter pertain to the ions that have been formed, either by strong electrolytes directly on their dissolution or by weak electrolytes in suitable media.

The generalized symbol of an ion (but not of a poly-ion) of any charge sign is $I^{z\pm}$, with an integral charge number z. As a part of the symbol for a quantity pertaining to an ion the subscript $_I$ is used without the charge. As a part of the symbol for a quantity pertaining to an electrolyte or to a neutral combination of ions the subscript $_E$ is used. Subscripts $_+$ and $_-$ represent generalized cations and anions with no regard to z.

Y. Marcus, *Ions in Water and Biophysical Implications,*
DOI 10.1007/978-94-007-4647-3_2, © Springer Science+Business Media Dordrecht 2012

2.1 The Properties of Isolated Ions

When an ion exists in an ideal gaseous state, that is, when it is devoid of interactions with other particles or its surroundings in general, it is termed an isolated ion. Commonly, isolated ions consist of relatively few atoms, but some quite large ones are produced in mass spectrometers. They may also be the centers of clusters consisting of the ion proper surrounded by a small number of solvent molecules.

The ionization process leading from an atom, a radical, or a molecule to a cation may proceed in several stages of losing an electron. It requires the investment of energy and is expressed by the ionization potential, $\sum I_p$, the sum being over the successive ionization stages. The electron capture by an atom, a radical, or a molecule to form an anion releases energy that is expressed as the electron affinity, *EA*, of such a moiety. However, the capture of an electron by an anion that already carries a negative charge is an unlikely event. Therefore, only a single electron may generally be added to a neutral species in the *EA* process. These energies, $\sum I_p$ and *EA*, in electron-volt units (1 eV/particle = 96.483 kJ mol^{-1}), have been reported for many ions in the book by Marcus (1997).

The primary characteristics of isolated ions are the amount of electrical charge they carry, their mass, their shape, and their size. The amount of charge is given in terms of a multiple, z_I, of the elementary units of the charge of a proton (positive) or an electron (negative), namely $e = 1.60218 \times 10^{-19}$ C. Within the scope of this book the absolute values of z_I for isolated ions range from 1 to 4 for monatomic ones and possibly somewhat larger for some complex ions. Highly ionized atoms that may be produced artificially or result from nuclear reactions are not considered here.

The masses of ions are generally specified as their molar mass, that is, of Avogadro's number, $N_A = 6.02214 \times 10^{23}$ mol^{-1}, of ions. The units of the molar mass, M_I, are therefore kg mol^{-1}, but generally M_I is given in g mol^{-1}.

The shape of monatomic ions is, of course, strictly spherical when isolated, but they may be deformed slightly by external forces (strong electrical fields). Ions that consist of several atoms may have any shape, but common ones are planar (NO_3^-, CO_3^{2-}), tetrahedral (NH_4^+, SO_4^{2-}), octahedral ($Fe(CN)_6^{4-}$), elongated (SCN^-), or more irregular ($CH_3CO_2^-$, HCO_3^-).

The sizes of ions in the isolated state, however, are difficult to specify, because the electrons in their periphery extend indefinitely around the inner electronic shells and the nuclei of the atoms. The sizes of monatomic ions may be compared with the iso-electronic noble gases (of known collision diameters), e.g., $O^{2-} > F^- > Ne > Na^+ > Mg^{2+}$. The sizes are expected to diminish in this series, because of the increasing positive nuclear charge that pulls-in the electrons. Stokes (1964) took up this idea with the quantum mechanical scaling principle, and calculated radii for isolated monatomic ions, $r_I^g = r(I^{z\pm}, g)$. These were then used to calculate the self-energy of the ions, used for the estimation of their Gibbs energies of hydration, see Sect. 2.3.3. However, such values of r_I^g have not been taken up by other investigators since then.

The self-energy of an isolated ion ($I^{z\pm}$, g) is due to its being charged and is

$$E_{\text{self}}(I^{z\pm}, g) = \frac{N_A z^2 e^2}{4\pi\varepsilon_0 r_I^g} \tag{2.1}$$

per mole of isolated ions. Here $\varepsilon_0 = 8.85419 \times 10^{-12} C^2\,J^{-1}m^{-1}$ is the permittivity of free space, and r_I^g is the radius of the ion. As stated above, the size of an isolated ion is an ill defined quantity, so must be its radius, hence the self-energy.

On the other hand, thermodynamic quantities that pertain to the formation of isolated ions from the elements in their standard states are well defined. The standard molar Gibbs energy and the enthalpy of formation, $\Delta_f G^\circ(I^{z\pm}, g)$ and $\Delta_f H^\circ(I^{z\pm}, g)$, of many ions have been reported. The standard molar entropy and constant-pressure heat capacity, $S^\circ(I^{z\pm}, g)$ and $C_P^\circ(I^{z\pm}, g)$, of isolated ions are also well defined quantities and have been reported. Such data are generally available for the standard temperature $T^\circ = 298.15$ K and pressure $P^\circ = 100$ kPa, and suitable sources are the NBS tables (Wagman et al. 1982) and the book by Marcus (1997). The standard molar volume of an isolated ion is trivial, being the same for all ions: $V^\circ(I^{z\pm}, g) = RT^\circ/P^\circ = 0.02479\,m^3\,mol^{-1}$, where $R = 8.31451\,J\,K^{-1}\,mol^{-1}$ is the gas constant.

Most ions are diamagnetic, that is, they are repulsed out from a magnetic field; their molar magnetic susceptibilities, χ_{Im}, range from a few to several tens of the unit (-10^{-12} m^3 mol^{-1}), as reported in (Marcus 1997). Ions that have one or more unpaired electrons in their electronic shells are paramagnetic and are attracted into a magnetic field. For a paramagnetic ion having n unpaired electrons $\chi_{Im} = +1.676n(n+2) \times 10^{-9}$ m^3 mol^{-1} at $T^\circ = 298.15$ K. Molar magnetic susceptibilities, thus, have the dimensions of molar volumes.

The polarizibility, α_I, of an ion also has the dimension of a volume, of the order of 10^{-30} m^3 per ion. The molar refractivity (at infinite frequency) is proportional to the polarizability:

$$R_{I\infty} = \left(\frac{4\pi N_A}{3}\right)\alpha_I = 2.5227 \times 10^{24}\alpha_I \tag{2.2}$$

The molar refractivity is obtained experimentally for neutral species, and generally the refractive index at the sodium D line (589 nm), n_D, is used to obtain the molar refractivity R_D in lieu of the infinite wavelength value R_∞. The Lorenz-Lorentz expression is used:

$$R_D = \frac{V(n_D{}^2 - 1)}{n_D{}^2 + 2} \tag{2.3}$$

where $V = (M/\rho)$ is the molar volume and M and ρ are the molar mass and the density. The molar refractivities are not very sensitive to the environment in which an ion is situate (in a condensed phase) nor to its concentration (when in solution). In order to ascribe a molar refractivity (and a polarizability) to an individual ion, the experimental values must be split appropriately between the cation and the anion.

There is no theoretically valid way to do this, so an empirical expedient is resorted to, namely $R_D(Na^+) = 0.65\,cm^3\ mol^{-1}$ at 25 °C (Heydweiler 1925). The temperature coefficient of R_D is rather small, approximately $+0.01\,cm^3\ mol^{-1}$.

A mild correlation of the polarizabilities exists with the 'softness' that can be ascribed to the ions. The softness is related to the difference between the energetics of formation of the ion from the neutral species on the one hand (loss or gain of electrons) and its enthalpy of hydration (Sect. 2.3.1) on the other. In the hydration process the charge on the ion itself is neutralized to some extent by the gain or loss of pairs of electrons by coordination with the solvent. The softness parameter was given normalized numerical values by Marcus (1986), for cations according to:

$$\sigma_+ = \frac{\frac{\sum I_p + \Delta_{hydr}H^\infty(C^{z+})}{z_+} - I_p(H^+) + \Delta_{hydr}H^\infty(H^+)}{I_p(H^+) + \Delta_{hydr}H^\infty(H^+)} \tag{2.4}$$

and for anions according to:

$$\sigma_- = \frac{\frac{-EA - \Delta_{hydr}H^\infty(A^{z-})}{z_-} - (EA(H)) - \Delta_{hydr}H^\infty(OH^-)}{-EA(H) - \Delta_{hydr}H^\infty(OH^-)} \tag{2.5}$$

The aqueous hydrogen and hydroxide ions are arbitrarily assigned softness values of zero and the dimensionless values for cations and anions are then related to these values. They have been listed for many ions (Marcus 1986, 1977); positive values of the softness parameter denote 'soft' ions and negative values denote 'hard' ions. As said, for soft ions there is some correlation with their polarizabilities but for hard ions the correlation is much better with the electric field strength, $z_1 e/r_1^2$, instead.

The properties of a selected list of ions in the isolated state are shown in Table 2.1.

2.2 The Properties of Aqueous Ions

The electrostatic interactions of the cations and anions making up an electrolyte in aqueous solutions compete with the thermal movement of all the particles in the solution, ions and water molecules, and are screened by the high dielectric permittivity of the water. The overall interactions, involving ion hydration and effects of ions on the water structure, in addition to ion-ion interactions and those of the hydrogen bonded network of water, are quite complicated. Approximations have to be applied in order to handle the resulting behavior of the ions theoretically or by means of computer simulations.

The simplest approximation is the '*restricted primitive model*' that considers the ions as charged conducting spheres dispersed uniformly in a continuum fluid made up of a compressible dielectric. The ions are characterized by their charges (sign and magnitude) and sizes (radii), and are assumed to be spherical. The solvent, whether single or a mixture, is characterized by its permittivity, compressibility, and

Table 2.1 Properties of some isolated ions (Marcus 1997)

Ion	z	M_I (g mol^{-1})	$\Delta_f H_I^\circ$ (kJ mol^{-1})	$\Delta_f G_I^\circ$ (kJ mol^{-1})	S_I° (J K^{-1} mol^{-1})	C_{pI}° (J K^{-1}mol^{-1})	$\sum I_p/EA$ (eV)	$\chi_{mI} - 10^{-12}$ (m^3 mol^{-1})	$R_{DI}10^{-6}$ (m^3 mol^{-1})	σ_+ or σ_-
H^+	1	1.008	1,536.2	1,523.2	108.9	20.8	1,318	−6.6	−0.1	0
Li^+	1	6.94	685.8	685.8	113.0	20.8	526	−3	0.08	−1.02
Na^+	1	22.94	609.4	580.5	148.0	20.8	502	2.3	0.65	−0.60
K^+	1	39.10	514.3	487.3	154.6	20.8	425	11.2	2.71	−0.53
Cs^+	1	132.91	458	433	169.9	20.8	382	34	6.89	−0.54
NH_4^+	1	18.04	630	681	186.3	34.9	458	11.5	4.7	−0.60
$(CH_3)_4N^+$	1	74.15	546	734	331.9	109.6		65	22.9	
Mg^{2+}	2	24.31	2,348.5	2,300.3	148.7	20.8	2,201		−0.7	−0.41
Ca^2	2	40.08	1,925.9	1,892.1	154.9	20.8	1,748	−1	1.59	−0.66
Ba^{2+}	2	137.33	1,660	1,628	170.4	20.8	1,480	21.5	5.17	−0.66
Fe^{2+}	2	55.85	2,749.9	2,689.6	180.3	25.9	2,334	19.6*	2.1	−0.16
Fe^{3+}	3	55.85	5,712.8	5,669.1	174.0	20.8	5,296	15.6*	3.2	0.33
La^{3+}	3	138.91	3,905	3,771	170.5	20.8	3,474	20	2.74	−0.75
F^-	−1	18.99	256	269	145.6	20.8	32.8	13	2.21	−0.66
Cl^-	−1	35.45	−233.1	−241.4	154.4	20.8	−349	28	8.63	−0.09
Br^-	−1	79.91	−219.1	−245.1	163.6	20.8	−324	39	12.24	0.17
I^-	−1	126.91	−197	−230.2	169.4	20.8	−295	57	18.95	0.50
SCN^-	−1	58.08			166.5	43.2	−207	35	17	0.85
NO_3^-	−1	62.01	−320	−272.8	245.2	44.7	−378	23	10.43	0.15
ClO_4^-	−1	99.45	−344	−266.8	263.0	62.0	−454	34	12.77	−0.30
$CH_3CO_2^-$	−1	59.04	−504.2	−464.1	278.7	61.4	326	32.4	13.87	−0.22
HCO_3^-	−1	61.02	−738	−702	257.9	50.6			10.9	
$H_2PO_4^-$	−1	96.99	−1,280	−1,190	286.7	62.5			14.6	
CO_3^{2-}	−2	60.01	−321	−300.9	246.1	44.4	226	34	11.45	−0.50
SO_4^{2-}	−2	96.07	−758	−704.8	363.6	62.4	1,660	40	13.79	−0.38
HPO_4^{2-}	−2	95.98			283.0	67.8				
PO_4^{3-}	−3	94.97			266.4	65.4	−657	50	15.1	−0.78

Paramagnetic ions are marked by *

thermal expansibility. The properties of the aqueous ions may then be estimated by the application of electrostatic theory and compared with the experimental values.

However, there are very few experimental determinations that can be applied unambiguously to individual ions in aqueous solution. Only as a thought process, may a single ion $I^{z\pm}$ be transferred from the ideal gas phase into water, but this process involves the passage through the gas-water interface. Such a passage is connected with not well defined consequences. Once an individual ion is in solution, its properties depend in principle on its location with respect to the surface and the walls of the vessel, due to its electric field. It is assumed that when such a thought process is carried out simultaneously for ions of opposite matching charges, the effects of the passage through the gas-water interface cancel out, so that valid quantities can be derived from the process.

The more common process that can be carried out experimentally is to dissolve in water an entire electrolyte, consisting of a matched number of cations and anions to produce a neutral species. Conditions can be chosen for approximating infinite dilution as a limit of extrapolation from low, finite concentrations. This limit corresponds to the dissolution of an infinitesimal amount of electrolyte in a finite amount of water or a mole of electrolyte in a huge amount of water. It is then possible to deal with the molar quantities pertaining to the aqueous electrolyte at infinite dilution. One must still devise some means to deduce from the measured quantities those pertaining to the individual ions.

At infinite dilution each ion is surrounded by solvent molecules only and is remote from other ions and does not interact with them. The individual ionic quantities contributing to the measured molar properties of the infinitely dilute electrolyte are, therefore, additive. They are weighted by their stoichiometric coefficients in the electrolyte: ν_+ cations C^{z+} and ν_- anions A^{z-}. For a 1:1 electrolyte such as KBr $\nu_+ = \nu_- = z_+ = |z_-| = 1$, for a 1:2 electrolyte such as $CaCl_2$ $\nu_+ = 1, z_+ = 2, \nu_- = 2$ and $|z_-| = 1$. From the additivity follows that if the value for some one ion is known, those of all other ions can be derived by subtraction of this value, appropriately weighted, from the values for electrolytes containing it, and so forth for other electrolytes. So-called '*conventional*' values are obtained when the value zero is assigned to the aqueous hydrogen ion, $Y^\infty(H^+, aq) = 0$ at all temperatures, Y^∞ being any additive property. Sums of appropriately weighted conventional values of cations, ${Y^\infty}_+^{conv}$, and of anions, ${Y^\infty}_-^{conv}$, represent the values for electrolytes, even those not measured directly. Values of ${Y^\infty}_+^{conv}$ of cations can be compared and discussed among themselves, and similarly for anions among themselves, but they may *not* be construed as representing the actual values that individual ions have these properties.

The problem of the validity of methods for obtaining the so-called '*absolute*' property values of individual aqueous ions was discussed by Conway (1978) and more recently by Marcus (2008a) and by Hünenberger and Reif (2010). These issues are treated in the following sections dealing with the properties of aqueous ions.

It is important to bear in mind the consequences of the electric charge on the ion in aqueous solutions. The electric field at the boundary between the ion and its hydration shell is huge, of the order of many GV m^{-1}. For instance, the field right

near the surface of a sodium ion, at 0.102 nm from its center, is 138.4 GV m^{-1}. Such fields surpass many-fold fields achievable experimentally in the laboratory, these being of the order of 1 GV m^{-1}. The two most important consequences of such large fields are a high compressive pressure and dielectric electrostatic saturation at the hydration layers around an ion. The permittivity of water at very high fields is given by the non-linear dielectric effect:

$$\varepsilon_W(E) = \varepsilon_W(0) + \beta E^2 \tag{2.6}$$

with $\beta = -1.080 \times 10^{-15}$ V^{-2} m^2 that is practically temperature-independent at very high fields. Dielectric saturation prevails at a short distance from the center of an ion, $\sim 0.40|z|^{1/2}$ nm, the relative permittivity diminishing to near the optical limit of n_∞^2 (the infinite frequency refractive index squared) $\approx$1.95 at 25 °C. The dipoles of the water molecules can then no longer be oriented by external fields and the residual permittivity is due to the electronic polarization of the water molecules. The other consequence is the large electrostriction produced by the compressive pressure that the field exerts on the water near the ion. Bockris and Saluja (1972) calculated the effective pressure in the middle of the first hydration shell of ions, the numerical coefficient being valid at 25 °C with the radii in nm:

$$\frac{P_{\text{eff}}}{\text{GPa}} = 0.18305(r_I + r_W)^{-3} \tag{2.7}$$

For the sodium ion the pressure is 13.2 GPa at this site, commensurate with the highest experimental pressures that can be applied to water or electrolyte solutions in the laboratory. At such large pressures the water in the hydration shell is highly compressed, it is strongly electrostricted.

2.2.1 Hydration Numbers

A Cation has the water molecules oriented towards it with one of their lone pairs of electrons, carrying a fractional negative charge, pointing at the cation. This may result in a coordinate bond, the fractional charge penetrating an unoccupied electronic orbital of the cation. Small multivalent cations, such as Mg^{2+}, tend to form such bonds with water, with definite coordination geometries and numbers of the water molecules in the first hydration shell: 6 in a regular octahedron for Mg^{2+}. These water molecules are polarized by the charge of the cation and are therefore strongly hydrogen-bond donors to water molecules in a second hydration shell that remains with the cation as it moves in the solution.

An anion in aqueous solutions has the water molecules pointing one (or both in some cases) of their hydrogen atoms towards it, resulting in hydrogen bonds. Anions tend to be large and have a relatively small electric field, and have no definite coordination number of water molecules hydrating them. For singly charged anions the average binding of water molecules is rather small (<2). Multivalent anions,

especially oxyanions, such as CO_3^{2-} or SO_4^{2-} bind more water molecules by accepting hydrogen bonds from them, and anions such as HSO_4^- or $H_2PO_4^-$ also donate hydrogen bonds to adjacent water molecules.

Ions containing hydrophobic parts, such as $C_2H_5CO_2^-$ and $C_6H_5NH_3^+$, arrange water molecules differently around such parts, $-C_2H_5$ and $-C_6H_5$, compared with the arrangement near the hydrophilic part, $-CO_2^-$ or $-NH_3^+$. This behavior is even more characteristic of ionic surfactants with long organic chains, such as $(C_8H_{17})_3NH^+$ or $C_{12}H_{25}OSO_3^-$. These tend to associate in aqueous solutions forming micelles or other structures. Ions with hydrophobic groups in their periphery around a buried charge, such as $(C_6H_5)_4B^-$ or $(C_4H_9)_4N^+$, are generally only poorly hydrated.

Water molecules around ions are arranged in concentric shells: the nearest ones, in the first hydration shell, are relatively strongly bound to the ion and move together with it, as do at least some of the water molecules in a second hydration shell, if present. Large monatomic ions (e.g., Cs^+ and I^-) lack a well-formed second hydration shell. A second shell characterizes multiply charged small ions (e.g., Al^{3+}), the water molecules in it being hydrogen-bonded to those in the first shell more strongly than are the hydrogen bonds in pure water. Large ions with a single charge (e.g., $(C_2H_5)_4N^+$ and larger tetraalkylammonium ions) may not have a hydration shell altogether, but have the water in clathrate-like or enhanced tetrahedral ice-like structures around them as for nonionic hydrophobic solutes. Beyond the hydration shells the water molecules are still affected by the electric field of the ionic charge and the possibility of being hydrogen bonded to the inner water molecules. In this region the hydrogen-bonded structure of the water is less ordered than in pure water (see Sect. 1.1.3). Only further out from the ion does the water become bulk water, having the properties of pure water.

Hydration numbers are the time-average numbers of water molecules residing in the first hydration shells of ions (and in the second, if formed). When coordinate bonds are formed between an ion and water molecules a definite integer (primary) hydration number results, equaling the coordination number, (e.g., 4 for Be^{2+}, 6 for Mg^{2+} and Al^{3+}). If only non-directional electrostatic association takes place, then geometric constraints may occur, smaller ions having smaller hydration numbers than larger ions, although the water molecules are bonded more energetically to the former. Fractional average hydration numbers then reflect the probabilities of the temporary localization of a certain number of water molecules around such ions. There is a dynamic exchange of water molecules with the bulk water outside the hydration shells. Over time, water molecules depart from the hydration shells and others come in, resulting in a non-integer hydration number. The rate of such exchanges may be as large as 10^9 per second when no coordinate bonds are formed (e.g., for Cs^+) and as small as $10^{5.2}$ exchanges per second for Mg^{2+}, and an even much smaller rate for an ion such as Cr^{3+}.

Consideration of hydration numbers requires, of course, departure from the strict primitive model (see p. 52) since it recognizes the molecular nature of the aqueous solvent. This number must be defined operationally, since diverse methods are sensitive in different ways to the number of water molecules in the hydration shells.

In an infinitely dilute solution of an ion in water the electric field of the ion causes compression of the water in its hydration shell, electrostriction. Independently of the nature of the ion, the compression of electrostricted water at 298.15 K per mole of water is $\Delta V_{\mathrm{Welec}} = -2.9\ \mathrm{cm^3\ mol^{-1}}$. This value is obtained from the isothermal compressibility of pure water, κ_{TW}, and the pressure derivative of its relative permittivity, $(\partial \ln \varepsilon / \partial P)_T$ (Marcus 2005, 2009).

The molar electrostriction of the water by an ion at infinite dilution, ${V_{\mathrm{Ielec}}}^{\infty}$, is obtainable from a stepwise, shell-by-shell electrostatic calculation (Marcus and Hefter 1999), see below, Sect. 2.2.2.

The ratio between the molar ionic electrostriction, ${V_{\mathrm{Ielec}}}^{\infty}$, and the molar electrostriction of the water, $\Delta V_{\mathrm{Welec}}$, is:

$$ {h_{\mathrm{Ielec}}}^{\infty} = \frac{{V_{\mathrm{Ielec}}}^{\infty}}{\Delta V_{\mathrm{Welec}}} \tag{2.8} $$

and can be construed to represent the time-average hydration number of the ion.

Alternatively, the ion and the water in its first hydration shell may be considered to be non-compressible by an external pressure, the electric field having already produced the maximal possible compression. Then the hydration number is defined by the standard molar ionic compression, $(\partial {V_{\mathrm{I}}}^{\infty}/\partial P)_T$, as:

$$ {h_{\mathrm{Icomp}}}^{\infty} = 1 - \frac{(\partial {V_{\mathrm{I}}}^{\infty}/\partial P)_T}{\kappa_{\mathrm{TW}} {V_{\mathrm{W}}}^{*}} \tag{2.9} $$

Here $(\partial {V_{\mathrm{I}}}^{\infty}/\partial P)_T$ is a negative quantity. Individual ionic values of $(\partial {V_{\mathrm{I}}}^{\infty}/\partial P)_T$ are obtained from experimental values for electrolytes by assuming a value for one ion. The value $(\partial {V_{\mathrm{I}}}^{\infty}/\partial P)_T(\mathrm{Cl^-,aq}) = -16.5 \pm 1.5\ \mathrm{cm^3\ GPa^{-1}\ mol^{-1}}$ at 298.15 K was suggested (Mathieson and Conway 1974). The hydration numbers from these two methods are shown in Table 2.2 and are compared with the approximation $h_{\mathrm{I}}^{\infty} = 0.360|z|/(r_{\mathrm{I}}/\mathrm{nm})$ (Marcus 1997) (see also the end of Sect. 2.2.5), that can be used for ions for which no other value of the hydration number is available.

Hydration numbers are expected to diminish as the concentration of the electrolyte increases, mildly at low concentrations but strongly when the hydration shells of oppositely charged ions start to overlap. This concentration can be estimated from the average distance between ions in a solution that is inversely proportional to the cube root of the concentration:

$$ d^{\mathrm{av}} = {N_A}^{-1/3}\left(\sum \nu_{\mathrm{I}} c_{\mathrm{I}}\right)^{-1/3} = 1.1844\left(\sum \nu_{\mathrm{I}} c_{\mathrm{I}}\right)^{-1/3}\mathrm{nm} \tag{2.10} $$

The summation extends over all the ions present at concentrations c_{I} in M multiplied by their stoichiometric coefficients ν_{I} (Marcus 2009b). The radius of a hydrated ion, r_{Ihydr}, may be taken as the sum of the ionic radius and the diameter of a water molecule (see below), so that it is possible to estimate the concentration at which the hydration shells start to overlap: $d^{\mathrm{av}} \leq r_{\mathrm{I+hydr}} + r_{\mathrm{I-hydr}}$. It is as low as 1.43 M for aqueous NaCl and is lower still for solutions of unsymmetrical multivalent electrolytes (1:2, etc.). Below the overlap limit experimental values of $(\partial V_{\mathrm{I}}/\partial P)_T$ may be used for the estimation of the hydration numbers at finite concentrations from the expression (2.10) for h_{Icomp} given above.

Table 2.2 Properties of some ions in aqueous solutions at 298.15 K (Marcus 1997)

Ion	r[a] (nm)	V_I^{∞} ($cm^3\ mol^{-1}$)	$V_{Ielec}^{\infty b}$ ($cm^3\ mol^{-1}$)	$h_{Ielec}^{\infty b}$	$h_{Icomp}^{\infty b}$	h_{Imodel}^{∞}	S_I^{∞} ($J\ K^{-1}\ mol^{-1}$)	C_{PI}^{∞} ($J\ K^{-1}\ mol^{-1}$)
H^+	0	−5.4					−22.2	−71
Li^+	0.069	−6.4	−12.9	4.4	4.0	5.2	−8.8	−9
Na^+	0.102	−6.7	−8.6	2.9	4.5	3.5	36.8	−28
K^+	0.138	3.5	−5.9	2.0	3.5	2.6	80.3	−58
Cs^+	0.170	15.8	−4.4	1.4	1.3	2.1	111.3	−94
NH_4^+	0.148	12.4				2.4	74.7	−1
$(CH_3)_4N^+$	0.280	84.1			0.4	1.3	187.8	166
Mg^{2+}	0.072	−32.2	−52.5	11.4[c]	10.0	10.0	−182.5	−158
Ca^2	0.100	−28.9	−38.5	10.0[c]	9.0	7.2	−97.5	−169
Ba^{2+}	0.136	−23.5	−27.5		10.3	5.3	−37.8	−188
Fe^{2+}	0.078	−34.4		(11.8)[c]		9.2	−182.1	−188
Fe^{3+}	0.065	−60.2		(21.1)[c]		16.6	−382.5	−204
La^{3+}	0.105	−55.6			15.1	10.3	−284.2	−339
F^-	0.133	4.3	−6.2	2.1	6.7	2.7	8.4	−45
Cl^-	0.181	23.3	−4.0	1.4	2.0	2.0	78.7	−56
Br^-	0.196	30.2	−3.5	1.2	1.8	1.8	104.6	−60
I^-	0.220	41.7	−2.8	1.0	1.5	1.6	133.5	−50
SCN^-	(0.213)	41.2		0.5[c]	0.1[b]	1.7	166.5	42
NO_3^-	(0.200)	34.5		1.4[c]	0.7[b]	1.8	168.8	−1
ClO_4^-	0.240	49.6	−2.4	0.8		1.5	206.2	46
$CH_3CO_2^-$	(0.232)	46.2			4.0[b]	1.6	108.8	97
HCO_3^-	(0.156)	28.9			1.7[b]	2.3	120.6	18
$H_2PO_4^-$	(0.200)	34.6				1.8	114.7	37
CO_3^{2-}	(0.178)	6.7		(10.9)[c]	14.4[b]	4.0	0.9	−159
SO_4^{2-}	0.230	25.0	−13.8	4.6	10.4[b]	3.1	63.2	−138
HPO_4^-	(0.200)	18.7				3.6	10.9	−102
PO_4^{3-}	0.238	−14.1				4.5	−155.4	−283

[a]Values in parentheses are approximate since ions are not nearly spherical; see text
[b]The values from (Marcus 2009), those in parenthesis are the mean values for ions of the given charge
[c]The values from (Marcus 2005), those in parenthesis are the mean values for ions of the given charge

2.2.2 Ionic Radii in Solution

The distances d_{I-O} between the centers of ions and those of the oxygen atoms of adjacent water molecules have been measured by x-ray and neutron diffraction methods and were summarized by Marcus (1988) and by Ohtaki and Radnai (1993). When the radius of a water molecule, $r_W = 0.138$ nm, is deducted from the d_{I-O} values the results correspond quite well with the set of Pauling radii, r_I^P, of the ions in crystals (Marcus 1983). The electrostatic forces acting on ions in condensed phases, crystals and solutions, are similar and the relevant energies, the lattice energies and energies of solvation, are of similar magnitude. Hence, the conclusion that the r_I^P, derived from measurements on crystals, are relevant for the radii of ions in solution is reasonable. The values of d_{I-O} reported by various authors for aqueous electrolyte solutions and pertaining to different concentrations have a mean uncertainty of ± 0.002 nm, much worse than the values in crystals (Shannon and Prewitt 1969, 1970). Within this uncertainty, the 'selected' (Marcus 1997) ionic radii r_I, listed in Table 2.2, added to r_W do yield the experimental d_{I-O} values, so that they validly represent the radii of aqueous ions.

David and Fourest (1990) challenged the concept of a constant radius for the water molecule, r_W. The electric field of the ions polarizes the water molecules adjacent to them and for multiply charged ions squeezes these molecules somewhat in the direction of the ions. The values of r_W decrease according to these authors from 0.143 nm for the alkali metal cations down to 0.133 nm for the trivalent lanthanide cations. Therefore, using the mean value, $r_W = 0.138$ nm, increases accordingly the uncertainty of the ionic radii in solution from ± 0.002 to ± 0.005 nm.

The radii of multi-atomic ions was estimated as thermochemical radii by Jenkins and co-workers (Jenkins and Thakur 1979; Jenkins et al. 1999; Roobottom et al. 1999) from the lattice potential energies U_{lat} of crystals containing them with a monatomic counter-ion of known radius. The sum of the radii of the cation and anion is:

$$r_{I+} + r_{I-} =$$
$$121.4(\nu_+ + \nu_-)z_+z_-[1 + \{1 - (0.138U_{lat}/121.4(\nu_+ + \nu_-)z_+z_-)\}^{1/2}]/2U_{lat} \quad (2.11)$$

So, if r_{I+} is known r_{I-} is obtained and vice versa.

The temperature dependence of the ionic radii of monatomic- as well as multi-atomic ions is negligible within the temperature range of the existence of water as a liquid at ambient pressures (Krestov 1991).

2.2.3 Ionic Volumes

The volumes that are to be assigned to ions in aqueous solutions are related to the measurable concentration-dependent densities, ρ, of the electrolyte solutions at

constant temperature and pressure. Consider a solution made up from n_W moles of water and n_E moles of electrolyte. The apparent molar volume of the latter:

$$^{\varphi}V_E = \frac{(V - n_W V_W{}^*)}{n_E} \tag{2.12}$$

is that part out of the total volume of the solution, V, remaining for the electrolyte per mole of it, once the volume assigned to the water, $n_W V_W{}^*$, is subtracted. The latter quantity is the volume that the water would have occupied if there was no effect due to the ions. In a solution of density ρ made up from $n_W = 55.51$ moles of water (1 kg) and $n_E = m_E$ moles of electrolyte (i.e., at a molality m_E) the apparent molar volume is obtained from the densities as:

$$^{\varphi}V_E = \frac{M_E}{\rho} + \frac{1000(\rho - \rho_W{}^*)}{\rho \rho_W{}^* m_E} \tag{2.13}$$

where M_E is the molar mass of the solute and $\rho_W{}^*$ the density of pure water. This apparent molar volume of the solute does not mean the actual volume that should be assigned to the electrolyte, because the water near ions does not have the same molar volume that pure water has. The water near the ions is compressed, electrostricted, by the electrical fields of the ions. The volume to be assigned to the ions is the partial molar volume, which for a solution of molality m_E is:

$$V_E = {}^{\varphi}V_E + m_E(\partial {}^{\varphi}V_E/\partial m_E)_T \tag{2.14}$$

Usually the second term of Eq. (2.14) is replaced by $m_E{}^{1/2}(\partial {}^{\varphi}V_E/\partial m_E{}^{1/2})_T$, because of the square root dependence of $^{\varphi}V_E$ on m_E in dilute solutions according to the Debye-Hückel theory. On extrapolation to infinite dilution $^{\varphi}V_E$ becomes equal to the standard partial molar volume of the electrolyte: $^{\varphi}V_E{}^{\infty} = V_E{}^{\infty}$.

At infinite dilution the properties of the cations and anions are additive as mentioned above, so that assuming the value of $V^{\infty}(I^{z\pm}, aq)$ for just one ion permits the splitting of the measured $V_E{}^{\infty}$ to the contributions from the individual ions. Conventional values $V_I{}^{conv}$, based on $V^{\infty}(H^+, aq)^{conv} = 0\,cm^3\,mol^{-1}$ at all temperatures, have been listed by Millero (1971) at several temperatures (0, 25, 50 and 75 °C); some of these values have since been revised (Marcus 2011). The temperature-dependent value for the aqueous hydrogen ion was suggested by Millero (1971), valid to 200 °C:

$$V^{\infty}(H^+, aq)/cm^3 mol^{-1} = -5.1 - 0.008(t/°C) - 1.7 \times 10^{-4}(t/°C)^2 \tag{2.15}$$

resulting in $V^{\infty}(H^+, aq) = -5.4\,cm^3\,mol^{-1}$ at 298.15 K. The derived so-called 'absolute' values are $V^{\infty}(I^{\pm}, aq) = V_I{}^{conv} + z_I V^{\infty}(H^+, aq)$. Those at 298.15 K for some ions are shown in Table 2.2. The steps that have led to Eq. (2.15) cause the ionic values to have uncertainties of at least $\pm 0.2 z_I\ cm^3\ mol^{-1}$, thus increasing with the ionic charges. For some cations, and in particular for multivalent ones, the values of $V^{\infty}(I^{z\pm}, aq)$ are negative: these ions cause a large electrostriction of the hydrating water.

The values of the individual ionic V_I at finite concentrations are not known as accurately, contrary to those at infinite dilution, ${V_I}^\infty$. This is due to interionic interactions causing the additivity of the individual volumes to breaks down. According to Redlich and Meyer (1964) the apparent molar volumes of electrolytes can be expressed as:

$$ {}^\varphi V_E = {}^\varphi {V_E}^\infty + S_V {c_E}^{1/2} + b_E c_E \tag{2.16} $$

where c_E is the molar concentration (in M), S_V is the theoretical slope of the square root term according to the Debye-Hückel theory (1.85 $dm^{3/2}$ $mol^{-1/2}$ at 298.15 K), and b_E is an empirical parameter specific for each electrolyte. Since ${}^\varphi {V_E}^\infty = {V_E}^\infty$ is known from additivity and S_V is independent of the electrolyte, knowledge of the b_E parameters should permit the splitting of measured (Eq. (2.13)) values of ${}^\varphi V_E$ at finite concentrations into the individual ionic contributions. Some progress in this direction was made when it was demonstrated that linear relationships exist between the b_E values and the B_η coefficients of the viscosities (Marcus 2006), the latter being additive and established for individual ions (see Sect. 2.4.3).

The standard partial molar volume of an ion in aqueous solution, ${V_I}^\infty$, is the actual volume to be assigned to the ion in the solution (at infinite dilution). It is the sum of its intrinsic volume, ${V_{IIntr}}^\infty$, and the electrostriction that the ion has caused in the water around it, ${V_{Ielec}}^\infty$, the latter being a negative quantity. The volume of a 'bare' unhydrated ion, $(4\pi N_A/3){r_I}^3$, cannot represent its intrinsic volume and must be enlarged to account for the void spaces between the water molecules and the ion and among themselves in order to represent the intrinsic volume of the ion in the solution. A factor of $k = 1.213$ was proposed by Mukerjee (1961) for the alkali metal and the halide ions, producing:

$$ {V_{I\,Intr}}^\infty = \left(\frac{4\pi N_A}{3} \right) (k r_I)^3 \tag{2.17} $$

The sums of the cation and anion values according to Eq. (2.17) agree with the intrinsic volumes obtained as the limits of V_E at very high concentrations, where all the water present is already completely compressed, so that $V_{Ielec} \to 0$ (Marcus 2010).

The electrostriction caused by an ion has been estimated on the basis of the electrostatic effects the very high electric field of an ion has on the water surrounding it. This field exerts a large pressure on the water and sharply decreases its permittivity, down to dielectric saturation. A stepwise shell-by-shell calculation (Marcus and Hefter 1999) yields the desired quantity:

$$ \begin{aligned} {V_{Ielec}}^\infty = & -(8\pi^2 N_A \varepsilon_0) \sum\nolimits_j (r(j)^3 - r(j-1)^3) \\ & \times \left\{ \varepsilon_W(j) \left[\left(\frac{\partial \ln \varepsilon_W}{\partial P} \right)_T - \kappa_{TW} \right] + \kappa_T \right\} E(j)^2 \end{aligned} \tag{2.18} $$

The summation extends over the shell numbers j from 1 up to such a value that the incremental change in ${V_{Ielec}}^\infty$ is negligible. In expression (2.18) $r(0) = r_I$, $\Delta r =$

$r(j) - r(j-1)$ is fixed at some small value, say 0.005 nm, $\varepsilon_W(j) = \varepsilon(j, E)$ is the electric field-dependent (hence pressure-dependent) relative permittivity in the jth shell, and $E(j) = E(j, \varepsilon_W)$ is the electric field strength in the jth shell. An iterative calculation is required due to the mutual dependence of E and ε_W.

The mutual dependences of the pressure, the compressibility, the permittivity, and the field strength complicate the electrostatic calculations. Marcus has recently calculated (Marcus 2009, 2012a) the ${V_{Ielec}}^{\infty}$ for the alkali metal and alkaline earth metal cations and the halide, perchlorate, and sulfate anions for aqueous solutions at five temperatures between 273.15 and 473.15 K (0 − 200 °C), those for 298.15 K being shown in Table 2.2. The corresponding intrinsic volumes are ${V_{I\ Intr}}^{\infty} = {V_I}^{\infty} - {V_{Ielec}}^{\infty}$, and, of course, all are positive.

2.2.4 *Molar Heat Capacities of Aqueous Ions*

When the heat of solution of an electrolyte in water to form a dilute solution is measured calorimetrically at several temperatures, the standard partial molar (constant pressure) heat capacity of the electrolyte, ${C_{PE}}^{\infty}$, is obtained from the temperature coefficient of these heats, extrapolated to infinite dilution. Alternatively, the difference between the specific heat of a dilute solution of the electrolyte and that of water is obtained by flow microcalorimetry to yield the same quantity. Accurate density data at the appropriate temperature are required for the use of this technique. A recent description of the methods available for the determination of the heat capacities of aqueous electrolytes is presented by Hakin and Bhuiyan (2010). Such determinations are accurate to ± 1 to ± 4 J K^{-1} mol^{-1} (Hepler and Hovey 1996)

Values of ${C_{PE}}^{\infty}$ have been critically compiled by Abraham and Marcus (1986) for many electrolytes. Some of the values have later been revised and supplemented by Criss and Millero (1996, 1999) and by Hepler and Hovey (1996). As for other pertinent quantities, it is necessary to assume a value for one ion in order to obtain the so-called 'absolute' standard molar ionic heat capacities, ${C_{PI}}^{\infty}$, these values being additive at infinite dilution. Criss and Millero (1996, 1999) presented values of the conventional standard molar ionic heat capacities at 298.15 K, based ${C_P}^{\infty}(H^+, aq)^{conv} = 0$. The 'absolute' value ${C_P}^{\infty}(H^+, aq) = -71 \pm 14$ J K^{-1} mol^{-1} at 298.15 K has been suggested (Abraham and Marcus 1986) on the basis of the TPTB assumption, equating the standard molar heat capacities of aqueous tetraphenylphosphonium and tetraphenylborate ions. These cation and anion should have similar values of ${C_{PI}}^{\infty}$, because they are chemically similar and have similar sizes, the charges being buried well inside the tetraphenyl structure (Marcus 1987). However, the ${C_{PI}}^{\infty}$ of these bulky ions are large, leading to a large uncertainty involved in equating them, because of slight differences in their sizes. Unfortunately, no more satisfactory method for splitting ${C_{PE}}^{\infty}$ into the ${C_{PI}}^{\infty}$ of the constituent ions has been found so far. Values of the latter are shown in Table 2.2.

Criss and Millero (1996, 1999) used the Pitzer formulation for activity coefficients (Pitzer and Mayoraga 1973) and presented the needed electrolyte specific parameters

for the calculation of the partial molar heat capacities of electrolyte solutions at appreciable concentrations. Hakin and Bhuiyan (2010) presented the semi-empirical Helgeson et al. (1981) expression for similar calculations, useful in particular for elevated temperatures.

2.2.5 Molar Entropies of Aqueous Ions

The standard molar entropies of aqueous electrolytes, S_E^∞, are obtained from the temperature coefficients of the electromotive forces of galvanic cells or of the solubilities of sparingly soluble salts. The values for individual ions need an assumption concerning the value of one ion, as in the cases of the standard molar volumes and heat capacities. The standard molar entropy of the hydrogen ion $S^\infty(H^+, aq)$ can be obtained from from thermocells or from the potential of a mercury electrode at the point of zero charge. The assumption involved in the former method relates to the entropy of transport across a boundary of similar solutions at different temperatures. The corresponding assumption for the latter method is that the temperature dependence of the surface potential of mercury in water is negligible. Consistent values are obtained from both methods: $S^\infty(H^+, aq) = -22.2 \pm 1.4\ J\ K^{-1}\ mol^{-1}$ (Conway 1978), a value that has not been seriously challenged since. Still, a much smaller negative value was suggested more recently by Schmid et al. (2000). It depends on the apparent similarity between the hydration and gas-phase clustering entropies of the hydrogen and the hydroxide ions. However, the adoption of the Schmid et al. value, $S^\infty(H^+, aq) = S^\infty(OH^-, aq) = -5.45\ J\ K^{-1}\ mol^{-1}$ would increase that of fluoride anions to $25.1\ J\ K^{-1}\ mol^{-1}$, much different from the hydroxide value. However, all measures of the hydration of hydroxide and fluoride anions in aqueous solutions lead to commensurate values. On the other hand,on the basis of Conway's choice (Conway 1978), the value of $S^\infty(OH^-, aq) = 11.3\ J\ K^{-1}\ mol^{-1}$, is quite near that of the fluoride anion, $S^\infty(F^-, aq) = 8.4\ J\ K^{-1}\ mol^{-1}$, and is to be preferred. The derived values for other ions are shown in Table 2.2.

Frank and Robinson (1940) suggested that partial molar entropy of the *water* in an electrolyte solution could be used for deciding on the structure-making or -breaking properties of the ions constituting the electrolyte. Gurney (1953) found a linear relationship between the partial molar entropy of aqueous monatomic *ions* and their viscosity B_η coefficients (see Sect. 2.4.3). Later investigators, such as Nightingale (1959), preferred to deal with the standard molar entropy of hydration, because it permitted the extension of such correlations to polyatomic ions due to cancellation of internal mode entropies of these ions and configurational contributions.

2.2.6 The Polarizabilities of Aqueous Ions

The molar refractivity R_D of an electrolyte is additive for the constituent ions if the ions are in an infinitely dilute solution. The expression used for the determination

of R_D uses the refractive index n_D at the sodium D-line (589 nm) for the solution and for pure water, n_{DW}. It is analogous to that for the apparent molar volume, Eq. (2.13), with the ratio $({n_D}^2 - 1)/({n_D}^2 + 2)$ replacing ρ^{-1} and similarly for ${\rho_W}^{-1}$ being replaced by $({n_{DW}}^2 - 1)/({n_{DW}}^2 + 2)$:

$$R_D = \frac{\left(\frac{1000}{\rho}\right)({n_D}^2 - 1)}{({n_D}^2 + 2)} - [(\rho/\rho_W) - c_E M_W/1000\rho_W]\,\frac{({n_{DW}}^2 - 1)}{({n_{DW}}^2 + 2)} \qquad (2.19)$$

Extrapolation to infinite dilution yields ${R_D}^\infty$ that has the dimension of a molar volume. The reported individual ionic values (Marcus 1997) are based on the arbitrary but reasonable value of ${R_D}^\infty(Na^+) = 0.65 \times 10^{-6}\ m^3\ mol^{-1}$, for the infinitely diluted aqueous sodium ions, the same as for isolated ions (See p. 52), because of the inappreciable dependence of the polarizability of the ions on their environment. The values shown in Table 2.1 for isolated ions, R_{DI}, are in fact those obtained for ions in infinitely dilute solutions, independent of the solvent (though mostly for aqueous ions). The polarizabilities of the ions are obtained from the ${R_{DI}}^\infty$ values by means of Eq. (2.2) and correlate to some extent with the sizes of the ions.

2.2.7 Ion Effects on the Surface Tension of Water

The surface tension of water, ${\gamma_W}^*$, is fairly large, 71.96 mN m^{-1} at 298.15 K, due to its hydrogen bonded network. Ions affect the surface tension of their solution, γ, because they are either preferentially sorbed at the surface layer of the water or, more commonly, desorbed from it, compared with their bulk concentrations. This subject is fully discussed in Sect. 4.4.1 and is not further dealt with here.

2.3 Thermodynamics of Ion Hydration

Ions in aqueous solutions are characterized by several thermodynamic quantities in addition to the molar volumes, heat capacities and entropies discussed above. These are the molar changes of enthalpy, entropy, and Gibbs energy on the transfer of an ion from its isolated state in the ideal gas to the aqueous solution. They pertain also to the dissolution of an electrolyte in water, since they can be considered as parts in a thermodynamic cycle in which the electrolyte is transferred to the gas phase, dissociates there into its constituent ions, which are then transferred into the solution. Contrary to thought processes, as described in Sect. 2.2., it is impossible to deal experimentally with individual ions but only with entire electrolytes or with such combinations (sums or differences) of ions that are neutral. The assignment of values to individual ions requires the splitting of the electrolyte values by some extra-thermodynamic assumption that cannot be proved or disproved within the framework of thermodynamics. However, for a theoretical estimation of the individual ionic

values a model is useful. Its success can be demonstrated if the calculated ionic values for the cations and anions add up to the experimental values for the corresponding electrolytes.

2.3.1 Experimental Enthalpies of Hydration of Ions

When an ion is transferred, in a thought process, from its isolated state in the ideal gas phase into water at infinite dilution a large amount of energy is released due to the interaction of the ion with the surrounding water, from which the work needed for creating a cavity for the accommodation of the ion in the water is subtracted. The molar volume of the ion is compressed in this process from RT/P° to the standard partial molar volume in the solution, V_I^∞. The net relevant energetic amount is the change in the enthalpy, $\Delta_{hydr}H_I^\infty$, but, as said, this cannot be determined experimentally for individual ions.

The standard molar enthalpy of hydration of a complete electrolyte, $\Delta_{hydr}H_E^\infty$, is obtained from its experimental heat of solution and theoretical lattice energy. It is also the difference between the critically compiled standard molar enthalpy of formation of the infinitely dilute aqueous electrolyte (Wagman et al. 1982) and the sum of the standard molar enthalpies of formation of the ideal gaseous ions (Table 2.1), weighted according to their stoichiometric coefficients.

$$\Delta_{hydr}H_E^\infty = \Delta_{soln}H_E^\infty - \Delta_{latt}H_E^\infty = \Delta_f H^\infty(\mathrm{E,aq}) - \sum \nu_I \cdot \Delta_f H^\circ(\mathrm{I^\pm, i.g.}) \tag{2.20}$$

In order to split the experimentally available $\Delta_{hydr}H_E^\infty$ values dealing with entire electrolytes into the ionic contribution a value must be estimated for just one ion. Conventional values are obtained on setting $\Delta_{hydr}H^\infty(\mathrm{H^+})^{conv} = 0$ at all temperatures. The 'absolute' value $\Delta_{hydr}H^\infty(\mathrm{H^+,\ aq}) = -1103 \pm 7$ kJ mol^{-1} at 298.15 K results (Marcus 1987) according to the TPTB assumption, equating the standard enthalpies of hydration of the tetraphenyphosphonium and tetraphenylborate ions:

$$\Delta_{hydr}H^\infty(\mathrm{Ph_4P^+}) = \Delta_{hydr}H^\infty(\mathrm{BPh_4^-}) \tag{2.21}$$

Contrary to the case of the heat capacities (Sect. 2.2.4), the values of $\Delta_{hydr}H_I^\infty$ for these bulky ions are quite low compared with those of small ions. Therefore, the uncertainty involved in equating the values for these reference ions is also small. This estimate for the hydrogen ion is compatible with several other reliable values suggested on the basis of other considerations, ranging from -1091 ± 10 to -1104 ± 17 kJ mol^{-1} (Conway 1978). The values for a number of ions are shown in Table 2.3 and are expected to be accurate to within $\pm 7 z_I$ kJ mol^{-1} (Marcus 1997). Since heat is released on the hydration of the ions, the values are all negative as expected and are of similar magnitude for singly charged ions, whether cations or anions. They become less negative with increasing sizes for a given ionic charge, but become considerably more negative, by a factor of the order of z_I^2, for multi-charged ions.

Table 2.3 Thermodynamic quantities of ion hydration at 298.15 K. (Marcus 1997)

Ion	$\Delta_{\text{hydr}} H_{\text{I}}^{\infty}$ kJ mol^{-1}	$\Delta_{\text{hydr}} S_{\text{I}}^{\infty}$ J K^{-1} mol^{-1}	$\Delta_{\text{hydr}} G_{\text{I}}^{\infty}$ kJ mol^{-1}
H^+	−1,103	−131	−1,064
Li^+	−531	−142	−489
Na^+	−416	−111	−383
K^+	−334	−74	−312
Cs^+	−283	−59	−258
NH_4^+	−329	−112	−296
$(CH_3)_4N^+$	−218	−144	
Mg^{2+}	−1,949	−331	−1,850
Ca^2	−1,602	−252	−1,527
Ba^{2+}	−1,332	−205	−1,258
Fe^{2+}	−1,972	−362	−1,864
Fe^{3+}	−4,462	−557	−4,296
La^{3+}	−3,312	−455	−3,155
F^-	−510	−137	−472
Cl^-	−367	−75	−345
Br^-	−336	−59	−318
I^-	−291	−36	−280
SCN^-	−311	−66	−291
NO_3^-	−312	−76	−289
ClO_4^-	−246	−57	−229
$CH_3CO_2^-$	−425	−170	−374
HCO_3^-	−384	−137	−343
$H_2PO_4^-$	−522	−166	−473
CO_3^{2-}	−1,397	−245	−1,324
SO_4^{2-}	−1,138	−249	−1,064
HPO_4^{2-}		−272	
PO_4^{3-}	−2,879	−421	−2,773

At finite concentrations the molar enthalpy of hydration of an electrolyte may be estimated by adding the relative partial molar heat content of the solute, L_{E}, to the sum of the cation and anion values of $\Delta_{\text{hydr}} H_{\text{I}}^{\infty}$. The value of L_{E} is numerically equal to and of opposite sign to the experimentally measurable (Harned and Owen 1958; Robinson and Stokes 1965) enthalpy of dilution of the electrolyte, $\Delta_{\text{dil}} H_{\text{E}}$. At finite concentrations the heat content and the enthalpy of hydration may therefore be smaller or larger than at infinite dilution, depending on the enthalpies involved in the interactions between neighboring ions.

The partial molar heat content of an electrolyte at molality m_{E} is obtainable from the temperature derivatives of the activity coefficient, $\gamma_{\pm}$:

$$L_{\text{E}} = -\nu R T^2 \left(\frac{\partial \ln \gamma_{\pm}}{\partial T} \right)_{P,m} \tag{2.22}$$

where ν is the number of ions in a formula of the solute electrolyte.

2.3.2 Experimental Entropies of Hydration of Ions

The standard molar entropy of hydration of an ion is:

$$\Delta_{\text{hydr}}S_{\text{I}}^{\infty} = S^{\infty}(\text{I}^{\pm}, \text{aq}) - S^{\circ}(\text{I}^{\pm}, \text{g}) \tag{2.23}$$

i. e., the difference between its standard molar ionic entropy in the aqueous solution (Table 2.2) and the standard molar entropy of the isolated ion in the ideal gas phase (Table 2.1). The former of these, the so called 'absolute' standard molar ionic entropies, are based on the chosen value $S^{\infty}(\text{H}^{+}, \text{aq}) = -22.2 \pm 1.4$ J K^{-1} mol^{-1} at 298.15 K, as discussed in Sect. 2.2.5. With the value of $S^{\circ}(\text{H}^{+}, \text{g}) = 108.9$ J K^{-1} mol^{-1} at 298.15 K shown in Table 2.1 this yields $\Delta_{\text{hydr}}S_{\text{I}}^{\infty}(\text{H}^{+}) = -131.1 \pm 1.4$ J K^{-1} mol^{-1} at this temperature.

These standard molar entropies of hydration of ions are related to the effect that ions have on the structure of water (Abraham et al. 1982; Marcus 1994), see Sect. 3.3.3.

2.3.3 Experimental Gibbs Energies of Hydration of Ions

The standard molar Gibbs energy of hydration of an ion, $\Delta_{\text{hydr}}G_{\text{I}}^{\infty}$, can now be obtained from a combination of the standard molar enthalpy and entropy of hydration:

$$\Delta_{\text{hydr}}G_{\text{I}}^{\infty} = \Delta_{\text{hydr}}H_{\text{I}}^{\infty} - T\Delta_{\text{hydr}}S_{\text{I}}^{\infty} \tag{2.24}$$

The value for the hydrogen ion, $\Delta_{\text{hydr}}G^{\infty}(\text{H}^{+}, \text{aq}) = -1,064 \pm 7$ kJ mol^{-1} is derived from the values of $\Delta_{\text{hydr}}H^{\infty}(\text{H}^{+})$ and $\Delta_{\text{hydr}}S^{\infty}(\text{H}^{+})$ given above. The resulting values of $\Delta_{\text{hydr}}G_{\text{I}}^{\infty}$ are shown in Table 2.3 for a number of ions.

The electrostatic component is the major contribution to the standard molar ionic Gibbs energy of hydration as it is for the enthalpy of hydration. Hence, $\Delta_{\text{hydr}}G_{\text{I}}^{\infty}$ can be estimated from the Born expression, resulting from the following thought process. Let an isolated ion in the gaseous phase, $\text{I}^{z\pm}(\text{g})$, be discharged, to produce a neutral particle, for which process the electric self energy $E_{\text{self}}(\text{I}^{z\pm}, \text{g})$ (Eq. (2.1)) must be provided. The neutral particle is then transferred into the bulk of liquid water with no electric energetic component for crossing the gas/liquid boundary being involved. The neutral particle is then charged up to the original value, producing the infinitely dilute aqueous ion, $\text{I}^{z\pm}, \text{aq}^{\infty}$. The energy of interaction with the surrounding water is thereby released, depending on the permittivity of the water $\varepsilon^{*} = 4\pi\varepsilon_0\varepsilon_{\text{W}}{}^{*}$. Here $\varepsilon_{\text{W}}{}^{*}$ is the temperature- and pressure-dependent relative permittivity, and at 298.15 K and ambient pressure $\varepsilon_{\text{W}}{}^{*} = 78.4$. The net effect of this thought process representing the hydration of the ion is the Born expression:

$$\Delta_{\text{hydr}}G_{\text{I}}^{\infty} = \left(\frac{N_{\text{A}}e^2}{4\pi\varepsilon_0}\right) z_{\text{I}}{}^2 r_{\text{I}}{}^{-1} \left(1 - \frac{1}{\varepsilon_{\text{W}}{}^{*}}\right) \tag{2.25}$$

The problem with this mode of calculation is the use of the same value of the radius r_{I} for the ion in the aqueous solution and the isolated state (see p. 50) and the use

of the relative permittivity of pure water for the description of the interaction of the ion with its immediate surroundings, where dielectric saturation, due to the high electric field of the ion, occurs. Various schemes have been proposed to counter these problems, such as adding a quantity Δr to the ionic radius and/or splitting the process into two spatial regions: one adjacent to the ion, where dielectric saturation occurs and $\varepsilon' \approx {n_{\mathrm{DW}}}^2$ (the square of the refractive index) and the other beyond this, where the bulk value $\varepsilon_{\mathrm{W}}{}^*$ prevails, as in the model described in Sect. 2.3.4. The use of such devices permits the estimation of reasonably correct $\Delta_{\mathrm{hydr}}{G_{\mathrm{I}}}^{\infty}$ values (Marcus 1991).

The standard molar Gibbs energy of hydration of the hydrogen ion noted above, $\Delta_{\mathrm{hydr}}G^{\infty}(\mathrm{H}^+, \mathrm{aq}) = -1,064 \pm 7\ \mathrm{kJ\ mol^{-1}}$ is compatible with the estimates $-1,056 \pm 6\ \mathrm{kJ\ mol^{-1}}$ (Marcus 1991) and $-1,066 \pm 17\ \mathrm{kJ\ mol^{-1}}$ (Conway 1978) but not with $-1,113 \pm 8\ \mathrm{kJ\ mol^{-1}}$ obtained from the cluster pair approximation used by Kelly et al. (2006). The assumptions involved in obtaining the latter value lead to a surface potential of water of $\Delta\chi = 0.34 \pm 0.08$ V (Marcus 2008), which, in turn, is not consistent with the recent estimate of $\Delta\chi = 0.1$ V (Parfenyuk 2002) deemed to be the most nearly correct one.

So called 'real' standard molar Gibbs energies of hydration are obtained from the electromotive force of specially constructed cells. These consist of a jet of aqueous solution flowing downward in the middle of a tube, along the inner surface of which another solution, concentric with the jet, flows with a narrow vapor gap between them. The measurable 'real' standard molar Gibbs energy of hydration is:

$$\Delta_{\mathrm{hydr}}{G_{\mathrm{I}}}^{\infty \mathrm{R}} = \Delta_{\mathrm{hydr}}{G_{\mathrm{I}}}^{\infty} + z_{\mathrm{I}} F \Delta\chi \tag{2.26}$$

where the algebraic value of the ionic charge z_{I} is to be used, $F = 96485.3\ \mathrm{C\ mol^{-1}}$ being the Faraday's constant. The uncertainties connected with the value of $\Delta\chi$ make the use of the measurable 'real' standard molar Gibbs energies of hydration unattractive for obtaining individual ionic values for the desired quantity, $\Delta_{\mathrm{hydr}}{G_{\mathrm{I}}}^{\infty}$.

2.3.4 A Common Model for Ion Hydration Thermodynamics

Marcus (1987, 1991) presented a model that is applicable to all the thermodynamic functions of hydration. It follows the thought process of dissolution described at the beginning of Sect. 2.2:

$$\Delta_{\mathrm{hyd}}Y^* = \Delta Y_{\mathrm{Nt}}(r) + \Delta Y_{\mathrm{El1}}(z, r) + \Delta Y_{\mathrm{El2}}(z, r) + \Delta Y_{\mathrm{St}}(z, r) \tag{2.27}$$

Here Y is, for the present purposes, H or S, Y^* is the 'unitary' part, describing the hydration process proper. At 25 °C $\Delta_{\mathrm{hyd}}H^*$ differs by 2.29 kJ mol^{-1} from the standard enthalpy $\Delta_{\mathrm{hyd}}H^{\circ}$ and $\Delta_{\mathrm{hyd}}S^*$ differs by $-18.9\ \mathrm{J\ K^{-1} \cdot mol^{-1}}$ from the standard entropy $\Delta_{\mathrm{hyd}}S^{\circ}$ per mole of ions. These difference quantities pertain to step 6 in the thought process: the relaxation of the fixed points in the ideal gas and solution phases and turning on the full translational degrees of freedom. The numerical values

depend on the standard states of the ions: 0.1 MPa pressure for the ideal gas state and 1 M for the solution.

The term $\Delta Y_{\mathrm{Nt}}(r)$ is the contribution from the hydration of a neutral solute of the same size of the ion (the r dependence), and is related to the cavity formation, step 2 in the thought process. For the enthalpy $\Delta H_{\mathrm{Nt}}(r) = 35 - 267(r_{\mathrm{I}}/\mathrm{nm})$ kJ mol^{-1} and for the entropy $\Delta S_{\mathrm{Nt}}(r) = -22 - 600(r_{\mathrm{I}}/\mathrm{nm})$ J K^{-1} mol^{-1}, obtained by Abraham et al. from gas solubilities (Abraham and Liszi 1980; Abraham et al. 1983).

The interaction of the solute ion with the water in its surrounding (step 4 in the thought process) is described by the electrostatic terms $\Delta Y_{\mathrm{El1}}(z, r) + \Delta Y_{\mathrm{El2}}(z, r)$. The first pertains to the first hydration shell of the ion and the second to water outside this shell. For the Gibbs energy of hydration these two terms read:

$$\Delta G_{\mathrm{El1}} + \Delta G_{\mathrm{El2}} = -\left(\frac{N_{\mathrm{A}} e^2}{8\pi\varepsilon_0}\right) z^2 \left[\left(1 - \frac{1}{\varepsilon'}\right) \frac{\Delta r_{\mathrm{I}}}{r_{\mathrm{I}}(r_{\mathrm{I}} + \Delta r_{\mathrm{I}})} + \frac{\left(1 - \frac{1}{\varepsilon}\right)}{(r_{\mathrm{I}} + \Delta r_{\mathrm{I}})}\right] \quad (2.28)$$

The second term in the square brackets is the Born expression applicable at distances $r_{\mathrm{I}} + \Delta r_{\mathrm{I}}$, i.e., beyond the first hydration shell of thickness Δr. The first term describes the electrostatic interaction inside this shell, characterized by a relative permittivity $\varepsilon' \approx {n_{\mathrm{DW}}}^2$, approximated by the square of the refractive index of water at the sodium D line. With the relevant dε'/dT and dε/dT values for water at 25 °C, the enthalpy of hydration Eq. (2.28) is $\Delta H_{\mathrm{El1}} + \Delta H_{\mathrm{El2}} = -69.5z^2[(0.35(\Delta r_{\mathrm{I}}/r_{\mathrm{I}}) + 1.005)/(r_{\mathrm{I}} + \Delta r_{\mathrm{I}})]$ kJ mol^{-1}. The entropy is then $\Delta S_{\mathrm{El1}} + \Delta S_{\mathrm{El2}} = -4.06z^2[(1.48(\Delta r_{\mathrm{I}}/r_{\mathrm{I}}) + 1.00)/(r_{\mathrm{I}} + \Delta r_{\mathrm{I}})]$ J K^{-1} mol^{-1}. The thickness of the first hydration shell, Δr, depends on the number of water molecules, h_{I}, in it, the hydration number. According to the model (Marcus 1987) $h_{\mathrm{I}} = 0.36|z_{\mathrm{I}}|/(r/\mathrm{nm})$, that is, it is proportional to the charge number of the ion and inversely proportional to its radius. The volume occupied by h_{I} water molecules is $\pi h_{\mathrm{I}} d_{\mathrm{W}}^3/6$, where $d_{\mathrm{W}} = 0.276$ nm is the diameter of a water molecule. Hence the volume of the first hydration shell is given by:

$$\left(\frac{4\pi}{3}\right)[(r_{\mathrm{I}} + \Delta r_{\mathrm{I}})^3 - {r_{\mathrm{I}}}^3] = \frac{\pi h_{\mathrm{I}} {d_{\mathrm{W}}}^3}{6} \quad (2.29)$$

from which the hydration shell thickness Δr_{I} is readily extracted.

The last term in Eq. (2.27), $\Delta Y_{\mathrm{St}}(z, r)$, pertains to the structural changes taking place in the water around the first hydration shell of the ion, step 5 of the thought process of dissolution. The hydrogen bonding in these surroundings is affected by the enhanced hydrogen bond acceptance of the hydration water of anions and the enhanced hydrogen bond donation of the hydration water of cations, and hydrophobic effects of ions such as the tetraalkylammonium ones also operate. The above described model, unfortunately, is not capable of specifying this term directly for the enthalpy of hydration, but it can be calculated from the experimental values. The structural entropy of ion hydration is more fully discussed in Sect. 3.3.3 in relation of the effects of ions on the structure of water.

Table 2.4 shows the various contributions to the enthalpy and entropy of hydration according to this model, Eq. (2.27). The sizes of the hydrated ions, i.e. $r_{\mathrm{I}} + \Delta r_{\mathrm{I}}$ are

Table 2.4 Calculated values of the thickness of the hydration shell, Δr_I, the hydration number h_I, and the contributions to the molar enthalpy and entropy of hydration of representative ions according to the model of Marcus (1987)

Ion	r_I/nm	Δr_I/nm$_I$	h_I	$\Delta_{hyd}H^*$/kJ mol^{-1}				$\Delta_{hyd}S^*$/J K^{-1} mol^{-1}			
				ΔH_{Nt}	$\Delta H_{El1}+\Delta H_{El2}$	ΔH_{St}	$\sum\Delta_{hyd}H$	ΔS_{Nt}	$\Delta S_{El1}+\Delta S_{El2}$	ΔS_{St}	$\sum\Delta_{hyd}S$
Li^+	0.069	0.171	5.2	17	−542	−14	−539	−63	−32	−48	−143
Na^+	0.102	0.116	3.5	8	−447	−3	−442	−83	−26	−11	−120
K^+	0.138	0.075	2.6	−2	−390	14	−378	−105	−22	45	−82
Cs^+	0.170	0.050	2.1	−10	−350	20	−340	−124	−20	68	−76
Me_4N^+	0.280	0.016	1.3	−40	−241	−10	−291	−190	−14	−34	−238
Pr_4N^+	0.379	0.006	0.9	−66	−182	−154	−402	−249	−11	−514	−774
F^-	0.133	0.081	2.7	−1	−396	−11	−408	−102	−23	−37	−162
Cl^-	0.181	0.044	2.0	−13	−337	13	−337	−131	−20	43	−108
I^-	0.220	0.028	1.6	−24	−294	25	−293	−154	−17	84	−87
ClO_4^-	0.240	0.023	1.5	−29	−274	23	−280	−166	−16	76	−106
Mg^{2+}	0.072	0.225	10.0	16	−1,964	−34	−1,982	−65	−130	−113	−308
Ca^{2+}	0.100	0.169	7.2	8	−1,650	−18	−1,660	−82	−101	−60	−243
Ba^{2+}	0.136	0.118	5.3	−1	−1,432	−6	−1,439	−104	−85	−19	−208
CO_3^{2-}	0.178	0.076	4.0	−13	−1,264	−14	−1,291	−129	−74	−48	−251
SO_4^{2-}	0.230	0.045	3.1	−26	−1,085	−2	−1,113	−160	−64	−5	−229
La^{3+}	0.105	0.197	10.3	7	−3,442	−32	−3,467	−85	−398	−108	−591
PO_4^{3-}	0.238	0.057	4.5	−29	−2,309	−35	−2,379	−165	−137	−117	−419
Th^{4+}	0.100	0.236	14.4	8	−6,060	−27	−6,079	−82	−420	−90	−592
$Fe(CN)_6^{4-}$	0.440	0.020	3.3	−83	−2,468	53	−2,498	−286	−146	176	−256

seen to cover a narrow range only, from a minimum of 0.213 nm for K^+ through not much larger values for the alkali metal and halide ions up to 0.385 or 0.460 nm for the bulky ions Pr_4N^+ and $Fe(CN)_6^{4-}$, a factor of ~2, compared to a factor of > 6 for the radii of the bare ions. The hydration numbers h_I derived from this model are similar to values obtained from diffraction or computer simulation studies or the compressibility of the solutions (Marcus 1997).

The molar enthalpy of hydration is seen to be strongly dominated by the combined electrostatic terms for all the ions, and increases (becomes more negative) sharply with the ionic charge, z_I. Except for the tetraalkylammonium ions the neutral and water- structural contributions tend to cancel each other to an appreciable extent. The hydrophobic effect ΔH_{St} is very marked for the tetrapropylammonium cation, and bulky ions have fairly important contributions from the cavity formation term, ΔH_{Nt}. The model does not distinguish between cations and anions, since the charge enters the expressions squared or as the absolute value.

On the contrary, the molar entropy of hydration is *not* dominated by the sum of the electrostatic terms except for small highly charged ions. The neutral and water-structural terms are of opposite sign for the alkali metal and halide ions but of the same, negative, sign for more highly charged ions. These two terms together are responsible to the large molar entropy of hydration of the tetrapropylammonium cation, but highly charged and highly hydrated small cations, such as La^{3+} and Th^{4+} also have large negative entropies of hydration, but for different reasons.

2.4 Ion Transport

Ions in solution move around spontaneously in an isotropic manner due to their thermal energy and they may carry some of their hydration shells with them, depending on how strong the bonding between the ion and the water of hydration is. The speed of their movements is a quantity that can be determined experimentally for individual ions, contrary to the thermodynamic quantities dealt with above. The directional movement of ions depends on the presence of fields, i.e., gradients in the forces that cause the ions to migrate. An external field could be a pressure gradient, causing the flow of the solution as a whole. It could be an electrical field, causing ions of opposite charges to move in opposite directions. A directional concentration gradient at finite concentration causes directional diffusion of ions. The inherent movement of ions in the absence of a field is their self-diffusion and can occur at infinite dilution or at finite ones in a homogeneous solution.

2.4.1 Self-diffusion of Ions

The rate of self-diffusion of ions is commonly obtained from other transport quantities, such as the conductivity. It may, however, be determined directly by labeling the ions isotopically. It is then assumed that the slight mass difference between ions that

Table 2.5 Transport properties of some ions at 298.15 K. (Marcus 1997)

Ion	D_I^∞ $10^{-9}m^2\ s^{-1}$	λ_I^∞ $cm^2\ \Omega^{-1}\ mol^{-1}$	r_{ISt} nm	B_I M^{-1}
H^+	9.311	349.8	0.026	0.068
Li^+	1.029	38.7	0.238	0.146
Na^+	1.334	50.1	0.184	0.085
K^+	1.957	73.5	0.125	−0.009
Cs^+	2.056	77.3	0.119	−0.047
NH_4^+	1.958[a]	73.6	0.125	−0.008
$(CH_3)_4N^+$	1.196	44.9	0.205	0.123
Mg^{2+}	0.706	106.1	0.174	0.385
Ca^2	0.792	119.0	0.155	0.298
Ba^{2+}	0.847	127.3	0.145	0.229
Fe^{2+}	0.719	107	0.172	0.42
Fe^{3+}	0.604	204	0.136	0.69
La^{3+}	0.619	209.1	0.232	0.582
F^-	1.475	55.4	0.167	0.127
Cl^-	2.032	76.4	0.121	−0.005
Br^-	2.08	78.1	0.118	−0.033
I^-	2.045	76.8	0.120	−0.073
SCN^-	1.758	66	0.142	−0.032[b]
NO_3^-	1.902	71.5	0.129	−0.045
ClO_4^-	1.792	67.4	0.137	−0.058
$CH_3CO_2^-$	1.089	40.9	0.225	0.246
HCO_3^-	1.185	44.5	0.207	0.13
$H_2PO_4^-$	0.879	33	0.279	0.34
CO_3^{2-}	0.923	138.6	0.133	0.294
SO_4^{2-}	1.065	160	0.115	0.206
HPO_4^{2-}	0.439	66	0.279	0.382
PO_4^{3-}	0.612	207	0.134	0.59

[a]Calculated from the molar conductivity
[b]From (Marcus 2012)

differ only by their isotopic composition does not affect their rate of diffusion. This should be valid the more so for diffusing hydrated ions for which their mass includes the mass of the water transported with them. A diaphragm cell is employed, with equal concentrations of the electrolyte in the two stirred compartments, in one of which ions of one kind are labeled by a radioactive isotopic tracer. Other methods of measuring diffusion of ions, e.g. by NMR with non-radioactive isotopes, have also been used. The rates of migration of the labeled ion truly measures self-diffusion at the nominal concentrations employed. The value of the limiting diffusion coefficient, D_I^∞, of the order of $10^{-9}\ m^2\ s^{-1}$, is obtained on extrapolation to infinite dilution.

Values of the limiting self-diffusion coefficients of certain common ions at 298.15 K are shown in Table 2.5. It is seen that the more strongly hydrated an ion is, the lower is its rate of self-diffusion, an exception being the hydrogen ion. This ion does not diffuse in water by massive movement of the ion carrying its hydration shell but by the Grotthuss mechanism, according to which the positive charge (i.e., a missing electron) is hopping from one water molecule in the hydrogen bonded network to the next, hence is much faster.

2.4.2 Ionic Conductivities

The most characteristic properties of ions are their abilities to carry an electric current. They do so by moving in the direction of an electrical field gradient imposed externally, cations towards the negatively charged cathode, anions in the opposite direction to the anode. The rate of movement of ions in an electric field is expressed by their mobilities u_I, measuring their speed at unit field, so that the units of u_I are $m\ s^{-1}/V\ m^{-1} = m^2\ s^{-1}\ V^{-1}$.

When an external electric field is imposed on an electrolyte solution by electrodes dipped into the solution, the electric current produced is proportional to the potential difference between the electrodes. The proportionality coefficient is the resistance of the solution, and its reciprocal, the conductivity, is readily measured accurately with an alternating potential at a rate of ~1 kHz in a virtually open circuit (zero current), in order to avoid electrolysis at the electrodes. The conductivity depends on the concentration of the ions, the carriers of the current, and can be determined per unit concentration as the molar conductivity Λ_E. At finite concentrations ion-ion interactions cause the conductivities of electrolytes to decrease, not only if ion pairs are formed (see Sect. 2.6.2) but also due to indirect causes. The molar conductivity Λ_E can be extrapolated to infinite dilution to yield ${\Lambda_E}^\infty$ by an appropriate theoretical expression. The modern theory, e.g., that of Fernandez-Prini (1969), takes into account the electrophoretic and ionic atmosphere relaxation effects. The molar conductivity of a completely dissociated electrolyte is:

$$\Lambda_E = {\Lambda_E}^\infty - S{c_E}^{1/2} + Ec_E \ln c_E + J'(R')c_E - J''(R'')c_E{}^{3/2} \tag{2.30}$$

Here *S*, *E*, *J'*, and *J"* are explicit expressions, containing contributions from relaxation and electrophoretic effects, the latter two depending also on ion-distance parameters *R*.

The limiting molar conductivity ${\Lambda_E}^\infty$ of an electrolyte can be split into the ionic contributions, the ionic limiting molar conductivities ${\lambda_I}^\infty$:

$$\Lambda_E^\infty = \nu_+ {\lambda_+}^\infty + \nu_- {\lambda_-}^\infty \tag{2.31}$$

with the appropriate stoichiometric coefficients. This is done by using experimentally measured (and extrapolated to infinite dilution) transference numbers, ${t_+}^\infty$ and ${t_-}^\infty = 1 - {t_+}^\infty$, such that ${\lambda_+}^\infty = {t_+}^\infty {\Lambda_E}^\infty$, etc. The commonly used units of the molar ionic conductivities are $S\ cm^2\ mol^{-1}$ ($S = \Omega^{-1}$). Values of the limiting ionic molar conductivities ${\lambda_I}^\infty$ for many ions in water at 298.15 K are shown in Table 2.5; they are accurate to $\pm 0.01\ S\ cm^2\ mol^{-1}$.

The mobilities of ions at infinite dilution, ${u_I}^\infty$, are directly proportional to the limiting ionic molar conductivities:

$${u_I}^\infty = \frac{{\lambda_I}^\infty}{|z|\,F} \tag{2.32}$$

as are also the self-diffusion coefficients:

$${D_I}^\infty = \frac{RT{\lambda_I}^\infty}{z^2F^2} \tag{2.33}$$

In fact, the latter have been obtained for most ions from the conductivities rather than from isotope labeling. Ion mobilities (hence molar conductivities and self-diffusion coefficients) increase with increasing temperatures. A five-fold increase in ${\Lambda_E}^\infty$ between 273 and 373 K has been noted. This is mainly because the viscosity of the solvent diminishes in this direction (Table 1.1 and see below). The transference numbers t_+ and t_- are temperature-sensitive too, though only mildly.

The mobility of an ion, hence its electric conductivity, depends on its size and on the viscosity of the solvent, ${\eta_W}^*$ for aqueous solutions. According to Nernst, Stokes, and Einstein, a quantity called the Stokes radius may be assigned to an ion:

$$r_{ISt} = \frac{\left(\frac{F^2}{6\pi N_A}\right)|z_I|}{{\eta_W}^* {\lambda_I}^\infty} \tag{2.34}$$

The parameter 6 in the denominator arises from the assumption of perfect sticking of the hydrated ion in the aqueous environment; otherwise, for perfect slipping, the parameter would be 4. Ionic Stokes radii, shown in Table 2.5, are of the same order of magnitude as the ionic radii r_I measuring the sizes of ions in crystals and solutions, shown in Table 2.2. However, the r_{ISt} are not directly related to the r_I, except for large tetraalkylammonium ions, for which they are substantially the same. In fact, in many cases the Stokes radii are smaller than the crystal ionic radii, although they are supposed to pertain to the hydrated ions and ought to be larger than the latter. Thus, although the r_{ISt} can be calculated formally by Eq. (2.34) they have no physical significance and their use ought to be discouraged (Marcus 2012b). The Walden products of the viscosities of the solvents and the limiting ionic molar conductivities, ${\eta_S}^*{\lambda_I}^\infty$, are approximately constant for the tetraalkylammonium cations (Marcus 2008). Hence, the Stokes radii of these ions are not sensitive to the solvents in which the ions are dissolved.

2.4.3 *Ionic Effects on the Viscosity*

The fluidity of a liquid, its rate of flow under a pressure gradient, is the reciprocal of its viscosity. The dynamic viscosity of water, ${\eta_W}^*$, although rather small compared with that of other liquids, is caused by the extensive network of hydrogen bonds existing in it that must be partly broken for the water to flow (Jenkins and Marcus 1995; Marcus 2009a). Ions affect the dynamic viscosity of the solution, η, some electrolytes enhancing it whereas others diminishing it. The effect is described up to fairly concentrated solutions by the Jones-Dole expression (Jones and Dole 1929):

$$\left(\frac{\eta}{{\eta_W}^*}\right) = 1 + A_\eta {c_E}^{1/2} + B_\eta c_E + \cdots \tag{2.35}$$

The A_η coefficients can be calculated theoretically from the conductivities according to Falkenhagen and Dole (1929):

$$A_\eta = \left(\frac{A_\eta^*}{\eta_W^*}(\varepsilon_W{}^* T)^{1/2}\right) f(\lambda_+{}^\infty, \lambda_-{}^\infty, z_+, z_-) \tag{2.36}$$

where $A_\eta{}^* = 1.113 \times 10^{-5}\ \mathrm{C^2(m\ K\ mol^{-3})^{1/2}}$ and the function $f(\lambda_+{}^\infty, \lambda_-{}^\infty, z_+, z_-)$ is for a symmetrical electrolyte ($z_+ = |z_-| = z$) approximately (Jenkins and Marcus 1995):

$$f = 0.0732 z^2 \frac{(\lambda_+{}^\infty + \lambda_-{}^\infty)}{\lambda_+{}^\infty \lambda_-{}^\infty} \tag{2.37}$$

On the other hand, the B_η coefficients are empirical. The are obtained as the limiting slopes of plots of $[(\eta/\eta_W{}^*) - 1]c_E^{-1/2}$ vs. $c_E^{1/2}$. The B_η coefficients are additive in terms of the constituent ions of the electrolyte and can be split into the ionic values by means of some reasonable assumption. The generally accepted assumption relates to the mobilities of the ions: $B_{\eta+}/B_{\eta-} \approx u_+/u_-$. The equality $B_\eta(\mathrm{K^+}, \mathrm{aq}) = B_\eta(\mathrm{Cl^-}, \mathrm{aq})$, valid over a narrow temperature range, has often been used, but $B_\eta(\mathrm{Rb^+}, \mathrm{aq}) = B_\eta(\mathrm{Br^-}, \mathrm{aq})$ holds over a fairly wide temperature range and is superior. The latter assumption differs by $-0.002 z_I\ \mathrm{M^{-1}}$ from the former (Jenkins and Marcus 1995). Viscosity B_η-coefficients of selected ions at 298.15 K are listed in Table 2.5 (see also Table 3.1 for data on some other ions and on the temperature coefficients dB_η/dT). They are positive for small and multivalent ions but negative for univalent large ions. As the temperature is increased the negative B_η values become less negative and may change sign at a characteristic temperature. This is explained by the diminishing extent of hydrogen bonded structure in the water as the temperature is raised, so that structure-breaking ions have less structure to break.

These algebraic signs have led to the classification of ions into water-structure-makers ($B_{\eta I} > 0$) and water-structure-breakers ($B_{\eta I} < 0$) (Gurney 1953), and such effects are fully discussed in Sect. 3.1.

2.5 Ion-Solvent Interactions

At infinite dilution in water an ion is surrounded by water molecules and its interactions with them are described in Sect. 2.2, 2.3, and 2.4 in terms of measurable quantities. The dependence of these on the concentration is also briefly described there. There are some further aspects of the ion-solvent interactions that merit discussion, as is done here.

The preference of ions to be hydrated rather than be solvated by non-aqueous solvents, as is manifested by the thermodynamic quantities of transfer from water to such solvents has been recently reviewed (Marcus 1996, 2007; Kalidas et al. 2000; Hefter et al. 2002). These quantities depend on the properties of the non-aqueous solvents and are outside the scope of the present book.

The mutual interactions of ions are treated in Sect. 2.6.

2.5.1 Salting-out and -in

Ions are hydrated and they bind water in their solvation shells, causing less 'free' water to be available to accommodate other solutes. Disregarding any direct ion-solute interactions, the presence of ions in a solution then cause an elevation of the activity coefficient y_N of a non-electrolyte solute, marked by subscript N, in a c_E molar solution of an electrolyte by a factor $1/[1-(V_W/1000)h_E c_E]$ in molar units. Here h_E is the sum of the hydration numbers of the ions constituting the electrolyte.

A result of this is a diminution of the solubility of the non-electrolyte solute N in a solvent containing the electrolyte E in order to maintain a constant activity of N at equilibrium with the pure solute. This phenomenon is called 'salting out' and is described up to fairly high c_E by the Setchenov expression:

$$\log\left(\frac{s_N{}^*}{s_N}\right) = k_{NE}c_E \tag{2.38}$$

Here $s_N{}^*$ is the solubility of N in water in the absence of E and s_N is that in its presence. The coefficient k_{NE} is called the Setchenov salting-out constant and depends on the natures of the non-electrolyte and of the electrolyte as well as on the temperature at ambient pressures. The Setchenov expression is taken as the limiting expression, valid for small solubilities, where self-interactions of the non-electrolyte can be disregarded. Because of the proportionality of the left hand side of Eq. (2.38) to c_E, the Setchenov expression pertains also to infinite dilution of the electrolyte and is additive with respect to the contribution of each ion, k_{NI}, to the total $k_{NE} = \Sigma_I\, \nu_I k_{NI}$, the index $_I$ pertaining to the individual ions of the salting agent (cations and anions, including those in mixed electrolytes) and the ν_I being their stoichiometric coefficients. There are some systems where the solubility is enhanced by the presence of the electrolyte so that $k_{NE} < 0$ and salting-in then occurs, but as a rule $k_{NE} > 0$ and the solubility is diminished.

Salting-out and salting-in pertain not only to the solubilities of the non-electrolyte solutes, but also to their volatility, their extractability by solvents immiscible with water, to phase-transfer catalysis, and other phenomena. The salting is not confined to aqueous solutions, where it was primarily studied and applied, but is found in all kinds of solutions of electrolytes, whatever the solvent. Typical solutes to which Eq. (2.38) pertains are non-reactive gases and organic compounds sparingly soluble in water.

The magnitude of k_{NE} for a given salt generally increases with the molar volume of the non-electrolyte, V_N, and for a given solute with the intensity of hydration of the electrolyte. The latter can be described by the electrostriction that the ion causes (Marcus 2011) and this leads to the McDevit and Long (1952) formulation for the Setchenov constant, rewritten as:

$$k_{NE} = \frac{-V_N V_{E\text{-elec}}}{(\ln 10)RT\kappa_{TW}} \tag{2.39}$$

where $V_{E\text{-elec}}$ is the (negative) molar electrostriction by the electrolyte. The direct interactions of the ions of the electrolyte with molecules of the non-electrolyte are

ignored in this approach. Actually, values of k_{NE} predicted by Eq. (2.39) are about three-fold larger than the experimental values (McDevit and Long 1952; Deno and Spink 1963).

Salting-in cannot be described by this formulation and occurs with poorly hydrated ions and/or with non-electrolytes that are more polar than the solvent (have a higher permittivity). An earlier theory, that of Debye and McAulay (1925), related the salting to the electrical work of charging the ions in water compared with that in the presence of the non-electrolyte. This work is proportional to the difference $(1/\varepsilon_r - 1/\varepsilon_{rW})$. When this difference is negative, that is, for highly polar solutes that increase the permittivity, salting-in is predicted. Other early theories of salting-out and -in were reviewed in the book by Marcus and Kertes (1969) and by Conway (1985) among others.

Shoor and Gubbins (1969) applied the scaled particle theory (SPT) to the salting-out and -in, specifically to the solubilities of non-polar gases in concentrated aqueous potassium hydroxide. Masterton and Lee (1970) derived the Setchenov constants from the SPT for more general systems. Their expression is the sum of three individually calculated terms: $k_{NE} = k_{\alpha NE} + k_{\beta NE} + k_{\gamma E}$, where $k_{\alpha NE}$ pertains to the work required for forming a cavity of the size of the solute, $k_{\beta NE}$ pertains to the interactions of the solute in the cavity with its surroundings, and $k_{\gamma E}$ converts from molar to mole-fraction units. The work $k_{\alpha NE}$ for cavity formation in the electrolyte solution does not equal that in the pure solvent, $k_{\alpha N}$, but is somewhat larger due to the increased tightness of the solvent in the presence of the electrolyte. For the calculation of the Setchenov constant for a particular system it is necessary to know the standard partial molar volume of the electrolyte, V_E^{∞}, the diameters σ_I and polarizabilities α_I of its ions, and the diameter σ_N, polarizability α_N, and Lennard-Jones energy parameter (e_N/k_B) of the solute. Fairly complicated expressions result from this theory for the quantities $k_{\alpha NE}$, $k_{\beta NE}$, and $k_{\gamma E}$. The values of $k_{\alpha NE}$ are positive, those of $k_{\beta NE}$ are negative, and salting-in would occur if $k_{\alpha NE} + k_{\beta NE}(+k_{\gamma E}) < 0$. The values of $k_{\gamma E}$ are much smaller than the other terms, and may have either sign, depending on V_E^{∞} but not on N. The SPT, essentially as developed by Masterton and Lee (1970), has since been applied by other authors to describe and predict salting behavior, e.g., (Fromon and Treiner 1979; Treiner 1981). Pawilkowski and Prausnitz (1983) showed that for a given salt k_{NE} follows the linear expression $a_E + b_E(e_N/k_B)$ for non-reactive gases, and listed the ionic a_I and b_I values (based on the convention that their values of OH^- are zero).

Ruckenstein and Shulgin (2002) used the Kirkwood-Buff fluctuation theory to obtain an expression for the salting out (of gases, but applicable to any non-electrolyte solute) in electrolyte solutions. The resulting expression can be re-written as:

$$k_{NE} = -(2.303 \times 2000)^{-1}(G_{WW} - G_{EE} - 2(G_{WN} - G_{WE})) \tag{2.40}$$

where $G_{\alpha\beta} = {}_0\int^{\infty}(g_{\alpha\beta} - 1)4\pi r^2 dr$ is the Kirkwood-Buff integral, $g_{\alpha\beta}$ is the pair correlation function for species α and β (being water W, electrolyte E, or non-electrolyte N) as a function of the distance r between the centers of their molecules. These integrals are related to the partial molar volumes and Eq. (2.40) can be transformed in

dilute solutions to:

$$k_{NE} = -(2.303 \times 2000)^{-1} \frac{-(\partial V_N / \partial c_E)}{V_E^{\infty}} + V_E^{\infty} - V_W^{*} \qquad (2.41)$$

The first term in the square brackets is generally small compared with the other two and may be neglected. Salting-in then occurs in systems where $V_E^{\infty} > V_W^{*}$, i.e., for bulky ions having a molar volume larger than that of pure water, but otherwise salting-out occurs. Mazo (2006) in an equivalent derivation used the measured k_{NE} to evaluate the Kirkwood-Buff integral G_{NE} not otherwise accessible.

On the practical level, another manner of looking at the salting-out, in the case of non-reactive gases, has been proposed by Weisenberger and Schumpe (1996) by means of the empirical expression:

$$k_{GE} = \Sigma_I \nu_I \left[k_I + k_{G25} + h_G \left(\frac{t}{°C} - 25 \right) \right] \qquad (2.42)$$

The index $_I$ pertains to the individual ions of the salting-out agent (cations and anions, including mixed electrolytes), k_I is an ion specific parameter that is relatively independent of the temperature, and k_{G25} and h_G are gas specific parameters. The conventional numerical values for the k_I are shown in Table 2.6, on the basis $k(H^+)^{conv} = 0$. For the cations to a good approximation $k_I/z_I = 0.080 \pm 0.002\ M^{-1}$, with a small increase in the alkaline earth and divalent transition metal series with the ionic radius, but for the alkali metal ions the opposite trend is observed, except for Li^+. The values of $k_I = 0.0648$ for Cr^{3+} and $k_I = 0.1161$ for Fe^{3+} appear to be outliers. For the anions less clear charge and size dependencies are seen, with $k_I/|z_I| = 0.072 \pm 0.007$, and for the halides k_I decreases with increasing size. The gas parameters are normalized to $k(O_2)^{conv} = 0$, with some positive k_I (e.g., 0.0120 for ethene) and some negative (e.g., −0.0159 for ethane) values for different gases, for most of which $h_G < 0$ for $273 \leq t/°C \leq 353$.

The salting out properties of organic solutes, mainly hydrocarbons, were compiled for many salts by Xie et al. (1997). The dependence on the molar volume of the solute, predicted by Eq. (2.39), was confirmed. Conventional salting constants k_I/M^{-1} on the basis $k(H^+)^{conv} = 0$ for benzene are shown in Table 2.6, the value for HCl yielding the Cl^- value, that for NaCl then the Na^+ value, and these served as secondary reference ions. For SCN^- the mean value for LiSCN and CsSCN was used, since otherwise the anion value would be an outlier. There is good qualitative agreement between the gas salting by the ions and the salting of benzene, but in the latter case instances of salting-in ($k_I < 0$) by large ions are noted.

2.5.2 *Preferential Solvation of Ions in Aqueous Mixed Solvents*

Different considerations are applied when the non-electrolyte is a solvent S miscible with water and is present at an appreciable concentration whereas the electrolyte is

Table 2.6 Ionic salting out parameters k_I/M^{-1} of gases according to Eq. (2.42) from (Weisenberger and Schumpe 1996) and of benzene from (Xie et al. 1997)

Cation	k_I(gases)	k_I(benzene)	Anion	k_I(gases)	k_I(benzene)
H^+	0	0	F^-	0.0920	0.115
Li^+	0.0754	0.094	Cl^-	0.0318	0.048
Na^+	0.1143	0.137	Br^-	0.0269	0.018
K^+	0.0922	0.108	I^-	0.0039	−0.042
Rb^+	0.0839	0.092	OH^-	0.0839	
Cs^+	0.0759	0.040	HS^-	0.0851	
NH_4^+	0.0556	0.055	CN^-	0.0679	
Mg^{2+}	0.1694	0.174	SCN^-	0.0627	−0.032
Ca^{2+}	0.1762		NO_2^-	0.0795	
Sr^{2+}	0.1881	0.176	NO_3^-	0.0128	−0.018
Ba^{2+}	0.2168	0.238	ClO_3^-	0.1348	−0.016
Mn^{2+}	0.1463		BrO_3^-	0.1116	
Fe^{2+}	0.1523		IO_3^-	0.0913	
Co^{2+}	0.1680		ClO_4^-	0.0492	−0.041
Ni^{2+}	0.1654		IO_4^-	0.1464	
Cu^{2+}	0.1675		HCO_3^-	0.0967	
Zn^{2+}	0.1537		HSO_3^-	0.0549	
Cd^{2+}	0.1869		$H_2PO_4^-$	0.0906	
Al^{3+}	0.2174		HCO_2^-		0.029
La^{3+}	0.2297		$CH_3CO_2^-$		0.028
Ce^{3+}	0.2406		$C_2H_5CO_2^-$		0.021
Th^{4+}	0.2709		CO_3^{2-}	0.1423	
$(CH_3)_4N^+$		−0.303	SO_3^{2-}	0.1270	
$(C_2H_5)_4N^+$		−0.625	SO_4^{2-}	0.1117	0.274
			HPO_4^{2-}	0.1499	
			$S_2O_3^{2-}$	0.1149	
			PO_4^{3-}	0.2119	
			$Fe(CN)_6^{4-}$	0.3574	

present at a low concentration. The ions are then solvated by both components of the mixed solvent: water (W) and the organic solvent (S). Its near environment generally has a composition differing from that of the bulk mixture due to preferential solvation of the ion by one of the components. If an ion $I^{\pm}$ has a favorable Gibbs energy of transfer from water into the pure organic component of the mixture: $\Delta_t G^{\infty}(I^{\pm}, W \rightarrow S) < 0$, then it will be preferentially surrounded by molecules of S, otherwise it will be preferentially hydrated. This statement must be modified in view of the mutual interactions of the solvent components of the mixture. When the preferential solvation (hydration) in the mixture is practically complete selective solvation (hydration) is said to takes place. It is of interest to enquire what fraction of the solvation shell of the ion is occupied by each solvent component, and there are two approaches that have been used in order to deal with this question (Marcus 2002).

The following model is employed in the quasi-lattice quasi-chemical (QLQC) approach (Marcus 1983a). The ion $I^{\pm}$ and the molecules of the two solvents, W and S, are distributed on sites of a quasi-lattice characterized by a lattice parameter Z that specifies the number of neighbors each particle has, independently of the nature of the

particles. Note the difference from the QLQC treatment of binary solvent mixtures dealt with in Sect. 1.2.4. The total configurational energy of the system is determined by the sum of the pair-wise interaction energies e_{IW}, e_{IS}, e_{WW}, e_{WS}, and e_{SS}, weighted according to the numbers of the corresponding nearest neighbors, N_{IW}, N_{IS}, etc. These pair-wise energies are assumed to be independent from the other neighbors the partners of the pair have. Ideal entropy of mixing of the particles on the quasi-lattice sites is assumed. The quasi-chemical aspect relates to the relative strength of the mutual interactions of the solvent molecules and those with the ion. A set of equations is provided by this approach to determine the local mole fraction of each of the mixed solvent components, made up from $n_W + n_S$ moles of the components around the ion present at infinite dilution. The relative interaction energy of the ion with W and S is obtained from its standard molar Gibbs energy of transfer from W to S:

$$\Delta E_{I,WS} = \frac{\Delta_t G^{\infty}(I^{\pm}, W \rightarrow S)}{Z} \tag{2.43}$$

The mutual interaction of W with S is obtained from the molar excess Gibbs energy at the equimolar composition in the absence of the ions:

$$\exp\left(\frac{\Delta E_{WS}}{RT}\right) = \left[\left\{2\exp\left(\frac{-G^{E}{}_{WS(x=0.5)}}{ZRT}\right)\right\} - 1\right]^2 \tag{2.44}$$

leading to:

$$\frac{N_{WS}}{Z(n_W + n_S)} = \frac{1 - \left\{1 - 4x_W x_S\left(1 - \exp\left(\frac{-\Delta E_{WS}}{RT}\right)\right)\right\}^{1/2}}{2\left(1 - \exp\left(\frac{-\Delta E_{WS}}{RT}\right)\right)} \tag{2.45}$$

The ratio of the like pairs of solvent molecules is:

$$\frac{N_{SS}}{N_{WW}} = x_S - \frac{\frac{N_{WS}}{Z(n_W + n_S)}}{x_W - \frac{N_{WS}}{Z(n_W + n_S)}} \tag{2.46}$$

The local mole fraction of component W is:

$${x_{IW}}^{L} = 1 - {x_{IS}}^{L} = \frac{1}{1 + (N_{SS}/N_{WW})^{1/2}\exp(\Delta E_{I,WS}/2RT)} \tag{2.47}$$

and the hydration number of the ion is then $Z \cdot {x_{IW}}^{L}$. The equilibrium constant for the replacement of S by W is (Marcus 1988a):

$${K_S}^{W} = \frac{{x_{IW}}^{L} x_S}{x_W {x_{IS}}^{L}} \tag{2.48}$$

The standard molar Gibbs energy of transfer of the ion $I^{\pm}$ from water to the mixture, $\Delta_t G^{\infty}(I^{\pm}, W \rightarrow W + S)$ serves to establish the lattice parameter Z within ± 2 units by fitting the data.

The inverse Kirkwood-Buff integral method (IKBI) does not involve a model such as the QLQC method does, hence is rigorous (Ben-Naim 1988). Note, again, the differences with respect to the treatment of binary solvent mixtures in Sect. 1.2.4. It requires the derivatives of the Gibbs energy of transfer:

$$D = \frac{\mathrm{d}\Delta_t G^{\infty}(I^{\pm}, W \rightarrow W + S)}{\mathrm{d}x_S} \tag{2.49}$$

and of the excess Gibbs energy of mixing with respect to the mixed solvent composition:

$$Q = RT + \frac{x_A x_B \mathrm{d}^2 G^E{}_{A,B}}{\mathrm{d}x_B{}^2} \tag{2.50}$$

These functions, however, may often not be known sufficiently accurately for obtaining meaningful derivatives. The Kirkwood-Buff integrals need for their evaluation in addition to these derivatives also the isothermal compressibility of the mixture, κ_T,and the partial molar volumes of the ion, V_I, and the two solvent components in the mixture as a function of the solvent composition. These integrals are then:

$$G_{W,I} = RT\kappa_T - V_I + \frac{x_S V_S D}{Q} \tag{2.51}$$

$$G_{S,I} = RT\kappa_T - V_I + \frac{x_W V_W D}{Q} \tag{2.52}$$

The expressions yielding the local mole fraction of water around the ion $x_{IW}{}^L$ requires furthermore an estimate of the correlation volume, i.e., the volume around the ion in which it affects the composition of the local solvent mixture. This must be calculated iteratively, because the volume occupied by the solvents around the ions depends on the composition when the components differ considerably in their molar volume, as is to be expected when one of them is water.

$$V_{cor} = 2522.5\ [r_I + 0.1363(x_{IW}{}^L V_W + x_{IS}{}^L V_S)^{1/3} - 0.085]^3 \tag{2.53}$$

The preferential hydration parameter is finally obtained as

$$\delta x_{IW} = x_{IW}{}^L - x_W = \frac{x_W x_S (G_{WI} - G_{S,I})}{(x_W G_{W,I} + x_S G_{S,I} + V_{cor})} \tag{2.54}$$

There exists also the problem in obtaining the required information from experimental data, in that the latter pertain to entire electrolytes, and their application to single ions has some bearing on the meaning of the Kirkwood-Buff integrals. Application of the TPTB assumption (see p. 65) to the splitting of the standard molar Gibbs

Table 2.7 Aqueous solvent mixtures in which the preferential solvation of ions was stutied by the QALQC and IKBI methods (Marcus 2002)

Co-solvent S	Ions	QLQC	IKBI
Methanol	Na^+, Cl^-	✓	✓
Ethanol	K^+, Cl^-	✓	✓
Tetrahydrofuran	H^+, $CH_3CO_2^-$	✓	
Dimethylsulfoxide	Li^+, Na^+, Cs^+, Ag^+, Cl^-, Br^-, I^-	✓	✓
Acetonitrile	H^+, Na^+, Ag^+, Cu^+, Cu^{2+}, Cl^-, $CH_3CO_2^-$	✓	✓
Pyridine	Zn^{2+}, F^-, Cl^-, Br^-, I^-, $C_6H_5CO_2^-$	✓	

energy of transfer of an electrolyte into the ionic contributions has been employed to circumvent this theoretical problem (Marcus 2002).

Both methods have been applied to several ions in aqueous solvent mixtures, with fair agreement when they have been applied to a given system (Marcus 2002). Some systems studied are presented in Table 2.7.

2.6 Ion-Ion Interactions

Beyond infinite dilution, at practical concentrations, ions in solution are sufficiently near each other to interact electrostatically: ions of like charge sign repel each other and those of unlike charge sign attract each other. The average distance apart of the ions, Sect. 2.2.1., is constrained by their concentrations:

$$d^{\mathrm{av}} = {N_{\mathrm{A}}}^{-1/3}\Big(\sum \nu_{\mathrm{I}} c_{\mathrm{I}}\Big)^{-1/3} = 1.1844\Big(\sum \nu_{\mathrm{I}} c_{\mathrm{I}}\Big)^{-1/3}\ \mathrm{nm} \qquad (2.11)$$

At 1 molar concentration and above d^{av} is commensurate with the sizes of ions with their hydration shells in solution: $r_{\mathrm{I}} + 2r_{\mathrm{W}} = d_{\mathrm{I\text{-}O}} + r_{\mathrm{W}}$ (Sect. 2.2.2) (Marcus 2009b).

The electrostatic interactions compete with the thermal movement of all the particles in the solution, ions and water molecules, and are screened by the high dielectric permittivity of the water. The overall interactions, involving ion hydration in addition to ion-ion interactions and the hydrogen bonded network of water are quite complicated. Approximations have to be applied in order to handle the resulting behavior of the ions theoretically.

The 'restricted primitive model' described at the beginning of Sect. 2.2. regards the ions as charged conducting spheres dispersed uniformly in a continuum made up of a compressible dielectric. Within this model and in very dilute solutions of electrolytes the well-known Debye-Hückel theory describes the chemical potentials of the electrolyte, μ_{E}, and that of the water, μ_{W}, sufficiently well.

2.6.1 Activity and Osmotic Coefficients

The chemical potential of the electrolyte, μ_{E}, is directly related to its activity and to its mean ionic activity coefficient, $\gamma_{\mathrm{E}\pm}$ (on the molal scale) or $y_{\mathrm{E}\pm}$ (on the molar

scale):

$$\mu_{\mathrm{E}} = \mu_{\mathrm{E(m)}}{}^{\infty} + \nu_{\mathrm{E}} RT \ln(m_{\mathrm{E}} \gamma_{\mathrm{E}\pm}) = \mu_{\mathrm{E(c)}}{}^{\infty} + \nu_{\mathrm{E}} RT \ln(c_{\mathrm{E}} y_{\mathrm{E}\pm}) \tag{2.55}$$

Here ν_{E} is the number of ions per formula of the electrolyte. The chemical potential of the water, μ_{W}, is directly related to its activity a_{W}:

$$\mu_{\mathrm{W}} = \mu_{\mathrm{W}}{}^{*} + RT \ln a_{\mathrm{W}} \tag{2.56}$$

The activity of the water is roughly equal to the ratio of its vapor pressure in the solution to that of the pure water: $p_{\mathrm{W}}/p_{\mathrm{W}}{}^{*}$ (when the vapor pressures are small and the vapors can be considered to approximate ideal gases). The activity of water in the electrolyte solution of molality m_{E} is related to its osmotic coefficient φ_{W} by:

$$\varphi_{\mathrm{W}} = -\left(\frac{1000}{\nu_{\mathrm{E}} m_{\mathrm{E}} M_{\mathrm{W}}}\right) \ln a_{\mathrm{W}} \tag{2.57}$$

where M_{W} is the molar mass of the water (in g mol^{-1}, 1,000/M_1 = 55.51). The osmotic coefficient is also related to the depression of the freezing point and elevation of the boiling point of the water. The vapor pressures and these quantities are used in order to obtain the water activity experimentally, and this, in turn, leads via the Gibbs-Duhem relationship to the activity coefficient of the electrolyte:

$$-55.51 \mathrm{d} \ln a_{\mathrm{W}} = \nu_{\mathrm{E}} m_{\mathrm{E}} \ln(m_{\mathrm{E}} \gamma_{\mathrm{E}\pm}) \tag{2.58}$$

The various methods to obtain the osmotic and activity coefficients experimentally (the latter also from galvanic cells) are described in the classical books by Harned and Owen (1958) and by Robinson and Stokes (1965).

Application of the restricted primitive model leads to the *limiting* Debye-Hückel expression for the mean molal activity coefficient of an electrolyte that pertains to very dilute solutions:

$$\log \gamma_{\mathrm{E}\pm} = -A z_{+} z_{-} I^{1/2} \tag{2.59}$$

where A depends on the temperature ($A = 0.5115$ in water at 298.15 K). The logarithm of $\gamma_{\mathrm{E}\pm}$ is thus proportional to the square root of the ionic strength:

$$I = 0.5 \sum\nolimits_{\mathrm{I}} m_{\mathrm{I}} z_{\mathrm{I}}{}^{2} \tag{2.60}$$

the summation extending over all the ions in the solution that may contain a mixture of electrolytes. This limiting expression is valid only in very dilute solutions, up to, say, $m = 0.01$ m ($\sim$0.01 M) for uni-univalent electrolytes.

Beyond this concentration, and still within the restricted primitive model, the *extended* Debye-Hückel expression should be used:

$$\log \gamma_{\mathrm{E}\pm} = \frac{-A z_{+} z_{-} I^{1/2}}{1 + B a I^{1/2}} \tag{2.61}$$

It is valid, in turn, up to, say, $m = 0.2\,m$ ($\sim$0.15 M). Beyond this concentration, again, or for higher-valent electrolytes, a linear term in the ionic strength, bI, has to be added, up to quite high concentrations. In these extended expressions, B is a temperature-dependent constant 3.291 $\mathrm{nm^{-1}(mol/kg)^{-1/2}}$ in water at 298.15 K and a is the mean distance of closest approach of the ions. This ought to be at least the sum of their radii: $a \geq r_+ + r_-$ or may be equated to their diameters, if considered the same for cations and anions. On the other hand, the coefficient b of the linear term is a completely empirical fitting parameter. For many purposes the universal product $Ba = 1.5\,\mathrm{kg^{1/2}\,mol^{-1/2}}$ at any temperature may be used in Eq. (2.61), leaving the responsibility for fitting the experimental values of $\log \gamma_{\mathrm{E}\pm}$ to the parameter b.

The added empirical quantity bI was replaced by Stokes and Robinson (1948) by an expression in the hydration number of the electrolyte $h_\mathrm{E} = \nu_+ h_+ + \nu_- h_-$, with the stoichiometric coefficients $\nu_+ + \nu_- = \nu_\mathrm{E}$, according to:

$$\log \gamma_{\mathrm{E}\pm} = \frac{-Az_+z_-I^{1/2}}{1 + BaI^{1/2}} - \frac{h_\mathrm{E}}{\nu_\mathrm{E}} \log a_\mathrm{W} - \log[1 + 0.001 M_\mathrm{W}(\nu_\mathrm{E} - h_\mathrm{E})m_\mathrm{E}] \qquad (2.62)$$

Here, again, there are two fitting parameters, the distance of closest approach a and the hydration number h_E. The expression (2.62) accounts for the amount of solvent, water, bound to the ions in the statistical part of the chemical potential.

A key quantity in the Debye-Hückel theory, leading to the values of the constants A and B, is the screening length, κ, the average reciprocal of the radius of the 'ionic atmosphere' surrounding an ion in the solution, made up essentially by ions of the opposite charge. The square of this quantity is proportional to the ionic strength of the solution and also to the reciprocal of the product $\varepsilon_\mathrm{W}{}^* T$:

$$\kappa^2 = \frac{{N_\mathrm{A}}^2 e^2}{1000 \varepsilon_0 \varepsilon_\mathrm{W}{}^* RT} I \qquad (2.63)$$

The numerical value of the screening length is $\kappa = 0.3556(\varepsilon_\mathrm{W}{}^* T/\mathrm{K})^{-1/2}(I/\mathrm{M})^{1/2}$ $\mathrm{nm^{-1}}$ and for water at 298.15 K it is $\kappa = 2.325 \times 10^{-3}(I/\mathrm{M})^{1/2}\ \mathrm{nm^{-1}}$. The dimensionless product κa features in the denominator of the extended Debye-Hückel expression for $\log \gamma_{\mathrm{E}\pm}$ and in the corresponding expression for the osmotic coefficient.

The logarithm of the water activity is given by the Debye-Hückel theory as:

$$\ln a_\mathrm{W} = -\ln \frac{1 + \nu_\mathrm{E} m_\mathrm{E} M_\mathrm{W}}{1000} + \frac{V_\mathrm{W}}{24\pi N_\mathrm{A}} \kappa^3 \sigma(\kappa a) \qquad (2.64)$$

The function $\sigma(\kappa\, a)$ is

$$\begin{aligned} \sigma(\kappa a) &= 3(\kappa a)^{-3}[(1 + \kappa a) - (1 + \kappa a)^{-1} - 2\ln(1 + \kappa a)] \\ &\approx 1 - 1.5(\kappa a) + 1.8(\kappa a)^2 - \ldots \end{aligned} \qquad (2.65)$$

where the approximation is valid for $\kappa a \leq 1$.

An alternative formulation for the activity and osmotic coefficients is that of Pitzer (1979). It includes the Debye-Hückel limiting law, but treats differently its extension

to practical concentrations for fully dissociated electrolytes up to several moles per kg or per dm^3. For 1:1 electrolytes the resulting expressions are:

$$\ln\gamma_{E\pm} = f_\gamma + B_\gamma m_E + C_\gamma {m_E}^2 \tag{2.66}$$

and

$$\varphi_W = 1 + f_\varphi + B_\varphi m_E + C_\varphi {m_E}^2 \tag{2.67}$$

The functions f are the electrostatic Debye-Hückel terms and the B and C coefficients are electrolyte-specific fitting parameters. Factors involving the charge numbers and stoichiometric coefficients have to be included for electrolyte types other than 1:1. Two universal constants, $b = 1.2$ and $\alpha = 2.0$ are employed in the full expressions for B and C as well as the solvent- and temperature-dependent A_φ arising from the Debye-Hückel theory. For details the series of papers by Pitzer and coworkers should be consulted, starting with (Pitzer and Mayoraga 1973).

For very concentrated solutions, in which the activity of the water is $a_W \leq 0.5$, another approach has been found to be useful. This is the BET approach that assumes that the water molecules are adsorbed on the ions of the salt. According to Stokes and Robinson (1948) the expression relating the salt molality m_E and the water activity a_W is:

$$\frac{m_E a_W M_W}{1 - a_W} = \frac{1}{c_{BET} r_{BET}} + \frac{(c_{BET} - 1) a_W}{c_{BET} r_{BET}} \tag{2.68}$$

A plot of the left hand side (with M_W in kg mol^{-1}) against a_W yields the product $c_{BET} r_{BET}$ as the intercept and $(c_{BET} - 1)/(c_{BET} r_{BET})$ as the slope, from which the two parameters r_{BET} and c_{BET} can be extricated. The former, r_{BET}, represents the number of 'binding sites' for water molecules per formula unit of the salt and the latter, $c_{BET} = \exp(\Delta H_{sorb}/RT)$ involves the difference ΔH_{sorb} between the molar enthalpy of 'sorption' of the water on the salt and the molar enthalpy of liquefaction of water vapor (the negative of the enthalpy of vaporization). The parameters r_{BET} and ΔH_{sorb} depend only moderately on the temperature and are shown in Table 2.8 for a number of salts for which a_W data are available at high concentrations (Marcus 2005a). Although the parameter r_{BET} plays the role of a hydration number, it is noted from the entries in Tables 2.3 and 2.8 that these two quantities do not correlate well, since h pertains to dilute solutions and r_{BET} to very concentrated ones, where hydration shells overlap.

2.6.2 Ion Pairing

In electrolyte solutions consisting of relatively poorly hydrated ions the screening of the charges by the aqueous solvent is inadequate to prevent ionic association at sufficiently high concentrations. In most cases the association stops at ion pairing:

Table 2.8 BET parameters for concentrated salt solutions at 25 °C (Marcus 2005a)

Salt	r_{BET}	ΔH_{sorb}/kJ mol^{-1}
LiCl	3.64	7.05
LiBr	3.82	9.32
$LiClO_4$	3.18	7.50
NaOH	3.20	7.34
KOH	3.25	8.26
$MgBr_2$	7.10	9.19
$CaCl_2$	6.73	5.58
$CaBr_2$	7.50	8.57
$Ca(NO_3)_2$	3.86	5.55
$Ca(ClO_4)_2$	6.83	8.68
$ZnCl_2$	3.69	7.73
$ZnBr_2$	4.01	7.40

one cation with one anion. The treatment of ion pairing according to Bjerrum, using the restricted primitive model (see p. 52), can be formulated as follows (Marcus and Hefter 2006). Ions that are nearer each other than the cut-off distance

$$q = \frac{z_+ z_- N_A e^2}{8\pi \varepsilon_0 \varepsilon_W RT} \tag{2.69}$$

are considered to be paired, those at larger distances from each other are free. The cut-off distance q is necessarily larger than the distance of closest approach a. Due to the electrostatic forces, only ions of opposite charge signs are likely to approach each other to a distance $\leq q$.

The equilibrium $C^{z+} + A^{z-} \leftrightarrows C^{z+}A^{z-}$ is governed by the equilibrium constant, K_A. If the fraction α of the c_E molar electrolyte is dissociated and the fraction $1 - \alpha$ is paired, then:

$$K_A = \frac{1-\alpha}{\alpha^2 c_E} \tag{2.70}$$

The association constant arising from Bjerrum's theory is:

$$K_A = \frac{4\pi N_A}{1000} b^3 Q(b) \tag{2.71}$$

where $b = q/a$ is a dimensionless parameter and the function $Q(b) = {}_2\int^b x^{-4}\exp(x)\mathrm{d}x$, with x as an auxiliary variable, is used, the integral being solved numerically. The value of the key variable b at 298.15 K for any solvent (characterized by its ε_r) is given by:

$$\log b = 1.448 + \log|z_+ z_-| - \log\varepsilon_r - \log(a/\mathrm{nm}) \tag{2.72}$$

At other temperatures $\log(298.15\ \mathrm{K}/T)$ should be added to the numerical constant, with the appropriate value of ε_r being used. The distance of closest approach a is taken as the mean diameter of the ions that should not be smaller than the sum of their ionic radii: $a \geq r_+ + r_-$. The values of $\log Q(b)$ have been tabulated (Marcus

1977) and range from −1.358 at $b = 2.1$ (the lowest practical value) through zero for $b = 5.9$ to positive values at large b, for which $Q(b) \approx \exp(b)/b^4$. The association constant K_A is readily calculated from the parameters b and $Q(b)$ and from it and Eq. (2.70) the fraction associated, $1 - \alpha$ is obtained as a function of the concentration c_E.

The dissociated fraction of the electrolyte, α, is commonly obtained from conductivity data, although other techniques have also been widely employed. In the case of the conductivities, expression (2.19) is replaced by:

$$\Lambda_2 = \Lambda_2^{\infty} - S(\alpha c_2)^{1/2} + E(\alpha c_2)\ln(\alpha c_2) + J'(R')(\alpha c_2) - J''(R'')(\alpha c_2)^{3/2} \quad (2.73)$$

recognizing that the actual concentration of the ions is αc_E instead of c_E.

Ion pairing between univalent ions in aqueous solutions with its high relative permittivity is rare, unless they are only poorly hydrated and can approach each other to within $q = 0.357$ nm (at 298.15 K). The ion-ion interactions that may lead to ion pairing of the alkali metal cations and halide anions were discussed by Collins (1997) in terms of their surface charge densities and the competition between ion-water and water-water interactions. He followed Morris (1968, 1969) who studied the solubilities and heats of solution of such salts and Diamond (1963) who pointed out the water-structure-enforced ion pairing that occurs when both cation and anion are large and poorly hydrated. This has recently been demonstrated by Heyda et al. (2010) using molecular dynamics simulations as well as experimental results concerning NH_4^+ ions on the one hand and for the poorly hydrated tetraalkylammonium ions on the other associating with halide anions. Whereas for the small well hydrated NH_4^+ the order of association is $F^- > Cl^- \geq Br^- \geq I^-$, the order is reversed for the poorly hydrated R_4N^+ ions: $F^- < Cl^- < Br^- < I^-$.

For more highly charged ions appreciable ion pairing does occur in aqueous solutions at concentrations of the order of 1 M for 1:2 or 2:1 type salts and even at concentrations of 0.1 M for 2:2 or salts with more highly charged ions. The equilibrium constants for association of the latter (e.g., $MgSO_4$) are of the order of 100–200 M^{-1}.

There is nothing in this formal electrostatic theory, based on the restricted primitive model of the electrolyte solution, to indicate how intimately the cation and anion are bound together in the ion pair. Water molecules penetrate the intervening space in cases where the cut-off distance q is manifold larger than the mean ionic diameters a. It is possible to specify how many solvent molecules separate the cation and the anion if the 'restricted' is removed from the model. A 'contact ion pair' (CIP) is formed if this number is zero, a 'solvent shared ion pair' (SIP) is formed if it is 1, and a 'solvent separated ion pair' (SSIP or S2IP) is formed if it is 2. Several forms of such ion pairs can exist at equilibrium with each other, depending on the electrolyte concentration. Methods for ascertaining the situation with regard to these forms of ion pairs have been reviewed (Marcus and Hefter 2006).

2.7 Charged Macromolecules

Soluble polymers that carry ionically dissociable groups are called polyelectrolytes, ionizing partly or completely to polyions. Synthetic polyelectrolytes generally have a linear polymeric chain, the hydrophobic backbone, to which side groups with hydrophilic ionizable groups are attached. An typical example of a polyelectrolyte is polystyrene sulfonic acid $-[CH_2CH(C_6H_5SO_3^-H^+)]_n-$, a strong, practically completely ionized electrolyte. The covalently attached ions, $-SO_3^-$, are the 'fixed ions' to which correspond mobile 'counter ions' of opposite charge, hydrated hydrogen ions. On the other hand, a weak polyelectrolyte, such as polymethacrylic acid $-[CH_2C(CH_3)(CO_2^-H^+)]_n-$, is only partly ionized, depending on the pH of the solution. Some polyions do not have a hydrophobic backbone but have long chains of hydrophilic moieties that are ionized, an example being polyphosphate detergents.

Such synthetic linear polyelectrolytes have a regularly repeating structure, but less regularity results from graft polymers, where randomly placed segments of different structures are connected in a row and may form polyelectrolytes having a branched backbone. Synthetic polyelectrolytes may also be cross-linked to form water-insoluble ion exchange resins and membranes that can exchange the counter ions with other ones in the imbibed or adjacent solution. Biological examples of polyelectrolytes are proteins and nucleic acids that share many features with synthetic polyelectrolytes, but they too do not have the regular repeating structures of the latter. However, synthetic polypeptides that mimic some of the properties of proteins do have regular repeating structures and therefore are more readily dealt with theoretically.

The special features exhibited by polyelectrolytes, when extensively ionized, compared with individual ions are due to the proximity along the polymeric backbone of charges of the same kind that repulse one another. The fixed ions attached to the polyelectrolyte can never be said to be at infinite dilution, even if the polyelectrolyte itself is at high dilution. Counter-ions with charges opposite to those of the fixed ions tend to associate electrostatically to some extent with the fixed ions or even may do so cooperatively to several fixed ions. The polymer chain itself is affected by the presence of charges of like sign, resulting in its being extended, in contrast with the coiling of uncharged linear polymers due to the entropic effect. If the degree of ionization is low, the polyelectrolyte will take up a more coiled conformation that maximizes the entropy.

Polyelectrolytes are characterized by their degree of polymerization, that is, their average molar mass (MW) and the dispersion of this average, the lengths, l, of the segments along the backbone that carry the charged groups, and the degree of ionization, $0 \leq \alpha \leq 1$. At low degrees of ionization ($\alpha \to 0$) the charged sites are hydrated individually, but as α is increased the hydration water shells start to overlap partly. A highly ionized ($\alpha \to 1$) linear polyion in aqueous solution may then be modeled, e.g., according to Fuoss et al. (1951), as an infinitely long rod with charges at its surface at a uniform charge density, with a cylindrical sheath of water of hydration around the rod. Still, the arrangement of water molecules near

the hydrophobic polymer backbone differs from that near the ionic groups. Counterions, attracted electrostatically to the fixed ions, bring with them their own hydration shells, and if ion pairs are formed, the hydration shells of fixed and counter ions overlap. The complicated picture of the hydration of polyelectrolytes that emerges depends on the flexibility of the polymeric backbone, the segment length l, the extent of ionization, α, the nature of the fixed ions and of the counter ions, and the presence or absence of additional electrolytes in the solution containing or in contact with the polyelectrolyte.

2.7.1 Electrostriction in Polyelectrolyte Solutions

The role played by electrostriction at biological polyelectrolytes, such as proteins and nucleic acids, has already been considered long ago. Cohn and Edsall (1943) concluded that due to the charged groups that ovalbumin contains, electrostriction reduces its specific volume by 2.43 % relative to the value calculated from its amino acid content (McMeekin and Maeshall 1952). The specific volume of rabbit myosin, rabbit tropomyosin, and Pinna tropomyosin (three muscle proteins) in water measured by Kay (1960) indicated a volume contraction by 0.028, 0.040, and 0.030 $cm^3\ g^{-1}$, respectively. These volume reductions were ascribed to electrostriction and were proportional to the number of charged groups (Mauzerall et al. 2002) in the proteins: 270, 376, and 315 per 10^5 g.

Mauzerall et al. employed pulsed photoacoustic measurements on the proteins involved in bacterial photosynthesis and applied the Drude-Nernst equation to estimate the electrostriction:

$$\Delta V = \frac{\kappa_T z_I{}^2 e^2}{8\pi\varepsilon_0 \varepsilon_W{}^2 r_I} \left(\frac{\partial \varepsilon_W}{\partial V}\right)_T \tag{2.74}$$

However, they used the compressibility κ_T of the protein rather than that of water, κ_{TW} that the equation requires. The calculated electrostriction of $-0.030\,nm^3$/pair of ions is compatible with an assumed compressibility of $0.170\,GPa^{-1}$ (that of water is $0.453\,GPa^{-1}$) and a relative permittivity in the immediate vicinity of the protein of 4 ± 1.

Experimental x-ray and neutron scattering data showed that the water in the hydration shell of a protein is 5–25 % denser than bulk water, i.e., it is highly electrostricted. The surface charge density of proteins (Mauzerall et al. 2002) is $\sigma = 0.08 - 0.48\ Cm^{-2}$ and the related field strength is $E = \sigma/\varepsilon_0\varepsilon_W$ (Danielewicz-Ferchmin et al 2003). The chemical potential of the water near the protein surface is reduced by the lower dipole orientation work (reflecting the lower ε_W) compared with pure water. In order for thermodynamic equilibrium to be established water therefore must flow into this high-field region and thereby compressing it. These aspects of protein hydration are further discussed in Chap. 5 (Sect. 5.3.2).

The charges on the walls of ion channels (see Sect. 5.3.3) and the ions passing through them also cause electrostriction of the water, as discussed by several authors

(Sancho et al. 1995; Duca and Jordan 1997; Krasilnikov et al. 2005; Danielewicz-Ferchmin and Ferchmin 2006). The duplex structures formed from single strand nucleic acids is also accompanied by volume changes and by the release of sodium ions to the solution, and appreciable electrostrictive volume diminution was observed for the B conformation of the duplex (Rentzeperis et al. 1993; Marky and Kupke 2000) in the presence of 0.1 M NaCl.

2.7.2 Ion Association of Polyions with Counter-ions

The drastic diminution of the permittivity of the water near the surface of biological polyelectrolytes noted above, is, of course common also to synthetic polyelectrolytes. The consequence of this diminution is association of the fixed ions with mobile counter ions in the solution. Three types of polyelectrolyte solutions are briefly discussed here: a linear strongly acid polyelectyrolyte, such as polystyrene sulfonic acid; a linear weakly acid polyelectyrolyte, such as (partly) neutralized polyacrylic acid; and a polyelectrolyte gel, such as the crosslinked polymethacrylic acid ion exchanger. In the latter, gel-type polyelectrolyte, two distinct phases exist in equilibrium: the gel phase and the outer solution. The treatment of polybases, e.g., (partly) protonated polyvinylpyridine as an example of a linear weak polybase and crosslinked polystryrene-benzyl-trimethyl-ammonium bromide as an example of a strongly basic anion exchanger are completely analogous to the examples discussed. A distinct class of polyelectyrolytes (polyampholytes), however, involves polypeptides and proteins that have both basic and acidic functions, such as arginine and glutamic acid moieties, on the same polymer chain. These are discussed briefly too.

According to the degree of sulfonation of polystyrene, the density of fully ionized groups along the chains can be varied from having only a few sulfonic groups along the polystyrene chain to having a sulfonic group on every phenyl ring. The variability of the relative molar mass M of the polystyrene chains is another parameter to be taken into account, even with fully sulfonated polystyrene. The osmotic pressures Π of aqueous solutions of the acid and sodium salt of sulfonated polystyrene of $M = 2 \times 10^4$ to 1.06×10^6 were related by Wang and Bloomfield (1990) to their mono-molarities c_{mono} (the molar concentration of styrene sulfonated groups) according to:

$$\Pi = RT\varphi c_{\text{mono}} \tag{2.75}$$

where φ is the osmotic coefficient, Eq. (2.57). The latter quantity is related to the charge density parameter ξ by:

$$\varphi = \frac{1}{2\xi} = \frac{1}{4(q/b_l)} \tag{2.76}$$

where q is the Bjerrum cut-off length (for univalent ions), Eq. (2.69), and b_l is the linear charge spacing along the polyelectrolyte chain (it corresponds to the segment

length l for a fully sulfonated polymer). Agreement with measured osmotic pressures of the calculated values was found with the value $\xi = 4.0$, corresponding with $b_l = 0.25$ nm, to $q = 0.5$ nm, and hence to $\varepsilon_W = 56$ in the near surroundings of the polystyrenesulfonate rods.

The expression (2.76) for the osmotic coefficient was previously derived by Lifson and Kachalsky (1954) and by Manning (1969) but shown by Manning to be valid only when $\xi > 1$. For polyelectrolyte solutions free from added salt with $\xi < 1$ the limiting value of the osmotic coefficient is $\varphi = 1 - {}^1/_2\xi$. Only when the fixed charges on the polyelectrolyte are densely spaced, that is, when the average distance b_l between them is smaller than $2q$ so that $\xi > 1$, would the electrical potential cause the (univalent) counter-ions to bind to ("condense on" (Manning 1969)) the fixed ions, thereby reducing the effective value of ξ to the critical value of unity.

The Donnan salt exclusion parameter Γ expresses a property of polyelectrolyte solutions. It describes the bias when a salt is present in the bulk of the solution against the presence of mobile ions in the vicinity of the polyelectrolyte. In the case of the two phase system of a cross-linked ion exchange gel and an outer solution the exclusion is directly measurable experimentally. If the concentration of the salt in the external solution is c_{Eex} and that in the vicinity of the polyelectrolyte is c_{Enear}, then the limiting value of Γ for a concentration c_{poly} of the polyelectrolyte tending to zero is formally defined by:

$$\Gamma = \lim(c_{\mathrm{poly}} \to 0)\frac{c_{\mathrm{Eex}} - c_{\mathrm{Enear}}}{c_{\mathrm{poly}}} \tag{2.77}$$

Manning (1969) showed that when $\xi < 1$ then $\Gamma = \frac{1}{2}(1 - \frac{1}{2}\xi)$ whereas if $\xi > 1$ then $\Gamma = 1/4\xi$. He compared these expectations with experimental data available to him for a variety of polyelectrolytes: sodium polyvinyl sulfate and sodium polyacrylate (of various degrees of neutralization α) and potassium polyphosphate and DNA, having ξ values ranging from 0.29 to 4.20, with good results. Also the expectations for the osmotic coefficients of the sodium polyacrylate and polymethacrylate were well vindicated.

Consider now an aqueous solution of polyacrylic acid that is being titrated with an aqueous sodium hydroxide solution in the absence of added salt in the solution. The degree of ionization of the polyelectrolyte, α, increases as the titration proceeds up to the equivalent point. Polyelectyrolytes tend to be polydisperse, i.e., have polymer chains of different lengths. It is therefore expedient to specify the concentration c_{poly} in terms of the total number of monomeric titratable groups per unit volume, c_{mono}. There are three different types of "sites" on the polymer chain, of which the relative abundance depends on the degree of ionization α and the concentration c_{mono}. The not-yet-neutralized protonated carboxylic groups constitute one type of "sites", the already ionized carboxylate groups constitute another, and carboxylate groups ion-paired with the sodium counter-ions are a third. When the titration is carried out in the presence of excess sodium chloride, the association of the sodium cations with the polyelectrolyte is enhanced due to the common ion effect, but it may be assumed that the chloride anions remain completely mobile. The environment of a given sodium cation at an appreciable value of α, even in very dilute solutions of

the polyelectrolyte, consists of many anions with which it can associate. The ionic atmosphere does not become infinitely dilute with decreasing concentrations of the polyelectrolyte, $c_{\text{poly}} \to 0$.

The course of the titration is described by the following operative expression according to Harris and Rice (1954):

$$p\text{H} + \log a_{\text{Na}+} + \log\left(\frac{1-\alpha}{\alpha}\right) - \log f = pK_{\text{a}} - pK_{\text{ip}} \tag{2.78}$$

Here f is the degree of binding of the sodium counter-ion, K_{a} is the intrinsic dissociation constant for the acid and K_{ip} is that of the ion pair (the reciprocal of its association constant). This treatment assumes random distribution of the three types of sites along the polyelectrolyte chain, but restrictions can be introduced, such as requiring an ionized site to be adjacent to the one where ion pairing takes place. Lifson and Katchalsky (1948) took into account the mutual interaction of neighboring ionized sites, but the final result was the same as Eq. (2.78), i.e., as for the case where no such interaction was considered.

The interactions of the polyion with the counter-ions may not follow the mass action law if the electrostatic potential around the polyelectrolyte is high. This quantity was calculated for polyelectrolyte gels according to several models. The model proposed by Gregor and Gregor (1977) involved a rod of infinite length of radius a, the fixed charges being located along it at random intervals. The solution region in which counter-ions are affected by the potential extended up to a distance R from the center of the rod. Counter-ions of different sizes, a smaller one with radius r_{sm} at a concentration c_{sm} and a larger one with radius r_{la} at a concentration c_{la}, can approach the rod to different distances. A selectivity constant (ratio of binding constants) arises from this difference in the distance of closest approach. The quantity $1/b_l$ is taken to be the average charge per unit length of the rod and leads to the parameter $\lambda = -2q/b_l$, with q given by Eq. (2.69) for univalent ions. Another quantity, α, is implicitly defined by:

$$2(\alpha^2+1)R^{-2}\left(\frac{4\pi\varepsilon_0\varepsilon k_{\text{B}}T}{\text{e}^2}\right) = c_{\text{la}} + c_{\text{sm}} \tag{2.79}$$

Then the selectivity coefficient between the two kinds of ions is:

$$K^{\text{la}}{}_{\text{sm}} = \frac{\lambda\dfrac{(c_{\text{la}}+c_{\text{sm}})}{c_{\text{sm}}}}{1+\alpha\cot(\alpha\ln)\dfrac{(a+r_{\text{la}})}{R} - \tan^{-1}\alpha} - \frac{c_{\text{la}}}{c_{\text{sm}}} \tag{2.80}$$

This expression was tested by Gregor and Greff (1977) with a completely ionized polymethacrylate gel, cross-linked to various extents, 0.2–24 mol %, by ethyleneglycol dimethacrylate (EGDM). They studied the exchange of the small cation K^+ (assigned $r_{\text{sm}} = 0.175\ nm$) and the large cation Me_4N^+ (assigned $r_{\text{la}} = 0.347$ nm) or Et_4N^+(assigned $r_{\text{la}} = 0.400$ nm), on this rod-like cross-linked polyelectrolyte, with a radius $a = 0.21$ nm and a charge density of $1/b_l = 3.23$ unit charges per

nm. The experimental selectivity coefficient, $K^{\mathrm{la}}_{\mathrm{sm\ expt}}$, has a contribution from the osmotic pressure Π and the difference in the partial molar volumes of the ions: $\exp[\Pi(V_{\mathrm{la}} - V_{\mathrm{sm}})/RT]$, a factor multiplying the electrostatic contribution expressed by Eq. (2.80). The values of Π and R are obtained from the swelling of the polyelectrolyte gels in water.

However, the permittivity ε_{W} of the water in the annular region around the polyelectrolyte defined by R, which enters the distance q according to Eq. (2.69), cannot be estimated independently. Considering Eq. (2.80) as valid, Gregor and Greff (1977) derived a value of the permittivity in the vicinity of the polyelectrolyte rod of $\varepsilon_{\mathrm{W}} = 30 \pm 3$ from the K^+/Me_4N^+ exchange for cross-linking with 4–24 mol % EGDM. However, when the data for the K^+/Et_4N^+ exchange were employed instead the even lower value $\varepsilon_{\mathrm{W}} = 15 \pm 5$ was obtained, for no apparent reason.

Lamm and Pack (1997) subsequently tackled the problem of the estimation of the solvent permittivity near the polyelectrolyte. They employed the finite difference Poisson-Boltzmann technique to calculate the permittivity of water at various distances from a charged cylinder. The effects of the surface boundary, the presence of the fixed ions, that of the counter-ions, and eventually of added electrolyte were considered, all leading in some manner to dielectric saturation, due to electrostriction of the water near the charges. They presented results for a cylinder of 1.0 nm radius and a charge density corresponding to B-DNA, showing the surface effect to be minor but both the fixed and the counter-ions causing a large decrease of the permittivity near the charged cylinder. The total relative permittivity ε_{W} rose from ∼5 at the surface of the cylinder to ∼28 at a distance of 0.5 nm, to ∼45 at 1.0 nm, and ∼58 at 2.0 nm, when there was 50 mM added salt present. In the absence of added salt the values at 0.5 nm (∼38) and at 1.0 nm (∼54) were appreciably larger. A low permittivity of the solvent near the polyelectrolyte is obviously conducive to electrostatic binding of counter-ions to fixed ions.

The association of multivalent ions may introduce complications at both low and high charge densities along the polyelectrolyte chain. When the charge density is low a z-valent cation associates with a single (univalent negative) fixed ion. This causes the sign of the charge of the site to reverse from -1 to $(z-1)^+$ and the site then interacts electrostatically with a neighboring (negatively charged) fixed ion. This may lead to precipitation, if the electrostatic repulsion between the negative sites becomes too small to keep the polyelectrolyte extended. However, when the charge density along the chain is high, multivalent counter-ions associate with several adjacent fixed ions and neutralize the charge. The multivalent counter-ions can also act as cross-linking agents between adjacent chains, when the concentration of the polyelectrolyte c_{poly} is large. This may cause precipitation of the thus crosslinked polyelectrolyte. When the added z-valent ion concentration is increased beyond a certain threshold, however, the screening of the electrostatic attractions permits the polyelectrolyte to be soluble again.

Porasso et al. (2001) showed that coordinative bonding between multivalent counter-ions and the fixed charges is possible beside electrostatic association. When a solution containing Cd^{2+} and polyacrylic acid is titrated with KOH, both 'territorial condensation' of the divalent cation and specific binding occur, whereas in

the presence of Ca^{2+} only the former kind does. Similarly, both condensation and specific binding occur on precipitation and re-solubilization of polyelectrolytes in the presence of multivalent ions, as shown by Sabbagh and Delsanti (2000). Barium ions were able to precipitate all kinds of anionic polyelectrolytes, whether carrying carboxylate, sulfonate, or sulfate fixed ions, whereas other divalent metal ions precipitated only the carboxylate-carrying polyelectrolyes.

Winkler et al. (1998) demonstrated by molecular dynamics the collapse of the extended rod-like polyelectrolyte structure to a coil-like conformation when, in the absence of added salt, the interaction energy of the fixed and counter-ions is increased beyond a certain threshold. Multivalent ions provided sufficiently large interaction energies for a given length of polyelectrolyte and distance between the fixed charges. Polyelectrolytes of finite length had to be used for these simulations, contrary to the infinitely long rods in the models considered above. The end-to-end extension or the radius of gyration was the measure for the collapse of the chain.

References

Abraham MH, Liszi J (1980) Calculations on ionic solvation, part 4. Further calculations in solvation of gaseous univalent ions using one-layer and two-layer continuum models. J Chem Soc, Faraday Trans 1(76):1219–1231

Abraham MH, Liszi J, Papp E (1982) Calculations on ionic solvation, part 6. Structure-making and structure-breaking effects of alkali halide ions from electrostatic entropies of solvation: correlation with viscosity B-coefficients, nuclear magnetic resonance B′-coefficients, and partial molal volumes. J Chem Soc Faraday Trans 78:197–211

Abraham MH, Marcus Y (1986) The thermodynamics of solvation of ions, part 1. The heat capacity of hydration at 298.15 K. J Chem Soc Faraday Trans 1(82):3255–3274

Abraham MH, Matteoli E, Liszi J (1983) Calculation of the thermodynamics of solvation of gaseous univalent ions in water from 273 to 573 K. J Chem Soc Faraday Trans 1(79):2781–2800

Ben-Naim A (1988) Theory of preferential solvation of nonelectrolytes. Cell Biophys 12:255–269

Bockris JO'M, Saluja PPS (1972) Ionic solvation numbers from compres-sibilities and ionic vibration potentials measurements. J Phys Chem 76:2140–2151

Cohn EJ, Edsall JT (1943) Proteins, amino acids, and peptides. Reinhold, New York, pp 370–81

Collins KD (1997) Charge density-dependent strength of hydration and biological structure. Biophys J 72:65–76

Conway BE (1978) The evaluation and use of properties of individual ions in solution. J Solution Chem 7:721–770

Conway BE (1985) Local changes of solubility induced by electrolytes: salting-out and ionic hydration. Pure Appl Chem 57:263–272

Criss CM, Millero FJ (1996) Modeling of the heat capacities of aqueous 1–1 electrolyte solutions with Pitzer's equations. J Phys Chem 100:1288–1294

Criss CM, Millero FJ (1999) Modeling of heat capacities of high-valence type electrolyte solutions with Pitzer's equations. J Solution Chem 28:849–867

Danielewicz-Ferchmin I, Banachowicz E, Ferchmin AR (2003) Protein hydration and the huge electrostriction. Biophys Chem 106:147–153

Danielewicz-Ferchmin I, Ferchmin AR (2006) Lowering of the freezing temperature of water at the protein surface due to electric field. J Mol Liquids 124:114–120

David FH, Fourest B (1990) Structure of trivalent lanthanide and actinide aquo ions. New J Chem 21:167–176

Debye P, McAulay J (1925) The electric field of ions and the action of neutral salts. Phys Z 26:22–29
Deno NC, Spink CH (1963) The McDevit-Long equation for salt effects on nonelectrolytes. J Phys Chem 67:1347–1349
Diamond RM (1963) The aqueous solution behavior of large univalwent ions: a new type of ion pairing. J Phys Chem 67:2513–2517
Duca KA, Jordan PC (1997) Ion-water and water-water interactions in a gramicidinlike channel: effects due to group polarizability and backbone flexibility. Biophys Chem 65:123–141
Falkenhagen H, Dole M (1929) Viscosity of electrolyte solutions and its significance to the Debye theory. Phys Z 30:611–622
Fernandez-Prini R (1969) Conductance of electrolyte solutions. Modified expression for its concentration dependence. Trans Faraday Soc 65:3311–3313
Frank HS, Robinson AL (1940) The entropy of dilution of strong electrolytes in aqueous solutions. J Chem Phys 8:933–938
Fromon M, Treiner C (1979) Scaled particle theory and salting constantof tetrahydrofuraqn in various aqueous electrolyte solutions at 298.15 K. J Chem Soc Faraday Trans 1(75):1837–1845
Fuoss RM, Kachalsky A, Lifson S (1951) The potential of an infinite rodlike molecule and the distribution of the counter ions. Proc Natl Acad Sci U S A 37:579–589
Gregor HP, Greff RJ (1977) Selective uptake of counterions of different size by ion-exchange gels: effect of swelling pressure and Coulombic interactions. J Chem Phys 67:5742–5751
Gregor HP, Gregor JM (1977) Coulombic reactions of polyelectrolytes with counterions of different sizes. J Chem Phys 66:1934–1939
Gurney RW (1953) Ionic processes in solution. McGraw-Hill, New York
Hakin AW, Bhuiyan MMH (2010) In: Wilhelm E, Letcher TM (eds) Heat capacities. RSC Publishing, Cambridge, p 132 ff
Harned HS, Owen BB (1958)The physical chemistry of electrolyte solutions, 3rd ed. Reinhold, New York
Harris FE, Rice SA (1954) A chain model for polyelectrolytes. Int J Phys Chem 58:725–732
Hefter GT, Marcus Y, Waghorne WE (2002) Enthalpies and entropies of transfer of electrolytes and ions from water to mixed aqueous organic solvents. Chem Rev 102:2773–2836
Helgeson HC, Kirkham DH, Flowers GC (1981) Theoretical prediction of the thermodynamic behavior of aqueous electrolytes at high pressures and temperatures: IV. Calculation of activity coefficients, osmotic coefficients, and apparent molal and standard and relative partial molal properties to 600 °C and 5 kb. Am J Sci 281:1249–1516
Hepler LG, Hovey JK (1996) Standard state heat capacities of aqueous electrolytes and some related undissociated species. Can J Chem 74:639–649
Heyda J, Lund M, Ončak M, Slaviček P, Jungwirth P (2010) Reversal of Hofmeister ordering for pairing of NH_{4+} vs alkylated ammonium cations with halide anions in water. J Phys Chem B114:1084310852
Heydweiler A (1925) Optical research on electrolytic aqueous solutions. Phys Z 26:526–556
Hünenberger P, Reif M (2010) Single-ion Solvation: experimental and theoretical approaches to elusive thermodynamic quantities. Royal Society of Chemistry, Cambridge
Jenkins HBD, Thakur KP (1979) Reappraisal of thermochemical radii for complex ions. J Chem Educ 56:576–577
Jenkins HBD, Marcus Y (1995) Ionic B-coefficients in solution. Chem Rev 95:2695–2726
Jenkins HDB, Roobottom HK, Passmore J, Glasser L (1999) Relationships among ionic lattice energies, molecular (formula unit) volumes, and thermochemical radii. Inorg Chem 38:3609–3620
Jones G, Dole M (1929) The viscosity of aqueous solutions of strong electrolytes with special reference to barium chloride. J Am Chem Soc 51:2950–2964
Kalidas C, Hefter GT, Marcus Y (2000) Gibbs energies of transfer of cations from water to aqueous organic solvents. Chem Rev 100:819–852
Kay CM (1960) Partial specific volume of muscle proteins. Biochim Biophys Acta 38:420–427

Kelly CP, Cramer CJ, Truhlar DJ (2006) Aqueous solvation free energies of ions and ion-water clusters based on an accurate value for the absolute aqueous solvation free energy of the proton. J Phys Chem B 110:16066–16081
Krasilnikov OV, Merzlyak PG, Yuldasheva LN, Capistrano MF (2005) Protein electrostriction: a possibility of elastic deformation of the α-hemolysin channel by the applied field. Eur Biophys J 34:997–1006
Krestov GA (1991) Thermodynamics of Solvation. Ellis-Horwood, Chichester, p 24
Lamm G, Pack GR (1997) Calculation of dielectric constants near polyelectrolytes in solution. J Phys Chem B 101:959–965
Lifson S, Kachalsky A (1954) The electrostatic free energy of polyelectrolyte solutions. II. Fully stretched macromolecules. J Polym Sci 13:43–55
Manning GS (1969) Limiting laws and counterion condensation in polyelectroyte solutions. I. Colligative properties. J Chem Phys 51:924–933
Marcus Y (1977) Introduction to liquid-state chemistry. Wiley, Chichester, pp 241–245, 267–279
Marcus Y (1983) Ionic radii in aqueous solutions. J Sol Chem 12:271–275
Marcus Y (1983a) A quasi-lattice quasi-chemical theory of preferential solvation of ions. Austr J Chem 36:1718–1738
Marcus Y (1986) Thermodynamics of transfer of single ions from water to non-aqueous and mixed solvents, 4. The selection of the extrathermodynamic assumptions. Pure Appl Chem 58:1721–1736
Marcus Y (1987) The thermodynamics of solvation of ions, part 2. The enthalpy of hydration at 298.15 K. J Chem Soc Faraday Trans 83:339–349
Marcus Y (1988) Ionic radii in aqueous solutions. Chem Rev 88:1475–1498
Marcus Y (1988a) Preferential solvation of ions, part 2. The solvent composition near the ion. J Chem Soc Faraday Trans 1(84):1465–1475
Marcus Y (1991) The thermodynamics of solvation of ions, part 5. The Gibbs free energy of hydration of ions at 298.15 K. J Chem Soc Faraday Trans 87:2995–2997
Marcus Y (1994) Viscosity B-coefficients, structural entropies and heat capacities, and the effect of ions on the structure of water. J Sol Chem 23:831–848
Marcus Y (1996) Transfer of ions between solvents: some new results on volumes, heat capacities and some other quantities. Pure Appl Chem 68:1495–1500
Marcus Y (1997) Ion properties. Dekker, New York
Marcus Y (2002) Solvent mixtures. Dekker, New York
Marcus Y (2005) Electrostriction, ion solvation, and solvent release on ion pairing. J Phys Chem B 109:18541–18549
Marcus Y (2005a) BET nodeling of solid-liquid phase diagrams of common ion binary salt hydrate mixtures. 1. The BET parameters. J Sol Chem 34:297–306
Marcus Y (2006) On the molar volumes and viscosities of electrolytes. J Sol Chem 35:1271–1286
Marcus Y (2007) Gibbs energies of transfer of anions from water to mixed aqueous organic solvents. Chem Rev 107:3880–3897
Marcus Y (2008) On the relation between thermodynamic, transport and structural properties of electrolyte solutions Russ. J Electrochem 44:16–27
Marcus Y (2008a) Properties of individual ions in solution. In: Bostrelli DV (ed) Solution chemistry research progress. Nova Science publishers, Inc., Hauppauge, 51–68
Marcus Y (2009) The standard partial molar volumes of ions in solution, part 4. Ionic volumes in water at 0–100 °C. J Phys Chem B 113:10285–10291
Marcus Y (2009a) The effects of ions on the structure of water: structure-breaking and—making. Chem Rev 109:1346–1370
Marcus Y (2009b) On water structure in concentrated salt solutions. J Sol Chem 38:513–516
Marcus Y (2010) On the intrinsic volumes of ions in aqueous solutions. J Sol Chem 39:1031–1038
Marcus Y (2011) Electrostriction in electrolyte solutions. Chem Rev 111:2761–2783
Marcus Y (2012) The viscosity B-coefficient of the thiocyanate anion. J Chem Eng Data 57:617–619

Marcus Y (2012a) The standard partial molar volumes of ions in solution. Part 5. Ionic volumes in water at 125–200 °C. J. Phys. Chem. B 117: http://dx.doi/10.1021/jp212518t
Marcus Y (2012b) Are ionic Stokes radii of any use? J. Solution Chem: in the press
Marcus Y, Hefter G (1999) On the pressure and electric field dependencies of the relative permittivity of liquids. J Sol Chem 28:575–591
Marcus Y, Hefter G (2006) Ion pairing. Chem Rev 106:4585–4621
Marcus Y, Kertes AS (1969) Ion Exchange and solvent extraction of metal complexes. Wiley, London, p 74 ff
Marky LA, Kupke DW (2000) Enthalpy-entropy compensations in nucleic acids: contribution of electrostriction and structural hydration. Meth Enzymol 323:419–441
Masterton WL, Lee TP (1970) A classical model for the low-energy electron(positron)-atomic hydrogen(1 s) elastic scattering. J Phys Chem 79:1776–1782
Mathieson JG, Conway BE (1974) Partial molal compressibilities of salts in aqueous solution and assignment of ionic contributions. J Sol Chem 3:455–477
Mauzerall D, Hou J-M, Boichenko VA (2002) Volume changes and electrostriction in the primary photoreactions of various photosynthetic systems: estimation of dielectric coefficient in bacterial reaction centers and of the observed volume changes with the Drude-Nernst equation. Photosyn Res 74:173–180
Mazo RM (2006) A fluctuation theory analysis of the salting-out effect. J Phys Chem B 110:24077–24082
Mcdevit WF, Long FA (1952) The activity coefficient of benzene in aqueous salt solutions. J Am Chem Soc 74:1773–1777
McMeekin TL, Marshall K (1952) Specific volumes of proteins and the relationship to their amino acid contents. Science 116:142–143
Millero FJ (1971) Molal volumes of electrolytes. Chem Rev 71:147–176
Morris DFC (1968) Ionic radii and enthalpies of hydration of ions. Struct Bond 4:63–82
Morris DFC (1969) Ionic radii and enthalpies of hydration of ions. Struct Bond 6:157–159
Mukerjee P (1961) Ion-solvent interactions, I. Partial molal volumes of ions in aqueous solutions, II. Internal pressure and electrostriction of aqueous-solutions of electrolytes. J Phys Chem 65:740–746
Nightingale ER (1959) Phenomenological theory of ion solvation. Effective radii of hydrated ions. J Phys Chem 63:1381–1387
Ohtaki H, Radnai T (1993) Structure and dynamics of hydrated ions. Chem Rev 93:1157–1204
Parfenyuk VI (2002) Surface potential at the gas-aqueous solution interface. Coll J 64:588–595
Pawilkowski EM, Prausnitz JM (1983) Estimation of Setchenow constants for nonpolar gases in common salts at moderate temperatures. Ind Eng Chem Fund 22:86–90
Pitzer KS (1979) Theory: ion interaction approach. In: Pytkovicz RM (ed) Activity coefficients in electrolyte solutions, Vol. 1. CRC Press, Boca Raton, (Chap. 7)
Pitzer KS, Mayorga G (1973) Thermodynamics of electrolytes, II. Activity and osmotic coefficients for strong electrolytes with one or both ions univalent. J Phys Chem 77:2300–2308
Porasso RD, Benegas JC, van den Hoop MAGT, Paoletti S (2001) Chemical bonding of divalent counterions to linear polyelectrolytes: theoretical treatment within the counterion condensation theory. Phys Chem Chem Phys 3:1057–1062
Redlich O, Meyer DM (1964) The molal volumes of electrolytes. Chem Rev 64:221–227
Rentzeperis D, Kupke DW, Marky LA (1993) Volume changes correlate with entropies and enthalpies in the formation of nucleic acid homoduplexes: differential hydration of A and B conformations. Biopolymers 33:117–125
Robinson RA, Stokes RH (1965) Electrolyte solutions, 2nd edn. Butterworths, London
Roobottom HK, Jenkins HDB, Passmore J, Glasser L (1999) Thermochemical radii of complex ions. J Chem Educ 76:1570–1573
Ruckenstein E, Shulgin I (2002) Salting-out or -in by fluctuation theory. Ind Eng Chem Res 41:4674–4680

Sabbagh I, Delsanti M (2000) Solubility of highly charged anionic poly-electrolytes in presence of multivalent cations: specific interaction effect. Europ Phys J E 1:75–86
Sancho M, Partenskii MB, Dorman V, Jordan PC (1995) Extended dipolar chain model for ion channels: electrostriction effects and the translocational energy barrier. Biophys J 68:427–433
Schmid R, Miah AM, Sapunov VN (2000) A new table of the thermodynamic quantities of ionic hydration: values and some applications (enthalpy-entropy compensation and Born radii). Phys Chem Chem Phys 2:97–102
Shannon RD, Prewitt CT (1969) Effective ionic radii in oxides and fluorides. Acta Cryst B 25:925–946
Shannon RD, Prewitt CT (1970) Revised values of effective ionic radii. Acta Cryst B 26:1046–1048
Shoor SK, Gubbins KE (1969) Solubility of nonpolar gases in concentrated electrolyte solutions. J Phys Chem 78:498–505
Stokes RH (1964) van der Waals radii of gaseous ions of the noble gas structure in relation to hydration energies. J Am Chem Soc 86:979–982
Stokes RH, Robinson RA (1948) Ionic hydration and activity in electrolyte solutions. J Am Chem Soc 70:1870–1877
Treiner C (1981) Some regularities in the behavior of salting constants for polar molecules in aqueous electrolyte solutions. Can J Chem 59:2518–2526
Wagman DD, Evans WH, Parker VB, Schumm RH, Halow I, Bailey SM, Churney KL, Nutall RL (1982) The NBS tables of chemical thermodynamic properties. Selected values for inorganic and C1 and C2 organic substances in SI Units. J Phys Chem Ref Data 11, Suppl 2:1–392
Wang L, Bloomfield VA (1990) Osmotic pressure of polyelectrolytes without added salt. Macromolecules 23:804–809
Weisenberger S, Schumpe A (1996) Estimation of gas solubilities in salt solutions at temperatures from 273 to 363 K. AIChE J 42:298–300
Winkler RG, Gold M, Reineker P (1998) Collapse of polyelectrolyte macromolecules by counterion condensation and ion pair formation: a molecular dynamics simulation study. Phys Rev Lett 80:3731–3734
Xie W-H, Shiu W-Y, Mackay D (1997) A review of the effect of salts on the solubility of organic compounds in seawater. Mar Environ Res 44:429–444

Chapter 3
Effects of Ions on Water Structure and Vice Versa

The structure of liquid water was dealt with in detail in Sect. 1.1.2. Once a solute, whether an ion or a neutral solute and whether hydrophilic or hydrophobic, is placed in the water, it is reasonable to expect it to affect the structure around it. The effects may be limited to a hydration shell surrounding the solute that has a structure differing from that in pure water. For instance, around monatomic ions the water molecules in the hydration shell are oriented towards the ion in a more or less spherical symmetry. Around hydrophobic solutes cages of water molecules are formed, that may be ice-like but also resemble the structure of clathrates or crystal hydrates. In many cases the effects of the presence of an ion are manifested also beyond the hydration shell or shells.

On the other hand, the hydrogen bonded structure of water affects the properties of the ions. Large univalent ions of opposite charges may be forced to pair-wise association by the water structure (cf. its tightness, Sect. 1.1.2) although they would not do so on electrostatic grounds (see Sect. 2.6.2). Ions may be sorbed at or desorbed from the surface layer of water, where its hydrogen bonded structure is not isotropic and weaker than in bulk water. Thus, the reciprocal effects of charge density of the ions and the water structure merit investigation.

Water structural effects of ions may be assessed by a variety of experimental methods as well as by computer simulations. These methods lead to the recognition that some ions enhance the native structure of the water whereas other ions destroy it, up to some distance in the water away from the ion. The former ions are called structure-makers, or cosmotropic, a term favoured in the biophysical literature, and the latter kind of ions are structure-breakers or chaotropic. Naturally, there are also ions that are borderline between these groups, neither structure-makers nor -breakers to a significant extent.

Following are the results of several of the methods that have been used to categorize ions as belonging to the structure-making or -breaking groups, the subject having been also recently reviewed (Marcus 2009, 2010).

Y. Marcus, *Ions in Water and Biophysical Implications,*
DOI 10.1007/978-94-007-4647-3_3, © Springer Science+Business Media Dordrecht 2012

3.1 Effects on Solvent Dynamics

There are both macroscopic effects of ions on the dynamics of electrolyte solutions relative to pure water and microscopic effects on the dynamics of the water molecules themselves. The former include the effects of ions on the fluidity of the solution as a whole, which is the reciprocal of its viscosity, and on the self-diffusion of the water. The latter pertain to the movements of individual water molecules: their mutual orientations, the rate of breaking or making of hydrogen bonds, etc. Such effects have been measured experimentally, as discussed in Sects. 3.1.1–3.1.5, and are complemented by computer simulations in Sect. 3.1.6.

3.1.1 Viscosity B*-coefficients*

Some questions arise from experimental facts pertaining to the relative viscosity, η/η_W, of certain dilute aqueous solutions, where η is the dynamic viscosity of the solution and η_W that of water at the same temperature. Jones and Stauffer (1936) reported that for 0.09966 M of cesium iodide at 25 °C $\eta/\eta_W = 0.98910$, i.e., it is <1. Laurence and Wolfenden (1934) reported that for 0.09393 M of lithium acetate at 25 °C $\eta/\eta_W = 1.0393_8$, i.e., it is >1. Essentially complete ionic dissociation of these solute electrolytes takes place in such dilute solutions. The question then arises: why do the cesium and iodide ions depress the relative viscosity of the solution whereas lithium and acetate ions enhance it?

The terms "structure making" and "structure breaking" are attributed to Gurney (1953), but Cox and Wolfenden (1934) were the first to mention the notion of "water structure" in the connection of the viscosities. Furthermore, Frank and Evans (1945) have already used the term "structure breaking" (but not "-making") with regard to effects of the alkali metal and halide ions, except Li^+ and F^-, on the partial molar entropies of dilute aqueous solutions. The Jones-Dole *B*-coefficient, Eq. (2.35), is the quantitative measure of this effect, and this equation may be recast in the form:

$$\frac{((\eta/\eta_W) - 1)}{{c_E}^{1/2}} = A_\eta + B_\eta {c_E}^{1/2} + \cdots \tag{3.1}$$

The A_η coefficients can be calculated from the conductivity of the salts, Eq. (2.36), but are generally obtained as the intercepts in plots of $((\eta/\eta^*) - 1)/{c_E}^{1/2}$ vs. the square root of the electrolyte concentration, ${c_E}^{1/2}$, and the B_η values are the limiting slopes of such plots. The B_η thus pertain to infinite dilution, and are, therefore, additive in the values for the constituent ions.

The splitting into individual ionic values is briefly described in Sect. 2.4.3. The splitting according to the assumption that $B_\eta(Rb^+) = B_\eta(Br^-)$ (Jenkins and Marcus 1995) over a wide temperature range around ambient is adopted here. It differs in a negligible manner (± 0.002 dm^3 mol^{-1}) from the commonly used assumption $B_\eta(K^+) = B_\eta(Cl^-)$, valid over a much narrower temperature range. These authors

(Jenkins and Marcus 1995) critically selected B_η values for over 70 aqueous ions from published data. It is worth noting that the few data available for ionic B_η values in heavy water are even more negative for structure breaking ions than in light water, because D_2O is more structured than H_2O (see the end of Sect. 1.1.3) so that there is more structure to break. Gurney (1953) *assumed* that loosening of the water structure, thus enhancing the fluidity, occurs locally near ions such as Cs^+ and I^- with $B_\eta < 0$ and deems them as "structure breaking". Similarly, the tightening of the hydrogen bonding near ions such as Li^+ and acetate having $B_\eta > 0$ designates them as "structure making".

Notwithstanding several attempts to develop a theory to account for the observed behaviour, no satisfactory theory has emerged so far. Not only the magnitudes and the signs of B_η are of importance in this respect, but also the signs of their temperature dependence, dB_η/dT, which have not yet been predictable on the basis of known ionic properties. Desnoyers and Perron (1972) showed that B_η in aqueous solutions of alkali metal halides should depend on the sizes of the hydrated ions through their partial molar volumes, but could not predict the structure making and breaking effects.

The mechanism by which the ions, given their assumed water structure modifying behaviour, affect the viscosity is not really known. For a macroscopic dispersion of particles in a fluid the Einstein relation

$$\left(\frac{\eta}{\eta^*} - 1\right) = 2.5\, v \tag{3.2}$$

holds, where v is the volume of the solute particles per unit volume of the dispersion. Taking this unit volume as 1 dm^3, then $v = c_E V_E$ where V_E is the partial molar volume of the electrolyte solute. Then, the larger the ion the larger the viscosity of the solution becomes, but this is contrary to the observed behaviour. Positive B_η could still be accounted for in principle by Eq. (3.2), but no plausible theory for negative values has been proposed. The sphere-in-continuum approach of Ibuki and Nakahara (1986) accounted partly for positive values of B_η only, but not for negative ones nor for the changes of B_η on transfer to heavy water.

Feakins et al. (1974) applied the absolute rate theory of Eyring to the estimation of the activation Gibbs energy, $\Delta G^\ddagger$, needed to reach the transition state of the flow process. This involves the creation of suitable cavities in the solvent and the jumping of solute and solvent particles between them, severing existing bonds and creating new ones. Applied to uni-univalent electrolytes rather than to individual ions this approach yields:

$$B_\eta = \left(\frac{V_W - V_E^\infty}{1000}\right) + V_W \left(\frac{\Delta G^\ddagger{}_E - \Delta G^\ddagger{}_W}{1000\ RT}\right) \tag{3.3}$$

Here the $\Delta G^\ddagger$ are the corresponding Gibbs energies of activation for the electrolyte solution and for water. The absolute rate theory yields for water $\Delta G^\ddagger{}_W = RT \ln(0.399(\eta_W/\text{mPa s})(V_W/\text{cm}^3\ \text{mol}^{-1}))$. However, there is no way for the independent estimation of $\Delta G^\ddagger{}_E$ for electrolytes and ions, although a model for it was

proposed later by Feakins et al. (1986). This approach, however, allows for $B_\eta < 0$ if the first term in Eq. (3.3) dominates over the second and if the limiting partial molar volume of the electrolyte is larger than the molar volume of water. The latter condition occurs for electrolytes made up from large univalent ions. Jiang and Sandler (2003) combined the absolute rate theory for the flow process with the mean spherical approximation for ion-ion and ion-solvent interactions employing four empirical parameters to model the viscosities of electrolyte solutions. However, the emphasis was not on explaining the structure-making and structure-breaking properties of the ions in dilute solutions but rather on high concentrations and engineering applications.

The relatively high viscosity of water with its small molecules is due to its hydrogen bonded network that must be disrupted dynamically for the water or the solution to flow. A rough consideration of the relative sizes of the average void spaces in water, $(V_W - V_{vdW})/N_A = 0.0094\ \text{nm}^3$, and the sizes of ions is instructive. Cavities to accommodate a moving ion need to be larger than this average void space, but are created randomly by the thermal movement of the water molecules. If small ions fit into such cavities and enhance the hydrogen bonding through their electric fields they are 'structure-makers' and slow down the rate of flow. Large ions, too large for moving into a randomly available hole near them, need to destroy some of the hydrogen bonded structure of the water in order to create a cavity sufficiently large to move into. They are 'structure-breakers' and should accelerate the flow of the solution, accounting for negative B_η values. In fact, cations with volumes $(4\pi/3)r_I^3 > 0.010\ \text{nm}^3$ have $B_\eta < 0$ and are structure-breaking and those with volumes $(4\pi/3)r_I^3 < 0.007\ \text{nm}^3$ have $B_\eta > 0$ and are structure-making. For anions the border between structure-making and -breaking is at $(4\pi/3)r_I^3/|z| \sim 0.02\ \text{nm}^3$, the magnitude of the charge also playing a role (Marcus 2011).

The absolute magnitudes of the $B_{\eta I}$-coefficients indicate the extents of the effects of the ions on the structure of water in the solution. They agree with other measures of such effects, e.g., those derived from the relaxation of NMR signals (B_{NMR}) and from the entropies of hydration of ions, see below. The values of B_η and of dB_η/dT for representative ions are shown in Table 3.1 and compared there with similar measures obtained by different techniques.

3.1.2 *Self-diffusion of Water Molecules*

The rate of exchange of water molecules between the hydration shells of ions and bulk water was considered by Samoilov (1957) to indicate the strength of the hydration and indirectly the effects of the ions on the water structure. The ratio of the average residence time of a water molecule near another one in the hydration shell of the ion, τ_I, to that in the bulk ($\tau_W = 17$ ps) was obtained from the activation Gibbs energy of the exchange, $\Delta G^{\ddagger}_{exch}$. This, in turn, was obtained from the temperature coefficients of the self diffusion coefficient of water, D_W, and of the ion mobility,

u_I (Sect. 2.4.1):

$$\frac{\mathrm{d}\ln u_{\mathrm{ion}}}{\mathrm{d}T} + T^{-1} - \frac{\mathrm{d}\ln D_W}{\mathrm{d}T} = \frac{(\Delta G^{\ddagger}_{\mathrm{exch}}/RT^2)}{(1 + 0.0655\exp(\Delta G^{\ddagger}_{\mathrm{exch}}/RT))} \tag{3.4}$$

The ratio τ_I/τ_W of the average residence times is then given by:

$$\frac{\tau_I}{\tau_W} = \exp\left(\frac{\Delta G^{\ddagger}_{\mathrm{exch}}}{RT}\right) \tag{3.5}$$

Some ions, such as Li^+, Na^+, Mg^{2+}, and Ca^{2+}, have $\Delta G^{\ddagger}_{\mathrm{exch}} > 0$ and $\tau_I > \tau_W$ and were called "positively hydrated". For some other ions: K^+, Cs^+, Cl^-, Br^-, and I^-, $\Delta G^{\ddagger}_{\mathrm{exch}} < 0$ and $\tau_I < \tau_W$ and they were designated as "negatively hydrated". These terms are not in general use now, however, but the relation of the residence times to the dynamic extent of hydrogen bonding in the solution is apparent. It should be noted that the residence time of a water molecule in the vicinity of another one, $\tau_W = 17$ ps is considerably longer than the rotational reorientation of a water molecule, around 2–3 ps, or the mean lifetime of a hydrogen bond, 0.2–0.4 ps, see Sect. 1.1.4.

In the case of cations, the values of τ_I deduced from Eq. (3.5) are expected to correspond with the unimolecular rate constants, k_r, for water release from their hydration shells, obtained from ultrasound absorption (Marcus 1985). These constants depend on the competition between water molecules and anions for sites in the coordination shell and need to be independent of the anion in order to be valid characteristics of the cation hydration. So far this has not been demonstrated.

The self diffusion coefficients of water molecules in electrolyte solutions, $D_{W(E)}$, were obtained by McCall and Douglas (1965) and by Endon et al. (1967) from NMR measurements, the former at 23 °C and the latter mostly at 0 °C but for some ions also at 25 °C, the reported data pertaining to 1 M, respectively m, alkali halide solutions. More recent data, for 25 °C, at $\geq$1 m and including some divalent metal chlorides are due to Müller and Hertz (1996). The quantity $(1 - D_{W(E)}/D_W)$ is negative when both cation and anion are structure-breakers, according to their being negatively solvated by Samoilov's criterion: KX, RbX, and CsX, where X = Cl, Br, and I. Contrarily, $(1 - D_{W(E)}/D_W)$ is positive when at least one of the ions is strongly structure making: LiX and NaX, where X = Cl and Br, and LiI; MF for M = K, Rb, and Cs; and $M'Cl_2$ for M′ = Mg, Ca, and Zn, but is near zero when these tendencies are opposite and of the same magnitude: NaI. Heil et al. (1995) added data on 0.2–4.0 m aqueous $NaClO_4$, $LiClO_4$, and $Mg(ClO_4)_2$ at 25 °C, reporting that the structure making properties of the cations predominate over those of the structure-breaking perchlorate anion so that $(1 - D_{W(E)}/D_W) > 0$ in the listed order. The ionic $(1 - D_{W(E)}/D_W)$ values, based on equating the values for K^+ and Cl^- and taking $D_W = 2.27 \times 10^{-9}$ m^2 s^{-1} at 25 °C (Table 2.3) are shown in Table 3.1.

Nowikow et al. (1999) measured the self diffusion of water in 0.94 m Bu_4NCl at room temperature using quasi-elastic neutron scattering. The residence times of water molecules in the hydration shell of the cation were twice longer than in bulk water. Still, $(1 - D_{W(E)}/D_W) > 0$ and the salt is a net structure maker. Sacco et al. (1994) measured the self diffusion coefficient of the water in aqueous CsCl in D_2O

Table 3.1 Comparison of selected ionic *B*-coefficients of viscosity, the relative self diffusion on function $(1 - D_{W(E)}/D_W)$, and the NMR relaxation and the sign of their temperature coefficients near 25 °C

Ion	B_η	dB_η/dT	$(1 - D_{W(I)}/D_W)$		B_{NMR}	dB_{NMR}/dT	B_{NMR}	dB_{NMR}/dT
Reference	Marcus (1994)	Jenkins and Marcus (1995)	McCall and Douglass (1965)	Müller and Hertz (1996)	^{1}H Engel and Hertz (1968)		^{17}O Yoshida et al. (1996); Fumino et al. (1996)	
Li^+	0.146	<0	0.11	0.113	0.14	~0	0.120	>0
Na^+	0.085	~0	0.08	0.077	0.06	>0	0.053	~0
K^+	−0.009	<0	0.00	−0.024	−0.01	>0	−0.017	>0
Rb^+	−0.033	<0		−0.041	−0.04	>0		
Cs^+	−0.047	<0	0.01	−0.048	−0.05	>0	−0.014	>0
Ag^+	0.090	<0			0.06	~0		
NH_4^+	−0.008	~0						
$H(D)_3O^+$					0.06	>0	0.036	>0
Me_4N^+	0.123	~0			0.18		0.165	>0
							(0.172)	
Et_4N^+	0.385						0.444	<0
							(0.421)	
Pr_4N^+	0.916	<0					0.889	<0
							(0.868)	
Bu_4N^+	1.275	<0					1.33	<0
							(1.24)	
Ph_4P^+	1.073	<0					0.831	<0
Be^{2+}	0.450		0.29					
Mg^{2+}	0.385	<0	0.26	0.236	0.50	>0		
Ca^{2+}	0.298	<0	0.19	0.124	0.27	<0		
Sr^{2+}	0.272	>0			0.23	>0		
Ba^{2+}	0.229	>0	0.17		0.18	>0		
Zn^{2+}	0.361		0.19					
Al^{3+}	0.750		0.41					
Th^{4+}	0.860		0.74					

Table 3.1 (continued)

Ion	B_η	dB_η/dT	$(1 - D_{W(I)}/D_W)$		B_{NMR}	dB_{NMR}/dT	B_{NMR}	dB_{NMR}/dT
Reference	Marcus (1994)	Jenkins and Marcus (1995)	McCall and Douglass (1965)	Müller and Hertz (1996)	^{1}H Engel and Hertz (1968)		^{17}O Yoshida et al. (1996); Fumino et al. (1996)	
F^-	0.127	< 0	0.11	0.086	0.14	< 0	0.120	< 0
Cl^-	− 0.005	< 0	0.00	− 0.024	− 0.01	> 0	− 0.017	> 0
Br^-	− 0.033	< 0	− 0.07	− 0.046	− 0.04	> 0	− 0.026	> 0
I^-	− 0.073	< 0	− 0.08	− 0.095	− 0.08	> 0	− 0.055	> 0
$OH(D)^-$	0.120	> 0	0.09		0.18	> 0	0.083	> 0
CN^-	− 0.024				− 0.04			
SCN^-	− 0.032[a]				− 0.07			
N_3^-	− 0.018				0.00			
ClO_3^-	− 0.024			− 0.046	− 0.08			
ClO_4^-	− 0.058		− 0.08		− 0.085	> 0		
BrO_3^-	0.007	> 0			− 0.06	∼0		
IO_3^-	0.138	< 0			0.02	> 0		
ReO_4^-	− 0.055				− 0.03	> 0		
NO_2^-	− 0.024				− 0.05			
NO_3^-	− 0.045	> 0	− 0.08		− 0.05	> 0		
$CH_3CO_2^-$	0.236		0.13					
BPh_4^-	1.115						0.928	< 0
CO_3^{2-}	0.278		0.19		0.25	∼ 0		
SO_3^{2-}	0.282		0.18		0.22			
SO_4^{2-}	0.206	> 0			0.12			

[a] Marcus (2012)

and H_2O and found the D/H isotope effect to be in agreement with the structure breaking properties of both ions of this salt and with the more extensive ("stronger") hydrogen bonded network of the D_2O (see Sect. 1.1.3).

3.1.3 NMR Signal Relaxation

Engel and Hertz (1968) measured the ^1H NMR longitudinal relaxation times of the water-proton, T_{1E}, in many aqueous electrolyte solutions mainly at 25 °C and for some salts also at 0 °C. An expression analogous to the Jones-Dole expression for the viscosities, Eq. (2.35), described the results very well:

$$\left(\frac{(1/T_{1E})}{(1/T_{1W})} - 1\right) = B_{nmr}c_E + \cdots \tag{3.6}$$

They employed the convention that $B_{nmr}(K^+) = B_{nmr}(Cl^-)$ to obtain the ionic values. The rotational correlation times τ_r of the water molecules near ions are $\tau_{rI}/\tau_{rW} = 1 + (55.51/h_I)B_{nmr}$, where the h_I are the hydration numbers of the ions. When the ions were classified according to the signs of their $\Delta G^{\ddagger}_{exch}$ values according to Samoilov (1957), the 'positively hydrated' ones had $B_{nmr} > 0$ (i.e., for structure-making ions) and the 'negaively hydrated' ones had $B_{nmr} < 0$ (i.e., for structure-breaking ones). A good correspondence was noted by (Engel and Hertz 1968) and by Abraham et al. (1982), among others, between these B_{nmr} values and the ionic B_η values (Sect. 3.1.1, see Table 3.1).

Only diamagnetic ions can be studied by means of ^1H NMR measurements of longitudinal relaxation times, T_1. Other kinds of NMR measurements are required for paramagnetic ones, e.g., transition metal cations. Yoshida et al. (1996) studied the ^{17}O NMR spin-lattice relaxation of D_2O molecules in aqueous salt solutions at five temperatures between 5 and 85 °C. They showed that splitting the salt data according to $B_{nmr}(K^+) = B_{nmr}(Cl^-)$ provides acceptable results, agreeing well in sign and generally in magnitude with the ^1H B_{nmr} values of Engel and Hertz (1968) and the viscosity B_η values Table 3.1. The signs of the temperature coefficients $\Delta B_{nmr}/\Delta T$ from 0 to 25 °C (Engel and Hertz 1968) and from 5 to 25 °C (Yoshida et al. 1996; Fumino et al. 1996) for the two NMR methods agree well. However, these signs are in most of the cases of structure-breaking ions opposite to those from viscosity, dB_η/dT. The reason for this is difficult to understand.

The B-coefficients obtained from viscosity and NMR signal relaxation rates pertain to dilute solutions (they are the limiting slopes towards infinite dilution). However, an equation of the form of Eq. (3.6) for NMR spin-lattice relaxation rates holds up to fairly large concentrations. Chizhik (1997) reported values of relative water molecule reorientation times τ_{rI}/τ_{rW} at 22 °C, being <1 for Br^-, I^-, NH_4^+, NO_3^-, and N_3^-, ~1.0 for K^+, and >1 for Li^+, Na^+, Mg^{2+}, Ca^{2+}, Sr^{2+}, Ba^{2+}, F^-, Cl^-, H_3O^+, SO_4^{2-}, and CO_3^{2-}, in more or less agreement with the signs of the B_{nmr} in dilute solutions, Table 3.1.

Table 3.2 Ratios of reorientation times of hydration water molecules in 1 M salt solutions at 25 °C, $\tau_{W(I)}$, to that in pure water, $\tau_W{}^*$, (Kaatze 1997)

Cation	$\tau_{W(I)}/\tau_W$	Anion	$\tau_{W(I)}/\tau_W$
Li^+	2.41	F^-	2.61
Na^+	1.53	Cl^-	0.90
K^+	0.90	Br^-	0.73
Rb^+	0.78	I^-	0.41
Cs^+	0.68	OH^-	2.44
H_3O^+	1.62	$NO_3{}^-$	0.73
$NH_4{}^+$	0.72		
Me_4N^+	1.59		
Et_4N^+	1.96		
Pr_4N^+	2.37		
Bu_4N^+	2.80		

3.1.4 Dilectric Relaxation

Dielectric relaxation times in aqueous alkali halide solutions were obtained by Kaatze et al. (Giese et al. 1970; Wen and Kaatze 1977; Kaatze 1997) from the complex permittivities as a function of the frequency. The relaxation data were analyzed by Kaatze (1997) in terms of the ratios of the cooperative reorientation times $\tau_{\theta I}$ of water molecules hydrating the ions in 1 M solutions to that, $\tau_{\theta W} = 8.27 \pm 0.02$ ps, of pure water at 25 °C. Individual ionic values are based on setting the values for K^+ and Cl^- as equal. The ratios $\tau_{\theta I}/\tau_{\theta W}$ are shown in Table 3.2, and are seen to follow the pattern shown in Table 3.1, namely, that structure-breaking ions have $\tau_{\theta I}/\tau_{\theta W} < 1$ and structure-making ones have $\tau_{\theta I}/\tau_{\theta WW} > 1$.

Dielectric relaxation measurements by Buchner, Wachter et al. (Buchner et al. 1994, 2002, Buchner and Hefter 2009; Chen et al. 2003; Tromans et al. 2004; Wachter et al. 2005, 2006, 2007) made mainly for studying ion association in aqueous solutions, yielded also the reorientation times of the water molecules. The cooperative reorientation time of bulk water, $\tau_{\theta E}$, decreases with increasing salt concentration, reflecting the weakening of the hydrogen bonded structure of the water. These measurements were made at salt concentrations, $c_E < 1$ M and yielded the coefficient b of Eq. (3.7):

$$\tau_{\theta E} = \tau_{\theta W} + a(\exp(-bc_E) - 1) \tag{3.7}$$

The values were not split into individual ionic ones, but for a series of sodium salts (Wachter et al. 2005) clearly show the effects of the anions on the b values: NaOH 0, Na_2CO_3 0.55, NaCl 0.79, NaBr 0.98, NaSCN 0.99, NaI 1.20, $NaNO_3$ 1.33, $NaClO_4$ 1.35, Na_2SO_4 1.8, and also sodium malonate 3.44, ranging from structure-makers to structure-breakers. Consideration of the b-coefficient of Eq. (3.7) for NaCl, 0.79, in conjunction with the values for KCl, 1.5, and CsCl, 2.1 (Chen et al. 2003) show them to be in the expected direction. Asaki et al. (2002) studied the solvent relaxation of aqueous lithium salts, and from their data the b-coefficients of Eq. (3.7) can be derived: LiCl 0.62, Li triflate 0.86, and Li imide 1.27. The value for LiCl fits in with those of NaCl, KCl, and CsCl.

The dielectric relaxation times of water molecules near hydrophobic solutes are some three times slower that of bulk water. This was established with solutes such as the larger tetraalkylammonium ions. Hindered orientation of the water molecules in the ice-like cages around the hydrophobic cations was said to be responsible for this behaviour, the sizes of the cages (the number of water molecules involved) increasing along the series (Barthel et al. 1998; Buchner et al. 2002). Another interpretation (Buchner and Hefter 2009) of the slowing down of the collective relaxation of the water molecules surrounding the hydrophobic parts of the ions is their being shielded by these parts from 'attack' by incoming water molecules that is responsible for the exchange of water molecules (Kropman et al. 2002). The concentration dependence of the solvent relaxation times, $\tau_{\theta E}$, for inorganic salt solutions is negative, $d\tau_{QE}/dc_E < 0$, but is positive for solutions of large hydrophobic ions such as the tetraalkylammonium halide, for which $d\tau_{\theta E}/dc_E > 0$. The values of $d\tau_{\theta E}/dc_E$ increase in the series: $Me_4NBr < Bu_4NBr < Et_4NBr \sim Pr_4NBr \sim Pe_4NBr < Et_4NCl$ (note that the position of Bu_4NBr is out-of-line) (Barthel et al. 1998; Buchner et al. 2002). The hydrophobic ions of aqueous Ph_4PCl and $NaBPh_4$ (Wachter et al. 2006) dominate over the small counter-ions, hence these salts have positive slopes $d\tau_{\theta E}/dc_E$.

3.1.5 Fast Vibrational Spectroscopy

Ultrafast (femtosecond) pulsed two-color mid-infrared spectroscopy was used by Bakker et al. in a series of papers to study the effect of ions on the structural dynamics of their aqueous solutions as recently reviewed (Bakker 2008). The first intense pulse (pump pulse) excites the O–H (or O–D) stretch vibration to the first excited state and the second pulse (probe pulse), red-shifted with respect to the first, probes the decay of this state. This technique has been applied to aqueous (0.1–0.5 M HDO in D_2O) solutions of LiX, NaX, and MgX_2 (X = Cl, Br, I), KF, $NaClO_4$, and $Mg(ClO_4)_2$ over wide concentration ranges, 0.5–10 mol dm^{-3}.

The reorientation dynamics of water molecules in the electrolyte solutions are related to the rotational anisotropy:

$$R = \frac{(\Delta\alpha_{\parallel} - \Delta\alpha_{\perp})}{(\Delta\alpha_{\parallel} + 2\Delta\alpha_{\perp})} \tag{3.8}$$

where $\Delta\alpha_{\parallel}$ and $\Delta\alpha_{\perp}$ are the absorption change for the probe pulse being parallel and perpendicular to the pump pulse. The reorientation times are obtained from $\tau_r = -t/\ln R(t)$. After a delay of 3 ps between pump and probe pulses the reorientation time of water molecules hydrogen bonded to the chloride anion in 3 M NaCl at 27 °C is 9.6 ps, compared with 2.6 ps in pure HOD/D_2O (Kropman et al. 2002). This time becomes faster as the temperature increases also for bromide and iodide anions, in agreement with the Stokes-Einstein expression (2.15), being related to the temperature-dependent viscosity. The rotational hydrodynamic radii of the anions are

larger than their translational (Stokes) radii, showing that the rotational dynamics involve the hydration shell, but they are smaller than the halide-O_W distances.

In similar investigations, of 3 and 6 M $Mg(ClO_4)_2$ and 0.5–6 M $NaClO_4$ in HOD-D_2O (with only ca. 0.25 M HOD), results specific to the O–H group hydrogen bonded to the perchlorate anion were obtained (Omta et al. 2003). The relaxation time of O–H stretch vibrations of perchlorate-bonded water molecules was 7.6 ± 0.3 ps (Kropman and Bakker 2003; Bakker et al. 2005). The orientational correlation times for bulk water molecules were deduced from the decay of the anisotropy parameter. These parameters in 0.5–6 M $NaClO_4$ as well as in 0.5 and 1 M $Mg(ClO_4)_2$ and 1 M Na_2SO_4 were independent of the salt concentration, 3.4 ± 0.1 ps, the same as for pure water. When the O–D stretch anisotropy was studied in H_2O with 4 % HOD and 1 and 3 M $Mg(ClO_4)_2$, the orientational correlation time was 2.5 ± 0.1 ps, as in pure HOD-H_2O. There was no relation of these results to the increased viscosity of the salt solutions. Only the firmly bound water molecules in the hydration shells, leading to the bulkiness of the ions, according to the Stokes-Einstein relationship, were in the view of the authors responsible for the enhanced viscosity of the solutions (positive B_η values).

3.1.6 Computer Simulations

Geiger (1981), following a suggestion by Gurney (1953), computed by molecular dynamics the self diffusion coefficient $D_{W(I)}$ of water molecules in the first and second hydration shells around particles of the size of a xenon atom. These had a Lennard-Jones diameter of 0.410 nm, i.e., between those of Cs^+, 0.340 nm and I^-, 0.440 nm. The particles were assigned discretely varying charges: 0, +0.67, +1, +2, and −1. Geiger found for lightly charged cations, + 0.67 and +1, that the self diffusion coefficient ratios for water in the first hydration shell to that of bulk water, $D_{W(I1)}/D_W$, are larger than unity, reaching 1.6 and 1.2, but for charges 0 (hydrophobic effect) and +2 it is smaller than unity, 0.7 and 0.5. For the anion, this ratio is 1.4. The effect persists to a smaller degree in the second hydration shell. A similar effect was noted for the reorientation times of the intermolecular H_W–H_W and O_W–H_W vectors, being shorter for the +0.67, +1, and −1 charged particles than for bulk water and longer for the uncharged and +2 charged particles. These findings are in agreement with the results of the measurements described in Sect. 3.1.2.

The results of early molecular dynamics simulations depend on the model potential functions and the number of particles used for the computations. Geiger (1981) employed the ST2-water model and 215 water molecules/charged particle.

Balbuena et al. (1998) studied the reorientation times of water molecules over a range of temperatures including supercritical ones, employing semi-continuum molecular dynamics by means of the SPC/E water model (500 water molecules per ion). The reorientation times in bulk water relative to those in the first hydration shell, assuming a coordination number of $N_{co} = 6$, are $\tau_{rw}/\tau_{rI} = 0.20, 0.47, 0.65$, and 0.90 for Na^+, K^+, Rb^+, and Cl^-, respectively, at 25 °C, showing faster reorientation as

the water binding weakens. The authors were mainly interested in the results for the higher temperatures and they did not discuss the discrepancy relative to Geiger's results.

The same water model, SPC/E at 25 °C was used by other authors too. Chowdhuri and Chandra (2001) employed 256 water molecules per ion, as well as lower ratios at increasing concentrations, and reported the average residence times of water molecules near ions in ps: Na^+ 18.5, K^+ 7.9, and Cl^- 10.0. Guardia et al. (2006) also reported residence times in ps of the water molecules in the first hydration shells of ions: Li^+ 101, Na^+ 25.0, K^+ 8.2, Cs^+ 6.9, F^- 35.5, Cl^- 14.0, and I^- 8.5, compared with 10 ± 1 for water molecules in the bulk. These values, resulting from detailed considerations of the hydrogen bond dynamics in water and near the ions, can be compared with experimental values derived from NMR. According to Bakker (2008) these are: Li^+ 39, Na^+ 27, K^+ 15, Cl^- 15 (by definition the same as for K^+), Br^- 10, and I^- 5 ps, and for water molecules in the bulk 17 ps, calculated from the self diffusion coefficient.

In the last dozen years or so Rode and his coworkers published an extensive program of study of the dynamics and structure of aqueous solutions of ions by means of quantum- mechanical combined with molecular-mechanical computer simulations. In the earlier studies the general methodology involved the quantum chemical treatment of the first hydration shell of an ion, with methods that have been progressively refined through the years. The water beyond the first hydration shell is then simulated by means of molecular dynamics methods, the interface between these two regions being also carefully treated. In general, 499 water molecules were employed at 298 K with one ion present as the solute. In later studies, employing the quantum mechanical charge field approach, the nearest two hydration shells were treated by quantum mechanics and 1,000 water molecules were employed. The mean residence times, *MRT*, of water molecules in the vicinity of ions, relative to those near water molecules in the bulk (*RMRT*s for the relative quantities) are indicative of the water structure-making (if they are longer) or structure-breaking (if they are shorter) effects of the ions. This aspect was stressed by Hofer et al. (2004), who also compared the methodologies employed and the results obtained by them. The computational program employed has evolved over the years as was the minimal time t^*, above which a molecule is deemed to have left its position, from 2 ps in the earlier studies to 0.5 ps used in the later ones. Therefore, not all the numerical values are comparable, Table 3.3.

The *MRT* of a water molecule near an F^- anion is twice longer than near another water molecule in the bulk, whereas for a Cl^- anion it is only 10 % longer. This shows F^- anions to be marked structure-makers and Cl^- anions to be only marginally so (Tongraar and Rode 2005). For I^- anions the corresponding *RMRT* is only 65 % of that of water in bulk, so that it can be deemed to be a water structure-breaker (Tongraar et al. 2010). For the oxo-anions: NO_3^- (Tongraar et al. 2006), ClO_4^-, CrO_4^{2-}, SO_4^{2-}, and PO_4^{3-} (Pribil et al. 2008; Hinteregger et al. 2010) the mean residence times of water molecules near them are 88, 88, 135, 153 and 229 % of those for water molecules in the bulk, again in agreement with their purported dynamical water structure-breaking and -making properties.

Table 3.3 The relative mean residence times, *RMRT* in %, for second shell water beyond $t^* = 0.5$ ps, obtained from (charge field) quantum mechanical/molecular dynamics simulations, with 1.7 ps residence time for bulk water molecules. Values in parenthesis are the second shell *MRT* in ps for $t^* = 2.0$ ps

Ion	Reference	*RMRT*	Ion	Reference	*RMRT*
Li^+	Loefler and Rode (2002)	?	Al^{3+}	Hofer et al. (2008a)	1060
Na^+	Azam et al. (2009a)	107	Ti^{3+}	Kritayakornupong et al. (2004)	2180 (37)
K^+	Azam et al. (2009a)	93	Cr^{3+}	Hofer et al. (2004)	440 (22)
Rb^+	Hofer et al. (2005)	88	Fe^{3+}	Moin et al. (2010)	240, 1160[e]
Cs^+	Schwenk et al. (2004)	76	Co^{3+}	Hofer et al. (2004)	650 (55)
Ag^+	Blauth et al. (2010)	80	Sb^{3+}	Lim et al. (2010a)	140
Au^+	Armunanto et al. (2004)	<100	Bi^{3+}	Durdagi et al. (2005)	500
Tl^+	Vchirawongwin et al. (2007)	76	La^{3+}	Hofer et al. (2006)	490
Be^{2+}	Azam et al. (2009a)	320	Tl^{3+}	Vchirawongwin et al. (2007a)	750
Mg^{2+}	Tongraar and Rode (2005a)	280, 240[c]	Zr^{4+}	Messner et al. (2011)	320
Ca^{2+}	Hofer et al. (2004)	260	Hf^{4+}	Messner et al. (2011)	910
Sr^{2+}	Hofer et al. (2006a)	350	U^{4+}	Messner et al. (2011)	480
Ba^{2+}	Hofer et al. (2004)	320	UO_2^+	Frick et al. (2009)	250
V^{2+}	Hofer et al. (2004)	440	UO_2^{2+}	Frick et al. (2010)	320
Mn^{2+}	Hofer et al. (2004)	400 (24)	F^-	Tongraar & Rode (2005)	~200
Fe^{2+}	Moin et al. (2010)	320, 180[d]	Cl^-	Tongraar & Rode (2005)	110
Co^{2+}	Kritayakornupong et al. (2003)	400 (26)	I^-	Tongraar et al. (2010)	65
Ni^{2+}	Inada et al. (2002)	?	HS^-	Kritayakornupong et al. (2010a)	161, 142[c]
Cu^{2+}	Hofer et al. (2004)	450	NO_3^-	Tongraar et al. (2006)	88
Zn^{2+}	Fatmi et al. (2005)	190	ClO_4^-	Pribil et al. (2008)	88
Cd^{2+}	Hofer et al. (2004)	270 (10)	HCO_2^-	Payaka et al. (2009)	132
Hg^{2+}	Hofer et al. (2004)	280 (13)	$CH_3CO_2^-$	Payaka et al. (2010)	172
Hg_2^{2-}	Hofer et al. (2008)	180	HCO_3^-	Vchirawongwin et al. (2010)	54, 76[a]
Ge^{2+}	Azam et al. (2010)	120	HSO_4^-	Vchirawongwin et al. (2010)	83, 167, 328[b]
Sn^{2+}	Lim et al. (2009)	110	$HAsO_4^{2-}$	Bhattacharjee et al. (2010)	109
Pb^{2+}	Bhattacharjee et al. (2009)	140	SO_4^{2-}	Pribil et al. (2008)	153
Pd^{2+}	Hofer et al. (2009)	270	CrO_4^{2-}	Pribil et al. (2008)	135
Pt^{2+}	Hofer et al. (2009)	?	PO_4^{3-}	Pribil et al. (2008)	229

[a] RMRT = 54 % near the H atom and 76 % near the O atoms
[b] *RMRT*=83 % near three of the O atom and 167 % near the fourth, and 324 % near the H atom
[c] *RMRT*=115 % near the S atom and 161 % near the H atom
[d] *RMRT* = 180 % was estimated in (Remsungen and Rode 2004)
[e] *RMRT* = 240 % from (Schwenk and Rode 2003)

The alkanoate anions, formate (Payaka et al. 2009) and acetate (Payaka et al. 2010) are both structure making, with mean *RMRT*s of 132 and 172 % respectively. A notable difference between the two oxygen atoms of $HCOO^-$ is noted, the *RMRT*s near them being 121 and 142 % but the difference in the case of acetate is negligible. For HS^- (Kritiyakornupong et al. 2010) there exists a difference in the *RMRT*s near the hydrogen atom, 161 %, and near the sulphur one 115 %, but in any case, this anion is a mild structure maker. Other protonated anions that were studied were the hydrogen carbonate (Vchirawongkwin et al. 2010a), hydrogen sulphate (Vchirawongkwin et al. 2010), and hydrogen arsenate (Bhattacharjee et al. 2010). In the case of HCO_3^- different *RMRT*s could be discerned near the hydrogen atom and the oxygen atom to which it is bound: 54 and 90 %, and the other two oxygen atoms: 69 %, but on the whole it is a structure breaking anion. For HSO_4^-, the hydrogen atom and the oxygen atom to which it is bound are strong structure making (*RMRT* = 328 and 167 %), but the other three oxygen atoms have structure breaking properties, their *RMRT*s are 83 %. For the bivalent $HAsO_4^{2-}$ anion only the overall *RMRT* = 109 % could be reported, making it a mild structure maker, in spite of its charge, but in view of its large bulk than, say, the divalent sulphate anion (*RMRT* = 153 %).

Little can be said about the water structure-making and -breaking properties of the hydrogen ion as derived from computer simulation. A recent quantum mechanical charge field (QMCF)/molecular dynamics (MD) simulation of dilute HCl (498 water molecules per HCl) (Kritiyakornupong et al. 2010) showed it to be simultaneously a weak structure-making and a weak structure-breaking species. The former effect should be attributed to the hydronium ion H_3O^+ ion and the latter to the Cl^- one, but the duration of the simulation, 10 ps, was too short to be definite on this point. The simulation of Li^+ hydration by similar methods (Loefler and Rode 2002) did not provide information about its water structure-making properties. An earlier quantum mechanical/MD simulation of Na^+ and K^+ hydration (Tongraar et al. 1998) showed a transition between structure-making (Na^+) and -breaking (K^+) properties beyond the first hydration shell. Recent re-examination of their hydration by QMCF/MD simulations (Azam et al. 2009) indeed showed *RMRT*s to be (in a possible second hydration shell) barely different from that in bulk water, 107 and 93 %, respectively and within the methodical uncertainty (Azam et al. 2009a). On the contrary, the water structure-breaking properties of Rb^+ (Hofer et al. 2005), *RMRT*= 88 %, and Cs^+ (Schwenk et al. 2004), *RMRT* = 76 % (65 % in Table 2 of (Hofer et al. 2004)) are clearly manifested by quantum mechanical/MD simulations, with the effect for Rb^+ being more pronounced than for K^+ but weaker than for Cs^+, as expected. For the latter cation a highly space-consuming second hydration sphere, disrupting the hydrogen bonded structure of the solvent, was observed.

The dynamics of water molecules near Ag^+ ions (Armunanto et al. 2003) showed the hydration shells to be non-symmetric, irregular, and labile. The *RMRT*s noted cannot be compared with those listed above because the *RMRT* value near a water molecule was not reported and the minimal time t^* above which a molecule is deemed to have left its position was set to 1 or 2 ps rather than 0.5 ps used in the other studies quoted above. This was amended in a subsequent paper (Blauth et al. 2010), where the *RMRT* was reported as 80 %, hence considering the ion as a

structure breaker. A similar problem is encountered with the study of the hydration of Au^+ ions (Armunanto et al. 2004), where absolute *MRT* values for t^* of 2 and 0.5 ps are reported (unusually shorter for the first than the second hydration sphere), but not the corresponding value for bulk water. The relative *MRT* values for the first and second shells were reversed in a more recent study (Lichtenberger et al. 2011). Still, also Au^+ was considered to be a structure-breaking ion. The hydration dynamics of Tl^+ (Vchirawongkwin et al. 2007) share with those of Au^+ the phenomenon that the *RMRT* of the first hydration sphere (76 %) is shorter than that of the second sphere (88 %) for t^* of 0.5 ps, but the list of *RMRT* values given in this paper for Rb^+, Cs^+, Ag^+, and Au^+ are at variance with their being classified as water structure breakers in the papers quoted above. This point has not been explained so far.

Turning to divalent alkaline earth cations, the *RMRT*s (Azam et al. 2009a) in the second hydration shell of Be^{2+} is 320 % and of Mg^{2+} is 280 % (240 % in (Tongraar and Rode 2005)). The corresponding second hydration shell values for Sr^{2+}, 350 % (Hofer et al. 2006), and Ba^{2+}, 320 % (Hofer et al. 2005a), are larger than those for Be^{2+} and Mg^{2+}, contrary to expectation from the sizes of the ions. For Ca^{2+} *RMRT* = 260 % was reported in (Hofer et al. 2004) and residence times in the first shell, 16.1 ps at 298.15 K and 8.5 ps at 368.15 K (Lim et al. 2010) show the effect of the temperature on the exchange rate of water molecules, hence on the effect of the ion on the structure of water.

For the divalent transition metal ions V^{2+} and Mn^{2+} the *RMRT*s in the second hydration shell are 280 and 160 % (Schwenk et al. 2003). However, the computational method at the time did not include the charge field correction to the quantum mechanical simulations. For second sphere water molecules near Fe^{2+} an *MRT* = 10 ps is reported in (Remsungnen and Rode 2004) but no corresponding value for bulk water. In a later paper (Moin et al. 2010) *MRT* = 5.4 ps (the *RMRT* = 320 %) was reported. For Co^{2+}, too, only an *MRT* = 28 ps (26 ps in (Kritayakornuong et al. 2003)) was reported (Armunanto et al. 2003) for second shell water molecules, with t^* = 2 ps, but subsequently *RMRT* = 400 was reported (Hofer et al. 2004). For Ni^{2+} mainly a static structure was obtained by the simulations (Inada et al. 2002) and the resources available at the time did not permit to obtain *RMRT* values comparable with the above. In the case of second shell Cu^{2+} water the *MRT* = 7.4 and 9.6 ps were reported for two acceptable computation methods, again for t^* = 2 ps, and a bulk water *MRT* = 2.9 ps by another computational method (Schwenk and Rode 2003). However, in unpublished work quoted in (Fatmi et al. 2005) the second shell *RMRT* = 180 % for t^* = 0.5 ps was obtained and for Zn^{2+} the corresponding value is 190 % (Fatmi et al. 2005), directly comparable with the values shown above. Again, for Cd^{2+} an *MRT* value for t^* = 2 ps was reported (Kritayakornupong et al. 2003b) as 10 ps, near that for Hg^{2+} of 13 ps (Kritayakornupong et al. 2003a) (a value later revised to be much shorter, 2.4 ps (Lichtenberger et al. 2011)) but two times shorter than for Co^{2+} (26 ps) or Mn^{2+} (24 ps). For the mercury(I) dimer, Hg_2^{2+}, the water binding is very weak, and for the *first* hydration shell a *RMRT* = 180 % was established, lower than that for Ba^{2+} as shown above. The *RMRT* values for t^* = 0.5 ps were subsequently reported as 270 % for Cd^{2+} and 280 % for Hg^{2+}, (Hofer et al. 2009). Aqueous Pd^{2+} has four firmly bound equatorial water molecules and two

more labile axial ones. The *MRT* of the axial water molecule of Pd^{2+} was said to be only 2.5 ps, whereas for aqueous Pt^{2+} the *MRT* of the axial water molecule is 3.9 ps (Hofer et al. 2009).

The dynamics of aqueous divalent post-transition-metal ions have also been studied by Rode's group (Lim et al. 2009; Bhattacharjee et al. 2009; Azam et al. 2010; Rode and Lim 2010). Their peculiar behaviour is ascribed to the lone pair electrons, so that in the proximal hydration hemisphere they are only slightly water structure makers, but in the distal hydration hemisphere they are slightly structure breakers. Even for the first hydration shell the *RMRT*s are much smaller than for the transition metal cations, and for the second shell the *RMRT*s are 120 % for Ge^{2+}, 107 % for Sn^{2+}, and 140 % for Pb^{2+}. The non-monotonically varying values with the atomic number should be noted.

For the trivalent cations, aqueous Al^{3+} has a *RMRT* = 1760 % for second sphere water molecules, reduced to 1040 % for charge field quantum mechanical simulations (Hofer 2008a; Azam et al. 2009). For aqueous Tl^{3+} the second sphere *RMRT* was 750 % (Vchirawongwin 2007a). For trivalent transition metals the second shell *RMRT* for Ti^{3+}, where the Jahn-Teller effect is involved, is 2180 % (but the same *MRT* of 37 ps was obtained for $t^* = 0.5$ and 2.0 ps) (Kritaryakornupong 2004). This paper also quotes *MRT* values for $t^* = 2.0$ ps of 22.4 ps for Cr^{3+} and 39.7 ps for Fe^{3+}, but given as 48 ps in (Remsungtnen et al. 2004) for the latter cation. Subsequently the *MRT* = 19.8 ps was reported (Moin et al. 2010), so the *RMRT* = 1160 % results. For aqueous Co^{3+} the *MRT* = 55 ps was reported for second shell water (Kritaryakornupong 2003). Aqueous La^{3+} has a much shorter *MRT*, the relative value being 490 % (compare Ba^{2+} 320 % and Cs^{+} 76 %) (Hofer et al. 2006a). Aqueous post-transition-metal cations, for which the presence of lone pair electrons makes the hydration shells asymmetric, have also been studied. For Sb^{3+} the second sphere *RMRT* = 140 % (Lim et al. 2010a) and for Bi^{3+} it is 500 % (Durdagi et al. 2005).

Aqueous quadrivalent ions have also been studied with respect to the residence time of water molecules in their second hydration spheres. The most recent publication (Messner et al. 2011) reports the *RMRT* values 320 % for Zr^{4+}, 910 % for Hf^{4+}, and 480 % for U^{4+} (also 1060 % for Al^{3+}). The non-monotonical variation of the *MRT* with the atomic number of the ion is to be noted. Finally, for the uranyl ions, the *RMRT* values 250 % for UO_2^{+} (Frick et al. 2010) and 320 % for UO_2^{2+} (Frick et al. 2009) were reported. The *MRT* values for second shell hydration of tri- and tetravalent cations were recently summarized by Hofer et al. (2011).

The first hydration shell water molecules for the multivalent ions have practically 'infinite' residence times, much longer than the duration of the simulations (tens of ps) can follow their movements. The relative mean residence times of water molecules near the ions are roughly proportional to the surface density of the charge on the ions. In fact, the $RMRT = 0.22 + 1.14(\sigma_I/\mathrm{C\ nm^{-2}})$, but exceptions are noted. It must be stressed, though, that the relative residence times depend strongly on the computational method. A further point to be noted is that the duration of the simulation runs is much too short to allow for hydrolysis of the ions that certainly takes place for tri- and quadrivalent cations.

3.2 Static Spectroscopic Studies

3.2.1 Vibrational Spectroscopy

Kujumzelis (1938) was among the first to apply Raman spectroscopy to electrolyte solutions with the express intent to study the alteration in the structure of water by ions. He studied solutions of chloride, bromide, iodide, nitrate, chlorate, iodate, perchlorate, carbonate, and sulphate salts of various cations. He concluded that the hydrogen bonds between the water molecules are distorted by these anions and that these effects differ from those produced by raising the temperature. Choppin and Buijs (1963) studied aqueous electrolyte solutions at several temperatures and various concentrations (mostly at 21–27 °C and 4.6 m). They used near-infrared spectroscopy and examined the resolved bands at 1.16, 1.20, and 1.25 μm, considering a model where these bands correspond to water molecules with none, one, or two hydrogen bonds. Water structure-making properties, i.e., shifts to more hydrogen bonds per water molecule, were assigned to La^{3+}, Mg^{2+}, H^+, Ca^{2+}, OH^-, and F^- according to the spectroscopic data. Structure-breaking properties, shifts to fewer hydrogen bonds, were accordingly assigned to K^+, Na^+, Li^+, Cs^+, Ag^+, $ClO_4{}^-$, I^-, Br^-, $NO_3{}^-$, Cl^-, and SCN^-.

Kecki et al. (1968) studied the infrared spectra of solutions of HDO in H_2O and in D_2O in the absence and presence of salts. The absorbance contours of OD and OH stretching were split in the presence of salts, and it was concluded that $ClO_4{}^-$does not hydrate but breaks down the water structure, contrary to the hydrating anions: Cl^-, Br^- and I^-. Bonner and Jumper (1973) compared the 1.15 μm infrared band of 1 M aqueous electrolyte solutions with that of water. The band consisted of two components, corresponding to hydrogen-bonded and non-bonded water groups. The fraction of the former (hydrogen- bonded water) was increased by cations relative to that in pure water at the same temperature whereas anions decreased it. How the observed changes were allocated to cations and anions is not clear, however.

Nickolov and Miller (2005) applied FTIR spectroscopy for analyzing the O–D stretching vibration in 8 mass% HOD in H_2O to study the water structure effects of KF, CsF, NaI, KI, and CsCl. They inferred water structure breaking from the narrowing and the blue-shifting of the peak of the non-deconvoluted 2380 cm^{-1} band and correspondingly structure making from the opposite trends. They required, however, appreciable concentrations of the salts in order to observe the effects, with water-to-salt ratios optimally < 20. Of the five salts, the two fluorides were deemed to be structure makers, the others structure breakers, the effects of cation and anion possibly compensating each other to some extent.

Walrafen (1970) studied Raman spectra of alkali metal perchlorate solutions in H_2O and D_2O containing HOD and found pronounced splitting of the OD and OH stretching bands in the presence of $ClO_4{}^-$, in agreement with the earlier infrared study of Kecki et al. (1968) mentioned above. It was concluded that the perchlorate anion did not form directed hydrogen bonds with water, contrary to those formed by halide anions, and that it was a strong water structure-breaker, reducing the fraction of fully

hydrogen bonded water molecules, in the same manner as raising the temperature does. The conclusion that the ClO_4^- anion is not hydrated is contrary to the results of Omta et al. (2003) from double pulse ultra-fast infrared spectroscopy that the O–H group in dilute HDO in D_2O is hydrogen bonded to the perchlorate anion. Walrafen (1970) also quoted unpublished Raman work of T. H. Lilley, who found that IO_4^- is also a structure breaking anion, possible more strongly than ClO_4^-.

Holba (1982) also used Raman spectroscopy for studying the extent of hydrogen bonding of water molecules in the presence of salts. The absorption intensities of the 6427 and 7062 cm^{-1} bands of 6 M HOD in D_2O were measured in the absence and presence of 0.5–2.0 M salts. Positive values of $1 - R_N$, where R_N is the ratio of the band absorption for 1 M salt solutions to that in the absence of salt, denote structure breaking effects and negative ones structure making ones, in the sense of decreasing and increasing the amounts of hydrogen bonded water molecules. No attempt to assign values to individual ions was made. The values for electrolytes are: 0.056 for NaCl, 0.068 for KCl, 0.061 for NaN_3, 0.124 for NaSCN, 0.122 for KSCN, 0.234 for $NaClO_4$, 0.275 for $Na_2S_2O_8$, 0.356 for $K_3Fe(CN)_6$, -0.016 for Li_2SO_4, -0.095 for Bu_4NBr, and -0.109 for $MgSO_4$.

Li et al. (2004) used Raman spectroscopy more recently to study the hydrogen bonded structure of water in the presence of sodium halide salts at various temperatures. They resolved the Raman band for the O–H stretching vibration of H_2O to five Gaussians (!) at 3051, 3233, 3393, 3511, and 3628 cm^{-1} and assigned the three lower wave-numbers to water molecules with all four ice-like hydrogen bonds intact. The two higher wave-numbers were assigned to water molecules with fewer than four hydrogen bonds, mainly in view of the temperature dependence of their intensities between 0 and 100 °C for pure water. Li et al. then showed that at 20 °C F^- does not affect the Raman spectrum appreciably, but Cl^-, Br^-, and I^- ions do so in increasing manner, in the direction of further breaking the ice-like hydrogen bonding, as expected.

3.2.2 The Structural Temperature

The concept of a 'structural temperature' of electrolyte solutions was introduced long ago by Bernal and Fowler (1933). This 'structural temperature', T_{str}, of an electrolyte solution at a given temperature T is that temperature, at which pure water would have effectively the same inner structure. They suggested that T_{str} could be estimated from viscosity, x-ray diffraction, Raman spectroscopy, etc., but did not provide explicit methods and values.

Bunzl (1967) used the shift of the 0.97 μm band of water in the infrared spectra of aqueous tetraalkylammonium bromides at 10–70 °C to establish their structural temperatures. The differences $\Delta T = T - T_{str}$ for 1 m solutions at 35 °C are 11–14 K, not showing a clear dependence on the nature of the cation, ranging from $(CH_3)_4N^+$ to $(C_4H_9)_4N^+$. The temperature dependence of the differences does show cation size

Table 3.4 The difference $\Delta T = T_{str} - T$ between the structural and the actual temperature of aqueous electrolytes, 1 m at 25 °C

Electrolyte	ΔT/K(IR)	ΔT/K(NMR)	Electrolyte	ΔT/K(IR)	ΔT/K(NMR)
LiCl	5		Na_2CO_3	−4.0	−6
LiI	8.0		Na_2SO_4	0.6	
NaCl	3.9	5	$(NH_4)_2SO_4$	−1.8	
NaI	6.5		$MgCl_2$	−3	
NaSCN	8.5		$MgSO_4$	−8.6	−8
$NaClO_4$	18.9	19	$BaCl_2$	−6	
KCl	4.6	3			
KBr	5.8	8			
KI	7[a]	6			
KSCN	9.6				
KNO_3	8.0	8			

[a]From (Worley and Klotz 1966)

effects: $d\Delta T/dT > 0$ for $(CH_3)_4N^+$, it is ~ 0 for $(C_2H_5)_4N^+$, and is < 0 for $(C_3H_9)_7N^+$ and $(C_4H_9)_4N^+$.

Luck (1965, 1975) used infrared spectroscopy to obtain the fraction of non-bonded OH groups at the wavelength of the peak of free OH in water at 200 °C. He then derived values of T_{str} ranging from 10–85 °C for salt solutions at T from 20–65 °C, but shown only in diagrams. Leyendekkers (1983) used these data at 25 °C to obtain the $\Delta T = T_{str} - T$ values shown as ΔT(IR) in Table 3.4. When the structure breaking properties of a salt dominate over the structure making ones ΔT is positive but is negative otherwise.

Structural temperatures of electrolyte solutions are unfortunately only operationally defined, i.e., in terms of the method used for their determination. The Raman scattering intensity ratio $I(2645\,cm^{-1})/I(2525\,cm^{-1})$ for 4 M $NaClO_4$ in HDO/H_2O at 25 °C corresponds according to Walrafen (1970) to as much as $\Delta T \sim 110$ K. More in line with Luck's (1965) $\Delta T \sim 19$ K infrared spectroscopic result for 1 m $NaClO_4$ in H_2O at 25 °C are the infrared absorbance intensities of Worley and Klotz (1966) corresponding to $\Delta T \sim 12$ and 37 K for 0.463 and 1.789 m $NaClO_4$ in HDO/H_2O solutions at 9.9 °C. These authors also reported $\Delta T = 9$ K for 1.033 m NaBr and $\Delta T = -3$ and -6 K for 0.641 and 2.151 m $(C_4H_9)_4NBr$ in HDO/H_2O solutions at 5.0 °C.

NMR data of Milovidova et al. (1970) of 1 M electrolytes in H_2O at 20 °C agree with infrared ΔT data and are shown in Table 3.4. The concentration and temperature dependences of ΔT do show differences between NMR and infrared results. Those for KI increase more strongly with the concentration in the NMR than in the infrared measurements whereas $d\Delta T/dT < 0$ for $NaClO_4$ in the former but ~ 0 in the latter ones (Milovidova et al. 1970). The temperature dependence $d\Delta T/dT$ (obtained from both infrared and NMR data) was stressed by Abrosimov (1973). It was shown to remain ~ 0 for NaSCN, $NaClO_4$, KSCN, and KNO_3 but to be < 0 for NaCl, KBr, Na_2SO_4 and $(NH_4)_2SO_4$ at 1 M concentration over the temperature range 20–65 °C. In fact, ΔT changes sign from positive to negative for NaCl near 43 °C and for KCl

near 67 °C. Thus, the balance between the structure breaking and structure making properties of the cation and anion, producing the sign and size of ΔT, is quite delicate.

The concept of structural temperature of aqueous electrolytes has more or less been abandoned in recent years.

3.2.3 X-ray Absorption and Scattering

Experimental x-ray absorption spectroscopy (XAS) and x-ray Raman scattering (XRS) at the oxygen K edge are able to probe the electronic structure of water and indirectly its hydrogen bonding structure. XAS is mainly sensitive to donor hydrogen bonds of the water molecules, and its use for elucidation of the structure of pure water has been discussed in Sect. 1.1.3. The absorption spectrum is characterized by a small pre-edge at 535 eV, a main peak around 538 eV and a post-peak (shoulder) near 541 eV. Two groups conducted such measurements, one based in Berkely (Cappa, Saykally, et al.) and the other in Stanford-Stockholm (Näslund, Nilsson, Cavalleri, et al.). The former stressed changes in the electronic structure of the unoccupied orbitals of the water molecules and the latter the hydrogen bonding (free –OH groups characterized by the pre-edge and double hydrogen bonded water molecules in the post-edge) as explanations of the observed results.

Both XAS and XRS have recently been employed in aqueous salt solutions by Näslund et al. (2005), aimed at the direct investigation of the hydrogen bond network. The main absorption or scattering edge is not sensitive to the presence of solutes, but the pre-edge, at 534–537 eV is. The 535 and 536.5 eV peaks are enhanced in 1 m aqueous NaCl and KCl compared with water, and even more so in 4 m KCl. On the contrary, in 2.7 m $AlCl_3$ the absorption at these energies is considerably less that in pure water. The authors attributed the changes in the absorption essentially to the effect of cations, assuming that the chloride anion has little or no effect on the hydrogen bonding of the water. On the basis of their experience with the hydrogen bonded structure of water they concluded that the fraction of single hydrogen bond donor water molecules increased by 2.3 % for KCl and 1.6 % for NaCl, relative to the fraction that exists in pure water. This is equivalent to a significant decrease of the fraction of tetrahedrally coordinated water, i.e., to water structure breaking by K^+ and Na^+.

Similar features in the oxygen K edge XAS have been observed at the same time by Cappa et al. (2005) in 0.8–4.0 M aqueous NaCl, NaBr, and NaI. Little enhancement of the pre-edge at 535 eV was observed for NaCl, but some enhancement of the main-edge at 537.5 eV was recorded for this salt. On the contrary, NaBr and NaI exhibited also appreciable enhancements of the 535 eV pre-edge, increasing in this order. The areas of the resolved pre- and main-edge features increase approximately linearly with the concentration (25 % up to 4 M) whereas those of the post-edge (540.5 eV) decrease similarly (10 % by 4 M) for all three salts. Cappa et al. (2006) proceeded to examine the oxygen K edge XAS of aqueous 2 and 4 M chlorides of Li^+, Na^+, K^+, NH_4^+, $C(NH_2)_3^+$ (guanidinium), Mg^{2+}, and Ca^{2+}. No profound differences

in the x-ray absorption spectra of solutions with different univalent cations were found, whereas the spectra of the divalent cations were quite different. Therefore, the perturbation of the electronic structure of the water leading to changes in the spectrum by the univalent cation salts is predominantly due to the Cl^- anions. This is contrary to the assumption of Näslund et al. (2005) that the chloride anion has little or no effect on the hydrogen bonding of the water. Specifically, since XAS is mainly sensitive to donor hydrogen bonds of the water molecules, these appear not to be differently affected by the rather dissimilar univalent cations: Li^+ is a strong structure-maker and $C(NH_2)_3^+$ is a mild structure-breaker. The divalent cation chloride spectra do not only differ from the univalent salt spectra but also between Mg^{2+} and Ca^{2+}. The surface charge densities, $z/(r/\text{nm})^2$ of Mg^{2+}(386) and Ca^{2+} (200) differ appreciably and differ also from those of the univalent cations Na^+ (96) and K^+ (53) (but not for Li^+ (210!), offering a possible explanation of the observed behaviour.

The two groups of authors cited above have also tackled aqueous HCl solutions (yielding protonated water species) by oxygen K edge XAS. Cappa et al. (2006a) compared the spectra of 2 and 4 m HCl and 4 m NaCl solutions, the latter confirming the earlier results (Näslund et al. 2005; Cappa et al. 2005, 2005), of enhanced pre- and main-edge absorption intensities and decreased post-edge intensities. On the contrary, the HCl spectra showed a diminution of the pre-edge intensity, no effect on the main-edge, and an increase of the post-edge intensity, linearly with the concentration. The formation of (hydrated) H_3O^+ in the HCl solutions counteracts the absorption intensity changes induced by the Cl^- anion. However, no conclusions could be reached concerning whether the protonated water is in the so-called Zundl configuration, $H_5O_2{}^+ = H_2O\cdots H\cdots OH_2$, with a proton shared between two water molecules, or the Eigen one, $H_9O_4{}^+ = O(H\cdots OH_2)_3$, with the central H_3O^+ donating hydrogen bonds to three water molecules. Cavalleri et al. (2006) reported the oxygen K edge XAS of 0.1, 1.0, 4, and 6 M aqueous HCl and found for the two more concentrated solutions results similar to those found by Cappa et al. (2006a): decreased intensity in the pre-edge and enhanced intensity in the post-edge absorption. However, the two more dilute solutions behaved in a different manner, 0.1 M HCl showed enhancement of the pre-edge and the main peak and 1.0 M HCl showed these effects as well as some enhancement of the post-edge. Cavalleri et al. (2006) suggested that in 4 and 6 M HCl the Eigen form predominates, with only one perturbed oxygen atom per proton (that of the central H_3O^+) and a hydrogen bond length of 0.155 nm, whereas in 1.0 M HCl a larger fraction of distorted Zundl forms with two perturbed oxygen atoms per proton and a hydrogen bond length of 0.170 nm exist.

Cappa et al. (2007) have also measured the oxygen K edge XAS of 4 and 6 M aqueous KOH solutions. They found a new spectral feature: a pre-pre-edge at 532.5 eV, attributed to the OH^- anions. The hydrated hydroxide anion shows a strong enhancement of the pre-edge, a strong diminution of the main-edge intensity, and an enhancement of the post-edge with a blue shift of its energy. The behaviour of the hydroxide anion is thus fundamentally different from that of halide anions.

In conclusion it must be said that little *new* insight on the effects of ions on the water structure has been gained by the XAS results. Most of these having been

obtained in rather concentrated solutions (> 1 M) and controversial interpretations between the two groups of researchers still hamper the understanding.

3.3 Evidence from Thermodynamic Quantities

3.3.1 Volumetric Properties

The effects of the ions on the structure of water have certain consequences for the thermodynamic properties of aqueous electrolyte solutions. These had been employed for the deduction of the structural effects already around 70 years ago. Steward (1939) found the rate of variation of the apparent molar volume of salts with their concentration to correspond to the alteration in the minor x-ray diffraction peak of their aqueous solutions. He argued that this indicated a lessening of the fraction of four-coordinated water molecules. Fajans and Johnson (1942) too used the apparent molar volume for the deduction of the water structural effects of ions. They considered that the ions of NH_4Cl, each ion having at 35 °C the same molar volume as a water molecule (18.1 cm^3 mol^{-1}), fit into the water structure without disturbing it. The thermal expansibility of much smaller or larger ions should then indicate the breaking of the water structure. Corey (1943) studied the adiabatic compressibility of salt solutions, finding a remarkable correlation with the corresponding partial molar volume of the water (not of the salt). He concluded that water had a liquid structure that became more highly coordinated and compacted with the introduction of ions.

Some two decades later Hepler (1969) employed the thermal expansion of salt solutions for the classification of ions as structure-makers or -breakers. He argued that positive values of $(\partial^2 V/\partial T^2)_P$ are characteristic of dilute solutions of the lower alcohols in water, known to be structure makers (water structure enhancement by the alcohols was later confirmed also by Marcus (2011a)). Positive values of $(\partial^2 V^\infty(\text{salt})/\partial T^2)_P$ were also quoted for tetraalkylammonium halide solutions, the cations of which again are considered to be water structure makers (more than the opposite effect of the heavier anions). Hence, negative values of $(\partial^2 V^\infty(\text{salt})/\partial T^2)_P$, found inter alia for aqueous LiCl, $MgCl_2$, and $CaCl_2$, should designate these salts as net structure breakers, as the negative values for KCl and CsCl indicate. However, for the former three salts this classification is contrary to all other accounts of their properties (the chloride anions have only small effects on the structure). Therefore, this use of the temperature derivative of the expansibility appears not to be substantiated.

These early studies, however, led to only qualitative views on the effects of individual ions on the structure of water. In a much more recent study Chalikian (2001) applied thermodynamic functions of hydration, in particular the partial molar volume and adiabatic compressibility, to the two-state model of liquid water (Sect. 1.1.3). According to this study, the fraction of high density domains in pure liquid water at 25 °C is 0.27, whereas it is raised to between 0.80 and 0.96 in dilute solutions of the alkali halides, that is, a large amount of (tetrahedral hydrogen bonded) structure breaking takes place. This conclusion is based on undefined ‘properties of water of

hydration' V_h° for which values are given in a table obtained from a misquoted reference, so that they cannot be traced. Within this range this fraction falls from sodium to cesium salts and from chloride to iodide salts for given counter-ions (lithium chloride is out of sequence), but this is counter-intuitive. Therefore, the entire study, as far as it concerns aqueous ions, is not valid.

3.3.2 *Internal Pressure*

The water structure-making and -breaking effects of salts, as obtainable from the internal pressure of their aqueous solutions, was discussed by Dack (1976). The internal pressure, P_i, is defined by the first equality:

$$P_i = \left(\frac{\partial U}{\partial V}\right)_T = T\left(\frac{\partial P}{\partial T}\right)_V - P \approx \frac{T\alpha_P}{\kappa_T} \tag{3.9}$$

and is measured by the thermal pressure coefficient (the second equality), as preferred by Dack (1976), or by the ratio $T\alpha_P/\kappa_T$ of the isobaric expansibility and the isothermal compressibility of the solution (the approximation neglects the vapour pressure or the ambient pressure (≤ 0.1 MPa) compared with the internal pressure (> 100 MPa). Dack argued (Dack 1975) that P_i measures the 'non-chemical interactions', or, in the case of water, the interactions except the hydrogen bonding. Adopting the two-state model of water (Sect. 1.1.3), Dack (1976a) suggested that the breakdown of the large aggregates in water should manifest itself in a greater number of non-chemical interactions and an increased P_i, as is observed when the temperature is raised. His experimental P_i values for 1 M salt solutions at 25 °C, accurate to 4–8 MPa, are shown in Table 3.5.

These values were compared with those of certain non-electrolytes (urea, formamide, acetonitrile, dioxane, and piperidine) that establish the size effect of the solutes as:

$$\frac{P_{i\,vol}}{\text{MPa}} = 190 + 0.509V/\text{cm}^3\,\text{mol}^{-1} \tag{3.10}$$

where $V = V_c$ is the molar volume of the solute, whether a non-electrolyte or a crystalline salt (molar mass divided by the density). The values of $\Delta P_i = P_i(1\,\text{M salt}) - P_{i\,vol}$ were shown in a figure (Dack 1976) to be either positive, for structure-breaking salts, or negative for a few structure-making salts. However, assignment of salts to these categories is problematic, in particular for non-uni-univalent salts, see Table 3.5. The values of P_i are linear with the concentration of the aqueous salt, hence, comparison of multivalent salts at 1 M concentration with uni-univalent ones over-estimates ΔP_i. A (negative) correction for this effect, namely $(P_{i\,W} - P_{i\,salt})/2$, where $P_{i\,W} = 168$ MPa is the internal pressure of water at 25 °C, when applied to ΔP_i in the fourth column of Table 3.5 appears to yield a more acceptable classification of the salts, although some questionable assignments are noted.

Table 3.5 The internal pressures, P_i, at 25 °C of aqueous salt solutions from Dack (1976) (1 M) and Leyendekkers (1983) (1 m), their crystal molar volumes, V_c, the excess internal pressures, ΔP_i, and their stoichiometry-corrected values, $\Delta P_{i\,corr}$

Salt	P_i/MPa	V_c/cm^3 mol^{-1}	ΔP_i/MPa	$\Delta P_{i\,corr}$/MPa
LiCl	187 (194)[a]	20.1	−13 (−6)[a]	
LiI	201 (204)[a]	38.3 (33.0)[b]	−8 (−6)	
Li_2SO_4	242 (251)[a]	49.5	27 (36)[a]	−10 (−1)
NaOH	248	18.8	48	
NaCl	234 (225)[a]	27.0	31 (26)[a]	
NaBr	239	32.1	28	
NaI	226[a]	40.8	15	
NaSCN	218[a]	46.7	5	
$NaClO_4$	226[a]	48.6	12	
Na_2CO_3	311 (299)[a]	41.9	100 (88)[a]	28 (14)
Na_2SO_4	306 (292)[a]	53.0	89 (75)[a]	20 (6)
KCl	229	37.6	21	
KBr	231[a]	43.4	19	
KNO_3	223[a]	47.9	9	
KSCN	226[a]	51.7	10	
$(NH_4)_2SO_4$	242[a]	74.7	14	−23
$(C_2H_5)_4NBr$	246	150	−21	
$MgCl_2$	224[a]	41.0	13	−10
$MgSO_4$	248	45.3	35	−5
$BaCl_2$	281 (270)[a]	54.0	64 (53)[a]	7 (−4)
$CuSO_4$	266	61.9	45	−4
$CdCl_2$	257	45.3	44	0

[a] From Table 3 in (Leyendekkers 1983)
[b] V_c calculated from the density, rather than the entry in (Dack 1976)

Leyendekkers (1983) obtained some additional internal pressure values, estimated according to several models of the solutions, and her P_i values are also included in Table 3.5, from which ΔP_i and $\Delta P_{i\,corr}$ values are derived as described above. In a following paper Leyendekkers (1983a) expressed the internal pressure as a sum of 6 terms:

$$P_i = P_W + P_{vol} + P_{WW} + P_{el} + P_{2c} + P_{ac} \tag{3.11}$$

with the following meanings. P_W is the internal pressure of pure water, P_{vol} is the pressure due to the inert volume of the solute, P_{WW} is the pressure change associated with the electrostatic effect of the change in hydrogen bonding, P_{el} is the pressure associated with the deformation of the water molecules by the ionic charge, P_{2c} is a pressure due to intermolecular energy changes, and P_{ac} is a pressure associated with the relative orientation of the cations and anions and the adjacent water molecules.

Individual ionic values of the terms in Eq. (3.11) are calculated as follows. $P_{vol} + P_{WW} = 1.173$ ($V_{TTG\,i}$/cm^3 mol^{-1}) MPa, where $V_{TTG\,i} = 2520(r_i + \Delta_g + \Delta_{el\,i})^3$ is the Tamman-Tait-Gibson ionic volume (Leyendekkers 1982) with the ionic radius r_i and the additives specified in nm. The geometrical factor $\Delta_g = 0.055$ nm is due to the packing and $\Delta_{el\,i}$ is an electric deformation term. $P_{el} + P_{2c} = -Ck(\Delta_{el\,i} + \Delta_{2c})$

z_i (m_i/mol kg^{-1}) with $Ck = 529$ MPa nm^{-1} and $\Delta_{2c} = 0.08$ nm. Note that in the last expression the algebraic value of the charge z_i is used, and that different signs are obtained for $\Delta_{el\,i}$ of cations (positive) and anions and tetraalkylammonium cations (negative). This causes P_{el} and P_{2c} to have opposite signs. Except P_{ac} all the terms are known and permit the calculation of the ionic contributions to the internal pressure. Values of $V_{TTG\,i}$ are listed (Leyendekkers 1982, 1983a), and $\Delta_{el\,i}$ values can be derived from them by inverting the expression given above. However, P_{ac} can be calculated from tabulated pressure components (Table 1 in (Leyendekkers 1983a): $P_{ac} = P_{Sv} - P_{lr} + P_{Born}$). With this analysis, Dack's ΔP_i should equal $P_i - (P_{vol} + P_{WW} + P_W) = P_{el} + P_{2c} + P_{ac}$, but this yields positive values for all cations (except Al^{3+}) and negative ones for all anions, with no bearing on their water structure effects.

A more direct correlation with such effects is obtained from the NMR chemical shifts of the water protons, δ_i, of 1 m cations at 25 °C according to Davies et al. (1971). Negative values of δ_i were obtained for Li^+, alkaline earth metal ions, and Al^{3+} whereas the other alkali metal cations have positive values. These are correlated with two terms in Eq. (3.11), namely as:

$$\frac{\delta_i}{\text{ppm}} = 4.215 \times 10^{-3} \left(\frac{P_{el}}{\text{MPa}}\right) + (2.11 \pm 0.35) \times 10^{-3} \left(\frac{P_{2c}}{\text{MPa}}\right) \tag{3.12}$$

The range of the coefficient of P_{2c} is due to that of the number of water molecules in the second hydration sphere of the cations. The opposite signs of P_{el} and P_{2c} and their partial compensation then produce the observed signs of δ_i, in agreement with the water structure-making and -breaking properties of the cations. For the anions the correlation is:

$$\frac{\delta_i}{\text{ppm}} = c \times 10^{-3} \left(\frac{P_{WW}}{\text{MPa}}\right) \tag{3.13}$$

with $c = 2.33$ for the halides and SCN^- and $c = 0.70$ for oxyanions. The values of P_{WW} were tabulated (Table 2 in Leyendekkers 1983a) and the resulting calculated δ_i have the expected signs for water structure-making and –breaking anions due to the signs of P_{WW}.

3.3.3 *Structural Entropy*

Frank and Robinson (1940) suggested that the partial molar entropy of the water in aqueous electrolyte solutions is affected by the structure-making or -breaking properties of their ions. Frank and Evans (1945) suggested that rather the entropies of hydration of the ions shed light on these properties. Gurney (1953) showed that a linear relationship exists between the partial molar entropy of monatomic ions, S_i^∞, and their viscosity B_η coefficients (see Sect. 3.1.1). Nightingale (1959) reverted to the Frank and Evans emphasize of partial molar entropies of *hydration* of the

ions, $\Delta_{hydr}S_i^{\infty}$, in that these exclude vibrational and rotational contributions to the entropies of the ions themselves, so that their relationship to the B_η coefficients may be generalized to polyatomic ions. These and the following considerations, using standard molar entropies, pertain to ions at infinite dilution in water.

The standard molar entropy of hydration of an ion, $\Delta_{hydr}S^{\infty}$, should contain contributions from the formation of the ionic hydration shell and also from the limitation of the ionic rotation of a multiatomic ion in the solution compared with the gas. Hence, such contributions should be deducted, according to Krestov (1962, 1962a), from $\Delta_{hydr}S^{\infty}$ in order to obtain the water structural effects of the ion beyond the hydration shell, $\Delta_{struc}S$ (ΔS_{II} in the notation of Krestov):

$$\Delta_{struc}S = \Delta_{hydr}S^{\infty} - 0.615S^{\circ}{}_{transl} - \eta S_{rot} \tag{3.14}$$

The hydration shell formation was estimated from the translational entropy loss, $0.615S^{\circ}{}_{transl}$, of inert gas atoms isoelectronic with monatomic ions on dissolution in water, but $0 \leq \eta \leq 1$ was an unknown numerical coefficient. Tables of values of $\Delta_{struc}S$ for many cations and anions, based on $S^{\infty}(H^+, aq) = -8.8$ J K^{-1} mol^{-1}, were shown in Krestov's book (Krestov 1991).

There are errors in this book: the reported signs of the $\Delta_{struc}S$ values for K^+, Rb^+, Tl^+, Br^- and At^- are negative instead of positive and the numerical value for Te^{2-}, -433.1, should be -33.1 instead. Furthermore, the value $S^{\infty}(H^+, aq) = -8.8$ J K^{-1} mol^{-1}, on which the reported data are based, is not acceptable and should be replaced by the more probably valid $S^{\infty}(H^+, aq) = -22.2$ J K^{-1} mol^{-1} (Sect. 2.2.5). This adjustment would change the values by $-13.4z$ units, where z is the charge number of the ion. Positive values of $\Delta_{struc}S$ resulting for K^+, Rb^+, Cs^+, Tl^+, Cl^-, Br^-, I^-, At^- and Po^{2-} among monatomic ions imply water structure breaking properties. Positive values are also shown (Krestov 1991) for many multiatomic ions, but the last term in Eq. (3.14) has been ignored in their derivation. The linear correlation: $B_\eta = 0.011 - 0.007\ \Delta_{struc}S$ resulted from Krestov's data.

Positive values of $\Delta_{struc}S$ at lower temperatures change over the temperature range 15–65 °C to negative ones at a characteristic temperature, called the limiting temperature (Krestov and Abrosimov 1964; Krestov 1991). The decreasing inherent structure of the water as the temperature is raised (Sect. 1.1.2 and Table 1.6) was offered as an explanation for the decrease in the structure breaking effect of those ions that do so at the lower temperatures and the eventual change of sign, signifying structure making properties at the higher temperatures.

The structural entropy according to Krestov (1991) was compared by Collins (1997) to the entropy of pure water, and $\Delta S = \Delta_{struc}S - S^*(H_2O)$ was plotted against the ionic radius for the alkali metal and halide ions. Those with $\Delta S < 0$ have large surface charge densities and are called kosmotropes (water structure making) whereas those with $\Delta S > 0$ have small surface charge densities and are chaotropes (water structure breaking). This view stresses the competition between the water-water interactions and the ion-water ones, an approach that has been proposed by others much earlier, e.g., by Diamond (1958).

Abraham et al. (Abraham and Liszi 1978; Abraham et al. 1982) derived in a different manner that part of $\Delta_{hydr}S^{\infty}$ that is relevant to the effects of the ions on

the structure of the water, $\Delta_{\text{struc}}S$ (the notation used was $\Delta S_{\text{I,II}}$, with a calculation involving two hydration layers). The contributions of a neutral part, ΔS_{n}, and of the bulk water dielectric effect ΔS_{el}, were deducted from $\Delta_{\text{hydr}}S^{\infty}$. The former were equated with the values for non-polar solutes of sizes (radii) similar to those of the ions: $\Delta S_{\text{n}} = 5.0 + 291(r_{\text{I}}/\text{nm})\ \text{J K}^{-1}\ \text{mol}^{-1}$, to be compare with the term $0.615 S^{\circ}_{\text{transl}}$ in Eq. (3.14)· The bulk water dielectric effect beyond the distance of one water molecular diameter, d_{W}, from the surface of the bare ion, i.e., beyond the first hydration shell, was calculated according to the Born expression,:

$$\Delta S_{\text{el}} = \left(\frac{N_{\text{A}}e^2}{8\pi\varepsilon_0}\right) z^2 (r + d_{\text{W}})^{-1} \varepsilon_{\text{r}}{}^{-1} \left(\frac{\partial \ln \varepsilon_{\text{r}}}{\partial T}\right)_P \tag{3.15}$$

The unusual mole fraction scale for the solution, with $S^{\infty}{}_{\text{x}}(\text{H}^+, \text{aq}) = -68.2\ \text{J K}^{-1}\ \text{mol}^{-1}$, was used for the calculation of values of $\Delta_{\text{struc}}S$ for the alkali metal and halide ions as well as Ag^+ and ClO_4^- (Abraham et al. 1982). However, the choices of the value of $S^{\infty}(\text{H}^+, \text{aq})$ and the mole fraction scale caused K^+ to appear as a structure making ion. This unacceptable result is corrected by adjustment to the molar scale with $S^{\infty}(\text{H}^+, \text{aq}) = -22.2\ \text{J K}^{-1}\ \text{mol}^{-1}$. Linear correlations of $\Delta_{\text{struc}}S$ with the viscosity B_{η} coefficients and with the NMR B_{nmr} coefficients (Sect. 3.1.3) and also with the ionic partial molar volumes or their electrostricted volumes were noted by Abraham et al. (1982).

Yet another model for obtaining $\Delta_{\text{struc}}S$ values from $\Delta_{\text{hydr}}S^{\infty}$ ones was suggested by Marcus and Loewenschuss (1985) and Marcus (1986). An irrelevant entropy of compression of $\Delta_{\text{comp}}S = -26.7\ \text{J K}^{-1}\ \text{mol}^{-1}$ is included in the absolute $\Delta_{\text{hydr}}S^{\infty}$ values, based on $S^{\infty}(\text{H}^+, \text{aq}) = -22.2\ \text{J K}^{-1}\ \text{mol}^{-1}$ using the standard state of 0.1 MPa for the ideal gaseous ions and 1 M for the aqueous ones. The electrostatic effect beyond the first hydration shell is: $\Delta S_{\text{el}} = (N_{\text{A}}e^2/8\pi\varepsilon_0) z^2 (r_{\text{i}} + d_{\text{W}})^{-1} \varepsilon_{\text{r}}{}^{-1} (\partial \ln \varepsilon_{\text{r}}/\partial T)_P$ from the Born expression, as in Eq. (3.15). However, the h water molecules within this hydration shell are translationally immobilized with a reduction of their entropy. This contribution to $\Delta_{\text{hydr}}S^{\infty}$ is:

$$\Delta_{\text{tr im}}S(\text{X}^z) = 1.5R \ln \left(\frac{M(\text{X}(\text{H}_2\text{O})_h)}{M(\text{X})}\right) - 26.0 h_{\text{I}} \tag{3.16}$$

The first term denotes the change of translational entropy due to the larger mass (M) of the hydrated ion and 26.0 is the molar translational entropy of water in its liquid form, that does not pertain to the water structural effects (Marcus 1986). On the supposition that sodium ions are indifferent with respect to the water structure-making and -breaking:

$$\Delta_{\text{struc}}S(\text{Na}^+) = \Delta_{\text{hydr}}S^{\infty}(\text{Na}^+) - \Delta_{\text{comp}}S - \Delta S_{\text{el}}(\text{Na}^+) - \Delta_{\text{tr im}}S(\text{Na}^+) = 0 \tag{3.17}$$

the value of h was obtained as $h_{\text{I}} = A|z|/(r_{\text{I}}/\text{nm})$ with $A = 0.355$. The assignments of ions to structure-making and -breaking categories conformed to those by other methods, such as the signs of B_{η} and B_{nmr}.

A subsequent development by Marcus (1994) of this concept for $\Delta_{\text{struc}}S$ is based on a model common for various thermodynamic functions of ion hydration (Marcus 1987) (Sect. 2.3.4). The width Δr_{I} of the electrostricted hydration shell is the key quantity of this model. The water molecules in this shell have a volume $\pi {d_{\text{W}}}^3/6$ each rather than $V_{\text{W}}/N_{\text{A}}$, that is, they are fully compacted, and $d_{\text{W}} = 0.276$ nm is the diameter of a water molecule. The value of Δr is obtained from the volume of the hydration shell with h_{I} water molecules:

$$\left(\frac{4\pi}{3}\right)\left((r_{\text{I}} + \Delta r_{\text{I}})^3 - {r_{\text{I}}}^3\right) = \frac{h_{\text{I}}\pi\, {d_{\text{W}}}^3}{6} \tag{3.18}$$

Here, as before, $h_{\text{I}} = A|z|/(r_{\text{I}}/\text{nm})$ with $A = 0.36$ (it is slightly different from the value 0.355 resulting from Eq. (3.17)).

The entropic effects of the creation of a cavity in the water to accommodate the ion (similar to ΔS_{n} in (Abraham et al. 1982)) and of the compression from the gas to the solution (similar to $\Delta_{\text{comp}}S$ in (Marcus 1986)) are taken care of together in a neutral term, ΔS_{nt}. It is calculated from the entropies of hydration of small neutral molecules or rare gas atoms, interpolated for a radius r_{I} the same as that of the ion: $\Delta S_{\text{nt}} = -3 - 600(r_{\text{I}}/\text{nm})\ \text{J K}^{-1}\ \text{mol}^{-1}$. In the electrostricted hydration shell the permittivity and its temperature derivative are assumed to have the infinitely large field values. Using for this purpose n_{D}, the refractive index of water at the sodium D line, $\varepsilon' = {n_{\text{D}}}^2 = 1.776$ and $(\partial\varepsilon'/\partial T)_P = 2(\partial n_{\text{D}}/\partial T)_P = -1 \times 10^{-4}\ \text{K}^{-1}$ (at 298.15 K). Then, in analogy with Eq. (3.15), the electrostatic entropic effect in this shell is:

$$\Delta S_{\text{el}\,1} = \left(\frac{N_{\text{A}}e^2}{8\pi\varepsilon_0}\right) z^2 \left(\Delta r(r + \Delta r)^{-1}\right) {\varepsilon'}^{-2} \left(\frac{\partial\varepsilon'}{\partial T}\right)_P \tag{3.19}$$

In the water layer beyond this shell the entropic effect is:

$$\Delta S_{\text{el}\,2} = \left(\frac{N_{\text{A}}e^2}{8\pi\varepsilon_0}\right) z^2 (r + \Delta r)^{-1} {\varepsilon_{\text{r}}}^{-2} \left(\frac{\partial\varepsilon_{\text{r}}}{\partial T}\right)_P \tag{3.20}$$

The structural entropy is then obtained from:

$$\Delta_{\text{struc}}S = \Delta_{\text{hydr}}S^{\infty} - (\Delta S_{\text{nt}} + \Delta S_{\text{el}\,1} + \Delta S_{\text{el}\,2}) \tag{3.21}$$

Cumulative errors incurred in such calculations mean that only values of $\Delta_{\text{struc}}S(\text{X}^z) > 20\ \text{J K}^{-1}\ \text{mol}^{-1}$ indicate that the ion X^z is definitely water structure-breaking and only values $< -20\ \text{J K}^{-1}\ \text{mol}^{-1}$ indicate it to be structure-making. In between values designate the ions to be borderline cases. This treatment could be applied to nearly 150 aqueous cations and anions, monatomic and polyatomic, with charges $-4 \le z_{\text{I}} \le 4$. The linear correlation with the viscosity B_η (except for tetraalkylammonium cations) is:

$$\Delta_{\text{struc}}S/\text{J K}^{-1}\ \text{mol}^{-1} = 20({z_{\text{I}}}^2 + |z_{\text{I}}|) - 605(B_\eta/\text{dm}^3\text{mol}^{-1}) \tag{3.22}$$

Table 3.6 Water structural entropy $\Delta_{struc}S$/J K^{-1} mol^{-1} and heat capacity $\Delta_{struc}C_P$/J K^{-1} mol^{-1} effects of representative ions according to three treatments. Adapted from (Marcus 2009) with kind permission of ©The American Chemical Society

Ion	Krestov (1962, 1991) $\Delta_{struc}S$	Abraham et al. (1982) $\Delta_{struc}S$	Marcus (1994)	
			$\Delta_{struc}S$	$\Delta_{struc}C_P$
Li^+	−69	−81	−52	147
Na^+	−19	−27	−14	83
K^+	21	40	47	0
Rb^+	39	50	52	−38
Cs^+	46	76	68	−83
Ag^+	−13	−20	−15	47
NH_4^+	−8[a]		5	28
Me_4N^+			41	−30
Ca^{2+}	−159		−59	215
La^{3+}	−300		−113	355
F^-	−57	−87	−27	20
Cl^-	20	−2	58	−62
Br^-	41	21	81	−88
I^-	68	52	117	−113
OH^-			−51	−187
NO_3^-	23		66	−59
SCN^-			83	−33
ClO_4-	44[a]	68	107	−87
$CH_3CO_2^-$			−32	−138
CO_3^{2-}	−160[a]		−52	68
SO_4^{2-}	−100[a]		8	−14
PO_4^{3-}	−319[a]		−131	103

[a]The contribution from hindered rotation, Eq. (3.14), could not be explicitly included in the $\Delta_{struc}S$ of the polyatomic ions

Values of $\Delta_{struc}S$ of representative ions, adjusted where applicable to the molar scale for $\Delta_{hydr}S^\infty$ and based on their absolute values with $S^\infty(H^+, aq) = -22.2$ J K^{-1} mol^{-1}. obtained according to the treatments of Krestov (1962) as reported in (Krestov 1991), Abraham et al. (1982), and Marcus (1994) are shown in Table 3.6, adopted from (Marcus 2009). The values of $\Delta_{struc}S$ are positive for large ions of low charge and negative for highly charged small ions.

The same model (Marcus 1987), but dealing with the structural heat capacity, $\Delta_{struc}C_P$, was also presented by Marcus (1994). Here C_P replaced S in Eqs. (3.19) to (3.21), and $\Delta C_{P\,nt} = -48 + 1380(r_I/\text{nm})$ J K^{-1} mol^{-1} on the same basis as before. The expressions $T(\partial^2\varepsilon'/\partial T^2)_P$ and $T(\partial^2\varepsilon_r/\partial T^2)_P$ replaced the corresponding factors in Eqs. (3.19) and (3.20). Due to the choice of $C_P{}^\infty(H^+, aq) = -71$ J K^{-1} mol^{-1} (Marcus 1994), a negative bias occurred in $\Delta_{struc}C_P$ calculated in this manner. In order to show the structure-making and -breaking properties of the ions, $175z_I$ J K^{-1} mol^{-1} were added to yield the values shown in Table 3.6, with positive values for structure making ions and negative ones for structure breaking ones, but allowing for a wide borderline region of ± 60 J K^{-1} mol^{-1}.

3.3.4 Transfer from Light to Heavy Water

In principle, the best estimation of the effects of ions on the structure of water is in terms of the changes in the average number of hydrogen bonds that characterize this structure (Sect. 1.1.3). According to Ben-Naim (1975), the pair potential between water molecules is written as a sum of two terms: one that describes the short range (repulsion) and long range (multipole) interactions and another that describes the hydrogen bonding. The latter is the product of the hydrogen bond energy e_{HB} and the geometrical factor $0 \leq G_{HB} \leq 1$, specifying whether a hydrogen bond exists or not. The difference in the standard chemical potentials $\Delta\mu_S{}^{\infty\,HD}$ of a solute particle S introduced into H_2O and into D_2O depends solely on changes in the hydrogen bonding structure of the water. This is based on the very similar properties of molecules of these two kinds of water with respect to solute-solvent interactions (Table 2.1). This difference can therefore be written as:

$$\Delta\mu_S{}^{\infty\,HD} = \Delta^{HD}e_{HB} \cdot \Delta G_{HB} \tag{3.23}$$

Here $\Delta^{HD}e_{HB}$ is the difference in the strengths of the hydrogen bonds in D_2O and H_2O and ΔG_{HB} is the change caused by the introduction of a particle of S in the average geometrical factors over all the configurations of the N water molecules of either kind:

$$\Delta G_{HB} = \left(\frac{2}{N}\right)\left(< \sum\nolimits_N G_{HB} >_S - < \sum\nolimits_N G_{HB} >_0\right) \tag{3.24}$$

Experimentally measurable quantities, such as solubilities, EMF data, etc., yield $\Delta\mu_S{}^{\infty\,HD}$ of Eq. (3.23) and the sublimation enthalpies of the D_2O and H_2O ices yield $\Delta^{HD}e_{HB}$ values. Hence, ΔG_{HB}, the effect of the solute S on the (hydrogen bonded) structure of water, can be determined. Non-ionic solutes, such as argon or methane, have positive values of ΔG_{HB} (Ben-Naim 1975) and are known from several approaches to enhance the structure of water, diminishing with increasing temperatures. This is expected from the structure of water being diminished in this direction (Table 1.6).

Marcus and Ben-Naim (1985) applied this approach to ionic solutes S. Unfortunately, the $\Delta\mu_S{}^{\infty HD}$ data for electrolytes are rather unsatisfactory and there are no definite data for ascribing $\Delta\mu_S{}^{\infty HD}$ to individual ions. The available $\Delta\mu_S{}^{\infty HD}$ values for various electrolytes are small and are comparable to their uncertainties, even in a recent electrochemical study (Gulaboski et al 2004). The 'best' available $\Delta\mu_S{}^{\infty HD}$/ J mol^{-1} values at 25 °C range from −950 for Bu_4N^+ to 1200 for Ba^{2+} with probable errors of ±100, as summarized by Marcus (2008). According to Eq. (2.11) a rather wide range is provided for $\Delta^{HD}e_{HB}$, but the value $\Delta^{HD}e_{HB} = -929$ J mol^{-1} has been previously employed (Marcus 1986, 1994, 2008). For the nine alkali metal and halide ions the values of $\Delta\mu_S{}^{\infty HD}$ are established better than for other ions, based on the assumption that they are equal for K^+ and Cl^-. Incidentally, this assumption also equalizes the values for $Ph_4\,As^+$ and $BPh_4{}^-$, for which no preference for hydration by H_2O or D_2O is expected. The ratios $\Delta G_{HB} = \Delta\mu_S{}^{\infty HD}/\Delta^{HD}e_{HB}$ are according to

Table 3.7 Ions arranged according to their effects on the structure of water at infinite dilution. Reproduced from (Marcus 2009) with kind permission of ©The American Chemical Society

Ions	ΔG_{HB}
Structure breaking ions	
I^-, I_3^-, ClO_4^-, BrO_4^-, IO_4^-, MnO_4^-, TcO_4^-, ReO_4^-, $AuCl_4^-$, $Ag(CN)_2^-$, $Au(CN)_2^-$, $S_2O_8^{2-}$, $S_4O_6^{2-}$, $Cr_2O_7^{2-}$, $PdCl_6^{2-}$, $PtCl_6^{2-}$, $Fe(CN)_6^{3-}$, $Co(CN)_6^{3-}$, $Fe(CN)_6^{4-}$	≤ -1.1
Br^-, Br_3^-, SCN^-, BF_4^-, SiF_6^{2-}	-1.1 to -0.9
K^+, Rb^+, Cs^+, Tl^+, Cl^-, SH^-, CN^-, N_3^-, OCN^-, NO_2^-, NO_3^-, ClO_3^-, $Al(OH)^-$, S^{2-}, Se^{2-}, $S_2O_6^{2-}$	-0.9 to -0.7
$CH_3NH_3^+$, $(CH_3)_4N^+$, Ra^{2+}, she^-, HF_2^-, ClO_2^-, BrO_3^-, HCO_2^-, HSO_3^-, HSO_4^-, SeO_4^{2-}, CrO_4^{2-}, $S_2O_3^{2-}$, $S_2O_4^{2-}$, $P_2O_7^{4-}$	-0.7 to -0.4
NH_4^+, $B(OH)_4^-$, SO_4^{2-}, MoO_4^{2-}, WO_4^{2-}, $C_2O_4^{2-}$	-0.4 to -0.1
Borderline ions	
Na^+, Ag^+, $(C_2H_5)_4N^+$, Ba^{2+}, Pb^{2+}, F^-, IO_3^-, HCO_3^-, $H_2PO_4^-$	$-0.1-0.1$
Structure making ions	
Li^+, Cu^+, Au^+, $(C_6H_5)_4As^+$, Sr^{2+}, Sn^{2+}, Al^{3+}, Cr^{3+}, Bi^{3+}, OH^-, $CH_3CO_2^-$, $B(C_6H_5)_4^-$, CO_3^{2-}, SO_3^{2-}	0.1–0.4
Ca^{2+}, Eu^{2+}, Hg_2^{2+}, Sc^{3+}, Co^{3+}, Tl^{3+}, Pu^{4+}, HPO_4^{2-}	0.4–0.7
$(C_3H_7)_4N^+$, V^{2+}, Cr^{2+}, Mn^{2+}, Cu^{2+}, Cd^{2+}, Sm^{2+}, Yb^{2+}, Gd^{3+}, V^{3+}, Fe^{3+}, Ga^{3+}, Rh^{3+}, U^{3+}, Pu^{3+}, AsO_4^{3-}	0.7–0.9
Mg^{2+}, Co^{2+}, Ni^{2+}, Zn^{2+}, Y^{3+}, La^{3+} to Eu^{3+}, Tb^{3+} to Lu^{3+}, Th^{4+}, U^{4+}, PO_4^{3-}	0.9–1.1
$(C_4H_9)_4N^+$, Fe^{2+}, UO_2^{2+}	≥ 1.1

Eq. (3.23) the geometrical hydrogen bonding parameters for the ions that describe their effects on the structure of the water. These may be taken for correlations with other quantities that describe the water structural effects of ions that are better established, such as B_η and $\Delta_{struc}S$. The resulting expressions, calculated with $\Delta^{HD}e_{HB} = -929$ J mol^{-1} are:

$$\Delta G_{HB} = -(0.54 \pm 0.11) + (4.75 \pm 1.39)(B_\eta/M^{-1}) \tag{3.25}$$

and

$$\Delta G_{HB} = -(0.14 \pm 0.06) - (8.16 \pm 1.01) \times 10^{-3}(\Delta S_{struc}/JK^{-1}mol^{-1}) \tag{3.26}$$

with standard errors of the fits of 0.2 units. Values of ΔG_{HB} can be generated by means of Eqs. (3.25) and (3.26) for a large number of ions, which do not describe, of course, the ionic water structural effects any better than the viscosity B_η coefficient and the structural entropy ΔS_{struc}, themselves. They do have the theoretical basis in terms of the effect on the extent of hydrogen bonding in the dilute solution that was provided by Ben-Naim (1975). The water structure effects of ions according to this criterion are shown in Table 3.7.

3.3.5 *Other Thermodynamic Evidence*

A comparison of the activity coefficient of water in aqueous electrolytes on the molar scale: $y_W = a_W/c_W$ with that of pure water: $1/55.51 = 0.0180$, was suggested by Dutkiewicz and Jakubowska (2002) to indicate the structure-making or -breaking effects of the ions. They obtained the data at fairly high concentrations, up to 2 M, in a round-about manner from the hydration of aldehydes. They assumed that Cl^- anions have a negligible effect on the structure of the water, and concluded that Na^+, NH_4^+, and Mg^{2+} are structure making, and K^+ and ClO_4^- are structure breaking. This conclusion does not produce any new insight.

A more refined examination of the water activity can be made (Marcus 2011) by a comparison of the osmotic coefficient φ at two electrolyte concentrations: $\Delta\varphi = \varphi(0.4\,\text{m}) - \varphi(0.2\,\text{m})$ at 25 °C, the values being taken from (Robinson and Stokes 1959). A combination of structure-making cations with structure breaking anions yields $\Delta\varphi > 0$ whereas structure-breaking cations combined with structure-making anions yields $\Delta\varphi < 0$. Other combinations lead to very small $\Delta\varphi$ values. Salts of multivalent cations have $\Delta\varphi > 0$ even with structure-breaking anions such as I^- or ClO_4^-. Salts of a multivalent anion, SO_4^{2-}, have $\Delta\varphi < 0$ even for multivalent, structure-making cations such as Mg^{2+} and Zn^{2+}. Such observations, however, do not provide more insight into the inherent properties of the ions with respect to their effects on the structure of water.

3.4 Computer Simulations of Structural Ionic Effects

Since the mid-1990s computer simulations have been directed at the elucidation of the effects of ions on the structure of the water in their aqueous solutions. They have several advantages over the many other methods: they consider individual ions and they can be applied to quite dilute solutions (water-to-ion ratios up to 500:1 in typical cases, corresponding to ~ 0.1 M solutions). A further advantage of such simulations is that their duration is on the ps time scale, before a reaction such as the hydrolysis of multivalent cations can take place, so that their hydration can be studied. However, in some cases sufficiently long simulation times were employed that described also the rate of the hydrolysis process, as, for example, for As(III) (Bhattacharjee et al. 2009a) and the group IV cations (Lim et al. 2010b). Computer simulations have often been applied in conjunction with diffraction studies in order to model the structures properly. The merits and disadvantages of the various computational methods employed cannot be discussed fully here. There are several potential functions for water, rigid and polarizable, that have been used: SPC and its extended form, SPC/E, as well as TIP3P and TIP4P among others. Classical molecular dynamics (MD) has been criticized for ignoring many-body interactions. Semi-empirical methods based on density functional theory also differ with respect to the functional used, e.g., Car-Parrinello, BP86, or B3LYP. Quantum mechanical simulations employed different levels of theory and base, e.g. Hartree-Fock *ab initio* or various approximations.

In a relatively early study, the ST2-water model was used by Szasz et al. (1981) with only 25 water molecules/pair of charged particles, Li^+I^- to study the hydration structure around these ions. Heinzinger's group subsequently studied other electrolytes by MD simulations (Heinzinger 1985; Heinzinger and Palinkas 1987) with the ST2 and later with more advanced water potential models (Kiselev et al. 1993; Heinzinger and Schäfer 1999). Monte Carlo simulations by Bernal-Uruchurtu and Ortega-Blake (Bernal-Uruchurtu and Ortega-Blake 1995) of Mg^{2+} at water-to-ion ratios up to 480:1 showed a well-formed second hydration shell, the water molecules being oriented not only by those in the first shell but also by those outside it. This is an indication of the presence of a third hydration shell, demonstrating the structure-making properties of this small doubly charged ion.

The major advance in this field resulted from the application by Rode and his group in Innsbruck since the late 1990s of quantum mechanical calculations to the first hydration shell (eventually also the second) and molecular mechanics calculations to the water beyond this shell, with attention paid to the interface between these regions. Their methods developed over the years to more and more sophisticated application of this basic approach. The results of the simulations are pair correlation functions involving the relevant atoms, g(X-O, r), g(X-H, r), g(O-O, r), g(O-H, r), and g(H-H, r), where X is the ion under investigation. From these functions inter-atomic distances and angles between groups of three atoms can be deduced, hence the structure of the water in the vicinity of the ion X. Further information from this approach include coordination numbers, vibrational and librational frequencies of the water molecules near the ion, strength (energy) of the water binding by the ion, and the dynamic aspects of the water molecule rotations and exchange between the hydration shell and the bulk water, already discussed fully in Sect. 3.1.6. These dynamics results show clearly the structure-making properties of multi-valent ions, both cations and anions, in that the exchange rate is retarded relative to water molecules exchanging positions in bulk water. Therefore, here the static evidence from the simulations concerning structure-breaking ions is mostly dealt with.

In an earlier paper Tongraar et al. (1998) showed that the configuration of the water molecules around Na^+ is due to the ability of this cation to order the structure of water molecules in its surroundings to a considerable extent and that this effect still finds some continuation beyond the first hydration shell, so that it is a structure-making ion. On the contrary, in the case of K^+ the unfavourable arrangement of a large portion of first-shell water molecules permits to regard the insertion of the ion as a perturbation of the hydrogen bond network structure, so that it is a structure-breaking ion. The hydration of these two ions was later re-considered by Azam et al. (2009) by means of the more sophisticated quantum mechanical charge field method and confirmed the earlier results, but stressed the dynamics of the water exchange.

In the case of Rb^+, the angular distribution functions showed a high degree of flexibility and a distorted hydration structure based on the large ionic radius and the low surface charge density, and is thus typical for structure breaking ions (Hofer et al. 2005). The g(O-O, r) functions for Cs^+ give clear indication for its structure breaking behaviour: the broad asymmetrical first-shell peak, the very flat but recognizable second shell, and numerous small inter-shell peaks, all typical for a very flexible

and irregular structure (Schwenk et al. 2004). The univalent gold ion, Au^+, features a broad distribution of coordination numbers of the first hydration shell and a very bulky second hydration shell that represents a far-reaching perturbation of the water structure (Armunanto et al. 2004), leading to a quite specific picture of a structure breaking effect. Finally, for Tl^+ too a second hydration shell exists, which is not the case for both K^+ and Cs^+, and this shell enables the structure-breaking effects to be extended beyond the first shell and thus to influence a larger space within the solution. It was deemed the strongest structure breaking cation in water (Vchirawongwin 2007).

Among the anions a study of F^- and Cl^- (Tongraar and Rode 2003) showed a preference for linear hydrogen bonds between F^- and water molecules in the first hydration shell, compared with no preference between linear and bridging hydrogen bonds in the case of Cl^-. A fluoride anion clearly forms its own framework of hydrogen bonds and is a structure maker, whereas Cl^- perturbs the solvent hydrogen bond network in its neighborhood without creating a specific new order and is a mild structure breaker (Tongraar and Rode 2005). In the case of I^-, the observed broad distribution of the $I^- \cdots H{-}O$ angle clearly indicates the flexibility of the weak iodide-water hydrogen bonds. The shape and height of the g(O-O, r) and g(O-H, r) reflect well the "structure-breaking" behavior of this anion (Tongraar et al. 2010).

For more quantitative information concerning the water structure making and breaking of these and other ions obtainable from the quantum mechanical/molecular mechanical computer simulations see Sect. 3.1.6.

References

Abraham MH, Liszi J (1978) Calculations on ionic solvation. Part 2. entropies of solvation of gaseous univalent ions using a one-layer continuum model. J Chem Soc Faraday Trans 1 74:2858–2867

Abraham MH, Liszi J, Papp E (1982) Calculations on ionic solvation. Part 6. Structure-making and structure-breaking effects of alkali halide ions from electrostatic entropies of solvation: correlation with viscosity B-coefficients, nuclear magnetic resonance B′-coefficients, and partial molal volumes. J Chem Soc Faraday Trans 78:197–211

Abrosimov VK (1973) The connection between the structural and the limiting temperature of aqueous solutions of electrolytes. Russ J Struct Chem 14:133–135 (Zh Strukt Khim 14:154–156)

Armunanto R, Schwenk CF, Rode BM (2003) Structure and dynamics of hydrated Ag (I): ab initio quantum mechanical-molecular mechanical molecular dynamics simulation. J Phys Chem A 107:3132–3138

Armunanto R, Schwenk CF, Tran HT, Rode BM (2004) Structure and dynamics of Au^+ ion in aqueous solution: ab initio QM/MM MD simulations. J Am Chem Soc 126:2582–2587

Asaki MLT, Redondo A, Zawodzinski TA, Taylor AJ (2002) Dielectric relaxation of electrolyte solutions using terahertz transmission spectroscopy. J Chem Phys 116:8469–8482

Azam SS, Hofer TS, Randolf BR, Rode BM (2009a) Hydration of sodium(I) and potassium(I) revisited: a comparative QM/MM and QMCF MD simulation study of weakly hydrated ions. J Phys Chem A 113:1827–1834

Azam SS, Hofer TS, Bhattacharjee A, Lim LHV, Pribil AB, Randolf BR, Rode BM (2009) Beryllium(II): the strongest structure-forming ion in water? A QMCF MD simulation study. J Phys Chem B 113:9289–9295

Azam SS, Lin LHV, Hofer TS, Randolf BR, Rode BM (2010) Hydrated germanium (II): Irregular structural and dynamical properties revealed by a quantum mechanical charge field molecular dynamics study. J Comput Chem 31:278–285

Bakker HJ (2008) Structual dynamics of aqueous salt solutions. Chem Rev 108:1456–1473

Bakker HJ, Kropman MF, Omta AW (2005) Effect of ions on the structure and dynamics of liquid water. J Phys Condens Matter 17:S3215–S3224

Balbuena PB, Johnston KP, Rossky PJ, Hyun J-K (1998) Aqueous ion transport properties and water reorientation dynamics from ambient to supercritical conditions. J Phys Chem B 102:3806–3814

Barthel J, Buchner R, Eberspächer P-N, Münsterer M, Stauber J, Wurm B (1998) Dielectric relaxation spectroscopy of electrolyte solutions. recent developments and prospects. J Mol Liq 78:83–109

Ben-Naim A (1975) Structure-breaking and structure-promoting processes in aqueous solutions. J Phys Chem 79:1268–1274

Bernal JD, Fowler RH (1933) A theory of water and ionic solution, with particular reference to hydrogen and hydroxyl ions. J Chem Phys 1:515–548

Bernal-Uruchurtu MI, Ortega-Blake I (1995) A refined Monte Carlo study of Mg^{2+} and Ca^{2+} hydration. J Chem Phys 103:1588–1598

Bhattacharjee A, Hofer TS, Pribil AB, Randolf BR, Lim LHV, Lichtenberger AF, Rode BM (2009) Revisiting the hydration of Pb(II): a QMCF MD approach. J Phys Chem B 113:13007–13013

Bhattacharjee A, Hofer TS, Pribil AB, Randolf BR, Rode BM (2009a) Hydrolysis of As(III): a femtosecond process. Chem Phys Lett 473:176–178

Bhattacharjee A, Pribil AB, Lim LHV, Hofer TS, Randolf BR, Rode BM (2010) Structural and dynamic aspects of hydration of $HAsO_4^{-2}$: An *ab initio* QMCF MD simulation. J Phys Chem B 114:3921–3926

Blauth M, Pribil AB, Randolf BR, Rode BM, Hofer TS (2010) Structure and dynamics of hydrated Ag^{+}: an ab initio quantum mechanical/charge field simulation. Chem Phys Lett 500:251–255

Bonner OD, Jumper CF (1973) Effect of ions on water structure. Infrared Phys 13:233–242

Buchner R, Hefter G (2009) Interactions and dynamics in electrolyte solutions by dielectric spectroscopy. Phys Chem Chem Phys 11:8984–8988

Buchner R, Hefter G, Barthel J (1994) Dielectric relaxation of aqueous NaF and KF solutions. J Chem Soc Faraday Trans 90:2475–2479

Buchner R, Hölzl C, Stauber J, Barthel J (2002) Dielectric spectroscopy mof ion-pairing and hydration in aqueous tetra-*n*alkylammonium halide solutions. Phys Chem Chem Phys 4:2169–2179

Bunzl KW (1967) Near-infrared spectra of aqueous solutions of some tetra-*n*-alkylammonium bromides. J Phys Chem 71:1358–1363

Cappa CD, Smith JD, Wilson KR, Messer BM, Gilles MK, Cohen RC, Saykally RJ (2005) Effects of alkali metal halide salts on the hydrogen bond network of liquid water. J Phys Chem B 109:7046–7052

Cappa CD, Smith JD, Messer BM, Cohen RC, Saykally RJ (2006) Effects of cations on the hydrogen bond network of liquid water: new results from x-ray absorptioin spectroscopy of liquid microjets. J Phys Chem B 110:5301–5309

Cappa CD, Smith JD, Messer BM, Cohen RC, Saykally RJ (2006a) The electronic structure of the hydrated proton: a comparative x-ray absorption study of aqueous HCl and NaCl solutions. J Phys Chem B 110:1166–1171

Cappa CD, Smith JD, Messer BM, Cohen RC, Saykally RJ (2007) Nature of aqueous hydroxide ion probed by x-ray absorption spectroscopy. J Phys Chem B 111:4776–4785

Cavalleri M, Näslund L-Å, Edwards DC, Wernet P, Ogasawara H, Myneni S, Ojamäe L, Odelius M, Nilsson A, Pettersson LGM (2006) The local structure of protonated water from x-ray absorptionh and density functional theory. J Chem Phys 124:1945081–1945088

Chalikian TV (2001) Structural thermodynamics of hydration. J Phys Chem B 105:12566–12578

Chen T, Hefter G, Buchner R (2003) Dielectric spectroscopy of aqueous solutions of KCl and CsCl. J Phys Chem A 107:4025–4031

Chizhik VI (1997) Estimated ionic B-coefficients from NMR measurements in aqueous electrolyte solutions. Mol Phys 90:653–659
Choppin GR, Buijs KJ (1963) Near-infrared studies of the structure of water. II. Ionic solutions. Chem Phys 39:2042–2050
Chowdhuri S, Chandra A (2001) Molecular dynamics simulations of aqueous NaCl and KCl solutions: effects of ion concentration on the single-particle, pair, and collective dynamical properties of ions and water molecules J Chem Phys 115:3732–3741
Collins KD (1997) Biophys J 72:65–76
Corey VB (1943) Adiabatic compressibilities of some aqueous ionic solutions and their variation with indicated liquid structure of the water. Phys Rev 64:350–357
Cox WM, Wolfenden JH (1934) Viscosity of strong electrolytes measured by a differential method. Proc Royal Soc (London) A 145:475–488
Dack MR (1975) The importance of solvent internal pressure and cohesion to solution phenomena. J Aust J Chem 28:211–229
Dack MR (1976) Solvent structure. II. a study of the structure-making and structure-breaking effects of dissolved species in water by internal pressure measurements. J Aust J Chem 29:771–778
Dack MR (1976a) Solvent structure. III. the dependence of partial molal volumes on internal pressure and solvent compressibility. J Aust J Chem 29:779–786
Davies J, Ormondroyd S, Symons MCR (1971) Solvation spectra. 41. Absolute proton magnetic resonance shifts for water protons induced by cations and anions in aqueous solutions. Trans Faraday Soc 67:3465–3473
Desnoyers JE, Perron G (1972) Viscosity of aqueous solutions of alkali and tetraalkylammonium halides at 25 deg. J Solution Chem 1:199–212
Diamond RM (1958) Activity coefficients of strong electrolytes. the halide salts J Am Chem Soc 80:48084812
Durdagi S, Hofer TS, Randolf BR, Rode BM (2005) Structural and dynamical properties of Bi^{3+} in water. Chem Phys Lett 406:20–23
Dutkiewicz E, Jakubowska A (2002) Water activity in aqueous solutions of homogeneous electrolytes: the effects of ions on the structure of water. Chem Phys Chem 3:221–224
Endon L, Hertz HG, Thuel B, Zeidler MD (1967) Microdynamic model of electrolyte solutions as derived from nuclear magnetic relaxation and self diffusion. Ber Bunsenges Phys Chem 71:1008–1031
Engel G, Hertz HG (1968) Negative hydration. a nuclear magnetic relaxation study. Ber Bunsenges Phys Chem 72:808–834
Fajans K, Johnson O (1942) Apparent volumes of individual ions in aqueous solution. J Am Chem Soc 64:668–678
Fatmi MQ, Hofer TS, Randolf BR, Rode BM (2005) An extended ab initio QM/MM MD approach to structure and dynamics of Zn(II) in aqueous solution. J Chem Phys 123:054514-1-8
Feakins D, Freemantle DJ, Lawrence KG (1974) Transition state treatment of the relative viscosity of electrolytic solutions. applications to aqueous, nonaqueous, and methanol + water systems. J Chem Soc Faraday Trans 70:795–806
Feakins D, Waghorne WE, Lawrence KG (1986) The viscosity and structure of solutions. Part 1. a new theory of the Jones-Dole B-coefficient and the related activation parameters: application to aqueous solutions. J Chem Soc Faraday Trans 82:563–568
Frank HS, Evans MW (1945) Free volume and entropy in condensed systems. III. entropy in binary liquid mixtures; partial molal entropy in dilute solutions; structure and thermodynamics in aqueous electrolytes. J Chem Phys 13:507–532
Frank HS, Robinson AL (1940) The entropy of dilution of strong electrolytes in aqueous solutions. J Chem Phys 8:933–938
Frick RJ, Hofer TS, Pribil AB, Randolf BR, Rode BM (2009) Structure and dynamics of the UO_2^{2+} ion in aqueous solution: an ab initio QMCF MD Study. J Phys Chem A 113:12496–12503
Frick RJ, Hofer TS, Pribil AB, Randolf BR, Rode BM (2010) Structure and dynamics of the $UO2^{+}$ ion in aqueous solution: an ab initio QMCF-MD study. Phys Chem Chem Phys 12:11736–11743

Fumino K, Yukiyasu K, Shimizu A, Taniguchi Y (1996) NMR studies on dynamic behavior of water molecules in tetraalkylammonium bromide-D2O solutions at 5–25 °C. J Mol Liq 75:1–12
Geiger A (1981) Molecular dynamics simulation of the negative hydration effect in aqueous electrolyte solutions. Ber Bunsenges Phys Chem 85, 52–63
Giese K, Kaatze U, Pottel RJ (1970) Permittivity and dielectric and proton magnetic relaxation of aqueous solutions of the alkali halides. Phys Chem 74:3718–3725
Guardia E, Laria D, Marti J (2006) Hydrogen bond structure and dynamics in aqueous electrolytes at ambient and supercritical conditions. J Phys Chem B 110:6332–6338
Gulaboski R, Caban K, Stojek Z, Scholz F (2004) The determination of the standard Gibbs energies of ion transfer between water and heavy water by using the three-phase electrode approach. Electrochem Commun 6:215–218
Gurney RW (1953) Ionic processes in solution. McGraw-Hill, New York
Heil SR, Holz M, Kastner TM, Weingärtner H (1995) Self-diffusion of the perchlorate ion in aqueous electrolyte solutions measured by 35Cl NMR spin-echo experiments. J Chem Soc Faraday Trans 91:1877–1880
Heinzinger K (1985) Computer simulations of aqueous electrolyte solutions Physica B 131:196–216
Heinzinger K, Palinkas G (1987) Interactions of water in ionic hydrates. in Kleeberg H ed. Interactions of Water and Nonionic Hydrates. Springer, Berlin, 1–22
Heinzinger K, Schäfer H (1999) On the hydration of ions. Cond Matter Phys 18:273–284
Hepler LG (1969) Thermal expansion and structure in water and aqueous solutions. Can J Chem 47:4613–4617
Hinteregger A, Pribil AB, Hofer TS, Randolf BR, Weiss AKH, Rode BM (2010) Structure and dynamics of the chromate ion in aqueous solution. An ab Initio QMCF-MD simulation. Inorg Chem 49:7964–7968
Hofer TS, Tran HT, Schwenk CF, Rode BM (2004) Characterization of dynamics and reactivities of solvated ions by ab initio simulations. J Comp Chem 25:211–217
Hofer TS, Randolf BR, Rode BM (2005) Structure-breaking effects of solvated Rb(I) in dilute aqueous solution-an ab initio QM/MM MD approach. J Comput Chem 26:949–956
Hofer TS, Rode BM, Randolf BR (2005a) Structure and dynamics of solvated Ba(II) in dilute aqueous solution—an ab initio QM/MM MD approach. Chem Phys 312:81–88
Hofer TS, Scharnagl H, Randolf BR, Rode BM (2006) Structure and dynamics of La(III) in aqueous solution—an ab initio QM/MM MD approach. Chem Phys 327:31–42
Hofer TS, Randolf BR, Rode BM (2006a) Sr(II) in water: a labile hydrate with a highly mobile structure. J Phys Chem B 110:20409–20417
Hofer TS, Randolf BR, Rode BM (2008) The hydration of the mercury(I)-dimer—a quantum mechanical charge field molecular dynamics study. Chem Phys 349:210–218
Hofer TS, Randolf BR, Rode BM (2008a) Al(III) hydration revisited. an ab initio quantum mechanical charge field molecular dynamics study. J Phys Chem B 112:11726–11733
Hofer TS, Randolf BR, Rode BM, Persson I (2009) The hydrated platinum(II) ion in aqueous solution—a combined theoretical and EXAFS spectroscopic study. Dalton Trans 1512–1515
Hofer TS, Weiss AKH, Randolf BR, Rode BM (2010) Hydration of highly charged ions. Chem Phys Lett 512:139–145
Holba V (1982) Spectroscopic study of the solute effect on the structure of liquid water. Coll Czech Chem Comm 47:2484–2490
Ibuki K, Nakahara M (1986) Dielectric friction theory of the viscosity of electrolyte solutions. J Chem Phys 85:7312–7317
Inada Y, Mohammed AM, Loeffler HH, Rode BM (2002) Hydration structure and water exchange reaction of Nickel(II) Ion: classical and QM/MM simulations. J Phys Chem A 106:6783–6791
Jenkins HBD, Marcus Y (1995) Viscosity B-coefficients of ions in solution. Chem Rev 95:2695–2724
Jiang J, Sandler S (2003) A New Model for the Viscosity of Electrolyte Solutions. Ind Eng Chem Res 42:6267–6272

Jones G, Stauffer RE (1936) Viscosity of aqueous solutions as a function of the concentration. IV. Potassium ferrocyanide. J Am Chem Soc 58:2558–2560

Kaatze U (1997) The dielectric properties of water in its different states of interaction. J Solution Chem 26:1049–1112

Kecki Z, Dryjanski P, Kozlowska E (1968) Effect of electrolytes on the intensity of the infrared band of water Rocz. Chem 42:1749–1754

Kiselev M, Poxleitner M, Seitz-Beyl J, Heinzinger K (1993) An investigation of the structure of aqueous electrolyte solutions by statistical geometry. Z Naturforsch A 48a:806–810

Krestov GA (1962) Thermodynamic characteristics of structural changes in water associated with the hydration of ions. Zh Strukt Khim 3:137–142

Krestov GA (1962a) Thermodynamic characteristics of the structural changes in water connected with the hydration of multiatomic and complex ions. Zh Strukt Khim 3:402–410

Krestov GA (1991) Thermodynamics of Solvation. Ellis Horwood, New York

Krestov GA, Abrosimov VK (1964) Thermodynamic characteristics of structural changes in water induced by ion hydration at various temperatures. Zh Strukt Khim 5:510–516

Kritayakornupong C, Plankensteiner K, Rode BM (2003) Structural and dynamical properties of Co(III) in aqueous solution: ab initio quantum mechanical/molecular mechanical molecular dynamics simulation. J Chem Phys 119:6068–6072

Kritayakornupong C, Plankensteiner K, Rode BM (2003a) Dynamics in the hydration shell of Hg^{2+} ion: classical and ab initio QM/MM molecular dynamics simulations. Chem Phys Lett 371:438–444

Kritayakornupong C, Plankensteiner K, Rode BM (2003b) Structure and dynamics of the Cd^{2+} Ion in aqueous solution: ab initio QM/MM molecular dynamics simulation. J Phys Chem A 107:10330–10334

Kritayakornupong C, Plankensteiner K, Rode BM (2004) The Jahn-Teller effect of the Ti(III) ion in aqueous solution: extended ab initio QM/MM molecular dynamics simulations. Chem Phys Chem 5:1499–1506

Kritayakornupong C, Vchirawongkwin V, Rode BM (2010) An ab initio quantum mechanical charge field molecular dynamics simulation of a dilute aqueous HCl solution. J Comput Chem 31:1785–1792

Kritayakornupong C, Vchirawongkwin V, Rode BM (2010a) Determination of structure and dynamics of the solvated bisulfide (HS-) ion by ab initio QMCF molecular dynamics. J Phys Chem B 114:12883–12887

Kropman MF, Bakker HJ (2003) Vibrational relaxation of liquid water in ionic solvation shells. Chem Phys Lett 370:741–746

Kropman MF, Nienhuys H-K, Bakker HJ (2002) Real-Time Measurement of the Orientational Dynamics of Aqueous Solvation Shells in Bulk Liquid Water. Phys Rev Lett 88:77601–1/4

Kujumzelis ThG (1938) The alterations in the structure of water produced by ions. Z Phys 110:742–759

Laurence VD, Wolfenden JH (1934) The viscosity of solutions of strong electrolytes. J Chem Soc 1144–1147

Leyendekkers JV (1982) Ionic contributions to partial molal volumes in aqueous solutions. J Chem Soc Faraday Trans 1 76:357–375

Leyendekkers JV (1983) Structure of aqueous electrolyte solutions. thermodynamic internal pressure. J Chem Soc Faraday Trans 1 79:1109–1121

Leyendekkers JV (1983a) Structure of aqueous electrolyte solutions. Ionic internal pressures and proton chemical shifts. J Chem Soc Faraday Trans 1 79:1123–1134

Li R, Jiang Zh, Chen F, Yang H, Guan Y (2004) Hydrogen bonded structure of water and aqueous solutions of sodium halides: a Raman spectroscopic study. J Mol Struct 707:83–88

Lichtenberger PM, Ellmerer AE, Hofer TS, Randolf BR, Rode BM (2011) Gold(I) and mercury(II)—isoelectronic ions with strongly different chemistry: ab initio QMCF molecular dynamics simulations of their hydration structure. J Phys Chem B 115:5993–5998

Lim LHV, Hofer TS, Pribil AB, Rode BM (2009) The hydration structure of Sn(II): An ab initio quantum mechanical charge field molecular dynamics study. J Phys Chem B 113:4372–4378
Lim LHV, Pribil AB, Ellmerer AE, Randolf BR, Rode BM (2010) Temperature dependence of structure and dynamics of the hydrated Ca^{2+} ion according to ab initio quantummechanical charge field and classical molecular dynamics. J Comput Chem 31:1195–1200
Lim LHV, Bhattacharjee A, Asam SS, Hofer TS, Randolf BR, Rode BM (2010a) Structural and dynamical aspects of the unsymmetric hydration of Sb(III): an ab initio quantum mechanical charge field molecular dynamics simulation. Inorg Chem 49:2132–2140
Lim LHV, Bhattacharjee A, Randolf BR, Rode BM (2010b) Hydrolysis of tetravalent group IV metal ions: an ab initio simulation study. Phys Chem Chem Phys 12:12423–12426
Loefler HH, Rode BM (2002) The hydration structure of the lithium ion. J Chem Phys 117:110–117
Luck W (1965) Association of water. II. Salt effects on the infrared bands of water. Ber. Bunsenges Phys Chem 69:69–76
Luck W (1975) In: Franks, F (ed) In water, a comprehensive treatise, Vol 2, Ch. 4. Plenum, New York
Marcus Y (1985) Ion Solvation. Wiley, Chichester, p. 66
Marcus Y (1986) The hydration entropies of ions and their effects on the structure of water. J Chem Soc Faraday Trans 1 82:233–240
Marcus Y (1987) Thermodynamics of ion hydration and its interpretation in terms of a common model. Pure Appl Chem 59:1093–1101
Marcus Y (1994) Viscosity B-coefficients, structural entropies and heat capacities, and the effects of ions on the structure of water. J Solution Chem 23:831–847
Marcus Y (2008) On the Relation between Thermodynamic, Transport and Structural Properties of Electrolyte Solutions. Elektrokhimiya 44:18–31 (Russ J Electrochem 44:16–27)
Marcus Y (2009) The effects of ions on the structure of water: structure breaking and – making. Chem Rev 109:1346–1370
Marcus Y (2010) The effect of ions on the structure of water. Pure Appl Chem 82:1889–1899
Marcus Y (2011) unpublished result
Marcus Y (2011a) Water structure enhancement in water-rich binary solvent mixtures. J Mol Liq 158:23–26
Marcus Y (2012) The viscosity *B*-coeffricient of the thiocyanate anion. J Chem Eng Data
Marcus Y, Ben-Naim A (1985) A study of the structure of water and its dependence on solutes, based on the isotope effects on solvation thermodynamics in water. J Chem Phys 83:4744–4759
Marcus Y, Loewenschuss A (1985) Standard entropies of hydration of ions Annu Rep Part C (Royal Soc Chem, London) 1984, 81–135
McCall DW, Douglass DC (1965) The effect of ions on the self-diffusion of water. I. Concentration dependence. J Phys Chem 69:2001–2011
Messner ChB, Hofer TS, Randolf BR, Rode BM (2011) Computational study of the hafnium (IV) ion in aqueous solution. Chem Phys Lett 501:292295
Milovidova ND, Moiseev BM, Fedorov LI (1970) Measurement of structural temperature of diamagnetic electrolyte solutions by nuclear magnetic resonance. Russ J Struct Chem 11:121–123 (Zh Strukt Khim 11:136–138)
Moin ST, Hofer TS, Pribil AB, Randolf BR, Rode BM (2010) A quantum mechanical charge field molecular dynamics study of Fe^{2+} and Fe^{3+} ions in aqueous solutions. Inorg Chem 49:5101–5106
Müller KJ, Hertz HG (1996) A parameter as an indicator for water-water association in solutions of strong electrolytes. J Phys Chem 100:1256–1265
Näslund L-Å, Edwards DC, Wernet P, Bergmann U, Ogasawara H, Pettersson LGM, Myneni S, Nilsson A (2005) X-ray absorption spectroscopy study of the hydrogen bond network in the bulk water of aqueous solutions. J Phys Chem A 109:5995–6002
Nickolov ZS, Miller JD (2005) J Coll Interf Sci 287:572–580
Nightingale ER (1959) Phenomenological theory of ion solvation. effective radii of hydrated ions. J Phys Chem 63:1381–1387

Nowikow A, Rodnikova M, Barthel J, Sobolev O (1999) Quasielastic neutron scattering of aqueous tetrabutylammonium chloride solutions. J Mol Liq 79:203–212

Omta AW, Kropman MF, Woutersen S, Bakker HJ (2003) Influence of ions on the hydrogen-bond structure in liquid water. J Chem Phys 119:12457–12461

Payaka A, Tongraar A, Rode BM (2009) Combined QM/MM MD study of $HCOO^-$-water hydrogen bonds in aqueous solution. J Phys Chem A 113:3291–3298

Payaka A, Tongraar A, Rode BM (2010) QM/MM dynamics of CH_3COO^-- water hydrogen bonds in aqueous solution. J Phys Chem A 114:10443–10453

Pribil AB, Hofer TS, Vchirawongkwin V, Randolf BR, Rode BM (2008) Quantum mechanical simulation studies of molecular vibrations and dynamics of oxo-anions in water. Chem Phys 346:182–185

Remsungnen T, Rode BM (2004) Molecular dynamics simulation of the hydration of transition metal ions: the role of non-additive effects in the hydration shells of Fe^{2+} and Fe^{3+} ions. Chem Phys Lett 385:491–497

Robinson RA, Stokes RH (1959) Electrolyte Solutions, 2nd edn. Butterworths, London

Rode BM, Lim LHV (2010) The influence of the lone electron pair on structure and dynamics of divalent group IV metal ion hydrates. J Mol Liq 157:79–82

Sacco A, Weingärtner H, Braun BM, Holz M (1994) Study of the structure-breaking effect on aqueous CsCl solutions based on H2O/D2O isotope effects on transport coefficients and microdynamical properties. J Chem Soc Faraday Trans 90:849–854

Samoilov OYa (1957) A new approach to the study of hydration of ions in aqueous solutions. Disc Faraday Soc 24:141–146

Schwenk CF, Rode BM (2003) Extended ab initio quantum mechanical/molecular mechanical molecular dynamics simulations of hydrated Cu^{2+}. J Chem Phys 119:9523–9531

Schwenk CF, Loeffler HH, Rode BM (2003) Structure and Dynamics of Metal Ions in Solution: QM/MM Molecular Dynamics Simulations of Mn^{2+} and V^{2+}. J Am Chem Soc 125:1618–1624

Schwenk CF, Hofer TS, Rode BM (2004) "Structure Breaking" Effect of Hydrated Cs^+. J Phys Chem A 108:1509–1514

Steward GW (1939) The variation in the structure of water in ionic solutions. J Chem Phys 7:869–877

Szasz GI, Heinzinger K, Palinkas G (1981) The structure of the hydration shell of the lithium ion. Chem Phys Lett 78:194–196

Tongraar A, Rode BM (2003) The hydration structures of F^- and Cl^- investigated by ab initio QM/MM molecular dynamics simulations. Phys Chem Chem Phys 5:357–362

Tongraar A, Rode BM (2005) Ab initio QM/MM dynamics of anion–water hydrogen bonds in aqueous solution. Chem Phys Lett 403:314–319

Tongraar A, Rode BM (2005a) Structural arrangement and dynamics of the hydrated Mg^{2+}: An ab initio QM/MM molecular dynamics simulation. Chem Phys Lett 409:304–309

Tongraar A, Liedl KR, Rode BM (1998) Born-Oppenheimer ab Initio QM/MM Dynamics Simulations of Na^+ and K^+ in Water: From Structure Making to Structure Breaking Effects. J Phys Chem A 102:10340–10347

Tongraar A, Tangkawanwanit P, Rode BM (2006) A combined QM/MM molecular dynamics simulations study of nitrate anion NO_3^- in aqueous solution. J Phys Chem A 110:12918–12926

Tongraar A, Hannongbua S, Rode BM (2010) QM/MM MD simulations of iodide ion (I-) in aqueous solution: a delicate balance between ion-water and water-water H-bond interactions. J Phys Chem A 114:43344339

Tromans A, May PM, Hefter G, Sato T, Buchner R (2004) Ion pairing and solvent relaxation processes in aqueous solutions of sodium malonate and sodium succinate. J Phys Chem B 108:13789–13795

Vchirawongwin V, Hofer TS, Randolf BR, Rode BM (2007) Tl(I)-the strongest structure-breaking metal ion in water? a quantum mechanical/molecular mechanical simulation study. J Comput Chem 28:100610016

Vchirawongwin V, Hofer TS, Randolf BR, Rode BM (2007a) Quantum mechanical/molecular mechanical mimulations of the Tl(III) ion in water. J Comput Chem 28:1057–1067

Vchirawongkwin V, Kritayakornupong C, Rode BM (2010) Structural and dynamical properties and vibrational spectra of bisulfate ion in water: a study by ab initio quantum mechanical charge field molecular dynamics. J Phys Chem B 114:11561–11569

Vchirawongkwin V, Pribil AB, Rode BM (2010a) Ab initio quantum mechanical charge field study of hydrated bicarbonate ion: structural and dynamical properties. J Comput Chem 31:249–257

Wachter W, Kunz W, Buchner R, Hefter G (2005) Is there an anionic Hofmeister effect on water dynamics? dielectric spectroscopy of aqueous solutions of NaBr, NaI, $NaNO_3$, $NaClO_4$, and NaSCN. J Phys Chem A 109:8675–8683

Wachter W, Buchner R, Hefter G (2006) Hydration of tetraphenylphosphonium and tetraphenylborate ions by dielectric relaxation spectroscopy. J Phys Chem B 110:5147–5154

Wachter W, Fernandez S, Buchner R, Hefter G (2007) J Phys Chem B 111:9010–9017

Walrafen GE (1970) Raman spectral studies of the effects of perchlorate ion on water structure. J Chem Phys 52:4176–4198

Wen W-Y, Kaatze U (1977) Aqueous solutions of azoniaspiroalkane halides. 3. dielectric relaxation. J Phys Chem 81:177–181

Worley JD, Klotz IM (1966) Near-infrared spectra of H_2O-D_2O solutions. J Chem Phys 45:2868–2071

Yoshida K, Ibuki K, Ueno M (1996) Estimated ionic B-coefficients from NMR measurements in aqueous electrolyte solutions. J Solution Chem 25:435–453

Chapter 4
Water Surfaces

Water as we know it, being a liquid in a gravitational field, has a flat free surface. When water is cooled down from ambient conditions to super-cooled conditions the surface persists, and of course also when it turns into the glassy state. When water is heated, the surface persists up to the critical point (Sect. 1.1.1), where it vanishes. Supercritical water has no *free* surface, although, of course, it has a surface with respect to its confining vessel. Due to the gravitational field, the surface of liquid water is horizontal and flat, except at the contact regions with the confining vessel, where it becomes curved, due to interaction with the wall.

Unconfined water, that is, water drops, have spherical surfaces when stationary, but the shape of drops varies when in motion. The spherical shape is due to the tendency of an unconfined liquid to minimize its surface area, because the surface has a higher energy than the bulk liquid. The surface of a liquid is maintained by the surface tension, γ, which is the energy that has to be applied in order to enlarge the surface area by one unit, and is thus measured in J m^{-2} or more commonly in mN m^{-1} units.

4.1 Surface Between Water and its Vapor or Air

The surface tension of water with respect to water vapor is listed as a function of the temperature at the standard pressure (0.1 MPa) in Table 1.2. The value with respect to air is lower by 0.03 % at room temperature (Richards and Carver 1921). Compared with other liquids the value is quite large: $\gamma = 71.96$ mN m^{-1} at 25 °C, exceeded only by that of hydrogen peroxide, 73.7 mN m^{-1}, and approached only by other highly hydrogen bonded liquids: such as glycerol, 63.3 mN m^{-1}, ethylene glycol, $\gamma = 48.0$ mN m^{-1}, and formamide $\gamma = 58.2$ mN m^{-1}. Other common liquids have definitely lower values, mostly in the range of 20–40 mN m^{-1} (Marcus 1998).

The temperature dependence of the surface tension of liquids is expressed well in terms of an empirical equation involving the critical temperature T_c (Guggenheim 1945):

$$\gamma(T) = \gamma_0 \left(1 - \frac{T}{T_c}\right)^{\frac{11}{9}} \tag{4.1}$$

Y. Marcus, *Ions in Water and Biophysical Implications,*
DOI 10.1007/978-94-007-4647-3_4, © Springer Science+Business Media Dordrecht 2012

The proportionality coefficient γ_0 is a function of the critical temperature T_c, the critical density ρ_c, and the acentric factor ω. For water, however, this expression is only approximate between 0 and 100 °C (with γ_0 = 157.7 mN m^{-1}) and a more accurate description is in terms of a linear dependence on $(1 - T/T_c)^{11/9}$:

$$\frac{\gamma(T)}{\text{mN m}^{-1}} = 22.93 + 104.02\left(1 - \frac{T}{T_c}\right)^{\frac{11}{9}} \tag{4.2}$$

One way to deal with the molecular aspects of the surface tension of a liquid is via the scaled particle theory (SPT) of Reiss et al. (1960). Mayer (1963) obtained an expression from this treatment, reformulated here as follows:

$$\gamma = \left(\frac{k_B T}{4\pi {\sigma_W}^2}\right)\left(\frac{12y}{(1-y)} + \frac{18y^2}{(1-y)^2}\right) - \frac{P\sigma_W}{2} \tag{4.3}$$

In this expression σ_W is the hard sphere diameter of the molecules of the liquid (in the present case of water) and $y = (\pi N_{Av}/6){\sigma_W}^3/V$ is the packing fraction of the liquid. The second term on the right hand side is generally negligible. The problem with this formulation is that the temperature dependence of this SPT value for the surface tension of water does not agree with the experimental values if a temperature-independent value of the diameter σ_W is used. The expedient of using $\sigma_W = f(T)$ derived from the experimental viscosity of the vapor which is proportional to $T^{1/2}{\sigma_W}^{-2}$ was suggested by Mayer (1963). This yields values of γ that decrease with increasing temperatures in agreement with experimental values (tested in the range from 10 to 60 °C). The required large temperature dependence: σ_W varying from 0.293 nm at 10 °C down to 0.271 nm at 100 °C (Mayer 1963a), was criticized by Pierotti (1967), who found a much milder dependence to be consistent with the compressibility of the water and with gas solubilities calculated by means of the SPT. He pointed out that the implicit assumption that the macroscopic surface tension of a liquid with respect to its vapor is the same as the microscopic one of a cavity in the liquid with respect to a hard sphere surface need not be correct.

Still, assuming that the SPT is applicable to macroscopic quantities, Mayer (1963a) related the surface tension of a liquid to its isothermal compressibility. He reformulated Eq. (4.3) again as:

$$\gamma = \frac{\sigma_W RT(2+y)}{4V(1-y)^2} \tag{4.4}$$

and the compressibility as:

$$k_T = \frac{V(1-y)^4}{RT(1+2y)^2} \tag{4.5}$$

Hence, the product of the surface tension and the compressibility becomes:

$$\gamma \cdot k_T = \frac{\sigma_W(2 - 3y + y^3)}{4(1+2y)^2} \tag{4.6}$$

Knowledge of the one quantity and the density then allows the calculation of the other. The diameter σ_W that features also in y is obtained from either γ or κ_T, whichever has been measured.

The macroscopic surface tension is defined with a flat surface between the liquid and its vapor, that is, a surface with an infinitely large radius of curvature, r_C. Tolman (1949) considered the dependence of the surface tension on the radius of curvature of droplets and arrived at the approximate expression:

$$\gamma(r_C) = \frac{\gamma(r_C = \infty)}{1 + \dfrac{2\delta}{r_C}} \tag{4.7}$$

Here δ is the thickness of the surface layer of the liquid that has a density differing from the bulk liquid density. It was estimated for water by Tolman (1949), increasing from 0.096 nm at 10 °C to 0.106 nm at 50 °C. This is only some 40 % of the molecular diameter of water, a value that appears to be too low.

The usual explanation given for the high surface tension of water is that at the surface a water molecule cannot form four tetrahedrally directed hydrogen bonds with other water molecules but only three, hence water tends to minimize the surface area in order to minimize the energetic expense of the loss of hydrogen bonds. Therefore, a value of δ of Eq. (4.7) of the order of two molecular diameters, 0.5 nm, should have been expected. Anyway, only very tiny droplets would have a surface tension smaller than that of bulk water with a flat surface. However, with regard to the application of the scaled particle theory, Eqs. (4.3) to (4.6), the question of the finite curvature of the cavity remains.

An approach alternative to the SPT, namely the domain model derived from the significant structure theory, was applied by Jhon et al. (1967) to the surface tension of water. According to the model, the water molecules at the surface layer are in an asymmetric field, having no neighbours in a direction perpendicular and outward from the surface. Water domains, the molecules of which are favourably oriented with respect to the field, then grow till equilibrium is reached. The surface tension is due to the orientation of molecules in the top layer and partly to changes in density within a few molecular diameters from the surface. The details of the calculation are, unfortunately, not provided in that paper. The values of γ calculated by this approach agree within 1 % with the experimental ones from 0 to 100 °C and provide also correct values for the surface entropy.

Still another approach to the theoretical estimation of the surface tension is the application of the gradient theory of Carey et al. (1978) to water by Guerrero and Davis (1980). According to this approach an equation of state is applied to the liquid, yielding the molecular interaction parameter $a(T)$, the excluded volume parameter $b = 2/3\pi\sigma_W{}^3$, and the Helmholtz energy density. An 'influence parameter' $c(\rho,T)$ is introduced, which determines the density gradient response to the local deviation in the chemical potential from its bulk phase value, ρ being the number density. The value $c(\rho,T) = Kab^{2/3}$, where K is calculated from the molecular properties of water and its pair correlation function. However, such values of K yield incorrect values when the resulting $c(\rho,T)$ is introduced into the expression for $\gamma(T)$ at $T \leq 500$ K.

A semi-empirical value, 0.888 K, does allow values of $\gamma(T)$ to be estimated adequately for $380 \leq T/\mathrm{K} \leq T_c$.

The problem of the number density profile at the liquid/vapor interface, $\rho(z, \theta)$, along the direction z perpendicular to the surface and as function of the molecular orientation θ, has been dealt with by Yang et al. (1991) in the case of water. It was concluded that there is a slight preference of the water dipoles at the surface to be directed downwards (i.e., with the hydrogen atoms towards the bulk liquid). This confirms earlier conclusions of Stillinger and Ben-Naim (1967), among others, who stressed the importance of the permanent quadrupole moment of the water molecules for the breaking of the symmetry in the direction of the dipole moment.

This issue is related to the surface potential difference between water and its vapor, $\Delta\chi$, and to the electrical double layer at the surface caused by the preferred orientation of the water dipoles. Parfenyuk (2002) has recently reviewed the values of $\Delta\chi$ proposed by many authors, ranging from -1.1 to $+0.5$ V. His experiments involved an electrochemical cell and a non-aqueous solvent S:

$$\mathrm{Ag, AgCl\,|HCl(W}, m)\,|\mathrm{air}\,|\mathrm{HCl(W} + x\mathrm{S}, m)\,|\mathrm{AgCl, Ag} \tag{4.8}$$

A double extrapolation to zero molality of HCl ($m \to 0$) and of the S content ($x \to 0$) in the right hand half-cell was performed. This should yield $\Delta\chi$ of the water/air interface, and is obtained as $+0.10$ V at room temperature. This value is in agreement with the estimate by Randles (1977): $+0.08$ V, by Trasatti (1974, 1987): $+0.13$ V, and by Krishtalik et al. (1992): 0.06 V, and also by several other authors as reported in the latter reference. However, an uncertainty of ± 0.05 V must be reckoned with for any of these estimates. The value of $\Delta\chi$ is of importance in the estimation of the standard chemical potentials of individual ions in aqueous solutions, ${\mu_\mathrm{I}}^\infty$ (Marcus 2008). Experimentally measurable 'real' chemical potentials, ${\mu_\mathrm{i}}^{\infty\mathrm{real}}$ or electrochemical potentials differ from the thermodynamic but unmeasurable ${\mu_\mathrm{I}}^\infty$ by the quantity $z_\mathrm{i}F\Delta\chi$, where F is the Faraday constant:

$${\mu_\mathrm{I}}^{\infty\mathrm{real}} = {\mu_\mathrm{I}}^\infty + z_\mathrm{I}F\Delta\chi \tag{4.9}$$

The probable error of ± 0.05 V in $\Delta\chi$ then causes a probable error of ± 5 kJ mol^{-1} in the values of ${\mu_\mathrm{I}}^\infty$estimated from Eq. (4.9) and accurate experimental ${\mu_\mathrm{I}}^{\infty\mathrm{real}}$ values (Marcus 2008).

Computer simulations have over the years contributed to our understanding of the liquid water/vapor interface. A fairly early study by Wilson et al. (1987) used the TIP4P water model with 342 molecules at a rather high temperature, 52 °C. They confirmed the preferred dipole orientation at the surface with the positive end (hydrogen atoms) towards the bulk liquid and considered the interfacial region to extend 0.75 nm into the liquid. However, the calculated surface tension, 132 ± 46 mN m^{-1}, is nearly twice the experimental value, so that the implementation of the model needed revision. Subsequent work by others improved on this situation. Taylor et al. (1996) used the SPC/E model of water with 526 molecules at several temperatures from -5 to 100 °C (and also with 1,052 molecules at 25 °C) at 0.1 MPa. A main conclusion is

that the interfacial region is not smooth. The density profile of the interfacial layer along the z axis perpendicular to the surface follows the hyperbolic tangent relation:

$$\rho(Z) = \frac{1}{2}(\rho_L + \rho_V) - (\rho_L - \rho_V)/2 \tanh\left(\frac{Z - Z_0}{d}\right) \tag{4.10}$$

where ρ_L and ρ_V are the densities of the liquid and vapor, z_0 is the locus of the Gibbs surface, where $\rho(z) = 1/2(\rho_\mathrm{L} + \rho_\mathrm{V})$, and $d = 0.4551 t_{9/1}$ is a thickness parameter. The thickness $t_{9/1}$ is that of the surface layer, over which the density falls from $0.9\rho_\mathrm{L}$ to $0.1\rho_\mathrm{L}$, and increases from 0.267 nm at −5 °C through 0.357 nm at 25 °C to 0.450 nm at 100 °C. The calculated surface tension values are, however, 10–20 % lower than the experimental ones over the temperature range tested, and have a more negative slope with respect to the temperature. The use of the same water model, SPC/E, but a different long range summation method (for coulombic interactions) for the molecular dynamics simulations by Alejandro et al. (1995) yielded the same thickness values, $t_{9/1}$, but a better agreement of the computed surface tension with the experimental values.

The surface water molecules, being less strongly hydrogen bonded to their neighbours, have larger self-diffusion coefficients in the plane parallel to the surface than those of molecules in the bulk of the liquid and the residence time of a molecule in the surface region is estimated as 2 ps (Taylor et al. 1996). Wang and Zeng (2009) reviewed computer simulation methods for the calculation of the surface tension of water, and arrived at values of γ at 55 °C of 53 ± 2 mN m^{-1} some 20 % below the experimental value, contrary to the earlier achievement of Alejandro et al. (1995).

The hydrogen bonds are longer, more bent, and weaker in the interfacial region than in the bulk, as was found by Jedlovszky (2004) from Monte Carlo simulations, but the structure of the water is more tetrahedral in the vicinity of the surface. Partay et al. (2008a) suggested a method (identification of truly interfacial molecules, ITIM) for the identification of the molecules residing at the liquid/vapor interface of water. A probe sphere of a definite size is moved in the vapor phase perpendicularly to the surface and the first water molecule it hits is noted. This systematic scanning of the surface thus determines the 'roughness' of the surface, the measure of which depends on the radius R_P of the probe sphere, since smaller probes can penetrate deeper into the surface layer before they are stopped by a water molecule. The simulations were carried out at 25 °C with 4000 TIP4P-model water molecules and a probe sphere radius $R_\mathrm{P} = 0.20$ nm was chosen as being most appropriate. The value of the $0.9\rho_\mathrm{L}$ to $0.1\rho_\mathrm{L}$ thickness parameter was $t_{9/1} = 0.423$ nm. The second layer is located at one molecular diameter below the interface on the average, indicating a strictly organized layering structure in the interfacial region. The probability of a molecule to belong to a two-dimensional percolation cluster in the bulk is 0.28, but that for a molecule in the first interfacial layer is nearly three times as large, 0.82, and is negligible for the second layer below the surface (Partay et al. 2008a). There occurs thus a strong lateral hydrogen bonding in the surface layer. This analysis was subsequently extended to a third sub-surface layer (Hantal et al. 2010). The thicknesses of the second and third layers are 6 and 10 % smaller than that of the first layer (0.415 nm)

and the residence time of a water molecule are 5.07, 1.89, and 1.77 ps in the 1st, 2nd, and 3rd layers. The roughness of the surface, $d(l)$ at large distances l parallel to the surface, can be described by means of two parameters: a, the saturation value of the mean vertical distance along the z axis between two surface points, and the slope ξ of the dependence of $d(l)$ at small l values:

$$d(l) = \frac{a\xi l}{a + \xi l} \tag{4.11}$$

The larger these parameters are, the rougher is the surface. For the free water surface $a = 0.304\,\text{nm}$ and $\xi = 11.2\,\text{nm}^{-1}$.

4.2 Surface Between Water and Another Liquid

The surfaces between water and a variety of immiscible solvents have been studied experimentally, theoretically, and by computer simulations. Volkov and Deamer (1996) edited a collective volume dedicated to liquid-liquid interfaces with some emphasis on the electrochemical aspects. 1,2-Dichloroethane (DCE) and nitrobenzene (NB) feature conspicuously in such studies, because they have reasonably large relative permittivities ($\varepsilon_{\text{rDCE}} = 10.36$ and $\varepsilon_{\text{rNB}} = 34.78$ at 25 °C) permitting electrolyte dissociation, and rather low miscibilities with water ($x_{\text{DCE}} = 1.48 \times 10^{-3}$ in water and $x_{\text{W}} = 1.02 \times 10^{-2}$ in DCE, and $x_{\text{NB}} = 2.78 \times 10^{-4}$ in water and $x_{\text{W}} = 1.62 \times 10^{-2}$ in NB). These liquids have been the basis of electrodes based on the interface between two immiscible electrolyte solutions (ITIES). Watts and VanderNoot (1996) briefly reviewed experimental methods for dealing with liquid-liquid interfaces, including surface tension (drop weight and drop time, Wilhelmy plate, drop profiles), electrocapillarity (thermal riplons and capillary waves), electro-chemical transient techniques (pulse and impedance methods), and spectroelectro-chemistry (laser scattering, ellipsometry, non-linear optics, Raman spectroscopy, fluorescence, and x-ray and neutron reflectivity).

An important quantity in this regards is the interfacial tension between the two liquids. Freitas et al. (1997) compiled a comprehensive list of γ_{WS} values for the surface tension between water and immiscible liquids S mostly at 20 °C or exceptionally at temperatures between 19 and 26 °C. Representative values are shown in Table 4.1. The larger the mutual solubility of water with the liquid S the smaller is the interfacial tension, until it vanishes, of course, for water-miscible liquids. Triethylamine is a case in point, since at 20 °C with $\gamma_{\text{WS}} = 0.1\,\text{mN m}^{-1}$ it is just 2 °C above the upper consolute temperature.

The interfacial tension is related to the work of adhesion between the two phases per unit surface area, W_{WS}, by:

$$\gamma_{\text{WS}} = (\gamma_{\text{W}} + \gamma_{\text{S}}) - W_{\text{WS}} \tag{4.12}$$

This work, on the other hand, is empirically related to the Ostwald coefficient L_{SW} for the solubility of the organic liquid as a gaseous solute in water, $L_{\text{SW}} = c_{\text{S-in-W}}/c_{\text{S-gas}}$,

Table 4.1 Interfacial tension, γ_{WS}/mN m^{-1}, between water and some immiscible, but mutually saturated, organic liquids S at 20 °C (Freitas et al. 1997) (γ_W 72.75 mN m^{-1})

Liquid S	γ_S	γ_{WS}	Liquid S	γ_S	γ_{WS}
n-Hexane	18.41	51.1	Hexanoic acid[a]	27.49	4.9
n-Octane	21.61	50.8	Ethyl acetate[a]	23.39	6.8
n-Decane[a]	23.89	51.2	Ethyl butyrate[a]	24.46	15.7
Tetradecane	26.56	52.2	Dichloromethane	27.84	28.3
Benzene	28.88	35.0	Chloroform	27.32	32.8
Toluene[a]	27.93	36.1	Tetrachloromethane	27.04	45.0
p-Xylene	28.55	37.7	1,2-Dichloroethane[a]	32.23	28.4
1-Butanol[a]	24.95	1.8	Bromoethane	24.20	31.2
1-Hexanol[a]	25.81	6.8	Iodoethane[c]	29.10	40.0
1-Octanol	27.50	8.5	Chlorobenzene	33.59	37.4
Benzyl alcohol[b]	39.72	4.8	Bromobenzene[a]	35.24	38.1
Phenol	40.90	0.8	Iodobenzene	39.27	41.8
Diethyl ether	17.11	10.7	Di-*n*-Butylamine	24.60	10.3
Di-*i*-Propyl ether[a]	17.27	17.9	Triethylamine	19.99	0.1
Anisole	35.70	25.8	Butyronitrile	27.44	10.4
2-Butanone[a]	23.96	1.0	Nitromethane	37.48	9.7
2-Hexanone	25.49	9.7	Nitrobenzene	43.38	25.6
Cyclohexanone[a]	35.23	3.9	Ethyl mercaptane	23.47	26.1
Acetophenone[a]	39.80	13.2	Carbon disulphide[a]	31.58	48.1

[a] At 25 °C
[b] At 22.5 °C
[c] At 16 °C

the reciprocal of its Henry's law constant. The relationship is:

$$\frac{W_{WS}}{\text{mN m}^{-1}} = 61.52 + 10.6 \log L_{SW} + 2.13(N_C - 6) \tag{4.13}$$

where the last term is applicable only to alkanes from hexane onwards and N_C is their number of carbon atoms. A linear solvation energy relationship (LSER) exists between L_{SW} and several properties of the organic solvent S as a solute, see Eq. (1.21) and the discussion in Sect. 1.2.2. However, in view of the limited span of the γ_{WS} values of only 52 mN m^{-1} (Freitas et al. 1997), the standard error of the fit, 4 mN m^{-1}, is rather poor and not conducive to a good prediction of the interfacial tension of a liquid immiscible with water from Eq. (4.12). Lee (2000) pointed out that values of γ_{WS} calculated from the properties of water and the pure liquid S are apt to disagree with the measured equilibrium interfacial tension because of the (limited) mutual solubility of water and S, each being saturated by the other.

Another way of looking at the surface tension between two liquids, in the present context between water and an immiscible liquid S, is in terms of the spreading coefficient of S, S_{SW}:

$$S_{SW} = \gamma_W - \gamma_S - \gamma_{WS} \tag{4.14}$$

When a drop of a liquid with small γ_S, such as benzene and long chain alcohols, is placed on water it is expected to spread, $S_{SW} > 0$, but for liquids such as CS_2

and CH_2I_2 $S_{SW} < 0$ and they do not spread, remaining as a distinct lens-form drop (Adamson 1990).

A related subject is the interfacial potential between water (W) and the liquid S, where the latter could be either miscible or immiscible with water. In the first case the individual surface potentials between W and air (A), $\Delta\chi^{WA}$, and between S and air, $\Delta\chi^{SA}$, are measured or estimated and the difference is taken $\Delta\chi^{WS} = \Delta\chi^{SA} - \Delta\chi^{WA}$. In the latter case direct measurements of the interfacial potential (at zero charge) between the mutually saturated W(S) and S(W) are possible. Koczorowski et al. (1989) presented values for many liquids S of both kinds, and these are compared with values for some water-miscible liquids obtained by other authors in Table 4.2. It should be noted that for the mutually immiscible pair water/nitrobenzene the interfacial potential, 0.105 ± 0.20 V (Koczorowski and Zagorska 1983), is considerable lower than that estimated for the neat liquids, 0.24 V.

The molecular structure of the interfacial region is obtainable from computer simulations (Benjamin 1996). Michael and Benjamin treated the water/hydrocarbon (Michael and Benjamin 1995) and water/nitrobenzene (Michael and Benjamin 1998) interfaces by molecular dynamics simulation. In the former system two hydrocarbons were treated: *n*-nonane and 'pseudononane' that consisted of globular molecules with the same mass and potential functions as the long chain actual *n*-nonane. The mean width δ_{WS} of the interfacial region is related to the macroscopic interfacial tension γ_{WS} by the approximate expression:

$$\delta_{WS}{}^2 = \left(\frac{k_B T}{4\pi}\right) \gamma_{WS}{}^{-1} \mathrm{In}\left(\frac{A}{\xi^2}\right) \tag{4.14}$$

Here A is the surface area of the interface and ξ is the bulk liquid correlation length, and $\ln(A/\xi^2) \sim 19$. Whereas the correlation length, 0.5–0.6 nm can be estimated separately, no indication how the applicable surface area A is to be estimated was given. The resulting value of δ_{WS} for *n*-nonane is 0.15 nm, for 'pseudononane' it is 0.17 nm (Michael and Benjamin 1995) and for nitrobenzene it is 0.19 nm (Michael and Benjamin 1998). The rate of molecular diffusion parallel to the surface (approximately the same as the bulk diffusion rate) is faster than that perpendicular to it by a factor near 2. The surface is rather rough, and water molecules may undergo excursions of up to 0.8 nm (nearly 3 molecular diameters) into the nitrobenzene phase. The probability of the existence of any given hydrogen bond in the water increases from 0.8 in the bulk to 0.9 at the interface, but since the average number of nearest neighbours is only 2.2 at the interface compared with 4.2 in the bulk, the average number of hydrogen bonds between water molecules drops from 3.6 in the bulk to 2.0 at the interface. The computed interfacial potential, 0.4 V (Michael and Benjamin 1998), is however manifold larger than the experimentally determined value of 0.105 ± 0.20 V.

Nitrobenzene (NB) is a highly polarizable molecule and so is carbon tetrachloride, the interface of which with water was studied by molecular dynamics simulation by Chang and Dang (1996). Whereas the density profile of the water in both systems is rather smooth, that of the organic liquid exhibits fluctuations. The interface induces

Table 4.2 Interfacial potentials, $\Delta\chi^{SW} = \Delta\chi^{WA} - \Delta\chi^{SA}$ between water (W) and other liquids (S), ±0.01 V

Liquid[a]	Koczorowski et al. (1989)	Trasatti (1987)	Krishtalik et al. (1992)	Petersen and Saykally (2004)
Methanol	0.31	0.31	0.17	0.28
Ethanol	0.31	0.25	0.35	0.36
1-Propanol				0.37
2-Propanol				0.38
1-Butanol				0.38
1,2-Ethanediol	0.23[b]			
1,2-Propanediol	0.24			
1,3-Propanediol	0.22			
2-Methoxyethanol	0.31			
2-Ethoxyethanol	0.25			
2-Butoxyethanol	0.31			
4-Butyrolactone	0.26[b]			
Acetone		0.47	0.46	0.44
Isobutyl methyl ketone	0.17[b]			
1,2-Dichloroethane[a]	0.08			
Acetonitrile	0.19	0.23		0.21
Propionitrile	0.18			
Benzonitrile[a]	0.21			
Nitroethane[a]	0.23			
Nitrobenzene[a]	0.24[c]			
Formamide		0.08		
N, N-Dimethylformamide		0.39	0.52	0.53
Dimethylsulfoxide		0.42	0.27	0.34

[a]The liquids S are immiscible with water
[b]From (Koczorowski and Zagorska 1985)
[c]From (Koczorowski and Zagorska 1983)

local order in both water and the organic liquid due to induced dipoles. An interfacial potential of ∼0.14 V was obtained between CCl_4 and water, not otherwise available because of the low solubility and low ionic dissociation of electrolytes in CCl_4. Monte Carlo computer simulations were applied to the interface between water and CCl_4 as well as between water and 1,2-dichloroethane (DCE) by Jedlovszky (2004) in order to investigate the hydrogen bonding of the water molecules. These bonds are weakened at the interface, being longer and more often bent than in bulk water, and there are fewer of them, although the overall structure of the water is more tetrahedral at the interface than in the bulk. Benjamin (2005) studied by molecular dynamics simulations the hydrogen bonding at the interfaces of water with CCl_4, DCE, and nitrobenzene (NB), increasing in polarity in this order. The thickness $t_{9/1}$ of the water layer over which its density falls from $0.9\rho_L$ to $0.1\rho_L$ (see Sect. 4.1) is 0.35, 0.54, and 0.53 nm for these three systems. In all the systems there is a gradual increase in the hydrogen bond lifetimes τ as the interface is approached from the bulk water side. They increase from 5 ps in bulk water to 7 ps at the interface with CCl_4, to 15 ps at that with DCE, and to 9.6 ps at that with NB, i.e., not in the order of the polarity of

the non-aqueous liquids. This was explained by the possibility of hydrogen bonding of water to the oxygen atoms of the nitro group of NB. Hydrogen bonds between water molecules in a layer of the non-aqueous liquid near the interface persist even longer.

The water/CCl_4 and water/DCE interfaces were also investigated experimentally by the vibrational sum frequency (VSF) method and by molecular dynamics simulations by Walker et al. (2007). The simulation results confirmed substantially the above conclusions and explained why the VSF spectra of the water/CCl_4 interfaces could be deconvoluted into free OH and hydrogen bonded OH vibrations but the water/DCE spectra could not, being broad and featureless. The interactions of water and DCE molecules are stronger than those of water and CCl_4 ones, leading to a red-shifted broadened total free OH peak that merges with hydrogen bonded OH modes. Hore et al. (2007) extended the molecular dynamics study to water/$CHCl_3$ and water/CH_2Cl_2 interfaces, in particular with regards to the orientations of the various molecules. The minimal energy structures involve a balance between dipole orientation and hydrogen bonding optimization. When the latter predominates then a significant net dipole moment exists perpendicular to the interface, resulting in the double layer potential. In the case of the water/$CHCl_3$ system the water side is slightly positively charged, but a more complex field pattern with a smaller excess charge was observed for the water/CH_2Cl_2 system.

The water/benzene interfaces were studied by Kereszturi and Jedlovszky (2005) by Monte Carlo simulations over wide temperature and pressure ranges, including states at which water and benzene become miscible. At ambient conditions the interfacial thickness $t_{9/1}$ of the water layer is 0.26 nm but it increases steadily with increasing temperatures. At a pressure of 100 MPa it increases from 0.27 nm at 27 °C to 0.31 nm at 102 °C, to 0.43 nm at 177 °C, to 0.67 nm at 202 °C, and to 1.09 nm at 377 °C (near the critical point of water) and diverges when the liquids become miscible. Both water and benzene molecules appear to be aligned parallel to the interface independently of the temperature.

The computational ITIM method of identification of the molecules that actually reside at the interface (Partay et al. 2008) described in Sect. 4.1 regarding the free surface of water was recently applied also to the interfaces of water with CCl_4, CH_2Cl_2, and CH_2ClCH_2Cl (DCE) by Hantal et al. (2010). The properties of the first interfacial layers are shown in Table 4.3. The width Δ of the interface is twice the distance between the midpoints of the two surface layers. The thickness of each layer $t_{9/1}$ is that defined above (Sect. 4.1) and the roughness parameters a and ξ are defined by Eq. (4.11). The residence time τ is the time interval for the probability of a molecule remaining in its layer to decrease to $1/e$ of that at the beginning of this time interval. It was found that the two liquid surfaces are not mutually close packed but there are voids between them. Molecules in the interface layers stay there longer than do molecules in layers removed from the interface. The values of τ(W) are 1.89, 2.06, 1.94, and 1.94 ps in the second layer of the W/vapor, W/CCl_4, W/CH_2Cl_2, and W/$C_2H_4Cl_2$ interfaces. The values of τ(RX) for the haloalkane molecules are respectively 12.7, 5.6, and 7.8 ps, about 27 % of the values in the interface layer. The longer τ values for the interface molecules are due to the single direction available

Table 4.3 Properties of the surface layers at the interface between water (W) and its vapor and between water and three haloalkanes (RX). (Adapted from Hore et al. 2007)

Property	W/vapor	W/CCl_4	W/CH_2Cl_2	W/$C_2H_4Cl_2$
Width, Δ/nm		0.928	0.798	0.816
W layer, $t_{9/1}$/nm	0.415	1.423	0.463	0.9204
W layer, a/nm	0.304	0.238	0.304	0.330
W layer, ξ/nm^{-1}	11.2	7.4	10.3	10.3
W layer, τ/ps	5.07	6.11	4.80	6.09
RX layer, $t_{9/1}$/nm		0.549	0.605	0.511
RX layer, a/nm		0.251	0.369	0.322
RX layer, ξ/nm^{-1}		8.5	11.8	9.4
RX layer, τ/ps		56.0	21.5	24.7

to them to leave their layers, compared to the double directions for molecules in the lower layers. The lateral binding energies of water molecules to each other in the surface layer are some 58 % stronger than for molecules in the deeper layers, but no such decrease was observed for the lateral mutual binding energies of the haloalkane molecules (Hantal et al. 2010).

4.3 Surface Between Water and a Solid

An extensive literature exists regarding the interface between water and solids, and only the main concepts are dealt with here. Two situations may be distinguished regarding the surface between water and a solid: in one case a gaseous phase (vapor and/or air) is also present, as when a drop of water is located on a solid support, and the other case is at a submerged solid in the water (or an aqueous solution), e.g., at an electrode.

Consider a drop of water on a solid support that is assumed to be perfectly smooth, with a gaseous phase above both. The so-called sessile drop of water may wet the solid to a greater or lesser extent, depending on whether the solid is hydrophilic or hydrophobic. There are three surfaces to be dealt with: the solid/gas one, with a surface tension γ_{SG}, the water/vapor one, with surface tension γ_{WG}, and the solid/water one, with surface tension γ_{SW}. Young's rule applies to the contact angle θ_{ca} between the tangent to the drop at its edge and the horizontal smooth surface of the solid (deGennes 1985):

$$\gamma_{WG} \cos \theta_{ca} = \gamma_{SG} - \gamma_{Sw} \tag{4.15}$$

The contact angle is $\theta_{ca} < 90°$ when the solid is hydrophilic (so-called high energy solid) and the water wets such a solid well; it is usually $< 30°$ and approaches zero when the water completely spreads over the solid. For hydrophobic solids (so-called low energy solids) $\theta_{ca} > 90°$ and may have values up to 150° for so-called superhydrophobic surfaces such as specially prepared (non-wettable) fluorohydrocarbons. There exists some hysteresis (amounting typically up to 10°) between the contact

Table 4.4 Some typical mean contact angles between water and solid surfaces

Solid	θ_{ca}
Glass	17 at 25 °C (Adamson 1968)
Carbon I, II	64, 72 at 21.5 °C (Tadros et al. 1974)
Graphite	86 at r.t. (Adamson 1990)
Polyethylene	89 at 21.5 °C (Tadros et al. 1974), 88–103 (Adamson 1990)
Paraffin wax	110 at r.t. (Adamson 1990)
Naphthalene	88 at r.t. (Adamson 1990)
Stearic acid	80 at 20.5 °C (Tadros et al. 1974)
Alumina	30 at 20 °C (Janczuk and Bialopiotroeicz 1988)
Marble ($CaCO_3$)	18 at 20 °C (Janczuk and Bialopiotroeicz 1988)
Quartzit	20 at 20 °C (Janczuk and Bialopiotroeicz 1988)
Sapphire	35 at 28.7 °C (Volyak et al. 1975)
Quartz	6 at 20 °C (Volyak et al. 1975)
Polyacrylamide	41 at r.t. (Kreuter 1983)
Polymethylmetacrylate	73 at r.t. (Kreuter 1983)
Polytetrafluoroethylene	99 at 23 °C (Kamusewitz and Possart 1985), 98–112 (Adamson 1990)
Silver	80 at r.t. (Erb 1968)
Gold	65 at r.t. (Erb 1968)
Palladium	63 at r.t. (Erb 1968)
Platinum	40 at r.t. (Erb 1968)
Ice	0 at 0 °C (Spagnoli et al. 2003)
Mica	23 at r.t. (Spagnoli et al. 2003)

angles subtended by an advancing and a receding water drop on a horizontal solid surface. Some typical mean θ_{ca} values for water on several kinds of solid supports in contact with air are shown in Table 4.4. Values obtained by different measurement techniques may vary by some 5°. It must also be realized that the nature of the surface of the solid (its smoothness, its purity) and any surface active solutes present in the water can change profoundly the contact angles, hence the wettability, of the solid. Water repellent coatings and spreading agents change surfaces to more hydrophobic and more hydrophilic, respectively. Trisiloxane is a superspreading agent permitting complete wetting by water of a hydrophobic surface (Hill 1998). When $\gamma_{SG} - (\gamma_{SW} + \gamma_{WG}) > 0$ spreading is energetically favoured as the contact angle becomes small. On the other hand, a certain roughness of the surface, with its micro- or nanometer scale grooves being filled by air, can transform a hydrophobic surface to a superhydrophobic one (Ferrari and Ravera 2010).

Vogler (1999) defined a transition region between hydrophobic and hydrophilic surfaces at contact angles between 74 and 56°, and distinguished two types of biological response to such surfaces. On hydrophobic surfaces the structure of the water is more nearly tetrahedral and open, whereas on the more hydrophilic surfaces it is more compact.

The surface energetics of wetting of solid substrates by water was discussed by Tarasevich (2008). When water is sorbed from the vapor on a vacuum-degassed solid

surface it may form a thin film on it of 8–15 nm thickness (total wetting). Then the heat released per unit surface area is given simply by $H_{WG} = \gamma_{WG} - T(d\gamma_{WG}/dT)$, independent of the nature of the support, because according to Young's rule, Eq. (4.15), the solid/liquid and solid/vapor interactions cancel out. However, when not sufficient water is sorbed to form a continuous film, the heat of wetting per unit area of surface, q, distinguished between different sorbents, i. e., adsorbing surfaces. Typical values of $q/\text{mJ m}^{-2}$ are 48 for graphite, 160 for Aerosil, 240 for silica gel, 335 for γ-alumina, and 430 for quartz. The interaction of water and well-characterized single crystal surfaces of metals, semiconductors and oxides was reviewed by Thiel and Madey (1987) and later by Henderson (2002) under conditions where no complete covering (film production) is achieved. Monolayers of water sorbed on metal surfaces were reviewed by Hodgson and Haq (2009).

The molecular structure of the water at interfaces, that is, wetting at the nanometer scale, was reviewed by Verdaguer et al. (2006). The structures were determined by atomic force microscopy (AMF) and scanning polarization force microscopy (SPFM). On mica a fully ordered monolayer of water is formed with all the hydrogen atoms in water either hydrogen bonded to another water molecule or to the mica substrate. At ambient temperatures the contact potential of the mica surface (relative to a hydrophobic tip) decreases from 400 mV at < 10 % relative humidity (RH) to a constant value $\sim$0 mV at 20–80 % RH, as a monolayer is formed without free OH groups, and increases at $>$ 80 % RH as multilayers of water are formed, with OH groups pointing towards the vapor phase. Substrates other than mica were also discussed as was water confined in pores and between flat surfaces.

A different situation arises at the interfaces between an immersed electrode and an aqueous solution, where no vapor needs to be taken into account. Trasatti (1983) dealt with uncharged metal surfaces in contact with solutions of not specifically adsorbed ions. In the case of transition metals water is chemisorbed on the metal surface with bond strengths correlated with the density of electronic states. The water molecules are oriented with the oxygen atom towards the metal, the acidity of the adsorbed water being enhanced. In a subsequent paper Trasatti (1995) compared results for metal surfaces adsorbing water molecules in vacuum (ultrahigh vacuum (UHV) results) with those for metal electrodes immersed in the solution. The potential of zero charge, $E_{\sigma=0}$, measured against a given reference electrode is related to the measurable electronic work function of the metal (in UHV), Φ^M/F, as $E_{\sigma=0} = \Phi^M/F + (\delta\chi^M + g^S)$, where $F$is Faraday's constant, $\delta\chi^M$ is the perturbation of the pristine surface potential of the metal by contact with the solution and g^S is the sum of the free surface energy of the liquid and its modification due to the orienting field of the metal. These two quantities, $\delta\chi^M$ and g^S, cannot be disentangled, and since measurement of $E_{\sigma=0}$ requires a reference electrode, measurements of $E_{\sigma=0}$ and Φ^M cannot either yield the sum $\delta\chi^M + g^S$. However, the difference (with a given reference electrode) for two metals (or two crystal faces of a given metal) can be obtained: $\Delta E_{\sigma=0} = \Delta\Phi^M/F + \Delta(\delta\chi^M + g^S)$.

The structure of the water in the double layer at the electrode surface was reviewed by Henderson (2002) and by Ito (2008). The orientation of the water dipoles and their ordering depends on the potential imposed on the electrode/solution interface.

4.4 Solutes at the Surface of Water

Up to this point the surfaces between pure water and its vapor (or air), or another liquid, or a solid substrate have been dealt with. The situation at the free surface of an aqueous solution is also relevant in the present context. The behaviour of simple ions at the surface is dealt with first, and that of non-electrolytes and of surface active agents, ionic or non-ionic, is dealt with in the following sections.

4.4.1 Sorption and Desorption of Simple Ions

The specific ion effects at the water/air interface have recently been reviewed by Jungwirth and Tobias (2006). Since the surface region of water with respect to air or water vapor differs in properties and structure from bulk water (Sect. 4.1), it is expected that ions react to these different environments by being either attracted to or repelled from the surface. In other words, ions may be sorbed at or desorbed from the surface of an electrolyte solution. The excess concentration Γ_E (the amount of an electrolyte sorbed per unit increase of the surface energy) at the surface relative to the bulk is governed by the Gibbs adsorption law:

$$\Gamma_E = -\left(\frac{a_E}{RT}\right)\left(\frac{\partial\gamma}{(\partial a_E)_{T,P}}\right) \tag{4.16}$$

where subscript $_E$ refers to the electrolyte, a is its activity, and γ is the surface tension of the solution, and Γ_E may be positive or negative. At low molar concentrations the concentration c_E approximates the activity a_E, hence the measurable surface tension increment (*STI*) $(\partial\gamma/\partial c_E)_{T,P}$ is a key quantity regarding the role of ions at the surface. As with other thermodynamic quantities, only the value of Γ_E pertaining to an electrolyte, but not that pertaining to individual ions, Γ_I, is experimentally accessible. The latter must be estimated by an extra-thermodynamic assumption.

The surface tension of aqueous electrolytes is linear with the concentration of the electrolyte up to fairly high concentrations. Surface tension increments, $(\partial\gamma/\partial c_E)_{T,P}$, were reported by several authors and recently critically compiled by Marcus (2010) for some 90 electrolytes. These data pertain to temperatures in the range 20–30 °C, their temperature dependence being ± 0.1 mN m^{-1} mol^{-1} dm^3 over the entire 10 °C range, commensurate with the expected uncertainty of the data at a given temperature. Hence the data are referred to as valid $d\gamma/dc_E$ values for 25 °C and 0.1 MPa, and are additive in the ionic values within ± 0.2 mN m^{-1} mol^{-1} dm^3. If only the alkali metal salts are considered, it appears as if only the anions have specific effects on the *STI* as generalized by some authors (Abramzon and Gaukberg 1993; LoNostro et al. 2002), but if a larger variety of salts is considered, both cations and anions are seen to show specific effects. The most extensive data are availablefor sodium and for chloride salts, hence the *arbitrary* assumption = 0.90 for Na^+ and = 1.20 for Cl^- was adopted (Marcus 2010), with results shown in Table 4.5. However, it

Table 4.5 Ionic surface tension increments, $d\gamma/dc_I$/mN m^{-1} mol^{-1} dm^3, of aqueous ions at ambient conditions. The improved values added $0.30z_I$ units to the cation values and subtracted $0.30|z_I|$ units from the anion values (see the text)

Cation	$d\gamma/dc_I$ (Marcus 2010)	$d\gamma/dc_I$ improved	Anion	$d\gamma/dc_I$ (Marcus 2010)	$d\gamma/dc_I$ improved
H^+	−1.35	−1.05	OH^-	1.35	1.05
Li^+	0.65	0.95	F^-	1.10	0.80
Na^+	0.90	1.20	Cl^-	1.20	0.90
K^+	0.80	1.10	Br^-	0.95	0.65
Rb^+	0.65	0.95	I^-	0.35	0.05
Cs^+	0.50	0.80	SCN^-	0.20	–0.10
NH_4^+	0.40	0.70	NO_3^-	0.45	0.15
$(CH_3)_4N^+$	−0.40	−0.10	ClO_3^-	0.00	–0.30
$C(NH_2)_3^{+a}$	−0.26	0.04	ClO_4^-	–0.50	–0.80
Ag^+	0.40	0.70	HCO_2^-	0.15	–0.15
Tl^+	0.30	0.60	$CH_3CO_2^-$	0.05	–0.25
Mg^{2+}	1.65	2.25	$H_2PO_4^-$	1.25	0.95
Ca^{2+}	1.50	2.10	CO_3^{2-}	0.95	0.30
Sr^{2+}	1.20	1.80	SO_4^{2-}	1.15	0.55
Ba^{2+}	0.50	1.10	CrO_4^{2-}	1.45	0.85
Mn^{2+}	0.75	1.35	$S_2O_3^{2-}$	1.45	0.85
Co^{2+}	1.05	1.65	PO_4^{3-}	2.00	1.10
Ni^{2+}	1.10	1.70			
Pb^{2+}	1.80	2.40			
UO_2^{2+}	1.40	2.00			
Al^{3+}	1.75	2.65			
La^{3+}	2.30	3.20			

[a]Guanidinium

was subsequently realized (Marcus 2011a) that improved values, obtained by adding $0.30z_I$ units to these cation values and subtracting $0.30|z_I|$ units from these anion values (still arbitrarily) more closely describe the sorption/desorption of ions at the water/vapour interface. This expedient would bring thiocyanate, chlorate, formate, and acetate (as well as perchlorate) into the category of surface active anions (enriched at the surface) and barium cations into the category of those attracted into the surface (as well as hydronium and tetramethyl-ammonium), while maintaining additivity and correct values for entire electrolytes. This operation may improve the situation regarding most of these ions but not of all the ions listed in the table.

The obvious feature exhibited by the *STI* data in the table is their being positive in the great majority of cases. This means that the ions are desorbed from the surface region of the solution according to Eq. (4.16). The trends among ions of a given sign class, cations or anions, are independent of the arbitrary splitting of the electrolyte values into individual ionic ones. The positive values of $d\gamma/dc_I$ increase with the charges of the ions but diminish with their increasing sizes; they thus increase with their solvation energies, a correlation noted by Boström et al. (2005). This behaviour can be ascribed to the increase of the sizes of the hydration spheres of small ions with their charges and diminishing sizes. The accommodation of such hydration spheres

within the more tightly bonded water molecules (Sect. 4.1) at the surface becomes less favourable than their accommodation in the less tightly hydrogen bonded bulk water, hence they are desorbed from the surface region. Linear correlations of $d\gamma/dc_I$ for series of chloride salts with the bulk water structure effects of the ions (Sect. 3), namely with the standard molar entropy of hydration ΔS_I and the Jones-Dole viscosity $B_{\eta I}$ were noted by Weissenborn and Pugh (1996). Cations that tend to promote and compact the bulk water structure have larger positive $d\gamma/dc_I$ values than ions that break up and expand the water structure. Similar correlations (not linear) for series of sodium slats with different anions with regard to the hydrated radius and the molar entropy of the anions were noted by Maheshwari et al. (2003).

Theoretical discussions of the surface tension increments try to explain the trends noted for the various ions. Aveyard and Saleem (1976) related the *STI* of an electrolyte solution to the product of its molality and its osmotic coefficient φ:

$$\frac{d\gamma}{d(m_E\varphi)} = \frac{\nu\delta RT}{1000} \tag{4.17}$$

where ν is the stoichiometric coefficient and δ is the thickness of the surface layer from which the ions are (completely) desorbed. Values of $\delta = 0.166\nu$ nm on the average were reported for LiCl, NaCl, KCl, KBr, KI, and Na_2SO_4. This is in accord with an electrostatic theory developed by Schmutzer (1955). A recent attempt (Kunz et al. 2004) to use computations that yield values for the osmotic coefficients of electrolyte solutions in reasonable agreement with experimental values to calculate also the *STI*s, however, failed to yield results in agreement with the experimental values. A further attempt (Boström et al. 2005) in this direction, including solvation energies and dispersion potentials did not either provide reliable predicted values.

The main point to consider in a theory of the *STI* by ions is the unequal surface/bulk concentration ratios of individual ions (Randles 1977). Pegram and Record (2007, 2008) arrived at an equation similar to Eq. (4.17), namely:

$$\frac{d\gamma}{d(m_E\varphi)} = \left(\frac{RT}{1000}\right) M_W b_W{}^{\sigma} \left[1 - \frac{(\nu_+ K_+ + \nu_- K_-)}{\nu}\right] \tag{4.18}$$

where M_W is the molar mass of the water (18.015 g mol^{-1}), $b_W{}^{\sigma} = n_W{}^{\sigma}/A$ is the number of water molecules per unit surface area in the surface region, and $K_{\pm} = m_{\pm}{}^{\sigma}/m_{\pm}{}^{b}$ (superscripts $^{\sigma}$ and ^{b} denote the surface region and the bulk) is the molality ratio of the ions of either sign in the respective regions. The quantity $b_W{}^{\sigma}$ takes the place of the thickness δ in the Aveyard and Saleem expression (4.17), designating a surface layer of thickness of ~0.6 nm, i.e., of two water molecules. However, contrary to Eqs. (4.17), (4.18) does allow for the presence of ions in this surface layer. On the assumption that $K(Na^+) = 0$, values for other cations studied are $K(Li^+) = 0.08$, $K(K^+) = 0.12$, $K(Cs^+) = 0.01$, $K(NH_4{}^+) = 0.25$, $K(GuH^+) = 0.67$, and $K(H^+) = 1.50$, all ± 0.06 except for Li^+ and GuH^+ (guanidinium) that are ± 0.21. Note that only $K(H^+) > 1$, i.e., the hydrogen ions are positively sorbed in the surface region, all the other cations mentioned here being desorbed from it. For the anions, $K(Cl^-) = 0.69 \pm 0.04$ on this scale, but iodide, acetate, chlorate,

thiocyanate and perchlorate anions have K_- values >1 and should be positively sorbed to the surface region to increasing extents in this order. The arbitrary choices of the splitting into individual ionic values by Pegram and Record (2007) and by Marcus (2010) (cf. Table 4.5) is demonstrated by the fact that only perchlorate is considered as positively sorbed by the latter author, although the sequences are substantially the same. A further indication of the arbitrariness of the absolute scale in Table 4.5 is the indication from molecular dynamics simulations that whereas formate anions, HCO_2^-, are repelled from the surface region, acetate anions, $CH_3CO_2^-$, are attracted into it (Minofar et al. 2007). The 'improved' *STI*s are more consistent with these trends.

The negative value of *STI* for H^+ means that the hydronium ion is positively sorbed at the surface layer of the acid solution. Several other ions share this property, but the main attribute of such ions is their being bulky and poorly hydrated (perchlorate) and/or containing many or large hydrophobic groups. Thus reported $d\gamma/dc_I$/mN m^{-1} mol^{-1} dm^3 values are -0.40 for tetramethylammonium, -2.95 for propionate, -6.45 for butyrate (Marcus 2010) and -5.5 for benzoate and -4.3 for phenolate (Minofar et al. 2007), values that illustrate this tendency. Still, the negative value of $d\gamma/dc_I$ for the H^+ ion that is small and strongly hydrated is unique among the surface seeking ions.

Molecular dynamics simulations on both finite water clusters containing ions and extended water/air surfaces have been reviewed by Jungwirth and Tobias (2006). They showed that the hydrogen ions, whether as hydronium ions H_3O^+, or as the Zundl $H_5O_2^+$ (i.e., $H_2O\cdots H^+\cdots OH_2$) or Eigen $H_9O_4^+$ (i.e., $O(H\cdots OH_2)_3^+$) species, are positively adsorbed at the water/air interface with the dipoles pointing into the interior. That is, the hydrogen atoms point towards the bulk and form hydrogen bonds with neighbouring water molecules. Such simulations also indicated the desorption of the alkali metal cations and of F^- and Cl^- anions from the interfacial region but that Br^-, I^-, NO_3^- and N_3^- anions are attracted into this region (contrary to the surface tension increment results). The simulations also confirm that OH^- and SO_4^{2-} anions are repelled from the surface region, in agreement with the surface tension results. At relatively large salt concentrations (1.2 M) simulation results show Br^- and I^- to be strongly and Cl^- only weakly concentrated in the surface layer, whereas Na^+ and F^- are repelled from it (Jungwirth and Tobias 2002).

Theoretical considerations showed that at moderate concentrations the dispersion forces dominate over the electrostatic ones and that $d\gamma/dc_I$ should be proportional to $B_I^{1/3}$, where B_I, in turn, is proportional to the static excess polarizability of the ion in water, $R_I - R_W$ (Boström et al. 2001). For multivalent anions (not considered in (Boström et al. 2001)) B_I/z_I^2 needs to be taken into account to obtain the excess polarizability, in terms of the molar refraction: $R_I/z_I^2 - R_W$, where $R_W = 3.67$ cm^3 mol^{-1} and some R_I values (taken from (Marcus 1998)) are shown in Table 2.1. The correlation is far from perfect, as seen in Fig. 4.1, but the general trend is confirmed.

Spectroscopic methods have recently been developed that are able to probe the surface species at the water/air interface. The use for this purpose of photoelectron spectroscopy depends on the short penetration depths of electrons and the electron binding energy specificity. Böhm et al. (1994) applied photoelectron spectroscopy

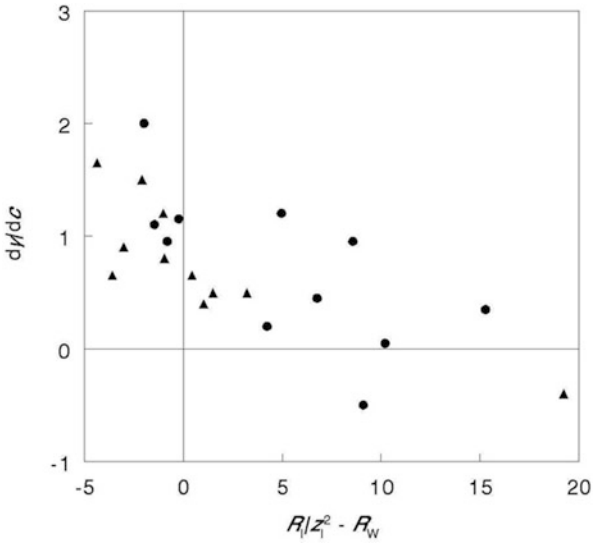

Fig. 4.1 The ionic surface tension decrement, $d\gamma/dc_I$/mN m^{-1} mol^{-1} dm^3, plotted against the ionic excess molar refractivity, $R_I/z_I^2 - R_W$ in cm^3 mol^{-1}: (●) anions and (▲) cations

to very concentrated aqueous CsF solutions and found that both ions are strongly repelled from the surface region of two water molecule thicknesses, in accord with surface tension increment results. Weber et al. (2004) and Winter et al. (2004) found similarly that both ions of NaI are repelled from the interface, but when tetrabutylammonium ions are present, iodide anions are dragged along with the bulky cations into the interfacial layer. Second harmonic generation (SHG) and vibrational sum frequency generation (VSFG) are spectroscopic methods that cannot provide signals in media with inversion symmetry, such as bulk solutions, but are allowed in asymmetrical media, such as surfaces. The results from the VSFG method on 1–2 M sodium halide solutions appear to be contradictory with respect to whether bromide and iodide are enriched in the interfacial layer with respect to their bulk concentrations (Jungwirth and Tobias 2006) but there is agreement that fluoride and chloride solutions yield VSFG spectra very similar to that of pure water. In solutions of the strong hydrohalic acids the VSFG spectra confirm enrichment of both hydrogen and halide ions at the surface, for the latter in the expected order of $Cl^- < Br^- < I^-$ (Schnitzer et al. 2000). The SHG method depends on the charge transfer to solvent spectrum measurable for polarizable (soft) anions, such as iodide, azide, and thiocyanate. All three are enhanced at the outermost surface layer, but are depleted in the sub-surface layer, whereas small, non-polarizable (hard) ions are repelled from the surface altogether. Hydrogen ions in iodide solutions are also found indirectly by the SHG method to be enhanced at the surface (with respect to sodium and potassium ions) (Petersen and Saykally 2004, 2005; Petersen et al. 2005).

Returning to traditional methods of investigation, the double layer at the surface of aqueous electrolytes described above by computer simulation and spectroscopic methods has long ago been probed by measuring the surface potential of the solutions relative to that of pure water (Randles 1957, 1977; Jarvis and Scheiman 1968). The

Table 4.6 The surface potentials of electrolyte solutions relative to that of pure water in 1 mol dm^3 aqueous solutions, $\Delta\Delta\chi$/mV at ambient temperatures (values read from figures, accurate to ±3 mV)

Anion	Cation = H^+ (Randles 1977)	Cation = Na^+ (Jarvis and Scheiman 1968)	Cation = K^+ (Randles 1977)
F^-			−3
Cl^-	22	2	3, 0[d]
Br^-	34	7	9
I^-	61	22	28, 23[d]
NO_3^-	49	8, 14[b]	
SCN^-		28	51, 53[c]
ClO_4^-	84	48[b]	
$CH_3CO_2^-$		−3	
PF_6^-			238[a, c]
CO_3^{2-}		−7	
SO_4^{2-}		−38[a]	

[a]Extrapolated to 1 mol dm^{-3}
[b]Randles (1977)
[c]Randles (1957)
[d]Jarvis and Scheiman (1968)

surface of the solutions is in most cases negatively charged with regards to the subsurface. The measurements of Randles (1957, 1977) were made with an air gap cell similar to that in Eq. (4.8), but with a jet of aqueous NaCl as the reference. The measurements of Jarvis and Scheiman (1968) were made with an ionizing electrode method instead, but with results in general agreement with the former ones. The values of $\Delta\Delta\chi = \Delta\chi(\text{electrolyte}) - \Delta\chi(\text{water})$ deduced from these papers for a 1 M solution are shown in Table 4.6. The trend of $\Delta\Delta\chi$ with the concentration is approximately linear up to this concentration. Not shown in Table 4.6 are trends with respect to further cations, which are: $Li^+ < Na^+ < K^+ \sim NH_4^+ \sim Cs^+$ for the chlorides and $Mg^{2+} > Ca^{2+} > Sr^{2+} > Ba^{2+}$ for chlorides and nitrates (the value for $BaCl_2$ is negative).

4.4.2 Surface Behaviour of Water-Miscible Non-Electrolytes

Contrary to electrolytes consisting of small ions that generally increase the surface tension of water, solutions of non-electrolytes tend to have surface tensions lower than that of water. Liquid non-electrolytes at ambient conditions, i.e., solvents that are immiscible with water but have a limited solubility in it, were already dealt with in Sect. 4.2. The surface tensions of aqueous organic solutes were reported in Adamson's book (Adamson 1990). The molecules of organic molecules tend to concentrate at the solution surface, they are surface active.

Molecules of substances that are miscible with water are rather small and of them alkanols have received the most attention. Bandyopadhyay et al. (2010) attempted to interpret the data in terms of the balance between hydrophobic and hydrophilic

groups. At low concentrations those of methanol, ethanol, 2-propanol and 2-methyl-2-propanol (*t*-butanol) and 1,2-ethanediol tend to be enhanced at the surface, their surface excesses being positive (at 25 °C, subscript$_S$ denotes the alkanol):

$$\Gamma_S = -(RT)^{-1}\left(\frac{\partial\gamma}{\partial \mathrm{Inc}_S}\right)_{T,P} > 0 \tag{4.19}$$

S-shaped curves $\Gamma_S(c_S)$ result for all the alkanols. Methanol, as well as 1,2-ethanediol, continue to have $\Gamma_S > 0$ values as the concentration increases. The other alkanols studied revert to negative values of Γ_S after the maximum but then increase again to positive values at higher concentrations. Water is desorbed from the surface, the Γ_W values are negative for all the alkanols over the entire concentration range, except for aqueous 2-methyl-2-propanol, where $\Gamma_W > 0$ was noted at $0.22 \leq x_S \leq 0.43$.

The excess surface tension values:

$$\gamma^E = \gamma - x_W\gamma_W{}^* - x_S\gamma_S{}^* \tag{4.20}$$

where the asterisks denote the pure substance are also instructive. The values of γ^E are negative for all the alkanols studied. Methanol has a minimal γ^E near $x_S = 0.23$. As more and more CH_3 groups replace the hydrogen atoms of methanol the minimum becomes deeper and shifts to lower x_S values: 0.17 in aqueous ethanol, 0.09 in 2-propanol, and 0.075 in 2-methyl-2-propanol, but at a higher $x_S = 0.29$ when a hydrophilic CH_2OH group replaces a hydrogen atom of the methanol methyl group in 1,2-ethanediol (Bandyopadhyay et al. 2010). This behaviour is similar to that observed for bulk properties, e.g., the excess partial molar volume of water in these mixtures, $V_W{}^E$, that describes the enhancement of the tetrahedral structure of the water (Marcus 2010b) (Sect. 1.2.4).

More sophisticated approaches than this discussion of the surface tensions of aqueous solutions of organic compounds miscible with water have also been applied. The surface of aqueous methanol mixtures has been studied both experimentally, with non-linear optical methods (Sect. 4.4.1), and by computer simulations, starting in the 1990's. The VSFG method was applied by Huang and Wu (1994) who found the methanol molecules at the surface to have an enhanced polar order, that is, the symmetry axis of the methyl groups which point towards the vapor phase has a smaller tilt angle θ from the vertical as the total methanol concentration increases. Molecular dynamics simulations by Matsumoto et al. (1993) confirm the accumulation of methanol at the surface, the surface layer becoming saturated with methanol even at low concentrations of the latter. The thickness of the surface layer, $t_{9/1}$ (Sect. 4.1) increases non-linearly with the composition from 0.40 nm in water to 0.76 nm in methanol. The VSFG method was again applied to aqueous methanol by Ma and Allen (2003) who found that at $x_{MeOH} > 0.57$ the tilt angle θ of the methanol axis (deviations from verticality) again increases, indicating less orientational order than at lower concentrations. Interfacial methanol is a more efficient hydrogen bond acceptor than bulk methanol. The molecular dynamics study of the surface of mixtures

of water and methanol by Chang and Dang (2005) substantially confirms the previous results. Furthermore, the number of hydrogen bonds between methanol and water molecules per methanol molecule diminishes as the total methanol concentration increases. A newly developed VSFG technique was applied by Chen et al. (2005) to show more ordered methanol orientations, i.e., tilt angles θ nearer zero, than previously found (Maheshwari et al. 2003). Although methanol is enriched in the surface layer, with an energy of adsorption of -7 kJ mol^{-1}, it is depleted at the next layer, with a desorption energy of ca. $+2$ kJ mol^{-1}. Partay et al. (2005, 2008) again used computer simulations for the surface of aqueous methanol mixtures. The Monte Carlo simulations (Partay et al. 2005) confirmed the methanol enrichment in the surface layer and its depletion in the first sub-surface layer, where the molecules are not correlated with those at the surface that are oriented perpendicularly to the surface.

Application of the truly interfacial molecular layer concept (ITIM, Sect. 4.1) to the aqueous methanol surfaces (Partay et al. 2008a) employed molecular dynamics simulations. Noting the roughness of the surface, methanol molecules prefer the humps and water molecules the depressions of the surface. A microscopic separation of the two kinds of molecules in the plane of the surface was also observed. The surface adsorption of the methanol molecules is attributed to their ability to remain at the surface without losing any of their hydrogen bonding with neighbours, contrary to water molecules. The residence time of methanol molecules at the surface is nearly an order of magnitude longer than that of water molecules. However, contrary to other studies, no depletion of methanol in the layer below the surface layer could be observed, and the properties of this layer are essentially the same as of the bulk mixture. The discrepancies noted among the results of different methods remain to be disentangled.

The surface of aqueous ethanol solutions was studied by molecular dynamics simulations at a single composition, $x_S = 0.1$ at 25 °C by Tarek et al. (1996). The computed surface tension of 55 mN m^{-1} was however much larger than the experimental value, so that the computed results were considered to apply to $x_S = 0.016$ instead of the nominal value of 0.1. The computed excess surface concentration $\Gamma_S = 3.6 \pm 0.5 \times 10^6$ mol m^{-2} agrees fairly well with the experimental value for this composition, 2.8×10^{-6} mol m^{-2} (Bandyopadhyay et al. 2010). The main result is the number density profiles for ethanol and water molecules, showing enrichment of the surface layer with ethanol but its depletion of the subsurface layer, where water is relatively enriched. Ethanol-ethanol hydrogen bonds are increased in number in the surface layer relative to bulk ethanol, but the hydrogen bonding of water with the ethanol as the acceptor are diminished by a factor of two (Tarek et al. 1996). A subsequent molecular dynamics study by Wilson and Pohorille (1997) at an even lower ethanol content, $x_S = 0.00204$, at 37 °C addressed mainly the dynamic effects of the surface sorption of the ethanol. Neutron and x-ray grazing incidence reflection were applied by Li et al. (1993) to dilute aqueous ethanol mixtures. The surface excess Γ_S values agreed approximately with the experimental values. The results suggested that the ethanol molecules are partially oriented with the ethyl group pointing towards the vapor phase.

Acetone at the surface of its aqueous solutions was studied by the VSFG method, probing the stretching mode of the methyl group, by Chen et al. (2005a) over the entire composition range. They found acetone to have the carbonyl group pointing into the solution and one methyl group directed towards the vapor phase and the other towards the solution. The effective average interfacial number density of methyl groups was calculated and showed a maximum near $x_S = 0.1$. This was interpreted as due to a well ordered surface layer becoming saturated with acetone molecules at this composition but having a partially ordered anti-parallel oriented layer of acetone molecules below it that grows as the bulk concentration of the acetone increases. Both layers can be described in terms of Langmuir sorption isotherms with a surface fractional coverage Θ:

$$\Theta = \frac{K x_S}{(1 - x_S + K x_S)} \tag{4.21}$$

with the equilibrium constant K for the surface layer being 5 times larger than that for the subsurface one.

Aqueous acetonitrile mixtures are interesting in that micro-heterogeneity sets in at ca. $x_S \geq 0.3$ in the bulk (Marcus and Migron 1991; Marcus 2008a), and is expected to be manifested at the surface starting at lower total acetonitrile concentrations, since the solute is enriched at the surface. Zhang et al. (1993) applied the VSFG technique and found an abrupt change in the CN stretching frequency as x_S increases above 0.07 in the bulk, changing from that characteristic of the C–N group hydrogen bonded to water to a frequency close to that in neat CH_3CN. The orientation of the CH_3CN molecules changed at this composition from one vertical to the surface (with methyl groups pointing towards the vapor) to one more parallel to the surface, as in the neat acetonitrile/vapor surface. A subsequent VSFG study by Kim et al. (2003) studied the C–H stretching mode of the CH_3CN at the surface and confirmed the near perpendicular orientation of the molecules with respect to the surface, with tilting angles up to 13°. No abrupt changed at $x_S = 0.07$ could be observed, but a maximal oscillator strength near $x_S = 0.1$ was found. This was ascribed to a combination of the excess surface concentration of acetonitrile (estimated from the surface tension) and its orientational preference. The surface mole fraction of CH_3CN increased steeply with x_S up to $x_S \sim 0.07$, where it is 0.45, then only slightly up to $x_S \sim 0.20$, beyond which it increases more gradually again.

The molecular dynamics simulation by Paul and Chandra (2005) of aqueous acetonitrile estimated the thickness of the interfacial layer $t_{9/1}$ (Sect. 4.1) that increases nearly linearly with x_S from 0.34 nm in water to 0.45 in CH_3CN. Contrary to the previous work, they found the orientation of the CH_3CN molecules to be parallel to the surface rather than perpendicular, but the models used for the simulations yielded surface tension values to be nearly twice the experimental ones at $x_S \geq 0.25$, so that some of the conclusions need revision. A subsequent molecular dynamics study by Partay et al. (2009) using the ITIM (Sect. 4.1) concept was applied at four concentrations up to $x_S = 0.15$. The strong interfacial enrichment of CH_3CN observed experimentally by VSFG was confirmed with compositions (total, surface) of (0.03, 0.23), (0.05, 0.42), (0.10, 0.70), and (0.15, 0.88). It was concluded that also

the sub-surface layer was enriched in acetonitrile and at sufficiently high x_S also the third layer was enriched. The molecules in the second layer are well correlated with those at the surface with strong dipolar interactions in the anti-parallel configuration. The orientational preferences of the CH_3CN molecules are dictated by the necessity to have as many methyl groups sticking outwards to the vapor as possible. Lateral association of like molecules at the surface was also found. The residence times of the acetonitrile molecules at the surface were manifold longer than those of the water molecules: 14.7 ps vs. 2.2 ps at $x_S = 0.15$.

Non-linear optical methods (Sect. 4.4.1) were applied to the surface of aqueous dimethylsulfoxide (DMSO) mixtures. Karpovich and Ray (1998) applied the SHG method and interpreted the results in terms of a Langmuir isotherm with a Gibbs energy of adsorption of -11.8 kJ mol^{-1}in agreement with the value derived from surface tension data and twice as large than the corresponding value deduced for the sorption of ethanol (Wilson and Pohorille 1997). Allen et al. (1999) applied the VSFG method and complemented it with surface tension measurements. Although DMSO hydrogen bonds readily with water, it is strongly accumulated at the surface at even very low concentrations. These authors found an even larger Gibb energy of adsorption of -19.8 kJ mol^{-1}for the DMSO at the surface than in (Karpovich and Ray 1998). A smaller Gibbs energy of adsorption of -9 kJ mol^{-1} resulted from the molecular dynamics simulations by Benjamin (1999) at four values of x_S: 0.05, 0.10, 0.15, and 0.20. There is a tendency for the DMSO at the surface to have its methyl groups pointing away from the bulk, as is observed for the other solutes examined above (methanol, ethanol, acetone and acetonitrile). The dipole axis is tilted about 60° from the perpendicular to the surface. A large negative surface potential of -0.5 to -0.7 V results from the sorption of DMSO at the interface in aqueous DMSO solutions according to the simulation, in agreement with experiment. The dynamics of the sorption of DMSO at the surface was also investigated.

4.5 Surfactants, Micelles and Vesicles

Hydrophobic groups tend to be driven out from the bulk aqueous solutions as seen above for both ions (alkylammonium ions, carboxylates, etc.) and water miscible organic solutes. When the hydrophobic group becomes large enough the solute becomes only partly soluble in water, and the exclusion of the hydrophobic parts of molecules and ions is intensified when long chain non-polar groups (tails) are attached to polar groups (heads, that may be neutral or ionic). The resultant solutes are called amphiphiles and are then surfactants and their sorption at the interface conveys onto the solutions special properties and structures.

There exists a plethora of books concerning surfactants (on the average of 60 per decade, for example (Adamson 1990) and more recently (Wendt and Hoysted 2010; Neumann et al. 2011; Tadros 2011), and review articles (increasing from ∼100 per year in 1982–1991 to ∼300 per year in 2002–2011), so it is counter-productive to

review the subject within the scope of the present book. Hence, only the broad outline of the subject and the main concepts involved are described here.

Typical ionic surfactants are sodium dodecylsulfonate, sodium dodecylsulfate and cetyltrimethylammonium bromide. Typical non-ionic surfactants are short copolymers $H(C_2H_4)_n(OC_2H_4)_mOH$ with $6 \leq n \leq 12$ and $6 \leq m \leq 10$ as well as certain bio-molecules such as diacylglycerides. Such molecules or electrolytes are soluble in water at low concentrations (and are the so-called monomers). They may form monolayers at the surface with the heads pointing towards the bulk aqueous phase and the tails pointing towards the vapor phase.

With longer tails (more than ca. 8 carbon atoms) the surfactants tend to aggregate. As the concentration of the surfactant increases above a certain concentration, called the critical micelle concentration (*cmc*) it may remain macroscopically in a homogeneous aqueous phase, but the molecules aggregate to micelles. These may be spherical or ellipsoidal, depending on the tail length and have the tails pointing towards the interior of the micelle and the heads at its surface. As the *cmc* is exceeded there occurs an abrupt change in the properties of the solutions, such as the surface tension and light scattering and in the case of ionic surfactants also the conductivity. With the latter surfactants a double layer is established at the outer layer of the micelle, with counter-ions being sorbed near the ionic groups fixed to the tails. An important feature of micelles is their ability to solubilize non-polar molecules, such as water-insoluble dyes, into their interiors. Added salts generally diminish the *cmc* of micelle formation, roughly according to the extent of the hydration of their ions, whereas urea acts in the opposite direction, it increases the *cmc*. The number of surfactant molecules per micelle is of the order of 50–100 and micelles have radii of the order of 1.5 nm. At low concentrations micelles tend to be spherical but non-spherical micelles result at higher concentrations, and they may be plate-like (oblate) or rod-like (prolate). Hydrodynamic methods yield information on the micellar shapes.

When micelles grow to very large sizes they tend to break into bilayers that form membranes or vesicles. The latter are structures with an outer layer of surfactant molecules with heads pointing towards the bulk aqueous solutions and tails pointing inwards, meeting the tails of the inner layer of surfactant molecules, the heads of which point towards an inner aqueous solution. Such vesicles (also termed vacuoles) may be used to transport drugs that are to be released slowly within the body. Bilayers play an important role in physiology as they constitute the membranes of cells, permitting some substances (or ions) to pass through them in either direction while stopping others. Diglycerides and phospholipids are typical examples of the constituents of such membranes. The former are di-esters of glycerol with fatty acids, such as oleic or palmitic acid. The latter have a further acidic group esterifying the glycerol, namely phosphoric acid, that may in turn be bound to choline in a typical phospholipid, namely the phosphatidylcholine known as lecithin of egg yolk. The main point here is that such membranes separate the intra-cellular aqueous solution of the cell from the extra-cellular one and act as gate-keepers between these two aqueous environments.

References

Abramzon AA, Gaukberg RD (1993) Surface tension of salt solutions. J Appl Chem 66:1139–1147, 1315–1320

Adamson AW (1968) An adsorption model for contact angle and spreading. J Coll Interf, Sci 27:180–181

Adamson AW (1990) Physical chemistry of surfaces, 5th ed. Wiley, New York, p 101 ff

Alejandro J, Tildesley DJ, Chapela GA (1995) Molecular dynamics simulation of the orthobaric densities and surface tension of water. J Chem Phys 102:4574–4583

Allen HC, Gregson DE, Richmond DL (1999) Molecular structure and adsorption of dimethyl sulfoxide at the surface of aqueous solutions. J Phys Chem B 103:660–666

Aveyard R, Saleem SM (1976) Interfacial tensions at alkane-aqueous electrolyte interfaces. J Chem Soc, Faraday Trans 1(72):1609–1617

Bandyopadhyay G, Dutta S, Lahiri SC (2010) Determination of surface tension, structural, and related properties of aquo-alcohol mixtures at 298 K. Z Phys Chem (Munich) 224:729–742

Benjamin I (1996) Chemical reactions and solvation at liquid interfaces: a microscopic perspective. Chem Rev 96:1449–1475

Benjamin I (1999) Structure, thermodynamics, and dynamics of the liquid/vapour interface of water/dimethylsulfoxide mixtures. J Chem Phys 110:8070–8079

Benjamin I (2005) Hydrogen bond dynamics at water/organic liquid interfaces. J Phys Chem B 109:13711–13715

Böhm R, Morgner H, Oberbrodhage J, Wulf M (1994) Strong salt depletion at the surface of highly concentrated aqueous solutions of CsF, studied by HeI-UPS. Surf Sci 317:407–421

Boström M, Kunz W, Ninham BW (2005) Hofmeister effects in surface tension of aqueous electrolyte solutions. Langmuir 21:2619–2623

Boström M, Williams DRM, Ninham BW (2001) Surface tension of electrolytes: specific ion effects explained by dispersion forces. Langmuir 17:4475–4478

Carey BS, Scriven LE, Davis HT (1978) Semiempirical theory of surface tensions of pure normal alkanes and alcohols. AIChE J 24:1076–1080

Chang T-M, Dang LX (1996) Molecular dynamics simulations of CCl_4-H_2O liquid-liquid interface with polariazble potential models. J Chem Phys 104:6772–6783

Chang T-M, Dang LX (2005) Liquid-vapor interface of methanol-water mixtures: a molecular dynamics study. J Phys Chem B 109:5759–5765

Chen H, Gan W, Lu R, Guo Y, Wang H-F (2005) Determination of structure and energetics for Gibbs surface adsorption layers of binary liquid mixture. 1. Acetone + water. J Phys Chem B 109:8053–8063

Chen H, Gan W, Lu R, Guo Y, Wang H-F (2005a) Determination of structure and energetics for Gibbs surface adsorption layers of binary liquid mixture. 2. Methanol + water. J Phys Chem B 109:8064–8075

de Gennes PG (1985) Wetting: statics and dynamics. Rev Mod Phys 57:827–863

Erb RA (1968) Wettability of metals under continuous condensing conditions. J Phys Chem 69:1306–1309

Ferrari M, Ravera F (2010) Surfactants and wetting at superhydrophobic surfaces: water solutions and non aqueous liquids. Adv Coll Interf Sci 161:22–28

Freitas AA, Quina FH, Carroll FA (1997) Estimation of water-organic interfacial tensions. A linear free energy relationship analysis of interfacial adhesion. J Phys Chem B 101:7488–7493

Guerrero MI, Davis HT (1980) Gradient theory of surface tension of water. Ind Eng Chem Fund 19:309–311

Guggenheim EA (1945) The principle of corresponding states. J Chem Phys 13:253–265

Hantal G, Darvas M, Partay LB, Horvai G, Jedlovszky P (2010) Molecular level properties of the free water surface and different organic liquid/water interfaces, as seen from ITIM analysis of computer simulation results. J Phys: Condens Matter 22(28):284112–1/14

Henderson MA (2002) The interaction of water with solid surfaces: fundamental aspects revisited. Surf Sci Rep 46:1–308

Hill RM (1998) Superspreading. Curr Opinion Coll Interf Sci 3:247–254
Hodgson A, Haq S (2009) Water adsorption and the wetting of metal surfaces. Surf Sci Rep 64:381–451
Hore DK, Walker DS, MacKinnon L, Richmond GL (2007) Molecular structure of the chloroform-water and dichloromethane-water interfaces. J Phys Chem C 111:8832–8842
Huang JY, Wu MH (1994) Nonlinear optical studies of binary mixtures of hydrogen bonded liquids. Phys Rev E 50:3737–3746
Ito M (2008) Structures of water at electrified interfaces: microscopic understanding of electrode potential in electric double layers on electrode surfaces. Surf Sci Rep 63:329–389
Janczuk B, Bialopiotroeicz T (1988) Components of surface free energy of some clay minerals. Clays Clay Min 36:243–248
Jarvis NL, Scheiman MA (1968) Surface potentials of aqueous electrolyte solutions. J Phys Chem 72:74–78
Jedlovszky P (2004) The hydrogen bonding structure of water in the vicinity of apolar interfaces: a computer simulation study. J Phys: Condens Matter 16:S5389–S5402
Jhon MS, van Artsdalen ER, Ghosh J, Eyring H (1967) J Chem Phys 47:2231–2238
Jungwirth P, Tobias DJ (2002) Molecular structure of salt solutions: a new view of the interface with implications for heterogeneous atmospheric chemistry. J Phys Chem B 105:10468–10472
Jungwirth P, Tobias DJ (2006) Specific ion effects aqt the air/water interface. Chem Rev 106:1259–1281
Kamusewitz H, Possart W (1985) The static contact angle hysteresis obtained by different experiments for nthe system PTFE/water. Int J Adhes Adhes 5:211–215
Karpovich DS, Ray DJ (1998) Adsorption of dimethyl sulfoxide to the liquid/vapor interface of water and the thermochemistry of transport across the Interface. Phys Chem B 102:649–652
Kereszturi A, Jedlovszky P (2005) Computer simulation investigation of the water-benzene interface in a broad range of thermodynamic states from ambient to supercritical conditions. J Phys Chem B 109:16782–16793
Kim J, Chou KC, Somorjai GA (2003) Structure and dynamics of acetonitrile at the air/liquid interface of binary solutions studied by infrared-visible sum frequency generation. J Phys Chem B 107:1592–1596
Koczorowski Z, Zagorska I (1983) Investigations on volta potentials in water-nitrobenzene systems and the surface potentials of these solvents. J Electroanal Chem 159:183–193
Koczorowski Z, Zagorska I (1985) On the surface and zero charge potentials at the water/nitrobenzene interface. J Electroanal Chem 190:257–260
Koczorowski Z, Zagorska I, Kalinska A (1989) Differences between surface potentials of water and some organic solvents. Electrochim Acta 34:1857–1862
Kreuter J (1983) Physicochemical characterization of polyacrilic nanoparticles. Int J Pharmaceut 14:43–58
Krishtalik LI, Alpatova NM, Ovsyannikova EV (1992) Determination of the surface potentials of solvents. J Electroanal Chem 329:1–8
Kunz W, Belloni L, Bernard O, Ninham BW (2004) Osmotic coefficients and surface tensions of aqueous electrolyte solutions: role of dispersion forces. J Phys Chem B 108:2398–2404
Lee L-H (2000) The gap between the measured and calculated liquid-liquid interfacial tensions derived from contact angles. J Adhesion Sci Technol 14:167–185
Li ZX, Lu JR, Styrkas SA, Thomas RK, Rennie AR, Penfold L (1993) The structure of the surface of ethanol/water mixtures. Mol Phys 80:925–939
LoNostro P, Fratoni L, Ninham BW, Baglioni P (2002) Water absorbency by wool fibers: hofmeiter effect. Biomacromol 3:1217–1224
Ma G, Allen HC (2003) Surface studies of aqueous methanol solutions by vibhrational broad bandwidth sum frequency generation spectroscopy. J Phys Chem B 107:6343–6349
Maheshwari R, Sreeram KJ, Dhathathreyan A (2003) Surface energy of aqueous msolutions of Hofmeister electrolytes at air/liquid and solid/liquid interface. Chem Phys Lett 375:157–161
Marcus Y (1998) The properties of solvents. Wiley, Chichester

Marcus Y (2008) Properties of individual ions in solution. In: Bostrelli DV (ed) Solution chemistry research progress. Nova Science publishers, Inc., Hauppauge, p 51–68
Marcus Y (2008a) Clustering in liquid mixtures of water and acetonitrile. In: Bostrelli DV (ed) Solution chemistry research progress. Nova Science, Publishers, Inc., Hauppauge pp 1–4
Marcus Y (2010) Surface tension of aqueous electrolytes and ions. J Chem Eng Data 55:3641–3644
Marcus Y (2011a) Unpublished results
Marcus Y (2011b) Water structure enhancement in water-rich binary solvent mixtures. J Mol Liq 158:23–26
Marcus Y, Migron Y (1991) On the polarity, hydrogen bonding, and structure of mixtures of water and cyanomethane. J Phys Chem 95:400–406
Matsumoto M, Takaoka Y, Kataoka Y (1993) Liquid/vapour interface of water-methanol mixture. 1. Computer simulation. J Chem Phys 96:1464–1472
Mayer SW (1963) Dependence of surface tension on temperature. J Chem Phys 38:1803–1808
Mayer SW (1963a) A molecular parameter relationship between surface tension and liquid compressibility. J Phys Chem 67:2160–2164
Michael D, Benjamin I (1995) Solute orientational dynamics and surface roughness of water/hydrocarbon interfaces. J Phys Chem 99:1530–1536
Michael D, Benjamin I (1998) Molecular dynamics simulation of the water/nitrobenzene interface. J Electroanal Chem 450:335–345
Minofar B, Jungwirth P, Das MR, Kunz W, Mahiuddin S (2007) Propensity of formate, acetate, benzoate, and phenolate for the aqueous solution/vapour interface: surface tension measurements and molecular dynamics simulations. J Phys Chem. C 111:8242–8247
Neumann AW, David R, Zuo Y, eds (2011) Applied surface thermo-dynamics, 2nd ed. CRC Press, Boca Raton, USA, pp 743
Parfenyuk VI (2002) Surface potential at the gas-aqueous solution interface. Coll J 64:588–595; Koll Zh 64:651–659
Partay L, Jedloszky P, Vincze A (2005) Structure of the liquid-vapor interface of water-methanol mixtures from Monte Carlo simulations. J Phys Chem B 109:20493–20503
Partay L, Jedloszky P, Vincze A, Horvai G (2008) Properties of free surface of water-methanol mixtures. An analysis of the truly interfacial molecular layer in computer simulation. J Phys Chem B 112:5428–5438
Partay LB, Hantal G, Jedlovszky P, Vincze A, Horvai G (2008a) A new method for determining the interfacial molecules and characterizing the surface roughness in computer simulations. Application to the liquid-vapor interface of water. J Comput Chem 29:945–956
Partay LB, Jedlovszky P, Horvai G (2009) Structure of the liquid-vapor interface of water-acetonitrile mixtures as seen from molecular dynamics simulations and identification of truly interfacial molecules analysis. J Phys Chem C 113:18173–18183
Paul S, Chandra A (2005) Liquid-vapor interfaces of water-acetonitrile mixtures of varying composition. J Chem Phys 123:184706–1/8
Pegram LM, Record MT Jr (2007) Hofmeister salt effects on surface tension arise from partitioning of anions and cations between bulk water and the air-water interface. J Phys Chem B 111:5411–5417
Pegram LM, Record MT Jr (2008) Quantifying accumulation or exclusion of H^+, OH^-, and Hofmeister salt ions near interfaces. Chem Phys Lett 467:1–8
Petersen PB, Saykally RJ (2004) Confirmation of enhanced anion concentration at the liquid water surface. Chem Phys Lett 397:51–55
Petersen PB, Saykally RJ (2005) Evidence for an enhanced hydronium concentration at the liquid water surface. J Phys Chem B 109:7976–7980
Petersen PB, Saykally RJ, Mucha M, Jungwirth P (2005) Enhanced concentration of polarizable anions at the liquid water surface: SHG spectroscopy and MD simulations of sodium thiocyanide. J Phys Chem B 109:10915–10921
Pierotti RA (1967) On the scaled-particle theory of dilute aqueous solutions. J Phys Chem 71:2366–2367

Randles JEB (1957) Ionic hydration and the surface potential of aqueous electrolytes. Disc Faraday Soc 24: 194–199
Randles JEB (1977) Structure of the free surface of water and electrolyte solutions. Phys Chem Liq 7:107–179
Reiss H, Frisch HL, Elfant E, Leibowitz JL (1960) Aspects of the statistical thermodynamics of real fluids. J Chem Phys 32:119–124
Richards TW, Carver, EK (1921) A critical study of the capillary-rise method of determining surface tension, with data for water, benzene, toluene, chloroform, carbon tetrachloride, ether and dimethylaniline. J Am Chem Soc 43:827–847
Schmutzer, E (1955) The theory of surface tension of solutions. The connection between radial distribution functions and the thermodynamic functions. Z Phys Chem (Leipzig) 204:131–156
Schnitzer C, Baldelli S, Schulz MK (2000) Sum frequency generation of water on NaCl, $NaNO_3$, $KHSO_4$, HCl, HNO_3, and H_2SO_4 aqueous solutions. J Phys Chem B 104:585–590
Spagnoli C, Loos K, Ulman A, Cowan MK (2003) Imaging structured water and bound polysaccharides on mica surface at ambient temperature. J Am Chem Soc 125:7124–7128
Stillinger PH, Ben-Naim A (1967) Liquid-vapor interface potential for water. J Chem Phys 47:4431–4437
Tadros ME, Hu P, Adamson AW (1974) Adsorption and contact angle studies. 1. Water and smooth carbon, linear polyethylene, and stearic acid-coated copper. J Coll Interf, Sci 49:184–195
Tadros TF, (ed) (2011) Self-organized surfactant structures. Wiley-VCH Verlag, Germany, pp 270
Tarasevich YuI (2008) Energetics of the interaction of water and other liquids with bthe surface of hydrophilic and hydrophobic sorbents according to data on the heats of wetting. Theor Exptl Chem 44:1–23
Tarek M, Tobias DJ, Klein ML (1996) Molecular dynamics investigation of the surface/bulk equilibrium in an ethanol-water solution. J Chem Soc, Faraday Trans 92:559–563
Taylor RS, Dang LX, Garrett BC (1996) Molecular dynamics simulations of the liquid/vapour interface of SPC/E water. J Phys Chem 100:11720–11725
Thiel PA, Madey TE (1987) The interaction of water with solid surfaces: fundamental aspects. Surf Sci Rep 7:211–385
Tolman RC (1949) The effect of droplet size on surface tension. J Chem Phys 17:118–128, 333–227
Trasatti S (1974) Relative and absolute electrochemical quantities. Components of the potential difference across the electrode-solution interface. J Chem Soc, Faraday Trans 1(70):1752–1768
Trasatti S (1983) Physical, chemical, and structural aspects of the electrode/solution interface. Electrochim Acta 28:1083–1091
Trasatti S (1987) Interfacial behaviour of non-aqueous solvents. Electrochim Acta 32:843–850
Trasatti S (1995) Surface science and electrochemistry: concepts and problems. Surf Sci 335: 1–9
Verdaguer A, Sacha GM, Bluhm H, Salmeron M (2006) Molecular structure of water at interfaces: wetting at the nanometer scale. Chem Rev 106:1478–1510
Vogler EA (1999) Water and the acute biological response to surfaces. J Biomater Sci Polymer Edn 10:1015–1045
Volkov AG, Deamer DW (1996) Liquid-liquid Interfaces. Theory and methods. CRC Press, Boca Raton, USA
Volyak LD, Stepanov VG, Tarlakov YV (1975) Temperature dependence of the angle of contact of water and water-d2 on quartz and sapphire. Zh Fiz Khim 49:2931–3133
Walker DS, Moore FG, Richmond GL (2007) Vibrational sum frequency spectroscopy and molecular dynamics simulations of the carbon tetrachloride-water and 1,2-dichloromethane-water interfaces. J Phys Chem C 111:6103–6112
Wang J, Zeng XC (2009) Computer simulation of liquid-vapor interfacial tension: Lennard-Jones fluid and water revisited. J Theo Comp Chem 8:733–763
Watts A, VanderNoot TJ (1996) The electrical double layer at liquid-liquid interfaces. In: Volkov AG, Deamer DW, (eds) Liquid-liquid Interfaces. Theory and methods. CRC Press, Boca Raton, USA, pp 77–102

Weber R, Winter B, Schmidt PM, Widdra W, Hertel IV, Dittmar M, Faubel M (2004) photoemission from aqueous alkali-metal-iodide salt solutions using EUV synchrotron radiation. J Phys Chem B 108:4729–4736

Weissenborn PK, Pugh RJ (1996) Surface tension of aqueous solutions of electyrolytes: relationship with ion hydration, oxygen solubility, and bubble coalescence. J Coll Interf Sci 184:550–563

Wendt PL, Hoysted D, (eds) (2010) Non-Ionic Surfactants. Nova Science Publishers, Hauppauge, New York, pp 360

Wilson MA, Pohorille A (1997) Adsorption and solvation of ethanol at the water liquid-vapor interface: a molecular dynamics study. J Phys Chem B 101:3130–3135

Wilson MA, Pohorille A, Pratt LR (1987) Molecular dynamics of the water liquid-vapor interface. J Phys Chem 91:4873–4878

Winter B, Weber R, Schmidt PM, Hertel IV, Faubel M, Vrbka L (2004) Molecular structure of surface-active salt solutions: photoelectron spectroscopy and molecular dynamics simulations of aqueous tetrabutylammonium iodide. J Phys Chem B 108:14558–14564

Yang B, Sullivan DE, Tjipo-Margo B, Gray CG (1991) Molecular orientational structure of the water liquid/vapour interfrace. J Phys Cond Matt 3:F109–F125

Zhang D, Gutow JH, Eisenthal KB, Heinz TF (1993) Sudden structural changes at an air/binary liquid interface: sum frequency study of the air/acetonitrile-water interface. J Chem Phys 98:5099–5101

Chapter 5
Biophysical Implications

Readers may have noticed that up to this point the "*Hofmeister series*" was not mentioned at all. This is, of course, not due to negligence, but to the insight that this concept has been mis-invoked by authors in many situations concerning ions in aqueous solutions, for which it is completely unnecessary, namely in dilute homogeneous aqueous solutions. Moreover, the concepts of water structure ordering and destruction (Chap. 3), i.e., the *kosmotropic* and *chaotropic* properties of ions, have also been mis-invoked by authors dealing with biophysical phenomena, for which alternative explanations in terms of dehydration energies or direct interactions should be better. These properties do have their place in certain biophysical implications of aqueous ions, and the Hofmeister series is a valuable phenomenological description when the aqueous ions are in the vicinity of a surface. It should also be noted that the Hofmeister series is *not identical* with the series of ions arranged according to their kosmotropic and chaotropic properties nor according to their lyotropic numbers.

Lyotropic numbers N_{lyo}, Table 5.1, were assigned to ions in the 30s of the last century by Büchner and Voet (Büchner et al. 1932; Voet 1937a, 1937b) according to their effects on colloidal systems. The lyotropic series has nowadays been to some extent superseded by the Hofmeister series, with which it is taken to be practically synonymous, but it is not so exactly. For the alkali metal cations and the halide anions the lyotropic numbers obtained from colloidal phenomena are linearly related to their enthalpies of hydration. Voet (1937a) concluded that the lyotropic series are simply related to the electric field strengths of the ions. Note that the N_{lyo} values for the alkali metal cations are not commensurate with those of the alkaline earth cations and with those of the anions.

Thus, it is urged on the researchers on solution chemistry and biophysics to call what they studied *specific ion effects* if the study does not pertain to aqueous electrolytes (ions) near surfaces at appreciable concentrations (where the *Hofmeister series* or *effect* is appropriate) nor should they invoke *kosmotropic* and *chaotropic* properties if their study does not pertain to dilute aqueous electrolytes (ions) in homogeneous solutions. The fact, that the order in a series of ions correlates with the Hofmeister series or with the series of ions according to their kosmotropic and chaotropic properties does not justify per se having such epithets in the title of the paper rather than *specific ion effects* with which the paper really deals. This field was

Y. Marcus, *Ions in Water and Biophysical Implications,*
DOI 10.1007/978-94-007-4647-3_5, © Springer Science+Business Media Dordrecht 2012

Table 5.1 Lyotropic numbers for colloidal systems. (Büchner et al. 1932; Voet 1937a)

Cation	*N*	Anion	*N*
Li^+	105.2	F^-	4.8
Na^+	100.0	OH^-	5.8
K^+	75.0	Cl^-	10.0
Rb^+	69.5	NO_2^-	10.1
Cs^+	60.0	NO_3^-	11.6
Ca^{2+}	10.0	ClO_3^-	10.65
Sr^{2+}	9.0	Br^-	11.3
Ba^{2+}	7.5	ClO_4^-	11.8
		SO_4^{2-}	2.0
		$H_2PO_4^-$	8.2
		PO_4^{3-}	3.2
		BrO_3^-	9.55
		SCN^-	13.25
		IO_3^-	6.25
		I^-	12.5

recently reviewed by Kunz (2010a) as well as in the multi-author book edited by him (Kunz 2010b).

A phenomenological term that is often used concerning biomolecules, especially proteins, but may cause confusion is "stability". Some ions have a high propensity to precipitate (salt-out) a protein but also have a diminished tendency to denaturate it and are said to stabilize the protein. Denaturaion of a protein involves destruction of its higher order structure (quaternary, tertiary, and secondary). This involves unfolding of the protein, disruption of internal hydrogen bonds and dipole interactions, and exposure of hydrophobic moieties to the external solution. On the contrary, certain other ions have a high ability to denature the protein, but although it keeps it in solution or increases its solubility (salting-in) it does so in an unfolded form, destabilizing it in terms of its biological function.

5.1 From Chaotropic to Kosmotropic Ions

The term "chaotropic" ions (anions) appears to have been coined first by Hamaguchi and Geiduschek (1962), but the introduction to and popularization in the biophysical literature of the couple of terms chaotropic and kosmotropic ions has generally been ascribed to Collins and Washabaugh (1985). These two terms derive from the Greek "chaos" (χάος), meaning disorder, "kosmos" (κόσμος), meaning order, harmony, and "tropos" (τρόπος), meaning tendency towards. When applied to ions they are in the present context synonymous with the terms "water-structure-breaking" and "water-structure-making" dealt with in Chap. 3. As discussed there, such properties are manifested at infinite dilution and pertain to ions surrounded by water. The effects on the structure of water persist also in homogeneous dilute solutions at finite concentrations, but when interionic forces become dominant or when the ions are in

a non-homogeneous region in the solution, other considerations than water structure play a role.

In dilute solutions the anions are ordered as follows, from chaotropic to kosmotropic, gleaned from Table 3.7:

$$\begin{aligned} &I^- \sim ClO_4^- > SCN^- \sim Br^- > NO_3^- \sim Cl^- > HCO_2^- \sim S_2O_3^{2-} \\ &> SO_4^{2-} > F^- \sim H_2PO_4^- > OH^- \sim CH_3CO_2^- > CO_3^{2-} > PO_4^{3-} \end{aligned} \quad (5.1)$$

Among these, F^- and $H_2PO_4^-$ are borderline anions, neither pronounced chaotropic nor kosmotropic. Those anions marked ($\sim$) as having nearly the same water structure affecting properties may have the order shown according to some criteria but a reversed order according to others. Such numerical criteria include the Jones-Dole viscosity B-coefficient B_η (Sect. 3.1.1), the NMR longitudinal relaxation time coefficient B_{NMR} (Sect. 3.1.3), the structural entropy $\Delta_{struc}S$ (Sect. 3.3.3), and the average change in hydrogen bonding geometrical factors on transfer from light to heavy water ΔG_{HB} (Sect. 3.3.4).

The corresponding series for the cations, but reversed (from kosmotropic to chaotropic) is:

$$Mg^{2+} > Ca^{2+} > Li^+ > Na^+ > NH_4^+ > (CH_3)_4N^+ > K^+ \sim Cs^+ \quad (5.2)$$

(Many more kosmotropic cations are listed in Table 3.7 and a few additional chaotropic ones too). In this series Na^+ occupies a borderline position, being neither pronounced kosmotropic nor chaotropic.

The ions listed in (5.1) and (5.2) are selected to be the same that are listed in the Hofmeister series dealt with in Sect. 5.2, but not necessarily in exactly the same order. Chapter 3 should be consulted for the details concerning the effects of ions on the structure of water in dilute solutions.

The question now arises, whether the biophysical phenomena ascribed to the ions being classified as chaotropic or kosmotropic indeed result from the effects the ions have on the structure of water or from other causes. This problem should be judged on the premise that water structure effects of ions are manifested in dilute homogeneous solutions. In fact, few biophysical phenomena take place in such solutions, since biomolecules such as proteins and nucleic acids tend to be large and colloidal, and when dispersed in water may form micro-heterogeneous domains.

1-Propanol has been promoted by Koga and coworkers as a moderately hydrophobic solute having a comparable ratio of hydrophobic and hydrophilic moieties to that of some soluble proteins, i.e., being sufficiently bio-mimetic to serve as a biophysical probe (Koga et al. 2004b; Miki et al. 2008). In an aqueous electrolyte system dilute in 1-propanol (1P), the excess enthalpic interaction, $H_{1P}{}^E = (\partial H^E/\partial n_{1P})_{n_W,n_E,P,T}$, (Koga et al. 2004a) and the excess chemical potential interaction $\mu_{1P}{}^E = (\partial \mu_{1P}{}^E/\partial n_E)_{n_W,n_{1P},P,T}$, from which $(\partial H_{1P}{}^E/\partial n_E)$ and $(\partial S_{1P}{}^E/\partial n_E)$ are derived (Miki et al. 2008), were used as thermodynamic probes. (Note that $H_{1P}{}^E$ is with respect to the amount of 1-propanol whereas $\mu_{1P}{}^E$ is with respect to the amount of electrolyte E, i.e., the salting-out or in agent). The electrolytes used were

sodium salts, since Na^+ has neither pronounced kosmotropic nor chaotropic properties. Fairly dilute solutions, $x_E \leq 0.02$, of the salts were used, so that the premise for characterizing the anions as kosmotropic or chaotropic are fulfilled, 1-propanol being molecularly dissolved in the homogeneous solutions. In the three relevant studies, the orders at a given salt and 1-propanol concentration are for ${H_{1P}}^E$(at $x_E = 0.02, x_{1P} \to 0$) $CH_3CO_2^- > Cl^- \sim {SO_4}^{2-} > {ClO_4}^- \sim SCN^-$ (Koga et al. 2004a) and $Cl^- > {B_r}^- > I^-$ (Westh et al. 2006) (F^- could be studied at only much more dilute solutions than $x_E = 0.02$, so that its position is not clear), and for ${\mu_{1P}}^E$(at $x_E = x_{1P} = 0.005$) ${SO_4}^{2-} > F^- > Cl^- > I^- \sim {ClO_4}^-$ (Miki et al. 2008).

These partial series correspond with eq. (5.1) with some significant reversals. However, the question arises: are these correspondences due to the water structure effects of the ions or may they have other causes? In fact, the latter partial series (that for ${\mu_{1P}}^E$) is no longer monotonic for the derived $(\partial {H_{1P}}^E/\partial n_E)$ and $(\partial {S_{1P}}^E/\partial n_E)$, which have minima near Cl^-. Although the epithets kosmotropic and chaotropic have been applied by the authors to the ions, the molecular interactions involved may have little to do with the structure of the water and the effects of the ions on it. The effects of the ions are complex and qualitatively different, involving the number of water molecules immobilized in their hydration shells, their fitting into the hydrogen bonded network of the water, and their retarding its fluctuations, and any direct interactions of them with the hydrophilic and hydrophobic parts of the 1-propanol.

Whereas 1-propanol is salted-out by all the five salts studied in (Miki et al. 2008), ${\mu_{1P}}^E > 0$, the abilities of salts to salt-out or salt-in hydrophobic solutes is not simply related to the kosmotropic or chaotropic properties of their constituent ions. Note, for instance, the position of k_I for Li^+ for the salting out of hydrophobic gases or benzene in Table 2.6. Whereas salting-out can generally be explained quantitatively by the electrostriction caused by the ions (Sect. 2.5.1), except in the case of Li^+, salting-in is more difficult to explain and is often due to direct interactions between the ions and the solute, which possibly but not necessarily are water-mediated.

Another relevant study is that of Bauduin et al. (2004a) of the effect of various sodium salts on the lower consolute temperature (LCST) of aqueous dipropylene glycol monopropyl ether. In the absence of salts and at a mole fraction of 0.11 of the ether in water this temperature is $t_{LCST} = 14\ ^\circ C$ but it is changed by salts in a linear fashion with their concentration, the values of dt_{LCST}/dc_E ranging from -14.4 for the salting-out Na_3PO_4 to $+3.2$ for the salting-in NaSCN (the units are K ($mmol_{salt}$/mole solvent mixture)$^{-1}$ and the uncertainty is ≤ 0.2 units). This linearity holds for the lowest concentrations of salt employed, thus pertain to the water-structure effecting properties of the anions (salts). The sequence of salts is similar to eq. (5.1) but deviates from it in several cases: Na_3PO_4, $Na_2SO_4 \sim Na_2CO_3$, $NaOH \sim NaCH_3CO_2$, NaCl, NaBr, NaI, $NaClO_4$, NaSCN. However, such deviations from the series in eq. (5.1) have already been noted for some of the criteria concerning the water-structure effects of the anions (see above). It should be emphasized that just below the LCST the solution is homogeneous, and the electrolytes change the chemical potential of the components towards phase separation. Thus there is no surface effect here, contrary to the suggestion of the authors, and the Hofmeister series should not have been mentioned in the title of the paper.

The question whether salting-out and salting-in ions can be classified as chaotropic or kosmotropic was raised by Zangi (2010). He used molecular dynamics simulations with 1030 water molecules and 60 ions (cations and anions of equal charge) with the surface charge density q being the variable studied. The values of q ranged from 0.5 to 1.4 elementary charges e per $\pi\sigma^2$ surface area, with $\sigma = 0.50$ nm being the fixed Lennard-Jones diameter of the ions. The boundary between salting-in (Setchenow constant $k_I < 0$) and salting-out ($k_I > 0$) ions for the association between two hydrophobic plates in the electrolyte solutions relative to that in neat water was at $q = 0.71\ e\ \text{nm}^{-2}$. This boundary nearly coincides with that ($q = 0.68\ e\ \text{nm}^{-2}$) between ions that enhance the viscosity of dilute aqueous solutions and those that reduce it. This coincidence, however, does not prove that the two phenomena are based on the water structure affecting properties of the ions, ascribed to their effects on the viscosity. Still, it was concluded that the hydrophobic association does not depend on the water structural effects of the ions, but on the direct interaction of low-q ions (poorly hydrated ones) with the hydrophobic entities. However, the association was simulated between *plates*, i.e., surfaces, and at appreciable ion concentrations, 1.31–1.46 M, which are somewhat outside the premise for chaotropic or kosmotropic ion effects postulated in this book.

A more satisfactory test of the importance of the surface charge density on the salting behavior of ions is with regards to molecularly dispersed solutes, such as the gases to which the data in Table 2.6 pertain. A clear dependence on the charge but not so clear on the size of the ions is demonstrated. The final conclusion from the study of Zangi (2010) is that the salting behavior of ions depends also on the properties of the solutes that are being salted: for small hydrophobic solutes the water structure effects of the ions may be dominant, but for large (and polar) hydrophobic solutes the direct interactions dominate.

Thomas and Elcock (2007) pointed out that surface charge density q is an insufficient criterion to place an ion in the Setchenow constant series, in that Li^+ has values close to those of Cs^+ or Rb^+, Table 2.6, rather than corresponding to its much higher charge density that should place it at the head of the series of alkali metal ions. Also, Table 2.6 shows that, say, Ba^{2+} has a much larger Setchenow constant than Mg^{2+}, although their q values are in the opposite direction. Thomas and Elcock (2007) applied molecular dynamics simulations with the TIP3P model of water and approximately 500 water molecules to pure water and to 1 M solutions of 20 halide salts of alkali metal, alkaline earth, as well as tetraalkylammonium cations. They defined the hydrogen bonding found by the simulations as $\theta_{HB} = N_{HB}/N_{\text{neighbors}}$, using geometrical criteria (Sect. 1.1.3) for the formation of a hydrogen bond between neighboring water molecules (for pure water $\theta_{HB} = 0.67$). The hydrophobic associations methane-methane and neopentane-neopentane (salting-out, $\theta_{HB} < 0.67$) are enhanced in NaF and KF solutions (more by the latter) relative to pure water and are diminished in LiCl and LiBr solutions, in agreement with the corresponding Setchenow constants k_E. When all the salts are considered there is a clear linear correlation between k_E and θ_{HB}, that ranges from the fluorides and divalent cation salts through the alkali metal and ammonium salts, water, reaching tetramethyl- and tetraethylammonium bromides (the latter have $\theta_{HB} > 0.67$). The authors stressed,

however, that the correlation of the Setchenow k_E with the ion effects on the hydrogen bonding (structure) of the water does not prove a causal relationship. The anomalous position of the lithium salts (at 1 M) was confirmed by the simulations, but is contrary to findings in which individual Li^+ ions were studied by simulations (Hribar et al. 2002).

Other simulation studies of salting-in or out of hydrophobic probes with ~ 1 M or higher concentrations of salts arrived at results conflicting with the above and among themselves. Smith (1999) studies the salting behavior of He, Ne, Ar, and methane in aqueous NaCl, $(NH_4)_2SO_4$, $CaCl_2$, $NH_4CH_3CO_2$, $(CH_3)_4NCl$, and $C(NH_2)_3Cl$ and concluded that the degree of preferential binding of the ions to the hydrophobic solutes was the dominant factor in the salting behavior. Karla et al. (2001) studied a hard sphere solute of the size of methane in aqueous solutions of $(CH_3)_4NF$, $(CH_3)_4NCl$, and $(CH_3)_4NBI$ (BI = big monatomic ion of radius ~ 0.25 nm). The dominant factor in the salting behavior ($k_E = 0.32, 0.22$, and $-0.09\,dm^3\,mol^{-1}$ respectively) is the structural hydration of the ions (the local water density) rather than the ion-solute interaction, the smaller anions being excluded from the vicinity of the hydrophobic solute. The discrepancy between the k_E value for $(CH_3)_4NCl$ obtained by these authors (Karla et al. 2001), 0.22, and that obtained by Smith (1999), 0.03, should be noted, throwing some light on the difficulties in the interpretation of the simulations in these ternary solutions: water + salt (ions) + solute (hydrophobic moiety).

5.2 The Hofmeister Series

When a surface is present as in colloidal solutions, to which essentially all physiological systems belong, it is justified to deal with the observed phenomenology in terms of the Hofmeister series. This concept was established in the late 19th century by Hofmeister (1888) as the series of aqueous sodium salts with various anions of which increasing concentrations were required in order to precipitate egg albumin from the solution. The series he presented was:

$$\begin{aligned} {SO_4}^{2-} \sim {HPO_4}^{2-} > {CH_3CO_2}^{-} > {HCO_3}^{-} > {CrO_4}^{2-} \\ > Cl^{-} > {NO_3}^{-} > {ClO_3}^{-} \end{aligned} \tag{5.3}$$

Many phenomena broadened the scope of the series since then, a corresponding cation series was added, and Collins and Washabaugh's comprehensive review of the field almost a century later listed nearly 1000 references (Collins and Washabaugh 1985). Very many more have been added since then and it has become fashionable in a sense in recent years to allude to the Hofmeister series or to the Hofmeister effect when specific ion effects are dealt with. It is generally agreed that water is the key solvent for the phenomena treated under such headings and that the specific ion effects are solvent (water) mediated. Although the Hofmeister series is a well documented phenomenological description of the results, no universal underlying principle has so far emerged for it. This is true concerning both the anion and the

cation series, and it is expedient to deal first separately with the two charge types, before trying to show principles valid for both.

Bio-macromolecules are generally studied in buffer solutions in order to maintain a given pH value, in view of the strong effect the pH has on the biological function, such as enzyme activity. However, it was noted by Bauduin et al. (2004b, 2006) that salts tend to change the pH of buffer solutions, causing effects beyond the specific ion effects on the biological activity. This was noted, for example for a 0.025 M citrate buffer at pH $\sim$ 4.7, where NaBr causes a catalytic activity of horseradish peroxidase at a lower pH similar to that in its absence whereas Na_2SO_4 causes an activity at a higher pH similar to that in its absence. Such effects should be taken into account when the specific ion effects on bio-systems and other colloidal systems are discussed.

5.2.1 The Anion Series

A representative anion Hofmeister series, resulting from elution from a Sephadex G-10 column, was shown by Collins and Washabaugh in their often quoted review (Collins and Washabaugh 1985):

$$SO_4^{2-} \sim HPO_4^{2-} > F^- > Cl^- > Br^- > I^- \sim ClO_4^- > SCN^- \tag{5.4}$$

Another version of the series was reported by Cacace et al. (1997) in their subsequent review:

$$F^- > PO_4^{3-} > SO_4^{2-} > CH_3CO_2^- > Cl^- > Br^- > I^- > SCN^- \tag{5.5}$$

A more comprehensive series is obtained by convolution (Marcus 2009) of the various series (Collins and Washabaugh 1985; Cacace et al. 1997; Pinna et al. 2005; Zhang and Cremer 2006):

$$\begin{aligned} PO_4^{3-} \sim CO_3^{2-} > SO_4^{2-} > S_2O_3^{2-} > H_2PO_4^- > OH^- > F^- > HCO_2^- \\ > CH_3CO_2^- > Cl^- > Br^- > NO_3^- > I^- > ClO_4^- > SCN^- \end{aligned} \tag{5.6}$$

Several organic anions, such as citrate, tartrate, and oxalate, are not included here, although Hofmeister alluded to some of them and other authors placed them in the series at various positions. It is generally agreed that Cl^- has little effect on the relevant phenomena and is used as a reference (dividing) point. If the numerical effects of the anions range from positive to negative (or vice versa) the value for Cl^- is near zero. The series starts with the most effective anion (lowest needed concentration of its salts with a given cation for precipitation of a protein), henceforth called "head anion" and continues to the least effective one or an even salting-in anion of a salt, called hereafter the "tail anion". These epithets, "head anions" near the beginning of the series and preceding Cl^- and "tail anions" subsequent to Cl^- and near the end of the series, are used here in order not to call them kosmotropic and chaotropic as

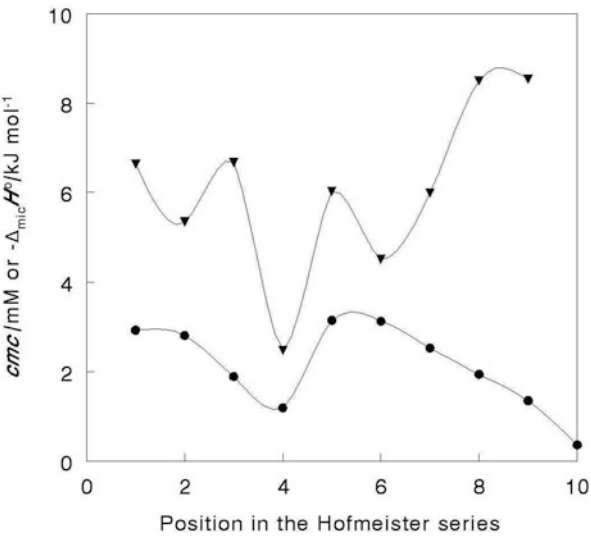

Fig. 5.1 Micellization parameters of tetradecyktrimethylammonium bromide in the present of sodium salts of: (*1*) PO_4^{3-}, (*2*) CO_3^{2-}, (*3*) SO_4^{2-}, (*4*) $S_2O_3^{2-}$, (*5*) F^-, (*6*) $CH_3CO_2^-$, (*7*) Cl^-, (*8*) Br^-, (*9*) NO_3^-, and (*10*) SCN^-. Plotted are the *cmc*/mM (●) and $-\Delta_{mic}H°$/kJ mol^{-1} (▼) (Maiti et al. 2009), the lines are guides to the eye

is often done, and to distinguish the specific ion effects in the presence of a surface, dealt with in this section, from those in its absence, see Sect. 5.1.

However, when several related phenomena are used to establish the series certain inversions of the positions of some anions in it are noted. For instance, Pinna et al. (2005) placed $H_2PO_4^-$ before SO_4^{2-} in their series of anion effects on the specific activity of an enzyme (lipase A) towards the hydrolysis of *p*-nitrophenyl acetate. Cacace et al. (1997), quoting Hochachka and Somero (1984) and Hall and Drake (1995), placed F^- at the head of the series, although other authors relegated it to nearer its middle. More serious deviations from the normal Hofmeister series were observed for three measures of the self aggregation of aqueous tetradecyltrimethylammonium bromide micelles (Maiti et al. 2009). These are the critical micelle concentration, *cmc*, the coefficient $\beta = (1-$ post*cmc*slope/pre*cmc*slope), where the slope pertains to conductivity vs. concentration, and the enthalpy of micellization, $-\Delta_{mic}H°$. Two of these three quantities are shown in Fig. 5.1. A few instances were noted, where a complete reversal of the series occurred, e.g., the stabilization of a-chymotrypsin against thermal inactivation by anions at the end of the series observed by Levitsky et al. (1994), which was explained by them ad hoc. A related series, that of the lyotropic numbers, Table 5.1 (Voet 1937a; Schott 1984; Lo Nostro et al 2002):

$$SO_4^{2-} < PO_4^{3-} < F^- < OH^- < IO_3^- < H_2PO_4^- < BrO_3^- < Cl^- \sim NO_2^- < ClO_3^- < Br^- < NO_3^- < I^- < ClO_4^- < I^- < SCN^- \qquad (5.7)$$

also has several reversals with respect to the Hofmeister series (5.6).

The phenomena described by means of the Hofmeister anion series cover a very broad spectrum. They range from the original one of protein precipitation to salting out of other solutes, enzyme activity, macromolecular conformational transitions,

critical micelle concentrations, and surface tension. A "head anion" that has a high propensity to precipitate a protein has also a small propensity to denaturalize it. On the contrary, a "tail anion" has a high ability to denature the protein, although it keeps it in solution. Cacace et al. (1997) among others reviewed the various effects of salts that conform to the Hofmeister series on biological systems. Studies of specific ion effects on such systems to which the Hofmeister series pertains generally involve salts at concentrations ≥ 0.1 M. At lower salt concentrations the electrostatic effects of the ions are of a general nature and no specific ion effects are to be expected. The binding of the water in the hydration shells of the ions at high salt concentrations makes less water available for hydrating other solutes, and this is, again, a general phenomenon that is outside the concept of specific ion effects, except where direct, chemical bonding between ions and the solute takes place. It is mainly the intermediate range of concentrations where the specific ion effects dealt with in this chapter are manifested.

The original Hofmeister series pertained to concentrations of the order of 1 M, but this was essentially due to the insufficient sensitivity of the methodology available at the time. More recent investigations pushed the limit of sensitivity down to 0.01 M. For example, at this ionic strength the relative effectiveness of anions in suppressing the heat induced transition and increasing thermo-stability of bovine serum albumin followed the *reverse* Hofmeister series, whereas at concentrations above 0.1 M the *normal* order is produced according to Yamasaki et al. (1991). Specific anion binding to amino acid sites was suggested as the stabilizing effect, made possible by the weaker hydration of the large anions.

Only very few of the protein-related studies and those that do not pertain to proteins are discussed in the following. They were chosen among the very many studies in order to bring out the underlying principles. Many different explanations of the Hofmeister series of anions have been proposed over the years. Collins and Washabaugh (1985) stressed the analogy of the surface tension and surface potential at the water/air surface with the series. Hofmeister series result when the anions in Tables 4.5 and 4.6 are ordered according to the sizes of $d\gamma/dc_i$ and of $\Delta\Delta\chi$. They proposed a three layer model for the water/air surface, the first two layers being of one water molecule thickness. These layers are: a region near the surface, I_1, where water molecules have fewer hydrogen bonds than in bulk water, an intermediate layer, I_2, and the bulk water, I_3. Layers I_1 and I_3 compete for hydrogen bonding interactions with layer I_2. The authors postulated the same structure near the surface of a solute as at the water/air surface, a relative competition for hydrogen bonding, and a charge transfer of the excess negative charge to adjacent water molecules as explanations for the specific ion effects. "Head anions" interact with the I_1 layer near solutes more strongly than bulk water, I_3, does, appropriating some of the water to themselves. For "tail anions" at the end of the Hofmeister series the binding of water is loose, so they do not dehydrate the solute.

Cacace et al. (1997) stressed several aspects of the Hofmeister series. The underlying concept is that biopolymer interactions are water-mediated and the anions affect both the surface of the biopolymer and the structure of the water. When a protein folds, aggregates or adsorbs, the solvent/protein interfacial area A_{WP} is diminished. Contrarily, when a protein is denatured, A_{WP} increases. Work needs to

be done to exclude an anion from an interface (e.g. protein/solvent). The larger the work that needs to be done, the greater the tendency to minimize that interface, by adsorption or aggregation and by the same token the native conformation (assumed more compact than any non-native one) is stabilized. On the other hand, anions are hydrated, and the more strongly they are hydrated the less readily they will give up their water of hydration when called upon to bind to positive sites of the protein. This may point to a more universal basis for the Hofmeister series than the surface tension of salt solutions in air. The exclusion of anions from the surface of a biomolecule is opposed by their enrichment, e.g. association with amino acid side chains and, especially, favorable arrangements of several neighboring amino acids to produce a binding site.

A different view was expressed by Baldwin (1996), who proposed that "head anions" affect the non-polar (hydrophobic) groups of proteins, the more the larger these groups are, whereas "tail anions" interact with the peptide group (Nandi and Robinson 1972a), loosing their hydration water more readily than the former anions.

Collins (1997) revised his previous views (Collins and Washabaugh 1985), concerning analogy with surface tension, and stressed the surface charge density, $q = z_I e/\pi\sigma_I{}^2$, as determining the strength of the water binding by the ions. The dividing line of strongly hydrated (relative to water-water interactions) from weakly hydrated ions was established according to the structural entropy (Sect. 3.3.3). For monovalent anions this corresponded to ions having a 0.178 nm radius (near that of Cl^-). Thus the water mediation of the interactions is relegated to a secondary place, the direct interactions of "head anions" with "solute head cations" and of "tail anions" with "solute tail cations" (Sect. 5.2.2) being the primary mechanism for the specific ion effects manifested by the Hofmeister series. Poorly hydrated "tail anions" adsorb to the hydrophobic positively charged amino acid side groups of proteins, such as those of arginine, histidine, and lysine, and neutralize the charges. On the contrary, a "head anion" such as F^- is unlikely to lose its water of hydration and form inner sphere ion pairs with protein cations, and has a similar effect as glutamate with two carboxylate groups on DNA-binding proteins.

The hypothesis that water structure effects dominate the protein stabilization or denaturalization by solutes was challenged by Batchelor et al. (2004), who used the pressure derivative of the heat capacity, $(\partial C_P/\partial P)_T$, to express the water structure effects. Solutes (most of them non-electrolytes) ordered according to their $(\partial C_P/\partial P)_T$ values, from positive to negative, correlated poorly with protein stability. The four electrolytes included did show the Hofmeister ordering $SO_4{}^{2-} > Cl^-$ for the ammonium salts, but for the guanidinium salts no conformation to it, $Cl^- \sim SCN^-$, was found.

Boström et al. emphasized the importance of dispersion forces regarding the specific ion effects on proteins and also regarding non protein-related Hofmeister effects. The charge on the protein lysozyme depends on the anion in salt solutions (Boström et al. 2003a), but only Cl^- and SCN^- (as their potassium salts) are compared. Phosphatidylglycerol bilayers (Boström et al. 2006a) are affected by Cl^-, Br^-, and SCN^- (as their sodium salts) in this order. Even silica membranes show Hofmeister series effects, namely in pH measurements with a glass electrode in fairly concentrated

Table 5.2 Parameters characterizing anion effects on the surface pressure of monolayers of dipalmitoyl phosphatidylcholine on water. (Leontidis and Aroti 2009)

Anion	$-U_i/k_BT$ (no Na^+ binding)	$-U_i/k_BT$ (with Na^+ binding)	$-B_i/10^{-50}$ J m^3
F^-		−2.0	
Cl^-	0.70	0.20	14.0 (3.6[a])
$CH_3CO_2^-$	1.40	0.95	16.5
Br^-	1.78	1.45	17.5 (10[a])
NO_3^-	2.50	1.85	18.5
ClO_3^-	2.90	2.50	19.8
I^-	3.15	2.95	20.9
BF_4^-	3.30	2.80	21.0
ClO_4^-	3.70	3.20	21.7
SCN^-	4.23	3.90	23.4 (15[a])
PF_6^-	4.50	4.05	24.6

[a]In parenthesis are the corresponding $-B_i/10^{-50}$ J m^3 values for anion effects on phosphatitylflycerol bilayers (Batchelor et al. 1996).

salt solutions (Boström et al. 2003b). At 0.8 M the order of decreasing pH in the salt solutions is NaCl > NaBr > $NaNO_3 \sim NaClO_4$, ascribed to competition between the polarizability of the anions and electrostatic interactions at the surface of the glass electrode. The importance of the dispersion forces, related to the polarizability of the anions in this respect, was stressed by Boström et al. (Sect. 4.4.1) (Boström et al. 2001a, 2001b). The order with respect to two ions, SCN^- and Cl^- is the reverse from the above in the presence of a dilute protein, cytochrome C (Boström et al. 2006b), for which the more polarizable SCN^- helps to bind hydrogen ions to the protein, depleting them from the bulk solution, thus increasing the pH. However, causes other than the anion polarizability, such as their sizes or hydration enthalpies could be responsible for the observed ordering.

Monolayers of octadecylamine on D_2O were studied by Gurau et al. (2004) using vibrational sum frequency spectroscopy that is sensitive to the ordering of the alkyl chains. "Tail anions" caused disordering of the monolayers, the effects conforming to the Hofmeister series. The effect is based on the ability of the anion to penetrate into the alkyl chain region of the monolayer, the highly hydrated "head anion" SO_4^{2-} having the least tendency to do so and the poorly hydrated SCN^- having the largest tendency. Leontidis et al. (2009) studied monolayers of dipalmitoyl phosphatidylcholine in the presence of sodium salts of a variety of anions. They measured the surface pressure at the monolayer and fitted the results in terms of several models. The ion partitioning (ion penetration) model pertains mainly to "tail anions" and presumes that Na^+ is excluded from the monolayer, whereas the anions partition between it and the bulk solution. Their study yields attraction potentials U_i/k_BT for fitting the surface pressure, which are listed in Table 5.2 and characterize the anions. Another model, emphasizing the dispersion forces is also able to fit the surface pressures well. It involves the dispersion coefficient B_i, proportional to the static excess polarizability of the ion in water (Sect. 4.4.1), as a fitting parameter, also

listed in Table 5.2. Among univalent "head anions" F^- was tested and no satisfactory fitting with the above models of the slight increase in the surface pressure by NaF could be achieved. However, a model that allows complexation of Na^+ with 3 lipid molecules but excludes F^- from the monolayer is able to fit the results. The allowance for Na^+ binding modifies the U_i/k_BT values, as is also shown in Table 5.2. The partitioning of the anions can be interpreted in terms of U_i/k_BT being the difference of a quantity describing the cavity formation energy and a Born-type quantity depending on transfer from a high permittivity medium (bulk water) to a low permittivity one (the lipid layer). The former is proportional to the surface area of the hydrated ion, the latter to the reciprocal of the size of the hydrated ion. A plot of U_i/k_BT vs. $(r_i + r_W)^2 - 0.029/(r_i + r_W)$ is in fact linear (SCN^- and $CH_3CO_2^-$ are outliers; being non-spherical or non-globular the radius r_i chosen for the plot being probably wrong).

Lipid bilayers with neutral phopsphatidylcholine head groups show according to Rydall and Macdonald effects on the conformation of the head groups in the order $NO_3^- < I^- < SCN^- < ClO_4^-$ (Rydall and Macdonald 1992). Molecular dynamics simulations with a bilayer involving palmatoyloleoylphosphatidylcholine (Sachs and Woolf 2003) showed similar effects, in that a big anion (BI, with radius 0.249 nm) penetrated more deeply into the bilayer than Cl^-, presumably because of its lower hydration and its ability to accommodate to the hydrophobic environment in the interior of the bilayer. The thickness of multilayers of two polyelectrolytes, poly(styrenesulfonate) and poly(diallyl-dimethylammonium) with their respective counter-ions, was measured by ellipsometry and atomic force microscopy, and was found to follow the Hofmeister series (Salomäki et al. 2004). The thickness increases some fourfold on going from F^- through HCO_2^-, BrO_3^-, Cl^-, ClO_3^-, NO_3^- to Br^- (SCN^-, ClO_4^-, and I^- precipitate the polyelectrolyte).

The lowering of the lower consolute temperature of aqueous poly(N-2-propylacrylamide) by a number of sodium salts follows roughly the Hofmeister series, from CO_3^{2-} through SO_4^{2-}, $S_2O_3^{2-}$, $H_2PO_4^-$, F^-, Cl^-, ClO_4^-, to Br^-, but NO_3^-, I^-, and SCN^- raise this temperature slightly (Zhang et al. 2005). The mechanism of the interactions of the anions with the polymer is said to involve polarization by the anion of the water molecules hydrating the amide group, effects on the hydrophobic hydration of the hydrophobic surfaces of the polymer, and direct association of the anion with the amide nitrogen that has a partial positive charge. Only the second effect is water-mediated, the first leading to salting out and the third to salting in. No single parameter, such as the surface tension increment by or the entropy of hydration of the anion, can explain the exact sequence noted, although the general trends agree with these parameters. "Tail anions" are correlated fairly well with the surface tension increment and "head anions" with the entropy of hydration.

As mentioned above, the exploration of the specific ion effects in bio-systems started with the Hofmeister series dealing with the precipitation of proteins. Proteins have surfaces that are roughly 1/3 hydrophobic and 2/3 hydrophilic, whereas their interiors are only 1/3 hydrophilic, mostly associated with the peptide backbone. However, proteins exhibit a rather narrow range of surface polarity and charge, and

therefore do not allow a wide variation of these variables, which artificial colloids do permit, as Schwierz et al. point out (Schwierz et al. 2010). The distinction between surface polarity (hydrophilic/hydrophobic balance) and net surface charge is of crucial importance, since it is related to reversals of the Hofmeister series.

Negatively charged colloids that are rather hydrophobic show the direct Hofmeister series but this is reversed for positively charged hydrophobic colloids. The opposite trends occur for very polar colloids. This has been demonstrated recently by Peula-Garcia et al. (2010) who studied the critical coagulation concentration, *ccc*, of various colloids in sodium salts with different anions. Hydrophobic colloids with positive surface charges showed the *ccc* order $IO_3^- > F^- > Cl^- > Br^- > NO_3^- > I^- > SCN^-$ but negatively charged ones showed the reverse order: $IO_3^- \leq F^- < Cl^- < Br^- < NO_3^- < I^- < SCN^-$. For hydrophilic colloids with positive surface charges the respective orders of the *ccc* were: $F^- < IO_3^- \sim Cl^- \sim Br^- \sim NO_3^- < I^- < SCN^-$, whereas those with negative surface charges did not show a clear *ccc* order of these ions. The interpretation of these results reverted to considerations of the effects of both the surface and the anions on the structure of the water, abandoned by other workers in recent years. The accumulation and exclusion of anions at interfaces are said to originate from the entropy forced attraction between ions and surfaces when they have similar water arrangements and their repulsion when the latter are dissimilar (Peula-Garcia et al. 2010).

Schwierz et al. (2010) provided a theoretical basis to the critical coagulation concentration of colloidal systems in the presence of anions and the resulting direct and inverse Hofmeister series. They dealt only with the univalent monatomic anions, F^-, Cl^- and I^-, corresponding to the start, middle, and end of the series. The surface tension increment $\Delta\gamma$ with respect to an uncharged surface is calculated as the sum of two terms, the one arising from the ionic surface excess Γ_I for zero surface charge and the other arising from the surface charge $\sigma_{surface}$, in e nm^{-2}. For neutral surfaces and also when $\sigma_{surface} = -0.1$ the surface tension increment $\Delta\gamma$ increases in the order $I^- < Cl^- < F^-$, the direct Hofmeister sequence, at a hydrophobic surface, but in the reverse order at a polar surface. The Debye-Hückel potential Φ_{DH} is related to the surface potential as $\Phi_{DH} = \sigma_{surface}/\varepsilon_r\varepsilon_0\kappa$, where κ is the Debye-Hückel screening length, proportional to the square root of the concentration. When the surface charge increases from -0.08 through 0.03–0.10 the electrostatic forces expressed by the Debye-Hückel potential change from $0 < |\Phi_{DH}(I^-)| < |\Phi_{DH}(Cl^-)| < |\Phi_{DH}(F^-)|$ at concentrations above 0.2 M to the opposite sequence through partially reversed sequences. It is the interplay of $\Delta\gamma$ with Φ_{DH} determined by $\sigma_{surface}$ that decides whether the direct or the reverse Hofmeister sequence will be followed, the properties of both the surface of the colloid and those of the anions being taken into account.

5.2.2 The Cation Series

Subsequent to Hofmeister's original series that involved only anions it was realized that the nature of the cations of the salts used for the denaturation of proteins also

plays a role, though subordinate to the dominating role of the anions. A Hofmeister series of cations was established for a given anion in the review by Cacace et al. (1997):

$$(CH_3)_4N^+ > (CH_3)_2NH_2{}^+ > NH_4{}^+ > K^+ \sim Na^+ > Cs^+ > Li^+ > Mg^{2+} > Ca^{2+} > Ba^{2+} \quad (5.8)$$

It is generally agreed that Na^+, being near the midpoint of the series, has a minimal effect; therefore it is almost universally used to study the anions effects of salts. Since also Cl^-, in the middle of the anion series (5.6) has a minimal effect, it is usually used to study the specific cation effects of a series of salts.

What is noteworthy about the series is that for the monatomic alkali metal cations their order does not agree with their size or charge density or their lyotropic series (Voet 1937b). This apparent disorder (note the position of Cs^+) is not universal, however, since cases where the lyotropic series is followed are also known. An instance is the rate of the penetration of the alkali metal cations through leaf cuticles that decreases in the order $Cs^+ \geq Rb^+ > K^+ > Na^+ > Li^+$, i.e., in the expected order according to their surface charge densities. The cuticular pores were supposed by McFarlane and Berry to be lined with a protein that has exposed positive sites (McFarlane and Berry 1974). The critical micelle concentration (*cmc*) of sodium dodecylsulphate increases in the reverse order by these cations (Maiti et al. 2009), where Cs^+ is at the expected position. The transition of a mixed surfactant (sodium dodecylsulfate + dodecyltrimethylammonium bromide with an excess of the former) from micelles to vesicles (Sect. 4.5) is also promoted in this sequence, explained by counter-ion association depending on relative ease of ion dehydration (Renoncourt et al. 2007).

The head groups of anionic surfactants, such as the dodecylsulfate mentioned above, can be changed, and carboxylate, phosphate, sulphate, and sulfonate groups have been investigated by Vlachy et al. (2009), noting that they become "softer" in this order, tending to form ion pairs increasingly with alkali metal cations as these are "softer" too as their size increases. That is, $-CO_2{}^-$ groups prefer association with Li^+ whereas $-SO_3{}^-$ groups prefer association with Cs^+, not in agreement with the position of Cs^+ in the "classical" cation Hofmeister series.

The critical coagulation concentration of alkali metal nitrates on negatively charged AgI sols also follows the lyotropic rather than the Hofmeister series: $LiNO_3 > NaNO_3 > KNO_3 > RbNO_3 > CsNO_3$ (Lyklema 2009).

Variants of the cation Hofmeister series (5.8) have been proposed, where the position of, say, $NH_4{}^+$ is shifted and guanidinium, $C(NH_2)_3{}^+$, is added, e.g.:

$$(CH_3)_4N^+ > (CH_3)_2NH_2{}^+ > K^+ \sim Na^+ > Cs^+ > Li^+ > NH_4{}^+ > Mg^{2+} > Ca^{2+} > C(NH_2)_3{}^+ \quad (5.9)$$

The series is extended as $Na^+ > Mg^{2+} > Ba^{2+} \sim > Ca^{2+} > Mn^{2+} > Ni^{2+}$ (Arakawa and Timasheff 1984), where the order among the divalent cations is more difficult to rationalize.

Many other reversals in the order have been noted over the years. The swelling of fibers was studied early in the 20th century with respect to the effects of salts, here different cations, on it. Fischer and Moore (1907) established the sequence of cations as dilute aqueous chlorides causing de-swelling of fibrin as: $K^+ < NH_4{}^+ < Na^+ < Ca^2 < Mg^{2+} \sim Sr^{2+} < Ba^{2+}$. The seemingly "anomalous" position of magnesium should be noted. Richter-Quittner (1921) quoted (as due to Fischer) the series: $Fe^{2+} > Cu^{2+} > Sr^{2+} > Ba^{2+} > Ca^{2+} > Mg^{2+} > NH_4{}^+ > Na^+ > K^+$ as effective fibrin de-swelling agents, not coinciding with the previous one. Thermal coagulation of plant protoplasma was found by Kahlo (1921) to proceed in the order $K^+ \sim NH_4{}^+ > Na^+ \sim Li^+ \sim Ca^{2+} > Mg^{2+} \sim Sr^{2+} \sim Ba^{2+}$ (Richter-Quittner 1921). Another apparently disordered series: $K^+ > Rb^+ > Cs^+ > Na^+ > Li^+$ was found by Carpenter and Lovelace for the influence of halide salts on the optical rotation of gelatine (Carpenter and Lovelace 1935).

It was later demonstrated that such fiber swelling effects are due to the helix-to-coil transitions of the collagen, increasing in the series (von Hippel and Wong 1964):

$$(CH_3)_4N^+ < NH_4{}^+ < Rb^+ \sim K^+ \sim Na^+ \sim Cs^+ < Li^+ < Mg^{2+} < Ca^{2+} < Ba^{2+} \tag{5.10}$$

The helix-to-coil transition of DNA also increased similarly: $(CH_3)_4N^+ < K^+ < Na^+ < Li^+$. The thermally induced cooperative unfolding of ribonuclease showed a similar sequence: $(CH_3)_4N^+ \sim NH_4{}^+ \sim K^+ \sim Na < Li^+ < Ca^{2+}$, but also $(C_2H_5)_4N^+ < (C_3H_7)_4N^+$ whereas for the collagen transition a much larger difference occurs $(C_2H_5)_4N^+ << (C_3H_7)_4N^+$. Von Hippel and Wong (1964) concluded that the sequence in the series does not depend on the effects of the salts on the water activity and that the specific biomolecule for which the series is established has little influence on the sequence.

Nandi and Robinson (1972b) distinguished between the salting effects of ions on the polar peptide group and on non-polar side chains of oligopeptides that can be considered as protein analogs. Peptide groups are *salted-in* (Sect. 2.5.1) in increasing order as: $(CH_3)_4N^+ < K^+ \sim Cs^+ \sim Li^+ < Na^+ < Ca^{2+}$, attributed to direct ion-peptide association. Ethyl esters of N-acetylaminoacids (L-valine, L-leucine, and L-phenylalanine) are *salted-out* in the order $Cs^+ < K^+ \sim Na^+ \sim Li^+ < Ca^{2+}$, as expected from the charge density and the electrostriction. The observed salting-out of proteins is therefore attributed to the salting out of the hydrophobic side groups. Baldwin (1996) interpreted these results in terms of the surface tension increment caused by the ions, hence in terms of the Gibbs energy of cavity formation for accommodation of the hydrophobic groups in the aqueous environment.

The position of guanidinium, $C(NH_2)_3{}^+$ in the cation series for the thermally induced cooperative unfolding of ribonuclease depends on the accompanying anion according to von Hippel and Wong (1964). On the other hand, for the salting-in of deoxygenated sickle haemoglobin its position between the alkali metal cations and the alkaline earth ones in the series $K^+ \sim Rb^+ < Na^+ \sim Cs^+ < Li^+ << C(NH_2)_3{}^+ < Mg^{2+} < Ca^{2+}$ is independent of the anion (Poillon and Bertles 1979).

The effects of divalent cations on bovine serum globulin in terms of salting-out and stabilization of the native form and salting-in and denaturation was studied by Arakawa and Timasheff (1984) in terms of the protein preferential hydration. This increased in the order $Mn^{2+} \sim Ni^{2+} < Ca^{2+} \sim Ba^{2+} < Mg^{2+} < Na^{+}$ leading to increased salting-out and stability of the protein against denaturation. The binding of the divalent salts to the protein overcomes the ion exclusion from the surface due to competition for water of hydration.

Further confusion in the order of cations in the Hofmeister series concerning the stability of a biomolecule (the enzyme halophilic malate dehydrogenase) arises from the reversal of the order when the cations are examined at low (≤ 1 M) or at high concentrations (Ebel et al. 1999). The order of efficiency of cations to maintain the folded form of the protein at low concentrations is $Ca^{2+} \sim Mg^{2+} > Li^{+} \sim NH_4^{+} \sim Na^{+} > K^{+} > Rb^{+} > Cs^{+}$, reverting to $Ca^{2+} < Mg^{2+} < Li^{+} < Cs^{+} \sim NH_4^{+} \sim Na^{+} \sim K^{+}$ at high concentrations. This reversal of the order is due to the compensation between direct interactions of the cations with the abundant acidic (carboxylate) groups at the surface of this particular protein, that absorbs a large amount of salt in its folded (natural) form, 0.2 g salt per 1 g protein, and the general electrostatic interactions prevailing at low salt concentrations. The unfolded (denatured) form exposes more of the peptide backbone where the latter interactions are the more important ones.

Still further confusion is seen in the various series listed by Zhao concerning enzyme activities and stabilities (Zhao 2005). Some series indeed conform to the Hofmeister series (5.8) but others show reversals, e.g., for prostatic specific antigen and for Candida rugosa lipase. An attempt to explain why direct or reverse series are obtained among Li^{+}, Na^{+}, and K^{+} with regard to double layer interactions between two negatively charged oxide surfaces in terms of ion hydration, dispersion forces, and ion sizes (Peula-Garcia et al. 2010) does not succeed, because it does not show why silica surfaces differ from alumina ones.

A conclusion from these often observed deviations from the "classical" Hofmeister series for cations is that specific ion interactions with specific sites of the biomolecules must be taken into account in proposed mechanisms leading to such a series. A subtle balance of several competing evenly matched interactions, such as dispersion forces, polarization, hydration strength, ion size effects, and the impact on interfacial water structure makes it hard to identify a universal law (Koelsch et al. 2007; Tobias and Hemminger 2008). Therefore, the view promoted by Collins and co-workers over the years till recently (Collins and Washabaugh 1985; Collins 1995, 1997; Collins et al. 2007), based only on the alkali metal cations, namely that the ion hydration strength, compared with water-water interaction strength, is the main driving force for the cation effects cannot be valid.

On the other hand, the further view promoted by these authors concerning the preferred interactions of weakly hydrated cations with weakly hydrated negatively charged side groups of the biomolecules and of strongly hydrated cations with strongly hydrated negatively charged groups, such as carboxylate and phosphate ones, appears to be useful. If water-shared ion pairs are formed, then the inverse order of Li^{+}, Na^{+} and K^{+} with respect to Cl^{-} (weakly hydrated) and RCO_2^{-} (strongly

hydrated), seen in computer simulations, can be explained, with relevance to the carboxylate side groups of proteins (Hess and Van der Vegt 2009). The tendency of counter-ions to form ion pairs with the head groups of micelle forming surfactants can therefore be invoked to explain the reversal of the alkali metal cation series with respect to magnitudes of the *cmc*s of dodecyl sulphate and dodecanoate micelles (Moreira and Firoozaqbadi 2010). The electrical double layer at the surface of negatively charged biomolecules or colloids must accommodate the counter-ions, and these are preferred according to their charge densities but also according to the sizes of their hydrated species. This may be a cause for the reversal of Cs^+ and Li^+ often observed (Koelsch et al. 2007).

The (water) accessible surface area (*ASA*) of a biomolecule or a small molecule analogue is an important attribute of such species according to Pegram and Record (2008), being measured with a probe of the size of a water molecule. (Compare the ITIM method for the surface of solutions, Sect. 4.1). The relative ability of ions to penetrate this hydrated surface is then said to yield the ion series for protein unfolding, depending on the change in *ASA* and the balance of hydrophilic (peptide) and hydrophobic groups occurring in such a process. This balance between hydrophilic and hydrophobic characters of surfaces in non biomolecules but other colloidal systems was in fact shown to determine whether the direct or reverse series is observed (Lopez-Leon et al. 2008).

5.2.3 Interpretation of the Hofmeister Series

For an ion to be found at a particular position in the Hofmeister series, a delicate balance between several kinds of interactions needs to be considered, as arises from all the above phenomena taken together. This balance depends to a large extent on the surface of the specific biomolecule or other colloid with which the ion interacts. The hydrophilic-hydrophobic balance of this surface, the sign of the charge on it, if any, and the existence of strongly ion binding groups at this surface, related to direct interaction of the ion with sites there, are as important as are general electrostatic and ion-water interactions that are independent of the surface of any given substrate.

Kunz et al. (2004) showed that correlations of the anion Hofmeister series with any one parameter of the anion, including ion polarizability, lyotropic number, Setchenow salting coefficient, and the surface tension decrement, are not successful, in that some ions are always outliers. Inclusion of the anion polarizability, important for "tail anions", does not help correlations when "head anions" are considered. A similar conclusion was presented by Abezgauz et al. (2010): "lyotropic number, anion size and shape, polarizability, and hydration energy all play a role in the interaction" regarding cetylpyridinium chloride micellization and micellar growth. The conclusion from the studies shown above is that although water-mediation probably plays a role in positioning anions in the series, whether direct or reverse, direct interactions with the surface of the solute dominate. The ease of desolvation of the anions is thus also a parameter that has to be taken into account. For a given colloidal or biomolecular surface a multidimensional correlation with several parameters

Table 5.3 Anion parameters that might be relevant to their ordering in the Hofmeister series, some of the values are taken from Table 2.2, others from (Marcus 1997). The anions are arranged arbitrarily according to their molar refractions, R_{DI}

Anion	R_{DI} ($cm^3\ mol^{-1}$)	r_I (Nm)	$-\Delta_{hyd}H_I$ ($kJ\ mol^{-1}$)	N_{lyoI}	$B_{\eta I}$ ($dm^3\ mol^{-1}$)	$d\Delta\gamma/dc_I$ ($mN\ m^{-1}\ mol^{-1}\ dm^3$)
F^-	2.21	0.133	510	4.8	0.127	1.10
OH^-	4.65	0.133	520	5.8	0.12	1.35
Cl^-	8.63	0.181	367	10.0	−0.005	1.20
NO_2^-	8.7	0.192	412	10.1	−0.024	
HCO_2^-	9.43	0.204	432		0.052	0.15
NO_3^-	10.43	0.200	312	11.6	−0.045	0.45
CO_3^{2-}	11.45	0.178	1397		0.278	0.95
ClO_3^-	12.1	0.200	299	10.65	−0.024	0.00
Br^-	12.24	0.196	336	11.3	−0.033	0.95
ClO_4^-	12.77	0.240	246	11.8	−0.060	−0.50
SO_4^{2-}	13.79	0.230	1035	2.0	0.206	1.15
$CH_3CO_2^-$	13.87	0.232	425		0.236	0.05
$H_2PO_4^-$	14.6	0.200	522	8.2	0.34	1.25
PO_4^{3-}	15.1	0.238	2879	3.2	0.59	2.00
BrO_3^-	15.2	0.191	376	9.55	0.007	
SCN^-	17	0.213	311	13.25	−0.032[a]	0.20
IO_3^-	18.85	0.181	450	6.25	0.138	
I^-	18.95	0.220	291	12.5	0.007	0.35
$S_2O_3^{2-}$	23.2	0.250				1.45

[a] From (Marcus 2012b).

(Table 5.3) appears to be called for, but when other surfaces are involved, the weights of the parameters will change, because of the varying properties of these surfaces. The parameters in Table 5.3 are not orthogonal to each other but they correlate only poorly with each other.

It is furthermore concluded that whereas the anion Hofmeister series is generally well established, with only few reversals that can be explained ad-hoc, this is not the case regarding the cation Hofmeister series. There are in general no "head cations" established in a series such as (5.8), erroneously termed chaotropic, nor general "tail cations", erroneously termed cosmotropic, but for each surface the hydrophilic and hydrophobic character or balance between these properties is responsible for the order of cations interacting directly with sites at the surface, in addition to the ion properties mentioned above, see Table 5.4 for the latter.

5.3 Some Further Comments on Aqueous Ions in Biophysics

The binding of counter-ions to polyions derived from polyelectrolytes is relevant to the biophysics of proteins, nucleic acids, and similar biomolecules. This is discussed in Sect. 2.7.2. Here some other aspects of aqueous ions of importance in the present context are dealt with.

Table 5.4 Cation parameters that might be relevant to their ordering in the Hofmeister series, some of the values are taken from Table 2.2, others from (Marcus 1997). The cations are arranged arbitrarily according to their surface charges, $z_I/4\pi r_I^2$

Cation	r_i (Nm)	$-\Delta_{hyd}H_i$ (kJ mol^{-1})	R_{Di} (cm^3 mol^{-1})	N_{lyoI}	$B_{\eta I}$ (dm^3 mol^{-1})	$d\Delta\gamma/dc_I$ (mN m^{-1} mol^{-1} dm^3)
$(C_2H_5)_4N^+$	0.337	206	43		0.385	
$(CH_3)_4N^+$	0.280	218	22.9		0.123	− 0.40
GuH^+[a]	0.20	602	11.21		0.058	− 0.26
Cs^+	0.170	283	6.89	60.0	− 0.047	0.50
Rb^+	0.149	308	4.1	69.5	− 0.033	0.65
NH_4^+	0.148	329	4.7		− 0.008	0.40
K^+	0.138	334	2.71	75.0	− 0.009	0.80
Na^+	0.102	416	0.65	100.0	0.085	0.90
Ba^{2+}	0.136	1332	5.17	7.5	0.229	0.50
Sr^{2+}	0.113	1470	2.65	9.0	0.272	1.20
Ca^{2+}	0.100	1602	1.59	10.0	0.298	1.50
Li^+	0.069	531	0.08	105.2	0.146	0.65
Mn^{2+}	0.083	1874	2.2		0.39	0.75
Ni^{2+}	0.072	2119	1.6		0.375	1.10
Mg^{2+}	0.072	1949	−0.7		0.385	1.65

[a] See Table 5.5.

5.3.1 The Guanidinium Ion

The guanidinium cation $C(NH_2)_3^+$ and its salts feature strongly in discussions of the stability and denaturation of proteins and other biomolecules. However, there is only scant information in the literature concerning their physicochemical properties and whatever is available is widely scattered, but see the recent review by Marcus (2012a). This applies to the ions and salts themselves and to their aqueous solutions, in which their physiological effects are manifested. It is, therefore, appropriate here to gather together the more important data that may be of use in the appreciation of the observed effects and compare them with values for other cations listed in Table 5.4, all the values being for 25 °C.

Guanidinium cations, in short GuH^+, are planar trigonal and of high symmetry, D_{3h}. The *size* of this cation can be estimated from its structure in chloride solution that has been reported by Mason et al. (2004). In the plane of the ion, with a Cl^- anion hydrogen bonded to two nitrogen atoms, the minimal distance C–Cl is 0.37 nm, but when a Cl^- anion is hydrogen bonded to a single nitrogen atom, having twice the statistical probability, the minimal distance is 0.41 nm. Since the radius of Cl^- is 0.18 nm, that of guanidinium (in the plane) is between 0.19 and 0.23 nm. The stacking of GuH^+ ions leads to a C–C distance of 0.40 nm, so the axial radius of GuH^+ (perpendicular to the plane) is 0.20 nm.

The mean radius of the ellipsoid of revolution of GuH^+, taken as the ionic radius for comparison with other ions, is then $r_I = [(0.67\times0.23 + 0.33\times0.19)^2\times0.20]^{1/3} = 0.21 \pm 0.02$ nm. However, the non-spherical shape of GuH^+ must be kept in mind,

Table 5.5 Properties of guanidinium ions at 298.15 K and 100 kPa possibly relevant to their biophysical effects. (Marcus 2012a)

Property	Symbol and units	Value
Properties pertaining to isolated (gaseous) ions		
Molar enthalpy of formation	$\Delta_f H°$/kJ mol^{-1}	462 ± 3
Molar enthalpy increment	$(H°–H_0°)$/kJ mol^{-1}	14.22
Molar constant pressure heat capacity	$C_P°$/J K^{-1} mol^{-1}	77.89
Molar entropy	$S°$/kJ mol^{-1}	264.54
Molar Gibbs energy function	$-(G°–H_0°)/T$/J K^1 mol^{-1}	216.94
Properties derived for ions in aqueous solutions		
Ionic radius	r/nm	0.21 ± 0.02
Surface charge density	σ/C m^{-2}	0.286
Polarizability	α/m^3	4.44×10^{-30}
Standard molar enthalpy of formation	$\Delta_f H^\infty$/kJ mol^{-1}	-140 ± 7
Standard molar entropy	S^∞/J K^{-1} mol^{-1}	201 ± 7
Standard molar heat capacity	C_P^∞/J K^{-1} mol^{-1}	103 ± 14
Standard molar volume	V^∞/cm^3 mol^{-1}	46.3 ± 3.3
Standard molar electrostriction volume	$\Delta_{electr} V^\infty$	~ 0
Standard molar refraction	R_D^∞/cm^3 mol^{-1}	11.21
Limiting molar conductivity	λ^∞/S cm^2 mol^{-1}	~ 39.6
Limiting self-diffusion coefficient	D^∞/m^2 s^{-1}	1.06×10^{-9}
Molar viscosity B-coefficient	B_η/dm^3 mol^{-1}	0.058 ± 0.006
Molar dielectric decrement (chloride salt)	$d\varepsilon_r/dc$/dm^3 mol^{-1}	-10.0
Molar surface tension decrement	$d\gamma/dc$/dm^3 mol^{-1}	0.04 ± 0.16
Values derived from a combination of the data for the gaseous and aqueous ions		
Standard molar enthalpy of hydration	$\Delta_{hydr} H^\infty$/kJ mol^{-1}	-602 ± 8
Standard molar entropy of hydration	$\Delta_{hydr} S^\infty$/J K^{-1} mol^{-1}	-63.7
Standard molar structural entropy	$\Delta_{struct} S^\infty$ = J K^{-1} mol^{-1}	83

and other species may approach it to a somewhat closer distance than this radius indicates. GuH^+ is, thus, intermediate in size between Cs^+ and $(CH_3)_4N^+$.

A thermodynamic datum that could be of interest for comparison with data for other cations is the *enthalpy of hydration* of the guanidinium cation, $\Delta_{hydr} H°(GuH^+)$. For its calculation are needed the enthalpy of formation of the gaseous cation, $\Delta_f H°(GuH^+,g)$ and that of the aqueous one, $\Delta_f H°(GuH^+,aq)$. For obtaining the former, its formation from guanidine by protonation in the gas phase:

$$(H_{2N})_2C = NH(g) + H^+(g) \rightarrow C(NH_2)_3{}^+(g) \tag{5.11}$$

is required. Such a calculation, based on literature values of the required quantities, has recently been made by the present author (Marcus 2012a). It involves the energy change for reaction (5.11) calculated theoretically (Schott 1984; Fülscher and Mehler 1991), and, converted to the enthalpy, the result is $\Delta_r H°(5.11) \approx -1106 \pm 3$ kJ mol^{-1}. The enthalpy of formation of guanidine in its standard state (crystalline) is $\Delta_f H°(Gu,c) = -56.1$ kJ mol^{-1} (Kirpichev et al. 1968; Wagman et al. 1982) and its enthalpy of sublimation is $\Delta_{subl}(Gu,c) \approx 87.9$ kJ mol^{-1} (Joshi 1982), yielding the enthalpy of formation of gaseous guanidine, $\Delta_f H°(Gu, g) = 31.8$ kJ mol^{-1}. With $\Delta_f H°(H^+,g) = 1536.2$ kJ mol^{-1} (Wagman et al. 1982) the re-

sulting enthalpy of formation of the gaseous cation is $\Delta_f H°(GuH^+, g) = 31.8 + 1536.2 - 1106 = 462 \pm 3$ kJ mol^{-1}.

The enthalpy of formation of the standard aqueous cation $\Delta_f H°(GuH^+,aq) = -139.1 \pm 0.7$ was estimated by Kon'kova et al. (2009). This is in agreement with values calculated (Marcus 2012a) from the enthalpies of formation of the nitrate and chloride salts, their enthalpies of solution, and the standard molar enthalpy of formation of the individual aqueous nitrate and chloride anions, based on the value assigned to the hydrogen ion of -1103 ± 7 kJ mol^{-1} (Marcus 1997). The mean value from these two salts is $\Delta_f H°(GuH^+,aq)$ -140 ± 7 kJ mol^{-1}.

Finally, the standard molar enthalpy of hydration of the guanidinium cation is $\Delta_{hydr} H°(GuH^+) = \Delta_f H°(GuH^+,aq) - \Delta_f H°(GuH^+,g) = -140 - 462 = -602 \pm 8$ kJ mol^{-1}.

The *molar refraction* of guanidinium is obtained from the density and refractive index data of Hunger et al. (2010) on aqueous GuHCl:

$$R_D = 1000\left(n_D{}^2 - 1\right)/\left(n_D{}^2 + 2\right) - \left(1000\rho - M_E\right)\rho_W{}^{-1}\left(n_{DW}{}^2 - 1\right)/\left(n_{DW}{}^2 + 2\right) \tag{5.12}$$

The density ρ is in g cm^{-3}, the refractive index n_D pertains to the Na line at 589 nm, and M_E is the molar mass of the salt in g mol^{-1}. Extrapolated to infinite dilution the result is $R_D{}^\infty(GuHCl) = 19.84$ cm^3 mol^{-1}. Taking the molar refraction of Cl^- from Table 5.3, $R_D{}^\infty(Cl^-) = 8.63$ cm^3 mol^{-1}, the remainder is $R_D{}^\infty(GuH^+) = 11.21$ cm^3 mol^{-1}. It is assumed that $R_D{}^\infty$ may be substituted for the infinite frequency molar refraction, R_∞, for the purpose of obtaining the polarizability of GuH^+, which is: $\alpha = (3/4\pi N_A)R_D{}^\infty = 4.44 \times 10^{-30}$ m^3. This is, again, intermediate between the values for Cs^+ and $(CH_3)_4N^+$.

The viscosity of aqueous guanidinium salts was measured by Kumar (2001a), yielding the values of the *viscosity B-coefficients*, B_η/dm^3 mol^{-1} according to Eq. (2.41) as 0.047 for GuHCl, 0.022 for GuHBr, 0.006 for $GuHClO_4$, and 0.325 for $(GuH)_2SO_4$. These are the limiting slopes of $(\eta/\eta_W - 1)/c^{1/2}$ against $c^{1/2}$, and as they pertain to infinite dilution they are additive in the values for the constituent ions. Subtraction of the anion values $B_\eta(Cl^-) = -0.005$, $B_\eta(Br^-) = -0.033$, and $B_\eta(ClO_4{}^-) = -0.060$, and $B_\eta(SO_4{}^{2-}) = 0.206$ yields the average $B_\eta(GuH^+) = 0.058 \pm 0.006$ dm^3 mol^{-1}. The data presented for guanidinium acetate are not consistent with those of the other four salts. The mean value for $B_\eta(GuH^+)$ makes guanidinium a mildly structure-making (kosmotropic) cation, somewhat less than Na^+. Other criteria of water structural effects (Chap. 3) regard GuH^+ as well as Na^+ as borderline cases, being neither pronounced structure makers nor breakers (Cappa et al. 2006).

The information regarding the *molar surface tension increment*, $d\gamma/dc$ is much less satisfactory, because it does not yield a constant increment for the GuH^+ cation. The molality based data of Kumar (2001a) were converted to the molarity base by means of the density data provided there to yield $(d\gamma/dc)/(mN\ m^{-1}\ mol^{-1}\ dm^3) = 0.75$ for GuHCl, 0.69 for GuHBr, and 1.00 for $(GuH)_2SO_4$, assigned large uncertainties, about ± 0.20 units, by Pegram and Record (2007). Subtraction of the

"improved" anion values from Table 4.5, yields the values for GuH^+ of −0.15, 0.04, and 0.23 mN m^{-1} mol^{-1} dm^3 from these three salts. An overall mean value of 0.04 ± 20 should best describe the value for the guanidinium cation. The values provided by Kumar (2001a) for the acetate and perchlorate salts yield sizable *positive* values for the GuH^+ cation, that are not compatible with that calculated from the chloride, bromide, and sulfate salts, for no apparent reason. According to this criterion GuH^+ is neither a structure-breaking nor a structure-making cation.

Some other data of interest are the standard *molar volumes* of the salts, $V_E^\infty/cm^3\ mol^{-1}$, reported by Kumar (2001b): GuHCl 69.9, GuHBr 79.8, $GuHClO_4$ 92.3. These values yield after subtraction of the anion values (Marcus 1997) the average $V_i^\infty(GuH^+) = 46.3 \pm 3.3\ cm^3\ mol^{-1}$. However, the reported (Kumar 2001b) values of V_E^∞ for the acetate and sulphate do not yield reasonable values for the cation. The specific conductance κ of aqueous GuHCl and $(GuH)_2CO_3$ was reported by Hunger et al. (2010), and for the former salt $\Lambda = \kappa/c$ extrapolates vs. $c^{1/2}$ to $\Lambda^\infty = 116.0\ S\ cm^2\ mol^{-1}$ (ignoring electrophoretic and ion atmosphere relaxation terms). On deduction of $\lambda^\infty(Cl^-) = 76.4\ S\ cm^2\ mol^{-1}$ (Marcus 1997), the *limiting ionic conductance* value $\lambda^\infty(CuH^+) = 39.6\ S\ cm^2\ mol^{-1}$ results.

The properties of the guanidinium cation described above as well as some others are summarized in Table 5.5 (Marcus 2012a). In conclusion, although GuH^+ has a large negative enthalpy of hydration, the water molecules are very labile (Mason et al. 2004), and in view of its viscosity B_η coefficient and its surface tension increment $d\gamma/dc$ it is a border-line cation between structure-making (kosmotropic) and structure-breaking (chaotropic) cations. The lability of its hydration shell and border-line position with regard to the structure of water should put GuH^+ near "head cations" such as NH_4^+ and K^+ in the Hofmeister series. On the other hand, it is a strong denaturant of proteins and should be placed near "tail cations" in this series (Kunz 2010b). This dual nature of GuH^+ is still baffling researchers.

5.3.2 *Some Aspects of Protein Hydration*

The hydration of proteins is widely described and discussed in the literature, but in this book, devoted to ions in water, only very limited aspects of this topic can be touched upon.

Native proteins in aqueous solutions, being in their folded form, consist of a mainly hydrophobic core that is little exposed to the solvent and a mainly hydrophilic periphery that borders on the solvent. The quantity that is relevant for the latter is the solvent accessible surface area (*SASA*), obtained by rolling a spherical probe having the diameter of a solvent molecule (water, 0.28 nm) on the surface of the protein according to Sanner et al. (1996). In a study by Saito et al. (2010) of five representative globular proteins (bovine pancreatic trypsin inhibitor, bovine pancreatic ribonuclease, hen egg-white lysozyme, bovine milk β-lactoglobulin A, and bovine pancreatic α-chymotrypsinogen A) the fraction of hydrophilic *SASA* ranged from 69 to 83 %, of which a portion was ionic, comprising from 27–50 % of the *SASA*. The

term 'ionic' was not clearly defined, but appears to pertain to the carboxylate and ammonium groups of the amino acid side chains. When these are ionized at appropriate pH values, then the protein surface has a considerable amount of electrical charges that interact with the hydrating water.

On the other hand, the protein surface is rough, having concave and convex regions, and the water molecules in such different geometrical environments must be subject to different forces as argued by Gerstein and Chothia (1996), who calculated the packing at the protein-water interface. For the 22 proteins studied the average number of surface atoms of was 420, of which 47 % were hydrated, i.e., in contact with water molecules. (There are also some 29 % of the total water hydrating molecules buried inside the core of the protein. These are strongly compressed, their molecular volume being $0.0229\,\mathrm{nm}^3$, not much above the van der Waals volume of $0.0206\,\mathrm{nm}^3$). The peripheral hydrating water molecules were calculated to have a molecular volume of $0.0245\,\mathrm{nm}^3$, that is, compressed by 22 % with respect to the molar volume of bulk water per molecule, $V_\mathrm{w}^*/N_\mathrm{A} = 0.0300$ nm at room temperature.

The compression of the water of hydration of proteins was studied experimentally by Svergun et al. (1998), using x-ray and neutron scattering. Three proteins (lysozyme, E. Coli thioredoxin reductase, and E. Coli ribonucleotide reductase protein R1) in aqueous solution were subjected to the scattering experiments. The known crystallographic structures of these proteins facilitated the interpretation of the results, and it was found that the density of the water of the first hydration shell differs from that of bulk water. The averages relative densities from x-ray and neutron diffraction (in H_2O and in D_2O solutions) were 1.08 ± 0.02, 1.16 ± 0.05, and 1.12 ± 0.06 for the three named proteins, respectively. These experimental values are smaller than those calculated from the packing (Gerstein and Chothia 1996), but still appreciable.

Perkins (2001) discussed x-ray and neutron diffraction from the hydration shell of proteins, but did not refer to the experimental results of Svergun et al. (1998). Instead he used the estimate of $0.0245\,\mathrm{nm}^3$ for a water molecule in the hydration shell by Gerstein and Chothia (1996) to explain the apparent different partial molar volume measured densitometrically for proteins in solution with the values calculated from their amino acid contents.

The source of the higher density of the water of hydration was then discussed by Merzel and Smith (2002) who computed by molecular dynamics simulation the small angle scattering profiles of the Svergun et al. experiments. They concluded that the variation in this density is determined by both topological and electrostatic properties of the protein surface. The simulation provided a measure for the surface roughness, $h(\Theta)$, ranging from -0.6 nm for depressions (concave regions, grooves) to $+0.4$ nm for ridges (convex regions) with respect to a perfectly flat and smooth surface. In the 0.3 nm thick hydration shell, the density of the water increased by up to 7 ± 2 % in the depressions but by only 2 ± 2 % at the ridges. Furthermore, where the electric field perpendicular to the surface was negative, corresponding to a surface charge density of 0.05 to 3.0 $e\,\mathrm{nm}^{-2}$ ($1\,e\,\mathrm{nm}^{-2} = 16\,\mathrm{C\,m}^{-2}$) the density was enhanced by up to 10 ± 3 %. The topological effect was explained by a water

molecule in a depression being less exposed to randomizing, disorienting effects of neighboring water molecules and being in closer contact with the protein surface, than water molecules at ridges.

Danielewicz-Ferchmin et al. (2003) took up the electrostatic explanation of the density enhancement of the water in the hydration shell, maintaining that the compression is due to the electrostriction of the water produced by the huge electric fields generated by the ions at the protein surface. The field $E = \sigma/\varepsilon_0\varepsilon_r(\sigma)$, is of the order of GV m^{-1}, and the relative permittivity in the hydration shell $\varepsilon_r(\sigma)$ depends on the charge density σ at the surface between the protein and this shell, being lower, down to much lower, than the bulk value. There being no way to determine independently the surface charge density σ, this was done by reversing the calculation of the resulting electrostriction. That is, the compression of the water deduced from the experimental x-ray and neutron scattering data (Svergun et al. 1998), yielded the values of σ required to produce this compression according to methods established for aqueous solutions of small ions (Danielewicz-Ferchmin et al. 1998). Up to surface charge densities of 0.24 C m^{-2} there is no appreciable density enhancement, but beyond this value and up to 0.41 C m^{-2} (where compression down to the van der Waals volume of the water molecules occurs) the surface densities are to a good approximation:

$$\sigma/\text{C m}^{-2} = -3.82 + 9.15(\rho/\rho_W) - 6.83(\rho/\rho_W)^2 + 1.74(\rho/\rho_W)^3 \qquad (5.13)$$

where (ρ/ρ_W) is the hydration water density relative to that of bulk water. Thus, if the total compression of the water is due to electrostriction, the charge densities σ/C m^{-2} at the surfaces of the three proteins studied by Svergun et al. (1998) are 0.294 ± 0.010, 0.326 ± 0.018, and 0.309 ± 0.025, respectively. These values of σ are within the range estimated by Merzel and Smith (2002), but there are no experimental values for comparison. If a part of the compression is due to the topological effect proposed by these authors, the resulting values of σ would be appreciably smaller. Still, a sizable fraction of the *SASA* is ionic (Saito et al. 2010), so that appreciable charges should occur at the protein surface to produce large electrostriction.

The molar volume of the water V_W at 298.15 K adjacent to the surface layer of the protein stays at 18.07 cm^{-3} mol^{-1} up to $\sigma = 0.24$ C m^{-2} but decreases to 16.57 cm^{-3} mol^{-1} at $\sigma = 0.3$ C m^{-2}, to 12.71 cm^{-3} mol^{-1} at $\sigma = 0.4$ C m^{-2} (Danielewicz-Ferchmin et al. 2003). Apparently, even smaller values are reached at larger charge densities, smaller than the van der Waals volume of 12.4 cm^3 mol^{-1}, an unlikely result. The density values reported for the surface layer of water of several proteins, such as chicken ovalbumin lysozyme (ranging from 1.08 to 1.22 g cm^{-3}) (Svergun et al. 1998) agreed with the values calculated from the surface charge densities and the corresponding electric fields (ranging from 2.34 to 5.69 GV m^{-1}) and permittivities. The permittivity of water, $\varepsilon_W{}^*$, is drastically reduced by high electric fields ($\sim$1 GV m^{-1}): from 82 (at 20 °C) at zero charge density to 79 at $\sigma = 0.1$ C m^{-2}, to 63 at 0.2 C m^{-2}, to 11 at 0.3 C m^{-2}, and to 4 at 0.4 C m^{-2} (Danielewicz-Ferchmin et al. 2003). This compacting of the water in the layer near a protein molecule also accounts for the non-freezing of this water when the temperature is

reduced below 0 °C, ascribable according to Sancho et al. to the electrostriction pressures generated by the charges (Sect. 2.2), ranging from 0.1–0.6 GPa (Sancho et al. 1995).

In a subsequent paper Danielewicz-Ferchmin et al. (2006) related the temperature and pressure dependence of native-to-denatured transition of proteins to local values of the charge density at the surface of the protein. They argued that water in the hydration shell, exchanging with bulk water, is at equilibrium with the latter, hence the work of orienting the molecular dipoles in the two environments, in the field of the surface charges and outside it, is equal. They set up an equation of state explicit in the electrostrictive pressure and the charge density and calculated temperature-pressure crossover points for the native-to-denatured transition dependence for six proteins (ribonuclease, human interferon γ, chymotrypsinogen, lysozyme, staphinococal nuclease, and ribonuclease A). Such crossover points occur over a narrow width of surface charges in the range 0.289–0.306 C m^{-2} for these six proteins. At these values of σ the energy of dipole orientation is commensurate with the energy for breaking a hydrogen bond between water molecules.

The dynamics of the water molecules in the hydration shells of proteins has also been the subject of much research. Modig et al. (2004) used the magnetic relaxation dispersion technique for the cyclic peptide oxytocin and the globular protein bovine pancreatic trypsin inhibitor (BPTI). The average rotational retardation factor of hydration shell water is in the range of 4–6, but this is an average over hundreds of water molecules. A few molecules located in depressions of the protein surface that are much more strongly retarded could produce these average values. The surface topography is, thus, of importance in controlling the hydration structure and dynamics. More direct information came from teraherz spectroscopy, applied by Ebbinghaus et al. (2007). Hydrogen bond lifetimes larger than those in bulk water (1.6 ps) were detected up to a distance of 0.6 nm from the protein surface (a synthetic five helix bundle λ^*_{6-85}), ranging up to 2.4 ps at 0.2 nm distance.

Priya et al. (2008) attempted to specify sites on the surfaces of proteins (lysozyme and staphilococal nuclease) where the water binding is particularly strong. However, they appear to have used unrealistically large densities of the water (>7 times the bulk density) as their criterion, to which water molecules cannot be compressed by any conceivable pressure, even not that generated by the huge electrostrictive fields. However, then the criterion was changed to:

$$\eta = 3.4 + \ln[\tau_1/(\tau_1 + \tau_0)] \tag{5.14}$$

where τ_1 is the average time a site is occupied by a water molecule and τ_0 the average time it is vacant. The criterion of $\eta > 2$ for strong binding does make sense, corresponding to ~25 % of the time occupancy of the site. Of the two proteins studied, the former has 150 sites of high occupancy and the other 242 such sites, 15 % and 10 % of which are with kinetically bound water ($\eta > 2.7$). Such sites appear to be the depressions in the rough topology of the protein surface, but according to Danielewicz-Ferchmin et al. (2006) could be at ionized amino acid side chains. Nucci et al. (2011) used NMR spectroscopy to study a protein (ubiquitin) encapsulated in a reversed micelle in a low viscosity solvent (to retard protein tumbling), thereby

being able to map regions at the protein surface where the water molecules cluster into slow, intermediate, and rapid average dynamics. Armstrong et al. (2011) used dynamic nuclear polarization of water and electron paramagnetic resonance to study the site-specific hydration dynamics by nitroxide, labelling the sites in apomyoglobin. Some surface sites of the native protein, identified by their amino acid sequences E41R1 and V66R1, show relatively fast hydration dynamics, only 2–4 times slower than bulk water. Other sites, F138R1 and M131R1 display water dynamics some 9–20 times slower than bulk water, deemed to indicate a 'dry' interior of the protein. For the unfolded protein all the sites display fast water dynamics.

This partial review of protein hydration shows that the water of hydration of protein surfaces is exposed to a heterogeneous assembly of sites: some highly ionic, some in concave depressions, and some at convex ridges. These contribute to the compression of the water, the orientation of the molecules, and the dynamics of their exchange and rotation. However, it is still not clear how important is each of these effects and at what specific sites of the protein surface do they take place.

5.3.3 *Some Aspects of K^+/Na^+ Selectivity in Ion Channels*

Sodium and potassium ions play key roles in several physiological processes, including homeostasis of blood and body fluids, cardiac, skeletal, and smooth muscle contraction, taste and pain sensation, hormone secretion, and signal transduction (Dudev and Lim 2010). Fenton (1977) described the transport of these ions by ionophores: biological, such as nonactin, and synthetic, such as crown ethers and cryptands, listing some requirements for the selective recognition of these ions by ligands that play their role in ion channels. Most of the very numerous studies of ion channels emphasize the structure of the pores in the protein membrane that hosts these channels. The charges on the walls of ion channels and the ions passing through them cause electrostriction of the water (see Sect. 2.7.3), as discussed by several authors (Sancho et al. 1995; Duca and Jordan 1997; Danielewicz-Ferchmin et al. 2006). In this book, devoted to ions in water, only the relevant properties of sodium and potassium ions are discussed that may lead to their preferences in the appropriate channels.

Relevant properties of the sodium and potassium ions, gleaned from Chap. 2 and elsewhere (Marcus 1997) are shown in Table 5.6. The bare potassium ion is larger than the sodium one and is more polarizable, as their crystal ion radii r_I (valid also in solutions) and molar refractivity R_{DI} show. However, the K^+ cations move faster in aqueous solutions as their mobilities u_I and diffusion coefficients D_I show, the K^+ ions having a smaller Stokes radius, r_{ISt}. The K^+ cations carry along when moving less of their hydration shells that are more loosely bound, the residence times of water molecules near K^+ being about one half that near Na^+. Also, the hydration number h_I of K^+ is smaller than that of Na^+, as derived from the compressibility of the solutions as well as other measures. Such numbers are smaller than the coordination numbers *CN* in solution, which are governed only by the sizes

Table 5.6 Properties of sodium and potassium ions relevant to their recognition in ion channels

Quantitity	Na^+	K^+
Crystal ionic radius, r_I/nm	0.102	0.138
Molar refraction, R_{DI}/cm^3 mol^{-1}	0.65	2.71
Softness parameter, σ_{+I}	−0.60	−0.53
Lewis acidity (Kamlet-Taft), α	0.89	0.85
Coordination number of aqueous ion, *CN*	6.0	6.3–7.8
Hydration number from compressibility, h_I	3.3	2.3
Water residence time near ion, τ_{WresI}/ps	9.9	4.8
Self-diffusion coefficient, $D_I^\infty/10^{-9}$ m^2 s^{-1}	1.33	1.96
Ion mobility, u_I^∞/cm^2 s^{-1} V^{-1}	51.8	76.0
Stokes radius, r_{ISt}/nm	0.184	0.125
Hydrated radius (Sect. 2.3.1), $(r_i + \Delta r_i)$/nm	0.218	0.213
Viscosity *B*-coefficient, $B_{\eta I}$/mol^{-1} dm^3	0.085	−0.009
Structural entropy, ΔS_{StrI}/J K^{-1} mol^{-1}	−11	45
Standard partial molar volume, V_I^∞/cm^3 mol^{-1}	−6.7	3.5
Molar electrostriction volume, $\Delta V_{I\,elec}{}^\infty$/cm^3 mol^{-1}	−8.6	−5.9
Setchenow salting coefficient for benzene, k_I/mol^{-1} dm^3	0.137	0.108
Molar Gibbs energy of hydration, $\Delta_{hydr}G_I^\infty$/kJ mol^{-1}	−383	−312
Molar enthalpy of hydration, $\Delta_{hydr}H_I^\infty$/kJ mol^{-1}	−416	−334
Molar entropy of hydration, $\Delta_{hydr}S_I^\infty$/J K^{-1} mol^{-1}	−111	−74
Molar surface tension increment, $d\gamma/dc_I$/mN m^{-1} mol^{-1} dm^3	1.20	1.10

of the bare ions and the geometrical packing of water molecules around them. Some other quantities do not appreciably distinguishing between Na^+ and K^+ cations: both are 'hard' ions ($\sigma_+ \leq 0$) with nearly the same Lewis acidity (Kamlet-Taft α) and they increase the surface tension of water ($d\gamma/dc_I$) similarly. On the other hand, other quantities are appreciably different for these two cations: the thermodynamic quantities of hydration, $\Delta_{hydr}G_I^\infty$ and $\Delta_{hydr}H_I^\infty$, show Na^+ to be more strongly (energetically) hydrated than K^+ by some 24 % and Na^+ ions cause considerably more electrostriction, $\Delta V_{I\,elec}{}^\infty$, of their hydration shells than K^+ ions. Hence, Na^+ ions are more effective salting out agents than K^+ ions, e.g., the Setchenow k_I for benzene. More striking are the opposite signs of the standard partial molar volumes, that of Na^+ being negative, the electrostriction caused by it being larger than its intrinsic volume, whereas the opposite holds for K^+, having a positive partial molar volume. Opposite signs pertain also to the effects of these cations on the structure of water: the viscosity *B*-coefficient, $B_{\eta I}$, and the (water-) structural entropy, ΔS_{StrI}. Potassium ions are considered to be water structure breaking (chaotropic), though only mildly, whereas sodium ions are water structure makers (kosmotropic), though only moderately, and by some criteria they are borderline cases, neither structure makers nor breakers.

The question arises now, that given these properties of sodium and potassium ions, how do ion channels recognise them, distinguish between them, and let the one or the other pass through them with high selectivity, as required for their proper physiological functioning.

Before answering this question a digression to the behaviour of the two cations towards small molecules, ionophores, that are able to carry them selectively from one

medium to another across lipid membranes, should be explored. The ionophores can be natural, such as nonactin and monensin, or synthetic crown ethers and cryptands. In the case of the crown ether 18C6, *c*-hexaethyleneoxide, with six donor oxygen atoms, the radius of the cavity is 0.130–0.143 nm (Arnaud-Neu et al. 2003), so that Na^+ ions would 'rattle' inside the cavity, if it were rigid, whereas K^+ ions sit snugly within. This difference is manifested by the equilibrium constants for complexation in aqueous solutions, $\log K_{comp}$ being < 0.3 and 2.05 for these two ions according to Frensdorff (1971). The difference in the enthalpies of the reaction, 14 kJ mol in favour of K^+ (Arnaud-Neu et al. 2003), compensates only partially for the difference in the enthalpies of hydration, 82 kJ mol^{-1}, signifying that only a part of the water of hydration is lost on complexation, water molecules still hydrate the ions perpendicularly to the plane of the crown ether. The crown ether 18C6 is flexible, but a more rigid ligand, dibenzo-18C6 shows less discrimination between the two cations $\log K_{comp}$ being 1.16 and 1.67 for aqueous Na^+ and K^+ (Shchori et al. 1975). The cryptand 222 wraps the ions completely inside a cage that has the same number of six oxygen donor atoms as the two crown ethers mentioned and in addition two nitrogen donor atoms. The respective complex formation constants are $\log K_{comp}$ 3.98 and 5.47, and the enthalpy difference of 16.5 kJ mol^{-1} pertains to replacement of the oxygen donor atoms of the hydrating water molecules by those of the cryptand (Marcus 2004). When carbonyl groups replace ether linkages, as in the ionophore valinomycin, the selectivity for K^+ increases many-fold over that shown by the crown or cryptand ligands, the relative complex formation constants are $\Delta \log K_{comp}$ 3–4, increasing with diminishing relative permittivity of the medium (Rose and Henkens 1974). The main conclusion is that discrimination between the two cations is larger when the encapsulating ligand is flexible, has stronger donor abilities of its donor atoms (carbonyl vs. ether oxygen atoms), and allows for some water of hydration to stick to the cations.

The insights gained from the ionophores may now be applied to the ion channels. It was concluded that for K^+-selective channels a rigid pore geometry that fits only K^+ but not the smaller (bare) Na^+ does *not* control the selectivity, since the fluctuations of the donor atom positions are 0.05–0.10 nm, larger than the difference in r_I of 0.036 nm. Rather, having 8 carbonyl oxygen donor atoms in the lining of the channel in a semi-rigid conformation favours binding to an ion with *CN* of 8 (K^+) over one with *CN* of 6 (Na^+). On top of this, an environment of low water accessibility, hence of low relative permittivity, leads to such selectivity that reaches 1000:1 (Dudev and Lim 2009).

On the contrary, the selectivity for Na^+ over K^+ in Na^+-channels is based on the pore providing three rather than four protein ligands that have strong donor abilities (such as carboxylate groups). Three carboxylate groups, with two donor atoms each, favour Na^+ having a *CN* of 6 relative to K^+ having a *CN* of 8. The pore of a Na^+ channel is narrow and rigid and exposed to the water, letting the smaller (bare) Na^+ to pass through it (Dudev and Lim 2010). The stronger donor ability of carboxylate vs. carbonyl groups helps to compensate for the unfavourable dehydration energies of Na^+ relative to K^+ and a selectivity for Na^+ of 500:1 is achieved. Smaller permeability ratios, of 10–40, are observed in certain voltage gated

Na^+-channels, which can transiently depolarize cell membranes by about + 130 mV. A lysine residue at the selectivity filter was found by Favre et al. to be essential for obtaining the Na^+ selectivity, but its function was not clear at the time (Favre et al. 1996). Subsequent work by Lipkind and Fozzard (2008) suggested that the glutamate site in the selectivity filter is normally blocked by hydrogen bonding to the lysine residue, but that a high charge density ion such as Na^+ (also Li^+) can compete and displace the ammonium group of the lysine. An ion with a smaller charge density, such as K^+, is not able to disrupt the hydrogen bond between lysine and glutamate.

References

Abezgauz L, Kuperkar K, Hassan PA, Ramon O, Bahadur P, Danino D (2010) Effect of Hofmeister anions on micellization and micellar growth of the surfactant cetylpyridinium chloride. J Coll Interf Sci 342:83–92

Arakawa T, Timasheff SN (1984) Mechanism of protein salting in and salting out by divalent cation salts: balance between hydration and salt binding. Biochemistry 23:5912–5923

Armstrong BD, Choi J, Lopez C, Wesener DA, Hubbell W, Cavagnero S, Han S (2011) Site-specific hydration dynamics in the nonpolar core of a molten globule by dynamic nuclear polarization of water. J Am Chem Soc 133:5987–5995

Arnaud-Neu F, Delgado R, Chaves S (2003) Critical evaluation of stability constants and thermodynamic functions of metal complexes of crown ethers. Pure Appl Chem 75:71–102

Baldwin RL (1996) How Hofmeister ion interactions affect protein stability. Biophys J 71:2056–2063

Batchelor JD, Olteanu A, Tripathy A, Pielak GJ (2004) Impact of protein denaturants and stabilizers on water structure. J Am Chem Soc 126:1958–1961

Bauduin P, Renoncourt A, Touraud D, Kunz W, Ninham BW (2004a) Hofmeister effect on enzymatic catalysis and colloidal structures. Curr Opin Coll Interf Sci 9:43–47

Bauduin P, Wattebled L, Touraud D, Kunz W (2004b) Hofmeister ion effects on the phase diagrams of water-propylene glycol propyl ethers. Z Phys Chem 218:631–641

Bauduin P, Nohmie F, Touraud D, Neuder R, Kunz W, Ninham BW (2006) Hofmeister specific-ion effects on enzyme activity and buffer pH: horseradish peroxidase in citrate buffer. J Mol Liq 123:14–19

Boström M, Williams DRM, Ninham BW (2001a) Specific ion effects. Why DLVO theory fails for biology and colloid systems. Phys Rev Lett 87:168103–1/4

Boström M, Williams DRM, Ninham BW (2001b) Surface tension of electrolytes: specific ion effects explained by dispersion forces. Langmuir 17:4475–4478

Boström M, Williams DRM, Ninham BW (2003a) Specific ion effects: why the properties of lysozyme in salt solutions follow a Hofmeister series. Biophys J 85:686–694

Boström M, Craig VSJ, Albion R, Williams DRM, Ninham BW (2003b) Hofmeister effects in pH measurements: role of added salt and co-ions. J Phys Chem B 107:2875–2878

Boström M, Deniz V, Ninham BW (2006a) Ion specific surface forces between membrane surfaces. J Phys Chem B 110:9645–9649

Boström M, Lonetti B, Fratini E, Baglioni P, Ninham BW (2006b) Why pH titration in protein solutions follows a Hofmeister series. J Phys Chem B 110:7563–7566

Büchner BH, Voet A, Bruins EM (1932) Lyotrope zahlen und ioneneigen-schaften. Proc Kong Neder Akad Veten 35:563–569

Cacace MG, Landau EM, Ramsden JJ (1997) The Hofmeister series: salt and solvent effects on interfacial phenomena. Quart Rev Biophys 30:241–277

Cappa CD, Smith JD, Messer BM, Cohen RC, Saykally RJ (2006) Effects of cations on the hydrogen bond network of liquid water: new results from x-ray absorption spectroscopy of liquid microjets. J Phys Chem B 110:5301–5309

Carpenter DC, Lovelace FE (1935) The influence of neutral salts on the optical rotation of gelatine. III. Effect of the halides of lithium, sodium, rubidium, and cesium. J Am Chem Soc 57:2337–2342

Collins KD (1995) Sticky ions in biological systems. Proc Natl Acad Sci U S A 92:5553–5557

Collins KD (1997) Charge density-dependent strength of hydration and biological structure. Biophys J 72:65–76

Collins KD, Washabaugh MW (1985) The Hofmeister effect and the behaviour of water at interfaces. Quart Rev Biophys 18:323–401

Collins KD, Neilson GW, Enderby JE (2007) Ions in water: characterizing the forces that control chemical processes and biological structure. Biophys Chem 128:95–104

Danielewicz-Ferchmin I, Ferchmin AR, Szlaferek A (1998) On the inter-relations between charge and mass densities within a double layer. Chem Phys Lett 288:197–202

Danielewicz-Ferchmin I, Banachowicz E, Ferchmin AR (2003) Protein hydration and the huge electrostriction. Biophys Chem 106:147–153

Danielewicz-Ferchmin I, Banachowicz E, Ferchmin AR (2006) Properties of hydration shells of protein molecules at their pressure—and temperature-induced native-denatured transition. ChemPhysChem 7:2126–2133

Duca KA, Jordan PC (1997) Ion-water and water-water interactions in a gramicidinlike channel: effects due to group polarizability and backbone flexibility. Biophys Chem 65:123–141

Dudev T, Lim C (2009) Determination of K^+ vs Na^+ selectivity in potassium channels. J Am Chem Soc 131:8092–8101

Dudev T, Lim C (2010) Factors governing the Na^+ vs. K^+ selectivity in sodium channels. J Am Chem Soc 132:2321–2332

Ebbinghaus S, Kim SJ, Heyden M, Yu X, Heugen U, Gruebele M, Leitner DM, Hevenith M (2007) An extended dynamical hydration shell around proteins. Proc Natl Acad Sci U S A 104:20749–20752

Ebel C, Faou P, Kernel B, Zaccai G (1999) Relative role of anions and cationsin the stabilization of halophilic malate dehydrogenase. Biochemistry 38:9039–9047

Favre I, Moczydlowski E, Schild L (1996) On the structural basis for ion selectivity among Na^+, K^+, and Ca^{2+} in the voltage-gated sodium channel. Biophys J 71:3110–3125

Fenton DE (1977) Across the living barrier. Chem Soc Rev 6:325–343

Fischer MH, Moore G (1907) On the swelling of fibrin. Am J Physiol 20:330–342

Frensdorff HK (1971) Stability constants of cyclic polyether complexes with univalent cations. J Am Chem Soc 93:600–606

Fülscher MP, Mehler EL (1991) Self-consistent, nonorthogonal group function approximation. III. Approaches for modeling intermolecular interactions. J Comput Chem 12:811–828

Gerstein M, Chothia C (1996) Packing at the protein-water interface. Proc Natl Acad Sci U S A 93:10167–172

Gurau MC, Lim S-M, Castellana ET, Albertorio F, Kataoka S, Cremer PS (2004) On the mechanism of the Hofmeister effect. J Am Chem Soc 126:10522–10523

Hall DL, Drake PL (1995) Activation of the herpes simplex virus type 1 protease. J Biol Chem 270:22697–22700

Hamaguchi K, Geiduschek EP (1962) Effect of electrolytes on the stability of the deoxyribonucleate helix. J Am Chem Soc 84:1329–1338

Hess B, Van Der Vegt NFA (2009) Cation specific binding with protein surface charges. Proc Natl Acad Sci U S A 106:13296–13300

Hochachka PW, Somero GN (1984) Biochemical Adaptation. Princeton Univ. press, Princeton

Hofmeister F (1888) About regularities in the protein precipitation effects of salts and the relation of these effects with the physiological behaviour of salts. Arch Exp Pathol Pharmakol 24:247–260

Hribar B, Southall NT, Vlachy V, Dill KA (2002) How ions affect the structure of water. J Am Chem Soc 124:12302–12311

Hunger J, Niedermayer S, Buchner R, Hefter G (2010) Are nanoscale ion aggregates present in aqueous solutions of guanidinium salts? J Phys Chem B 114:13617–13627
Joshi RM (1982) Bond energy scheme for estimating heats of formation of monomers and polymers. VII. Nitrogen compounds. J Macromol Sci-Chem A18:861–911 (p 886)
Kahlo H (1921) Ueber die beeinflussung der hitzekoagulation des pflanzen-protoplasmas duch neutralsalze. Biochem Z 117:87–95
Karla A, Tukgu N, Cramer SM, Garde S (2001) Salting-in sna salting-out of hydrophobic solutes in aqueous salt solutions. J Phys Chem B 105:6380–6386
Kirpichev EP, Titov LV, Rubtsov YuI, Gavrilova LA (1968) Determination of the heat of formation of guanidine. Russ J Phys Chem 42:269–270
Koelsch P, Viswanath P, Motschmann H, Shapovalov VL, Brezesinski G, Möhwald H, Horinek D, Netz RR, Giewekemeyer K, Salditt T, Schollmeyer H, von Klitzing R, Daillant J, Guenoun P (2007) Specific ion effects in physicochemical and biological systems: simulations, theory and experiments. Coll Surf Sci A Physicochem Eng Aspects 303:110–136
Koga Y, Westh P, Davies JV, Miki K, Nishikawa K, Katayanagi H (2004a) Toward understanding the Hofmeister series. I. Effects of sodium salts of some anions on the molecular organization of H_2O. J Phys Chem A 108:8533–8541
Koga Y, Westh P, Nishikawa K (2004b) Effects of Na_2SO_4 and $NaClO_4$ on the molecular organization of H_2O. J Phys Chem A 108:1635–1637
Kon'kova TS, Matyushin YuN, Miroshnichenko EA, Vorob'ev AB (2009) Thermochemical properties of dinitramidic acid salts. Russ Chem Bull Intl Ed 58:2020–2027
Kumar A (2001a) Aqueous guanidinium salts Part II. Isopiestic osmotic coefficients of guanidinium sulphate and viscosity and surface tension of guanidinium chloride, bromide, acetate, perchlorate and sulphate solutions at 298.15 K. Fluid Phase Equil 180:195–204
Kumar A (2001b) Aqueous guanidinium salts: part I. Densities, ultrasonic velocities, and apparent molar properties. J Solution Chem 30:281–290
Kunz W (2010a) Specific ion effects in colloidal and biological systems. Curr Opin Coll Interf Sci 15:34–39
Kunz W (2010b) Specific Ion Effects. World Scientific, Singapore
Kunz W, Lo Nostro P, Ninham BW (2004) The present state of affairs with Hofmeister effects. Curr Opin Coll Interf Sci 9:1–18
Leontidis E, Aroti A (2009) Liquid expanded monolayers of lipids as model systems to understand the anionic Hofmeister series: 2. Ion partitioning is mostly a matter of size. J Phys Chem B 113:1460–1467
Leontidis E, Aroti A, Belloni L (2009) Liquid expanded monolayers of lipids as model systems to understand the anionic Hofmeister series: 1. A tale of model. J Phys Chem B 113:1447–1459
Levitsky VY, Panova AA, Mozhaev VV (1994) Correlation of high-temperature stability of α-chymotrypsin with 'salting-in' properties of solution. Eur J Biochem 219:231–236
Lipkind GM, Fozzard HA (2008) Voltage-gated Na channel selectivity: the role of the conserved domain III lysine residue. J Gen Physiol 131:523–529
Lo Nostro P, Fratoni L, Ninham BW, Baglioni P (2002) Water absorbency by wool fibers: Hofmeister effect. Biomacromolecules 3:1217–1224
Lopez-Leon T, Santander-Ortega MJ, Ortega-Vinuesa JL, Bastos-Gonzalez D (2008) Hofmeister effects in colloidal systems: influence of the surface nature. J Phys Chem C 112:16060–16069
Lyklema J (2009) Simple Hofmeister series. Chem Phys Lett 467:217–222
Maiti K, Mitra D, Guha S, Moulik AP (2009) Salt effect on self-aggregation of sodium dodecylsulfate (SDS) and tetradecyltrimethylammonium bromide (TTAB): physicochemical correlations and assessment in the light of Hofmeister (lyotropic) effect. J Mol Liq 146:44–51
Marcus Y (1997) Ion properties. Dekker, New York
Marcus Y (2004) Metal ion complexation by cryptand 222. A thermodynamic approach. Rev Anal Chem 23:269–302
Marcus Y (2009) The effects of ions on the structure of water: structure breaking and—making. Chem Rev 109:1346–1370

Marcus Y (2012a) The guanidinium ion. J Chem Thermodyn 48:70–74
Marcus Y (2012b) The viscosity *B*-coeffricient of the thiocyanate anion. J Chem Eng Data 57:617–619
Mason PE, Neilson GW, Enderby JE, Saboungi M-L, Dempsey CE, MacKerell AD Jr, Brady JW (2004) The structure of aqueous guanidinium chloride solutions. J Am Chem Soc 126:11462–11470
McFarlane JC, Berry WL (1974) Cation penetration through isolated leaf cuticles. Plant Phys 53:723–727
Merzel F, Smith JC (2002) Is the first hydration shell of lysozyme of higher density than bulk water? Proc Natl Acad Sci U S A 99:5378–5383
Miki K, Westh P, Koga Y (2008) Interactions of Na-salts and 1-propanol in 1-propanol-Na-salt-H_2O systems: toward an understanding of the Hofmeister series (IV). J Phys Chem B 112:4680–4686
Modig K, Liepinsh E, Otting G, Halle B (2004) Dynamics of protein and peptide hydration. J Am Chem Soc 126:102–114
Moreira L, Firoozaqbadi A (2010) Molecular thermodynamics modelling of specific ion effects on micellization of ionic surfactants. Langmuir 26:15177–15191
Nandi PK, Robinson DR (1972a) The effects of salts on the free energy of the peptide group. J Am Chem Soc 94:1299–1308
Nandi PK, Robinson DR (1972b) The effects of salts on the free energy of nonpolar groups in model peptides. J Am Chem Soc 94:1308–1315
Nucci NV, Prometun MS, Wand AJ (2011) Stie-resolved measurement of water-protein interactions by solution NMR. Nat Struct Mol Biol 18:245–249
Pegram LM, Record MT Jr (2007) Hofmeister salt effects on surface tension arise from partitioning of anions and cations between bulk water and the air-water interface. J Phys Chem B 111:5411–5417
Pegram LM, Record MT Jr (2008) Thermodynamic origin of Hofmeister ion effects. J Phys Chem B 112:9428–9436
Perkins SJ (2001) X-ray and neutron scattering analyses of hydration shells: a molecular interpretation based on sequence predictions and modelling fits. Biophys Chem 93:129–138
Peula-Garcia JM, Ortega-Vinuesa JL, Bastos-Gonzalez D (2010) Inversion of Hofmeister series by changing the surface of colloidal particles from hydrophobic to hydrophilic. J Phys Chem C 114:11133–11139
Pinna MC, Salis A, Monduzzi M, Ninham BW (2005) Hofmeister series: the hydrolytic activity of Aspergillus niger lipase depends on specific anion effects. J Phys Chem B 109:5406–5408
Poillon WN, Bertles JF (1979) Deoxygenated sickle hemoglobin. Effects of lyotropic salts on its solubility. J Bio Chem 254:3462–3467
Priya MH, Shah JK, Asthagiri D, Paulaitis ME (2008) Distinguishing thermodynamic and kinetic views of the preferential hydration of protein surfaces. Biophys J 95:2219–2225
Renoncourt A, Vlachy N, Bauduin P, Drechsler M, Touraud D, Verbavatz J-M, Dubois M, Kunz W, Ninham BW (2007) Specific alkali cation effects in the transition from micelles to vesicles through salt addition. Langmuir 23:2376–2381
Richter-Quittner M (1921) Die Bedeutung der Quellung und Entquellung fuer einige Fragen der Biochemie. Biochem Z 121:273–292
Rose MC, Henkens RW (1974) Stability of sodium and potassium complexes of valinomycin. Biophys Acta 372:426–435
Rydall JR, Macdonald PM (1992) Investigation of anion binding to neutral lipid mem branes using deuterium NMR. Biochemistry 31:1092–1099
Sachs JN, Woolf TB (2003) Understanding the Hofmeister effect between chaotropic anions and lipid bilayers: molecular dynamics simulations. J Am Chem Soc 125:8742–8743
Saito H, Matubayashi N, Nishikawa K, Nagao H (2010) Hydration propertiy of globular proteins: an analysis of solvation free energy by energy representation method. Chem Phys Lett 497:218–222
Salomäki M, Tervasmäki P, Areva S, Kankare J (2004) The Hofmeister anion effect and the growth of polyelectrolyte multilayers. Langmuir 20:3679–3683

Sancho M, Partenskii MB, Dorman V, Jordan PC (1995) Extended dipolar chain Model for ion channels: electrostriction effects and the translational energy barrier. Biophys. J 68:427–433
Sanner MF, Olson AJ, Spehner J-C (1996) Reduced surface: an efficient way to compute molecular surfaces. Biopolymers 38:305–320
Schott H (1984) Lyotropic numbers of anions from cloud point changes of non-ionic surfactants. Coll Surf 11:51–54
Schwierz N, Horineck D, Netz RR (2010) Reversed anionic Hofmeister series: the interplay of surface charge and surface polarity. Langmuir 26:7370–7379
Shchori E, Nae N, Jagur-Grodzinski J (1975) Stability constants of metal cations with dibenzo-18-crown-6 in aqueous solutions. J Chem Soc Dalton Trans 1975:2381–2386
Smith PE (1999) Computer simulation of cosolvent effects on hydrophobic hydration. J Phys Chem B 103:525–534
Svergun DI, Richard S, Koch MHJ, Sayers Z, Kuprin S, Zaccai G (1998) Protein hydration in solution: experimental observation by x-ray and neutron scattering. Proc Natl Acad Sci U S A 95:2267–2272
Thomas AS, Elcock AH (2007) Molecular dynamics simulations of hydrophobic associations in aqueous salt solutions indicates a connection between water hydrogen bonding and the Hofmeister effect. J Am Chem Soc 129:14887–14898
Tobias DJ, Hemminger JC (2008) Getting specific about specific ion effects. Science 319:1197–1198
Vlachy N, Jagoda-Cwiklik B, Vacha R, Touraod D, Jungwirth P, Kunz W (2009) Hofmeister series and specific interactions of charged headgroups with aqueous ions. Adv Coll Interf Sci 146:42–47
Voet A (1937a) Quantitative lyotropy. Chem Rev 20:169–179
Voet A (1937b) Zur numerischen Feststellungder lyotropen Reihe der einwertigen Kationen. Koll Z 78:201–204
von Hippel PH, Wong K-Y (1964) Neutral salts. The generality of their effects on the stability of macromolecular conformations. Science 145:577–580
Wagman DD, Evans WH, Parker VB, Schumm RH, Halow I, Bailey SM, Churney KL, Nutall RL (1982) The NBS tables of chemical thermodynamic properties. Selected values for inorganic and C1 and C2 organic substances in SI units. J Phys Chem Ref Data 11(2):1–392
Westh P, Kato H, Nishikawa K, Koga Y (2006) Towards understanding the Hofmeister series. 3. Effects of sodium halides on the molecular organization of H_2O as probed by 1-propanol. J Phys Chem A 110:2072–2078
Yamasaki M, Yano H, Aoki K (1991) Differential scanning calorimetric studies on bovine serum albumin. II. Effects of neutral salts and urea. Intl J Biol Macromol 13:322–328
Zangi R (2010) Can salting-in/salting-out ions be classified as chaotropes/kosmotropes? J Phys Chem B 114:643–6350
Zhang Y, Cremer PS (2006) Interactions between macromoleculesw and ions: the Hofmeister series. Curr Opin Chem Biol 10:658–663
Zhang Y, Furyk S, Bergbreiter DE, Cremer PS (2005) Specific ion effects on the water solubility of macromolecules: PNIPAM and the Hofmeister series. J Am Chem Soc 127:14505–14510
Zhao HJ (2005) Effects of ions and other compatible solutes on enzymatic activity, and its implication for biocatalysis using ionic liquids. Mol Catal B Enzym 37:16–25

Author Index

Y. Marcus, *Ions in Water and Biophysical Implications,*
DOI 10.1007/978-94-007-4647-3, © Springer Science+Business Media Dordrecht 2012

Subject Index

Y. Marcus, *Ions in Water and Biophysical Implications,*
DOI 10.1007/978-94-007-4647-3, © Springer Science+Business Media Dordrecht 2012